USAAMRDL-TR-76-9

DEVELOPMENT PROGRAM FOR FIELD-REPAIRABLE/EXPENDABLE MAIN ROTOR BLADES

Kaman Aerospace Corporation
Old Windsor Road
Bloomfield, Conn. 06002

September 1976

Final Report

Prepared for

EUSTIS DIRECTORATE
U. S. ARMY AIR MOBILITY RESEARCH AND DEVELOPMENT LABORATORY
Fort Eustis, Va. 23604

EUSTIS DIRECTORATE POSITION STATEMENT

This report reflects the positive results that can evolve from the inclusion of reliability and maintainability (R&M) considerations in the structural design of a new component. In this particular case, one important result is lower initial and life-cycle rotor blade cost. A second important outcome of this work was the development of a repair technique that appears to be acceptable, with some engineering development, to other rotor blade designs including metal skin and honeycomb structures.

Original studies indicate that low blade acquisition costs could not be readily achieved using composite spars, and therefore an aluminum spar was selected for this design. Subsequent efforts, including the development of more acceptable manufacturing processes and the use of high-modulus composite materials, have indicated that an all-composite blade could be cost effective.

Mr. Arthur J. Gustafson of the Technology Applications Division served as project engineer for this effort.

UNCLASSIFIED

SECURITY CLASSIFICATION OF THIS PAGE (When Data Entered)

REPORT DOCUMENTATION PAGE	READ INSTRUCTIONS BEFORE COMPLETING FORM
1. REPORT NUMBER: USAAMRDL-TR-76-9	2. GOVT ACCESSION NO. / 3. RECIPIENT'S CATALOG NUMBER
4. TITLE (and Subtitle): Development Program for Field-Repairable/ Expendable Main Rotor Blades	5. TYPE OF REPORT & PERIOD COVERED: Final Report
	6. PERFORMING ORG. REPORT NUMBER: R-1387
7. AUTHOR(s): J. E. Miller, T. N. Cook	8. CONTRACT OR GRANT NUMBER(s): DAAJ02-73-C-0006
9. PERFORMING ORGANIZATION NAME AND ADDRESS: Kaman Aerospace Corporation, Old Windsor Road, Bloomfield, Connecticut 06002	10. PROGRAM ELEMENT, PROJECT, TASK AREA & WORK UNIT NUMBERS: 63209A 1F163209DB38 00 011 EK
11. CONTROLLING OFFICE NAME AND ADDRESS: Eustis Directorate, U. S. Army Air Mobility R & D Laboratory, Fort Eustis, Virginia 23604	12. REPORT DATE: September 1976 / 13. NUMBER OF PAGES: 274
14. MONITORING AGENCY NAME & ADDRESS(if different from Controlling Office)	15. SECURITY CLASS. (of this report): Unclassified / 15a. DECLASSIFICATION/DOWNGRADING SCHEDULE
16. DISTRIBUTION STATEMENT (of this Report): Approved for public release; distribution unlimited.	
17. DISTRIBUTION STATEMENT (of the abstract entered in Block 20, if different from Report)	
18. SUPPLEMENTARY NOTES	
19. KEY WORDS (Continue on reverse side if necessary and identify by block number): Blade, Main Rotor, Helicopter, Expendable, Field-Repairable, Repair Costs, Reliability, Maintainability	
20. ABSTRACT (Continue on reverse side if necessary and identify by block number): This report details the work completed in designing and developing a main rotor blade for the UH-1D/H helicopter which would reduce the Army's blade-related helicopter costs. This cost reduction results from designing a blade with high repairability to reduce damage-related repair and scrappage costs, high survivability so that required repairs are minimized and low production cost so that the blade could be economically discarded in case of severe damage.	

DD FORM 1 JAN 73 1473 EDITION OF 1 NOV 65 IS OBSOLETE

404 307

UNCLASSIFIED

SECURITY CLASSIFICATION OF THIS PAGE (When Data Entered)

BLOCK 20:

The program was unique in that reliability and maintainability personnel had inputs to the designs from their inception in the comparison of candidate designs and the selection of the final design concept. A maintenance philosophy was developed for the blade, and the repair techniques developed were proven to be easy to apply, and structurally sound during fatigue and whirl testing. Thus, the blade was shown to be repairable after extensive damage, and the repairs required less time than is normally required for blade removal and replacement.

During the design of the blade, components were evaluated for their durability under the extremes of the Army's operating environment prior to their incorporation into the final design concept, and the design was analyzed and projected to be no less durable than the present UH-1D/H blade.

The survivability, acquisition cost, repair cost, and replacement costs were all used to predict the life-cycle costs of the new blade in comparison to that already in use. This comparison showed that a substantial cost saving could accrue to the Army as a result of employing this new design philosophy on helicopter blade acquisitions.

PREFACE

The Field Repairable/Expendable Main Rotor Blade Development Program was performed under Contract DAAJ02-73-C-0006 with the Eustis Directorate, U. S. Army Air Mobility Research and Development Laboratory, Fort Eustis, Virginia, and under the general technical cognizance of Mr. Arthur J. Gustafson, of the Structures Area; Messrs. Royace H. Prather and J. H. McGarvey, Reliability and Subsystems Area; and Messrs T. L. House and J. W. Sobczak of the Reliability and Maintainability Area.

The authors acknowledge the contributions made by Messrs. J. Carver (Rockwell International, Tulsa); S. Barlow and J. Wynkoop (Adhesive Engineering, Airline Systems Division); and W. A. Alex, G. P. Basile, A. Belbruno, M. A. Bowes, J. E. Fitzpatrick, M. C. Frengley, P. F. Maloney, D. Ojantakanan, H. Pelletier, M. Powers, W. A. Smyth, W. Spurr, F. E. Starses, M. White, E. Wilk and R. L. Young, and many other members of the Kaman Aerospace Corporation staff.

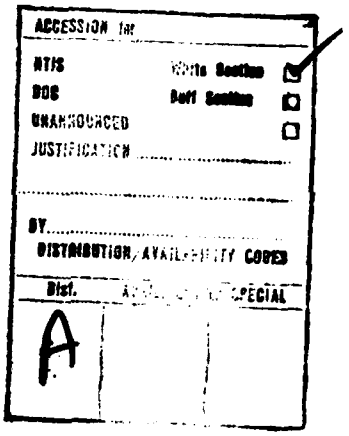

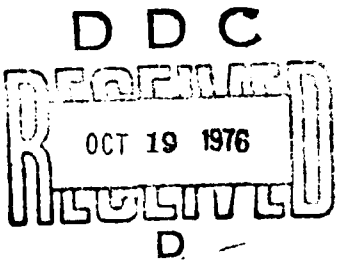

TABLE OF CONTENTS

TABLE OF CONTENTS (continued)

LIST OF ILLUSTRATIONS

LIST OF ILLUSTRATIONS (continued)

LIST OF ILLUSTRATIONS (continued)

LIST OF ILLUSTRATIONS (continued)

LIST OF ILLUSTRATIONS (continued)

LIST OF ILLUSTRATIONS (continued)

LIST OF TABLES

LIST OF TABLES (continued)

LIST OF TABLES (continued)

LIST OF TABLES (continued)

INTRODUCTION

The high cost of maintaining helicopter rotor blades in the field can be traced to several factors. The critical nature of the application, combined with the generally poor reliability these components experience, contributes heavily to high cost. Subject to severe operating and environmental stresses and vulnerable to handling and foreign object damage, rotor blades suffer high failure rates; few survive to complete their fatigue-limited operating life. The problem of poor reliability is magnified by the very limited repairability of present-day rotor blades. Many types of damage are not repairable at all, resulting in high scrap rates and blade replenishment costs. Blade repair is rarely capable of being performed in the field, and this necessitates removal and shipment of the blade to higher maintenance levels, usually a depot. This results in excessive aircraft downtime for maintenance and supply, and incurs heavy costs in packaging, transportation and depot repair. Many blades are damaged, or corroded, in transit and arrive at the depot only to be scrapped. Overall, poor reliability and the inability to repair rotor blades in the field have contributed, very substantially, to the operating costs of helicopters.

In the several exploratory Army R&D programs leading to development of the Field Repairable/Expendable Blade (FREB), the Army investigated various approaches to lowering rotor blade life-cycle costs. One program examined design and fabrication techniques aimed at making rotor blades highly repairable in the field, with the intent of lowering scrap rates and depot maintenance costs. Another studied the feasibility of an expendable rotor blade design, one whose acquisition cost was sufficiently low that damage beyond minor field repair would justify scrapping the blade. In seeking the benefits of improved repairability and economic expendability, these programs sought to equal or improve upon the reliability of existing rotor blades without suffering unacceptable degradation in blade performance.

The results of the conceptual design studies, while demonstrating that definite benefits were achievable in the design of rotor blades, indicated that neither the repairability concept nor the expendability concept, alone, provided the optimum solution and that the most cost-effective approach would be achieved from a mix of both attributes. This led to the concept of the FREB program.

The program had two major objectives. The first was to design and develop a main rotor blade for the UH-1D/H helicopter possessing improved life-cycle cost characteristics over those of

the existing blade, without degrading safety, performance or flying qualities. Life-cycle cost reductions were to be sought in both manufacture and support. The second objective was to develop improvements in the definition and specification of design requirements which could be used as a model for future blade development programs.

The approach to meeting these objectives involved, first, a comprehensive review and analysis of the twenty-six blade design concepts evolved from earlier programs. Trade-off analyses were conducted to establish the optimum mix of design characteristics (materials, fabrication techniques, reliability, repairability, etc.) from the standpoint of minimizing the total life-cycle costs of the blade. Together with other technical requirements for the blade, such as strength, stiffness and weight, these goals were incorporated into a specification for design.

Following these initial concept analyses, the six most promising concepts were chosen for in-depth evaluation. Maintenance methods were proposed and life-cycle cost predictions were made for each concept. This information, when added to stress and aeroelastic analyses, allowed selection of a design concept with an extruded spar and spline and a composite afterbody as that most likely to meet program objectives.

The maintenance methodology was further developed and tested on both blades and blade sections, following detail design and blade fabrication. A maintainability demonstration was conducted which proved the blade's maintainability under simulated field conditions. Both repairs of relatively deep metal damage and replacement of substantial portions of afterbody were demonstrated under simulated field conditions. Static, fatigue and whirl testing of undamaged, damaged and repaired blades and blade components confirmed earlier predictions of blade repairability and life, building confidence in earlier projections of blade life-cycle costs.

It was concluded that a blade designed around maintainability requirements could be built for the UH-1D/H helicopter, and such a blade would produce substantial savings in blade-related helicopter life-cycle costs.

DESIGN SPECIFICATION

The method chosen for integration of the maintainability requirements into the other design requirements for the FREB was the compilation of a design specification which enumerated both the normal design and performance requirements and the reliability and maintainability requirements which would best serve the overall program objectives.

In addition to the maintainability requirements given in the Design Specification (Appendix A), other requirements relating to performance, UH-1H system capability, aerodynamic and aeroelastic system compatibility, blade strength, and blade radar and acoustic detectability were included. All the candidate concepts were screened with respect to all of the items in the Design Specification, and only those which had high probability of specification conformity were examined more closely during the concept selection phase of the program.

Adherence to the items at the beginning of the Design Specification insures that the blade will not adversely affect the life or structural integrity of any of the existing UH-1H components. The requirements for weight, balance, center of gravity, dynamic mass axis location and rotor inertia were all intended to maintain aeroelastic stability at least equal to that of the present blade. The weight and balance requirements eliminated several design candidates, as will be discussed later in this report. A rather thorough treatment of blade internal components and structure was intended to insure that the blade has sufficient structural integrity to remain serviceable throughout its fatigue life, thus eliminating blade overhaul expenses. The requirements for radar and acoustic detectability acted against design concepts with high percentages of metallic components and also against those designs which adversely affected the rotor's acoustic characteristics through airfoil deviations from the present blade's NACA 0012 airfoil with 21.0 inch chord.

RELIABILITY AND MAINTAINABILITY

The life-cycle costs of helicopter rotor blades are very much related to their reliability (resistance to failure and damage) and their maintainability (ability to be repaired). Deficiencies in these two areas have been one of the principal causes of the cost problems of the past. It was necessary, therefore, in establishing requirements for design of the FREB, to insure that R&M goals were among the priority considerations. The contractor's prior work in the study of repairable and expendable blade concepts (Contracts DAAJ02-70-C-0070 and DAAJ02-71-C-0041) established a framework for developing the R&M requirements.

FAILURE MODES AND RATES

While the thrust of the R&M effort was to improve field repairability in design of the FREB, reliability also received heavy emphasis. Life-cycle cost reductions would be achieved if blades could be made more repairable in the field, but not if blade reliability were seriously compromised in the process. Any increase in the frequency of failure would tend to nullify the benefit of improved repairability.

Among the reliability objectives for the FREB was the desire to eliminate failure modes which have historically contributed to the high incidence of blade removal and scrap. In some cases, this would be accomplished through changes in materials and methods of construction. In others, the failure mode might not be eliminated entirely in the FREB design, but would be made less serious in effect through the ability to repair.

Also sought in the design were materials and construction features that would make the FREB more inherently reliable and resistant to external damage than the blades presently used. The use of composite materials with their inherent resiliency and low notch sensitivity held promise in this regard. Safety, also stressed in the design, was pursued through such features as structural redundancy, alternate load paths, and materials with low crack propagation rates. In seeking to avoid the reliability problems of prior blade designs, great care would be needed to insure that no new failure modes, particularly critical ones, were introduced in the FREB design.

REPAIRABILITY CRITERIA

A major improvement in field repairability was foremost among the FREB design goals. It was recognized that real improvements in repairability would only be brought about, however, if

repairs could be accomplished on the installed rotor blade. Repairs that require removal of the blade from the helicopter are undesirable since the repair task becomes more difficult than replacing and scrapping the damaged blade. Despite policies to the contrary, experience has shown that maintenance personnel tend to take the most expedient route to restoring aircraft readiness, particularly under the stress of field operations. This being the case, repair of rotor blades would be undertaken, primarily, when blade replacement became a more difficult and time-consuming alternative.

Guidelines for developing the blade maintenance concepts and repair techniques were established by the Army. All maintenance was to be performed at the using unit level. The number of different repair kits and special tools were to be kept to a minimum, consistent with the goal of maximum field repairability, and their use was to be adapted to the skill level of a UH-1 helicopter repairman, MOS 67N20. Cure time for adhesives and fillers would have to be of such duration as to allow repairs to be made within the time goals specified.

Repair Time Goal

Only one quantitative repair time goal was specified by the Army: a 95th percentile maximum repair time of 3 elapsed hours. This was to include the tasks of locating, isolating and correcting the fault (including any adhesive curing time), and placing the aircraft in an operational status. A maximum of two helicopter repairmen was to be required for any one repair task.

Data supplied by the Army, with the contract work statement, listed an average removal and installation time for the UH-1 main rotor blade of 7.5 man-hours (3.75 elapsed hours, assuming two men for the task). This required that a qualification be placed on the maximum repair time requirement. In developing concepts for the FREB design, the ratio of blade repairability to expendability would be dictated by the cost effectiveness characteristics of various design approaches, moving in the direction of expendability as the cost of scrapping the blade became less than that of repair. Obviously, the selected concept might, conceivably, be a nearly expendable rotor blade, one whose cost of fabrication was so low that scrapping the blade would be economically justified whenever damage exceeded minor surface repair. With an expendable rotor blade, the maintenance task, in the event of damage or failure, is to replace the blade. But this task alone would exceed the 95th percentile corrective maintenance time specified by the Army.

Since it was not within the scope of the contract to improve the design of the blade installation, there was no opportunity

for reducing blade replacement time other than to, perhaps, facilitate the balancing and tracking tasks to some degree. It might be possible to recommend improvements in the maintenance procedures associated with blade replacement, although the possibilities here were very remote in view of the Army's long experience with the UH-1 aircraft. It was reasonable to conclude, therefore, that the time required to remove and install the rotor blade should be accounted for in the maximum repair time requirements only when removal would be required to effect an off-aircraft repair. In cases where the blade was to be scrapped, replacement time would be accounted for only in the cost analysis.

One other qualification of the 3-hour 95th percentile repair time was necessary. The 3-hour goal could be attained, realistically, only if painting time were excluded, since the time required to apply primer and lacquer, allowing for drying, would alone exceed 3 hours. If the 3-hour requirement was intended to place a limit on the time required to restore the aircraft to operational readiness, after having sustained blade damage, excluding painting time was reasonable, since the aircraft would be safely flyable without paint. (The painting operation could await the next scheduled downing of the aircraft.) Attempting to improve existing paint systems in order to meet the 3-hour requirement would be far beyond the scope of the program.

TRADE-OFF CONSIDERATIONS

The process of identifying and evaluating design concepts for the FREB would involve a large number of trade-offs in such areas as material selection, manufacturing methods and repairability. Within the R&M area itself, several trade-off possibilities were apparent.

Expendability/Repairability Trade-off

The FREB, as already brought out, had as its ultimate design objective the attainment of the lowest possible life-cycle costs consistent with other technical constraints. The degree of blade repairability desired would be decided on the basis of the cost of repair, including the cost of providing the logistics resources, versus the cost of scrapping blades when a given level of damage had been exceeded. This suggested that design for expendability should be pursued when the alternative was an involved and costly off-aircraft repair. Conversely, repairability would be the preferred approach when the repair lent itself to a relatively simple, quickly performed task on the installed rotor. Economic considerations would not permit rigid adherence to this philosophy in every instance, however. The ultimate aim was to provide the best overall cost effectiveness, and the maintenance policy would have to satisfy that objective.

Reliability/Repair Time Trade-off

In terms of achieving the Army's one quantitative maintainability goal for the FREB, the 95th percentile maximum repair time, only two factors assumed importance: the mix of repair tasks and their relative frequency. The absolute frequency of repair was not really pertinent since it would be possible to obtain the same repair time distribution at entirely different levels of overall blade reliability. The reliability characteristics of the blade would become important only insofar as they affected the distribution of tasks; i.e., made certain tasks occur more or less frequently in relation to the overall population of repair tasks. A reliability/repair time trade-off would be required when the blade design characteristics were such that an involved repair task occurred too frequently. The decision here would be to increase the reliability (or reduce the vulnerability) of the blade in that area so as to reduce the frequency of that task or to design to make the task easier to perform. Overall reliability/maintainability relationships would be of major importance, moreover, in the analysis of blade life-cycle costs.

Mean/Maximum Repair Time Trade-off

The Army's one quantitative maintainability goal, the maximum repair time, allowed considerable flexibility in the design of the FREB and its associated repair system. It was seen that the maximum repair time could be controlled, both in terms of the average task duration and the variability in task performance. A larger mean task time could be tolerated if the variance in task performance could be kept small. With a fixed maximum repair time, the expected variance would define the mean repair time.

Figure 1 shows the area of trade-off between the mean repair time (MTTR) and the variance for a log normal repair time distribution at 95th percentile repair times (M_{max}) of 3 hours, 2 hours and 1 hour. (Rationale for selection of a log normal distribution of repair times is discussed in Reference 1.) MTTR and the geometric mean repair time, $\bar{t}_g$, are shown plotted against the standard deviation of the distributed repair times. The area under the MTTR curves is the mean/variance trade-off area, with the shaded area representing the range of realistic alternatives. Also shown on the figure is a plot of the standard deviation as a function of the MTTR based on a regression equation developed by Kaman for use in maintainability predictions. (The equation and its derivation are also described in Reference 1.) The portion of this curve which intersects the potential trade-off area was viewed as the region of most likely mean/variance combinations, based on past history.

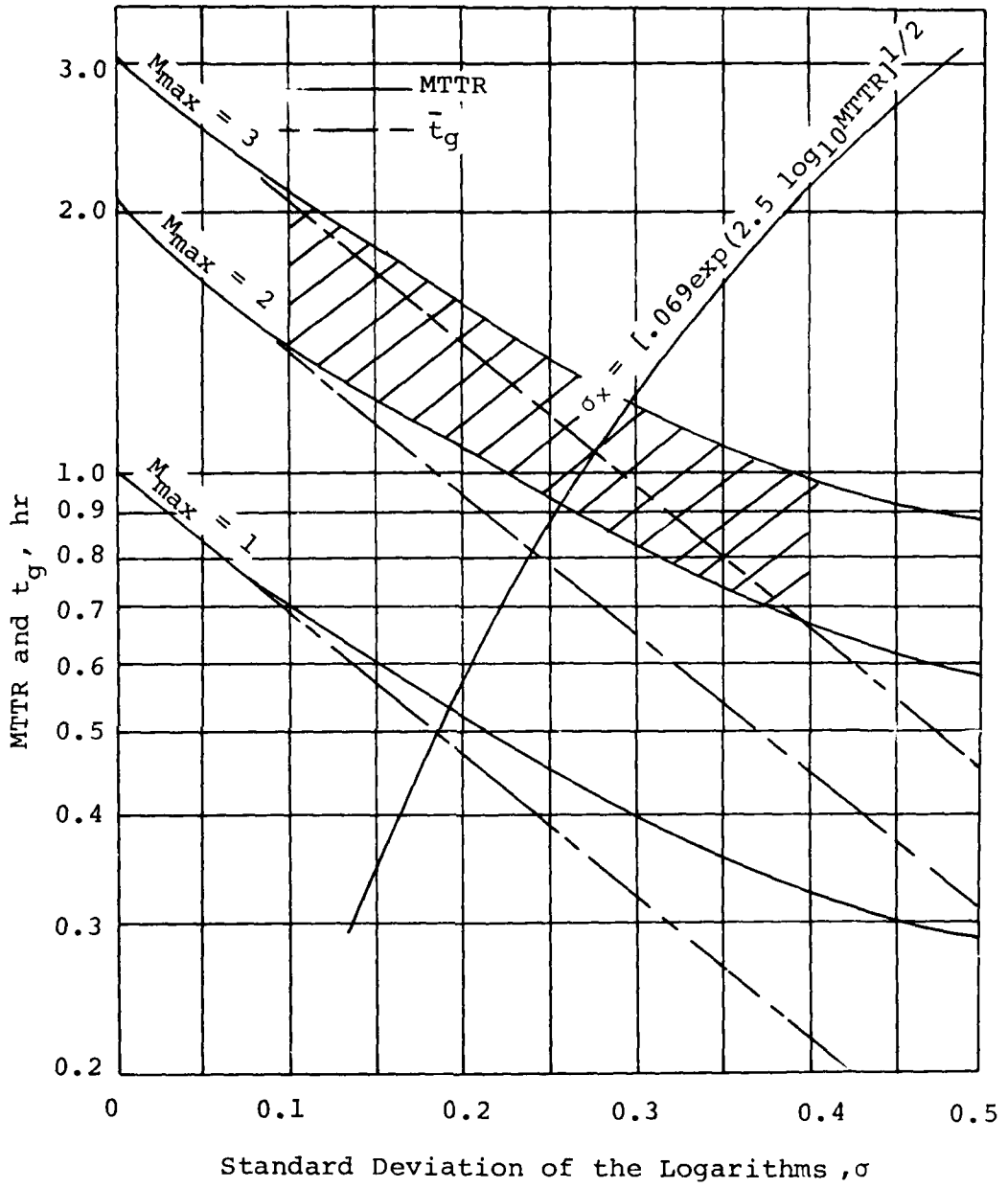

Figure 1. Maintainability Trade-Offs.

LIFE-CYCLE COST PREDICTION

Ordinarily, the objectives of a blade development program are limited to performance, fatigue life, acquisition cost, stability and weight considerations. Experience with the present UH-1H blade, however, shows that the blades are normally removed because of inherent or external (including combat) damage before they approach their fatigue life. This premature removal has substantial cost repercussions in the form of increased aircraft downtime and increased spares requirements. By properly integrating reliability and maintainability requirements into the FREB program at the design phase, overall blade-related life-cycle costs could be reduced by extending average blade life, decreasing aircraft downtime and decreasing spares requirements.

In order to optimize all of the parameters which could decrease blade-related helicopter life-cycle costs, it was necessary to develop a method for predicting these costs that could be used to evaluate tradeoffs as they came up within the program.

Two time-sharing computer programs were developed to fill this need. The first program merely recorded all of the failure modes projected for the blade, their frequency of occurrence, and repair requirements. This program allowed evaluation of overall MTBFs and repair time, and comparison of the effect on these parameters of elimination of certain failure modes or improvements in repair time. The second and more useful program was a life-cycle cost model which allowed studies of life-cycle cost sensitivity to initial blade cost, MTBF, repairability, repair time, etc. This program uses the flow chart given in Figure 2 to predict blade-related aircraft life-cycle costs.

This approach of real-time evaluation of cost parameters allowed the various candidate designs to be compared in terms of their reliability and maintainability, and its effect on overall blade-related helicopter life-cycle costs. This relative measure of each blade's cost effectiveness was then used in the selection of the final design concept. This concept's repairability could then be optimized, again by studying trade-offs by use of the life-cycle cost program.

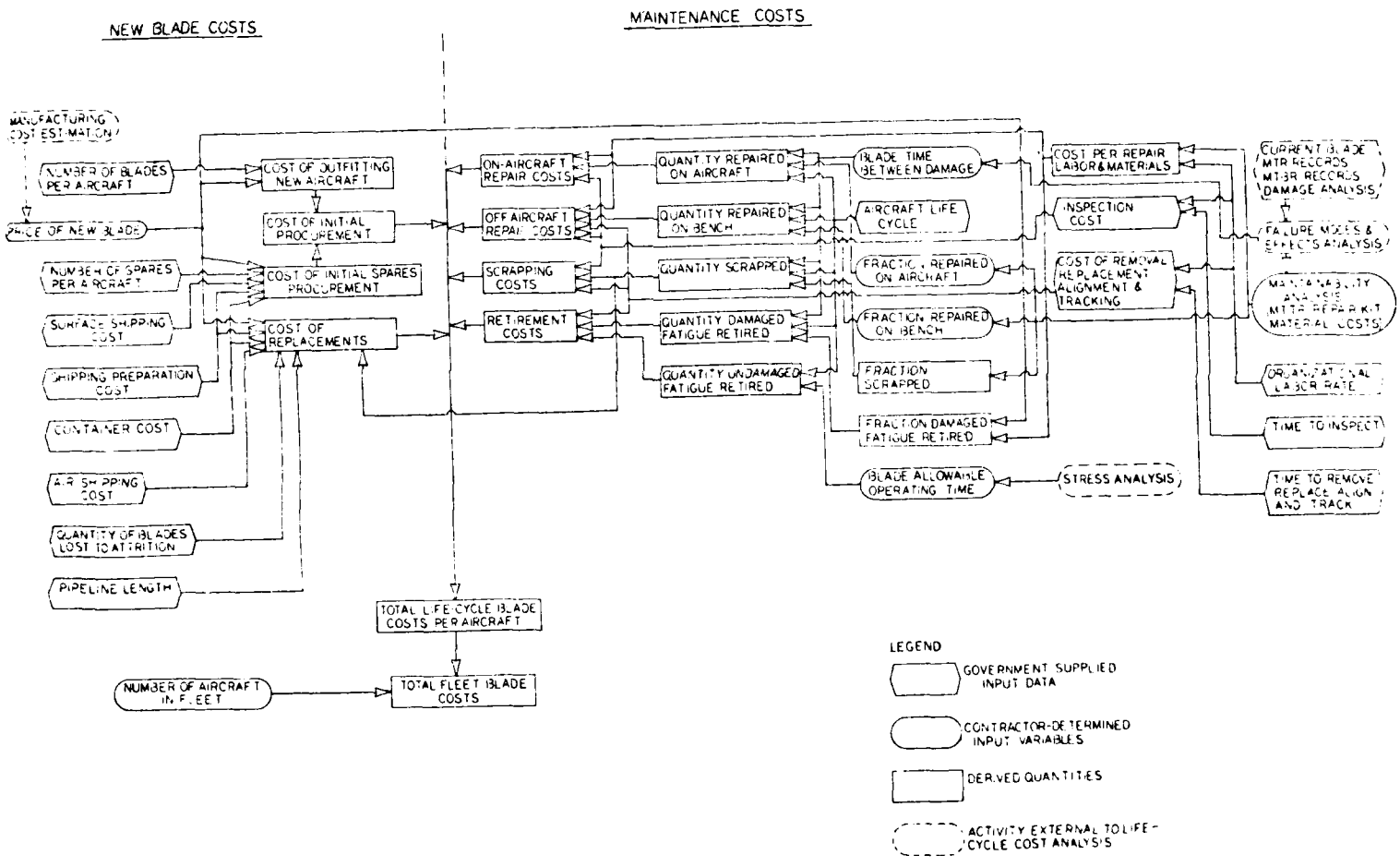

Figure 2. Life-Cycle Cost Model Flow Chart.

PRELIMINARY DESIGN

EVALUATION OF DESIGN CONCEPTS

At the beginning of the program, twenty-six candidate design concepts were listed on the basis of all rotor blade fabrication methods which may be able to meet program goals (see Table 1). Several concepts were very similar except for detail changes, and all had either a material choice which forced certain fabrication methods, or a fabrication method which forced a material choice.

Materials possibilities for spars were extruded or formed metals, filament wound, mold formed or pultruded glass fiber reinforced plastic (GFRP), and wood. Metal spars have the bearing strength necessary for root and tip weight attachment, while both wood and GFRP require local reinforcement to provide the required attachment points. Wood, in addition, is hydroscopic and as such requires very effective sealing. Woods vary considerably in strength and density, even within the same species. These problems, as well as the decreasing availability of aircraft-quality lumber, make wood an undesirable choice for rotor blades. Glass-fiber reinforced plastic spars require fiber orientation at an angle to the spar axis to provide the required spar torsional stiffness. The efficiency of these transverse fibers in providing spar spanwise stiffness decreases as the efficiency of providing torsional stiffness increases, as shown in Figure 3, thus detracting from one of the normal benefits of GFRP components. Although this problem could have been minimized by the use of high modulus fibers, at the time of the original studies the additional expense was not justified in light of the program's emphasis on low blade acquisition cost. In addition, the exposed surface of an all-GFRP spar would have required some form of erosion protection.

Metal spars, similar to those presently used in helicopter blades, offer adequate shear and bearing strengths for the FREB application, but they reflect radar energy in a manner that may prove to be detrimental in a combat environment. In addition, metal spars reduce the possibility of spar repair. This problem can be reduced by use of a titanium spar of minimum chordal dimension, but again this method entails substantial extra cost. Metal spars have the advantage of being usable without abrasion protection, due to abrasion resistance superior to that in all GFRP unprotected spars.

The skins of a rotor blade should ideally be light. This would favorably affect chordal balance and tend to decrease reliance upon the skins for structure, thus increasing skin repair latitude. Light aluminum skins, as used on the present UH-1H blade,

TABLE 1. DESIGN CONCEPTS FOR PRELIMINARY EVALUATION

	DESIGN CONCEPT	COMMENTS
a.	One-piece extruded aluminum alloy spar, glass-fiber-reinforced aft skins, aluminum honeycomb aft core, and extruded aluminum alloy trailing-edge spline (Reference 2, Configuration V).	This concept is a compromise arrived at in the design study of Reference 2, and it represents the most cost-effective approach to a repairable blade.
b.	Glass-fiber-reinforced aft skins but otherwise unchanged from the current UH-1H blade (Reference 2, Configuration I).	The best feature of this concept, the reinforced plastic aft skins, was incorporated in (a).
C.	Narrow chord titanium spar, glass-fiber-reinforced-plastic aft skins, titanium spline (Reference 2, Configuration II).	The titanium spar increases the repairable area, but it adds unacceptably to the cost.
d.	One-piece extruded aluminum alloy spar with integral root buildup, glass-fiber aft skins, aluminum alloy spline (Reference 2, Configuration III).	This concept has characteristics similar to those of (a), but the stepped extrusion providing the root end integral with the spar is more expensive than the laminated buildup.
e.	Unidirectional glass-fiber-reinforced-plastic spar and spline, glass-fiber aft skins (Reference 2, Configuration IV).	At the time of these studies, a composite spar would have been relatively costly. In addition, adequate torsional stiffness would have been difficult to achieve.
f.	All-aluminum alloy blade with one-piece extruded spar (Reference 3, Design 1).	This concept is the least expensive of the expendable blades, but the aft section is neither damage resistant nor very repairable.
g.	Stretch-formed stainless-steel sheet three-piece spar, drawn stainless-steel nose ballast, glass-fiber-reinforced aft skins, polyamide paper honeycomb aft core, unidirectional glass-fiber-reinforced-plastic spline (Reference 3, Design 2).	This blade concept gave the lowest life-cycle costs of the four studied in Reference 3, but subsequent study showed that the stainles-steel spar was priced unrealistically low and that the basic advantages lie with the repairability of the aft section, although the rugged spar is a contributor.
h.	One-piece extruded aluminum alloy spar, glass-fiber-reinforced-plastic aft skins, sheet aluminum shear web on chord plane, polyamide paper aft cores, extruded aluminum spline (Reference 3, Design 3).	The chord-plane shear web is attractive because of its anticipated reduced vulnerability. However, the extra pair of glue lines and the third sheet of material mean that the external skins have to be very light to maintain section balance. Through damage is unrepairable.

TABLE 1. – CONTINUED

DESIGN CONCEPT	COMMENTS
i. Extruded aluminum alloy spar, extruded aluminum alloy aft section (Reference 3, Design 4).	The thin-walled extruded aft section is extremely expensive, if not impossible to obtain.
j. Aft fairing sectionalized into short, bolted-on boxes, but otherwise changed only as necessary from the current UH-1H blade (Reference 4, Figure 14).	In common with the other sectionalized blades, the necessity for providing a solid trailing-edge spline, for in-plane stiffness, forces the cost of the removable aft section pockets and the accompanying fastener provisions to go so high that the concept is not cost-effective.
k. Sectionalized glass-fiber-reinforced-plastic spar, bolted removable leading-edge member (Reference 4, Figure 14).	Again, the sectionalized approach is not cost-effective, and the all-glass-fiber-reinforced-plastic construction may give difficulty in meeting dynamic requirements.
l. Four-component bolted spar with sectionalized aft fairing (Reference 4, Figure 16).	This concept was abandoned from the study in Reference 4 because of its complexity.
m. Wraparound steel tube spar with sectionalized aft fairing (Reference 4, Figure 17).	In addition to the inherent disadvantage of the sectionalized approach, a seamless tube more than twice the length of the blade is currently impractical.
n. Extruded aluminum spar, bolted removable leading edge sections, sectionalized aft fairings bolted in place (Reference 4, Figure 18).	Although simplified from (j), this version of the sectionalized blade is not cost-effective.
o. As (n), but sectionalized aft fairings bonded in place (Reference 4, Figure 19).	Using bonded attachments, the cost and complexity of the blade are reduced, but the replaceability of the aft boxes suffers to the extent that (n) is preferred.
p. Two-piece extruded aluminum alloy spar, glass-fiber-reinforced-plastic aft skins, aluminum honeycomb core, glass-fiber-reinforced-plastic trailing-edge spline (Reference 5, Configuration I).	This concept is similar to (a), but the spar can be a one-piece extrusion to reduce cost, while the degree of repairability available at the spline does not justify the use of fiber-reinforced plastic.

TABLE 1. – CONTINUED

	DESIGN CONCEPT	COMMENTS
q.	Three-piece spar of stainless steel and aluminum sheet, aft section and spline as (p) (Reference 5, Configuration II).	The acquisition cost of the three-piece sheet-metal spar is slightly higher than that of (p), while the vulnerability and repairability remain approximately the same.
r.	Glass-fiber- and carbon-fiber-reinforced-plastic spar, aft section and spline as (p) (Reference 5, Configuration III).	The cost and torsional stiffness objections to a composite spar apply to this blade, although Reference 5 suggests that costs will become competitive by 1980.
s.	Glass-fiber- and carbon-fiber-reinforced-plastic twin-beam spar, aft section and spline as (p) (Reference 5, Configuration IV).	Again, the cost and stiffness questions do not appear to be adequately answered.
t.	Spar as (s), integrally supported carbon-fiber- and glass-fiber-reinforced-plastic aft skin produced by pultrusion process, carbon-fiber-reinforced-plastic spline (Reference 5, Configuration VI).	The pultrusion process, when fully developed, may reduce costs, while the use of high-modulus carbon fibers in the skin may provide adequate stiffness. These developments are not expected during the time frame of this program.
u.	Spar as (p), pultruded integrally supported glass-fiber-reinforced-plastic aft skins, glass-fiber-reinforced-plastic spline (Reference 5, Configuration VI).	This is similar to (p) in characteristics, and the pultruded skins may reduce costs sufficiently to offset the anticipated increase in spar extrusion costs. Again, this is a future development not ready for this program.
v.	Multispar construction utilizing a series of filament-wound glass-fiber-reinforced-plastic tubes enclosed in a filament-wound glass-fiber-reinforced-plastic skin, with other structural and mass elements in the interstices between tubes (Reference 6).	This is a very interesting concept because of its evident survivability after ballistic damage. However, the torsional stiffness is inadequate, and the design of the root retention must be complex and expensive because of the necessity for attaching a multitude of basic structural members. Through damage is probably unrepairable because almost all of the planform encloses primary structure. The unusual internal configuration would require special tools for patch procedures. The filament winding process is highly automated and inexpensive, but the costs of the root and tip must yet be defined.

TABLE 1. - CONTINUED

	DESIGN CONCEPT	COMMENT
w.	As (v), with high-modulus fiber filament-wound skins for added torsional stiffness.	The use of high-modulus organic fiber in the skins restores adequate torsional stiffness, as well as increases damage resistance. However, development of this concept has not yet progressed to a point where the basic goal of the program, that of determining reliability and maintainability design methodology, can be met with the certainty that an extensive technology development diversion can be avoided.
x.	Multicell structure formed from glass fibers or advanced fibers laid up on mandrels, loaded with resin, and cured in a mold. This type of construction can have many variations in materials used, fiber orientation, resin impregnation processes, final contour mold, and the proportion of automated procedures to manual labor.	The varieties of this concept all leave the basic torsional stiffness concern unanswered. Material costs are higher than those of aluminum, although it is possible that automatic processing can reduce fabrication costs.
y.	Combinations of metal structural members (spar and, possibly, spline) and molded reinforced-plastic contour. This hybrid construction can have as many variations as (x) above. (Reference 7 provides one example.)	The metal structural members provide hard points at root and tip, and add torsional stiffness, but the production cost adds that of the metal-forming technique to that of the fiber impregnation, layup, and cure. This may be a relatively inexpensive and reliable way to achieve advanced geometry in the near future.
z.	Various types of wooden construction, which may or may not incorporate metal or plastic.	The objections to wood in series production have been outlined above.

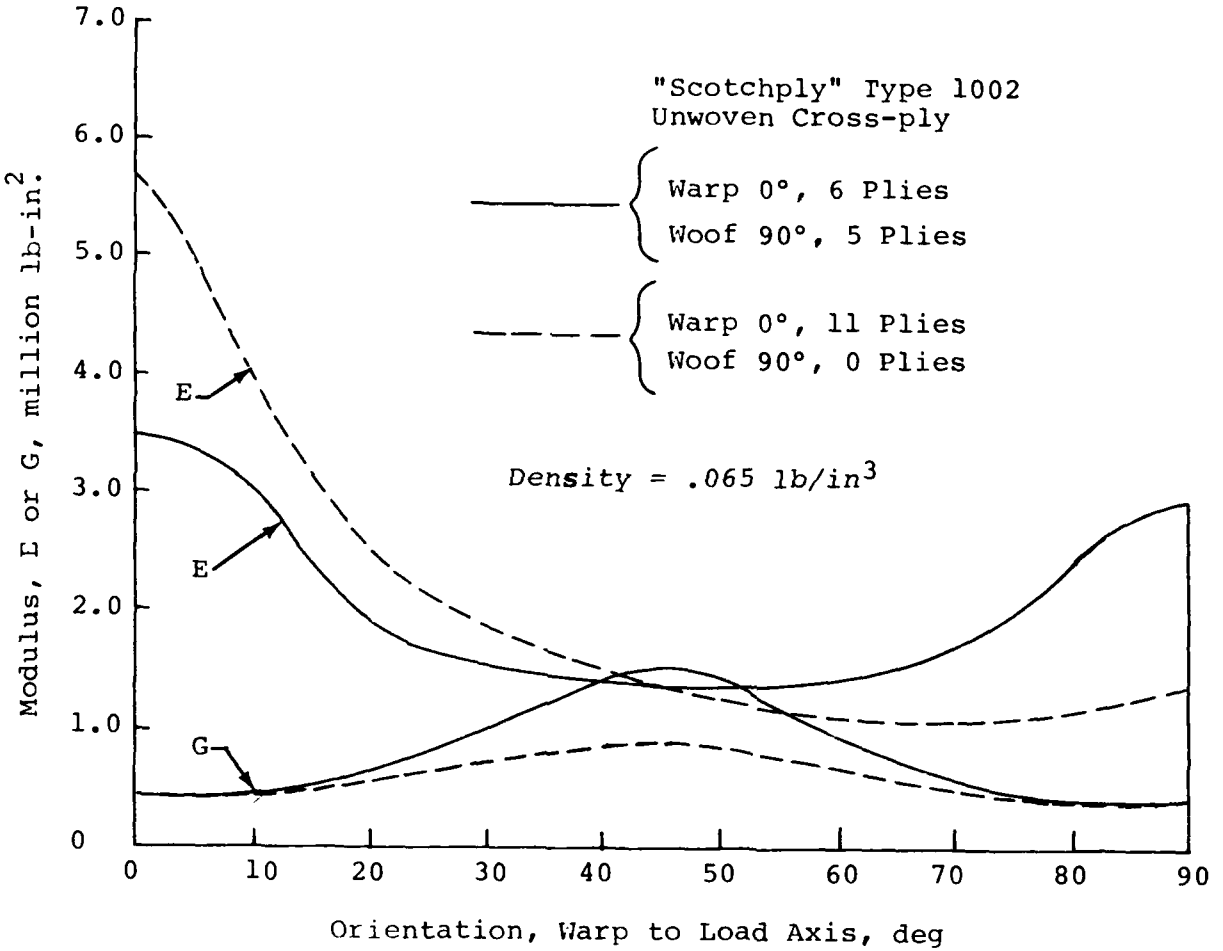

Figure 3. Modulus Variation With Fiber Orientation, Glass-Fiber-Reinforced Plastic.

are very susceptible to dents and corrosion and their attendant stress concentration factors. In addition, aluminum skins would require special treating, both before and after repair application. GFRP skins, on the other hand, can have fibers running both spanwise and at large angles to the span for shear stiffness. This crisscross of fibers actually decreases notch sensitivity by presenting high probability that crack growth will be impeded by fibers running across the crack. GFRP skins are also highly resistant to dents and almost impervious to corrosion. This last consideration would reduce required repair application and corrosion protection efforts below those required for aluminum skins. One problem with bonded composites is the change in bond strength and laminate stiffness as a function of temperature and humidity, and testing would be required to show that the properties do not deteriorate below acceptable limits for the blade's requirements before the material was incorporated into the design.

Consideration of afterbody fillers was limited to foam, balsa wood and aluminum or polyamide paper core. Balsa wood has all of the problems associated with wood, and low-density foams tend to brake up under periodic loading. Aluminum core is more susceptible to handling and induced damage, and to corrosion than polyamide paper honeycomb of the same density. In addition, a conductive blade interior not only tends to attract lightning strikes, but explosively vaporizes upon being hit by lightning, destroying the blade. Nonconductive blade afterbody fillers are far less susceptible to lightning damage. Polyamide paper honeycomb, in its lowest density, seemed to be the best choice for a repairable blade afterbody filler.

The FREB is intended to be usable on the two-bladed teetering rigid-in-plane rotor system of the UH-1H helicopter. The spline, therefore, must have sufficient structural integrity to contribute to edgewise stiffness. This member should also have thermal compatibility with the spar in order to minimize locked-in strains resulting from blade bonding. Metal spars, would, therefore, work best with either a metal spline or a high expansion fiberglass spline. A stainless steel spar could be used with a stainless steel spline, but the spline would probably taper to a planform smaller than that required for adequate skin bond. A fiberglass spline would, therefore, seem to work best with a fiberglass spar. An aluminum spline could be quite easily used with an aluminum spar. Composite spars would be used with composite splines with a possible increase in repairability, due to the fiberglass spline. Any repairability increase is small, however, because of the relatively small spline planform area.

In order to collect and concentrate the blade root loads, a doubler system is required on the FREB blade. A stiffness gradient nearly identical to that of the current UH-1H blade,

including the grip and drag pads, would have the advantage of reducing the risk that a new root end load path would have to be developed as part of the program. A doubler system could be made integral with the spar, but would greatly increase spar machining requirements. Composite spars could be bonded to a pre-machined monolithic reinforcement, or could have metal sheets bonded in during spar fabrication. Metal spars lend themselves to external doubler systems in which thin sheets are draped over the blade contour and bonded on during a "one-shot" blade final assembly. The choice of doubler system is secondary to the choice of spar material and will be made after basic component selection.

FABRICATION TECHNIQUES

Blade assembly could either be by mechanical fasteners or adhesive bonding. Mechanical fasteners lend themselves to blade repair, by removal and replacement of damaged sections, but blade operation in a fatigue environment would require very careful design and testing of any mechanical fastening system. In addition, experience with the design of other dynamically loaded components shows that an appreciable portion of program funds would have to be used in just developing mechanically fastened joints. Adhesive bonding minimizes stress concentrations at component interfaces, but limits component replacement capability. Despite this limitation, adhesive bonding is the standard industry practice, and the best available assembly technique for meeting the FREB program objectives. Forming of individual blade components is largely dependent upon material choices.

Metal spars would be formed by extrusion, rolling, or stretch-forming. Titanium and aluminum are readily and inexpensively extruded, but require an additional twisting process for torsionally stiff extrusions. Stainless steel sheet is readily formed by rolling and stretch-forming. This method could be used to produce torsionally flexible open sections which could be twisted during the final blade bonding process, at which time closed torsionally stiff sections would result from closing the sections. This type of assembly, however, has caused difficulties with such blades as the AH-1 main rotor blade.

Composite spars can be manufactured by filament winding, molding and pultrusion. Filament winding and pultrusion require less hand work and can, therefore, be less expensive than molding.

For the reasons outlined above, consideration of skin material was limited to composites, which could be made by either fabric layup or filament winding. Fabric layup is relatively simple using prepreg materials cut to shape and mated to the other blade components in a "one-shot" bond. Filament winding, on

the other hand, requires mandrels and end fittings to be made up, as well as machine running time, but results in less waste from cutting. On production runs, both methods of skin manufacture may be competitive.

Splines can be either extruded, pultruded, or hand laid-up, depending upon material. Again, the material chosen will be the primary factor in influencing the method of fabrication. An appreciable part of the blade component manufacturing costs is involved in shaping the core used to fill the afterbody. Cost reductions may result from adjusting the airfoil contour to allow for linear thickness taper in the afterbody. A simplified airfoil based on an NACA 0015 airfoil with a 16.8-inch chord extended by straight lines tangent to this surface to give a total chord of 21.0 inches could provide this cost reduction at a minimum change to airfoil performance. This simplified airfoil provides some advantages in chordwise balance, because the point of maximum thickness is moved closer to the leading edge. More volume is available in the leading edge than in that of the standard section, and the aft section is thinner.

PRELIMINARY CONCEPT SELECTION

Based upon the previously stated considerations, the twelve concepts listed in Table 2 were selected for further consideration. Representative cross sections of these concepts are given in Figures 4, 5 and 6. Concepts 1 through 6 are shown in these figures. Concepts 7 through 12 have the same basic configurations as Concepts 1 through 4, differing only in doubler makeup, skin composition, and the use of an abrasion strip. Further description of these concepts is given in Reference 1. Although the inexpensive composite materials lend themselves to relatively inexpensive fabrication techniques, the questionable torsional stiffness of composite spars eliminated them from further consideration. Glass fiber reinforced plastic skins and polyamide paper core were chosen as the best skin and afterbody filler for the reasons given above. The metal for the spars could be either stainless steel with an S-glass spline or extruded aluminum.

AISI 301 stainless steel was chosen as a spar material candidate because of favorable industry experience with this material in rotor blades. Procured in the 1/4 to 1/2 hard condition, 301 stainless is amenable to either stretch- or roll-forming. For the extruded blade components, 6061 T651 was chosen because it is readily extruded and exhibits fracture toughness, endurance strength, and erosion and corrosion resistance comparable to that of other commonly used aluminum alloys.

Cost estimates, failure predictions, maintainability estimates, repair schemes, and technical analyses were performed on the

TABLE 2. FREB CANDIDATE DESIGN CONCEPT SUMMARY

DESIGN	AIRFOIL SECTION	MATERIALS AND FORMING PROCESSES						PRICE ($)	
		ABRASION SHEATH	MAIN SPAR	AFT SKIN	AFT CORE	T E SPLINE	ROOT DOUBLERS	MID-1971	MID-1976
1	Modified 12% NACA 0012	None	6061 Al. Alloy Extruded	Glass-Fiber Reinforced Epoxy	Polyamide Paper Honeycomb	6061 Al. Alloy Extruded	2024 Al. Alloy Sheet	2,815	3,659
2								2,888	3,756
3	Modified 12% NACA 0012	None	AISI 301 St. Steel Stretch Formed	Glass-Fiber Reinforced Epoxy	Polyamide Paper Honeycomb	Unidirectional S-Glass Reinforced Epoxy	AISI 301 St. Steel Sheet	3,765	4,926
4								3,839	5,024
5	Modified 12% NACA 0012	None	AISI 301 St. Steel Roll Formed	Glass-Fiber Reinforced Epoxy	Polyamide Paper Honeycomb	Unidirectional S-Glass Reinforced Epoxy	AISI 301 St. Steel Sheet	3,581	4,666
6								3,654	4,764
7	Modified 12% NACA 0012	Strippable Polyurethane	6061 Al. Alloy Extruded	Glass-Fiber Reinforced Epoxy	Polyamide Paper Honeycomb	6061 Al. Alloy Extruded	2024 Al. Alloy Sheet	2,840	3,691
8								2,913	3,788
9	Modified 12% NACA 0012	None	6061 Al. Alloy Extruded	Glass-Fiber Reinforced Epoxy	Polyamide Paper Honeycomb	6061 Al. Alloy Extruded	AISI 301 St. Steel Sheet	2,838	3,688
10								2,911	3,785
11	Modified 12% NACA 0012	None	6061 Al. Alloy Extruded	PRD-49 Fiber Filament-Wound Reinforced Epoxy	Polyamide Paper Honeycomb	6061 Al. Alloy Extruded	2024 Al. Alloy Sheet	3,315	4,159
12								3,388	4,256
Current UH-1H Blade	NACA 0012	St. Steel & Cobalt Alloy	5-Member Steel/Al. Box Beam	2024 Al. Alloy Sheet	Aluminum Honeycomb	2014 Al. Alloy Extruded	2024 Al. Alloy Sheet	3,000	--

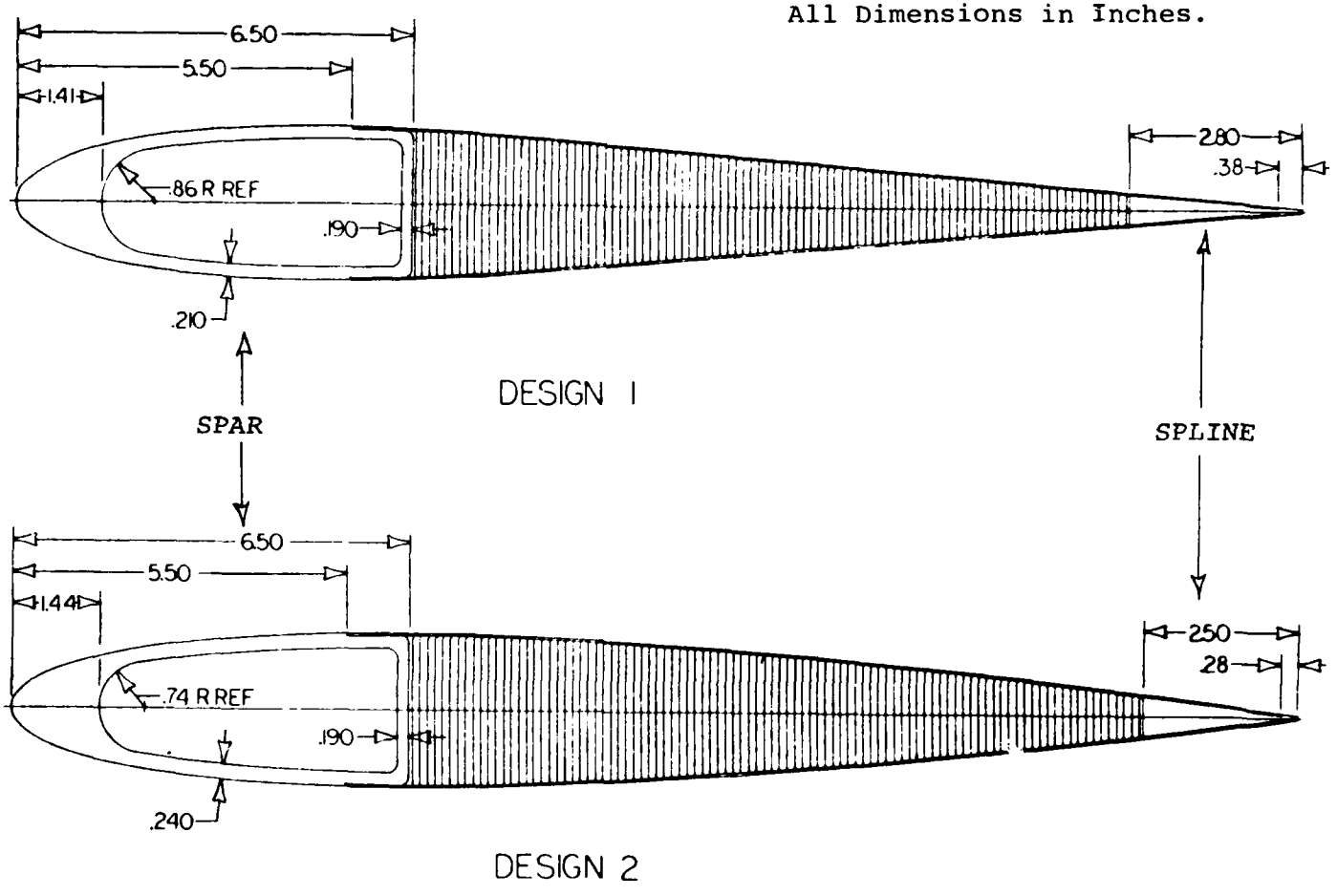

Figure 4. Cross Sections Through Concepts 1 and 2 at Station 81.

All Dimensions in Inches.

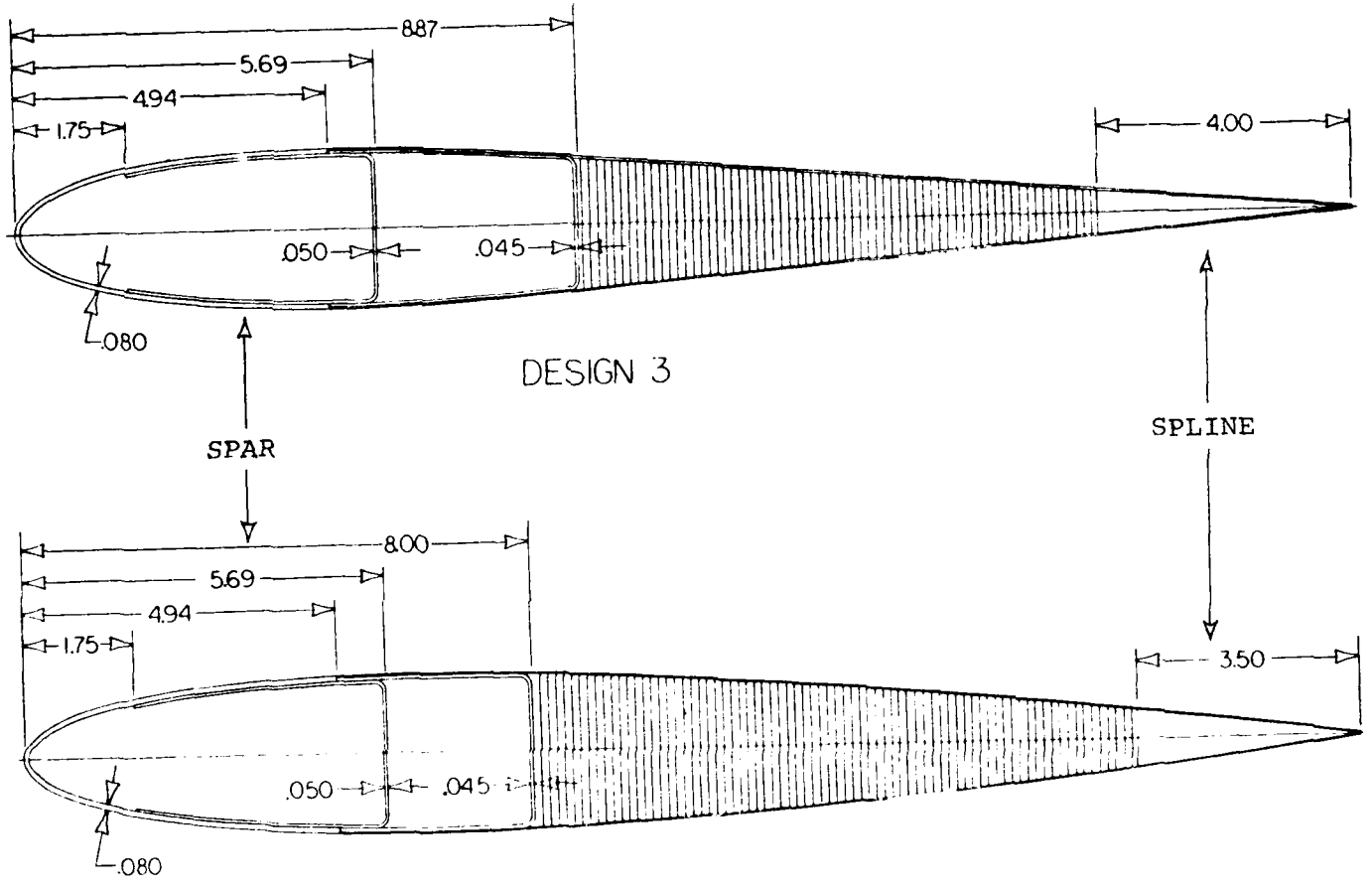

Figure 5. Cross Sections Through Concepts 3 and 4 at Station 81.

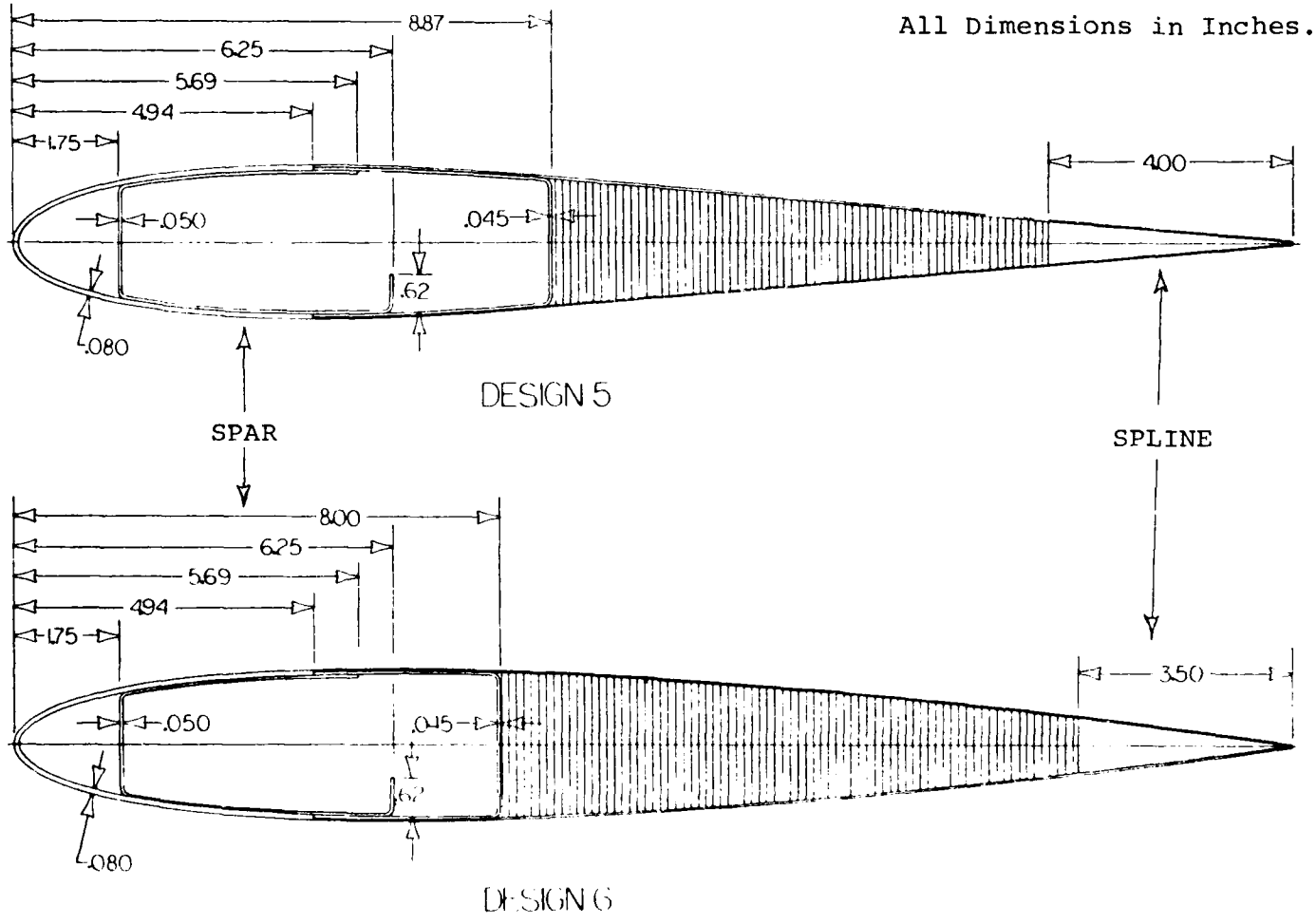

Figure 6. Cross Sections Through Concepts 5 and 6 at Station 81.

twelve concepts, taking advantage of design similarities wherever possible. The mid 1971 and mid 1976 estimated costs are given in Table 2, where the even-numbered concepts have the standard NACA 0012 airfoil presently used on the UH-1H and the odd-numbered concepts have the modified airfoil discussed elsewhere in this report.

All of the design concepts considered have structural elements that are continuous along the spar. This commonality of structure, as well as uniform weight and balance requirements on the candidate concepts, forces a high degree of similarity on the section properties and resultant bending moments and natural frequencies of the twelve concepts.

Figures 7 through 12 allow comparison of the weight properties, pertinent section parameters, natural frequencies and bending moments at 107 knots for the current UH-1H blade and for Concept 2. Table 3 summarizes the weight and balance of the six design candidates. Concept 2 is representative of the section properties for all of the candidate concepts considered. As can be seen from these plots, the present blade has a number of discontinuities. These are due to the large number of pieces from which it is made. All of the candidate concepts utilize main structural elements that extend from the root to the tip, decreasing cost and fabrication difficulty and increasing reliability by reduction of joints within the structure.

TECHNICAL ANALYSES

Design concepts 1 through 6, as well as the present UH-1 design, were analyzed with the contractor's computer programs to predict the natural frequencies, static and dynamic bending moments, and stresses at critical points on the blades.

Figures 13 and 14 give Campbell diagrams for Concept 2 and the present blade. Again, Concept 2 displayed natural frequencies representative of the twelve candidate design concepts. The in-plane and out-of-plane cantilever and out-of-plane pin end modes for Concept 2 are very close to those of the present blade, and are predicted to produce negligible change in the vibration characteristics of the UH-1 system.

Figures 15 and 16 give plots of the in- and out-of-plane dynamic bending moments predicted for Concept 2, as well as the current design. Again, there is very little change between the moment levels predicted for the present design and those for Concept 2. The 107-knot condition was chosen as representative of the UH-1 flight spectrum.

Table 4 summarizes the results of a stress analysis performed on the candidate design concepts. [illegible], where the

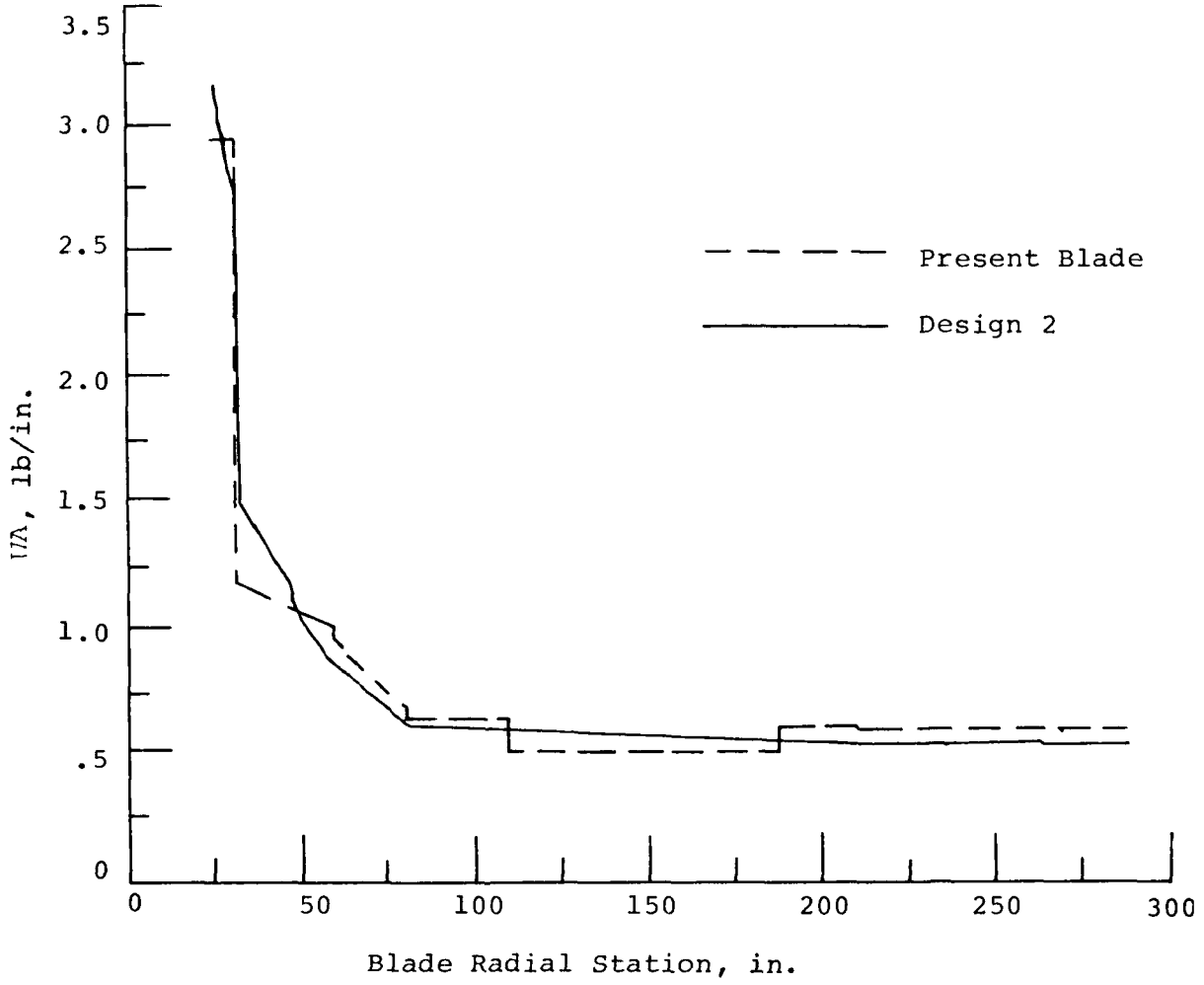

Figure 7. Concept 2, Current Blade Section Weight Distribution Comparison.

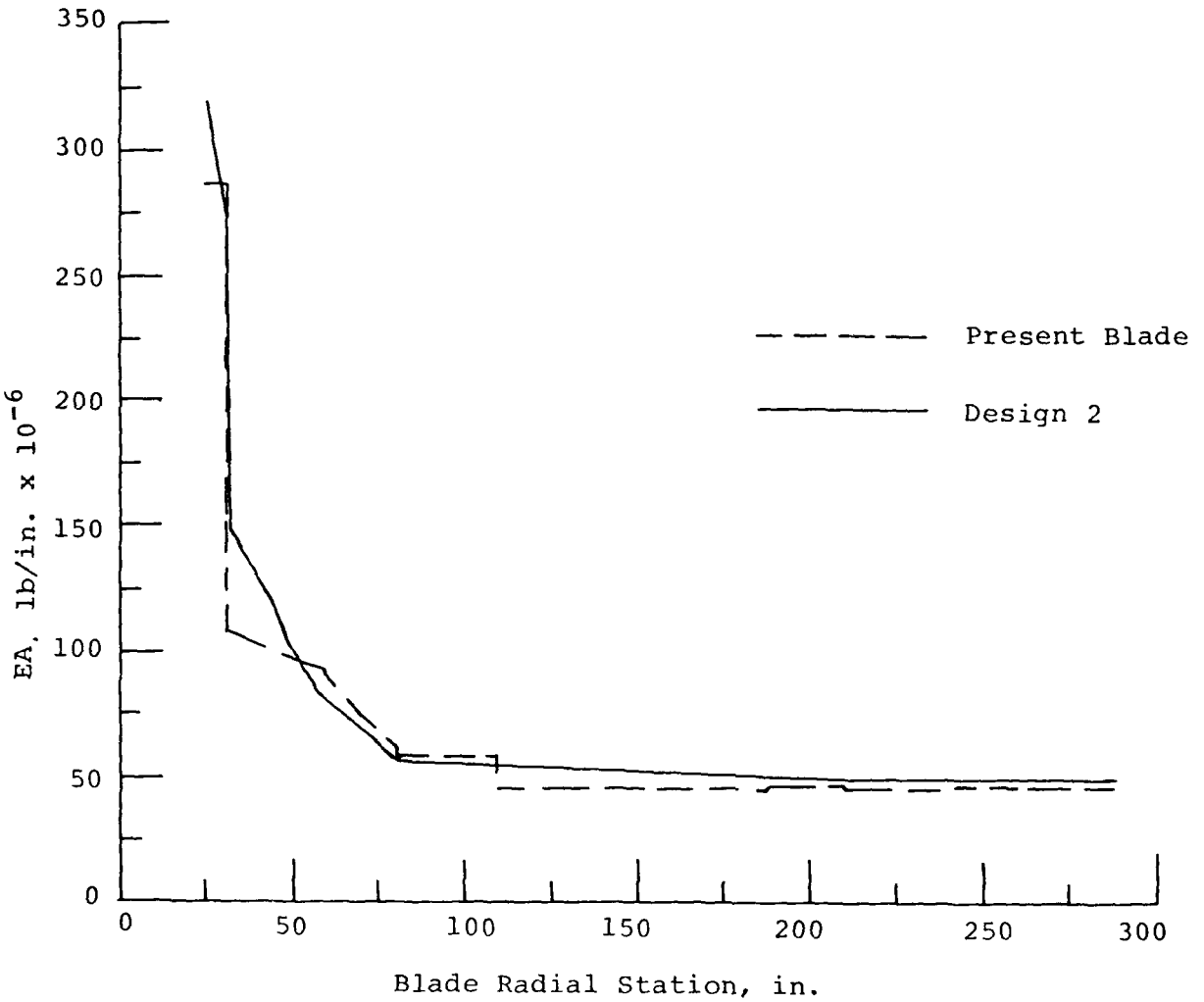

Figure 8. Concept 2, Current Blade Tensile Stiffness Distribution Comparison.

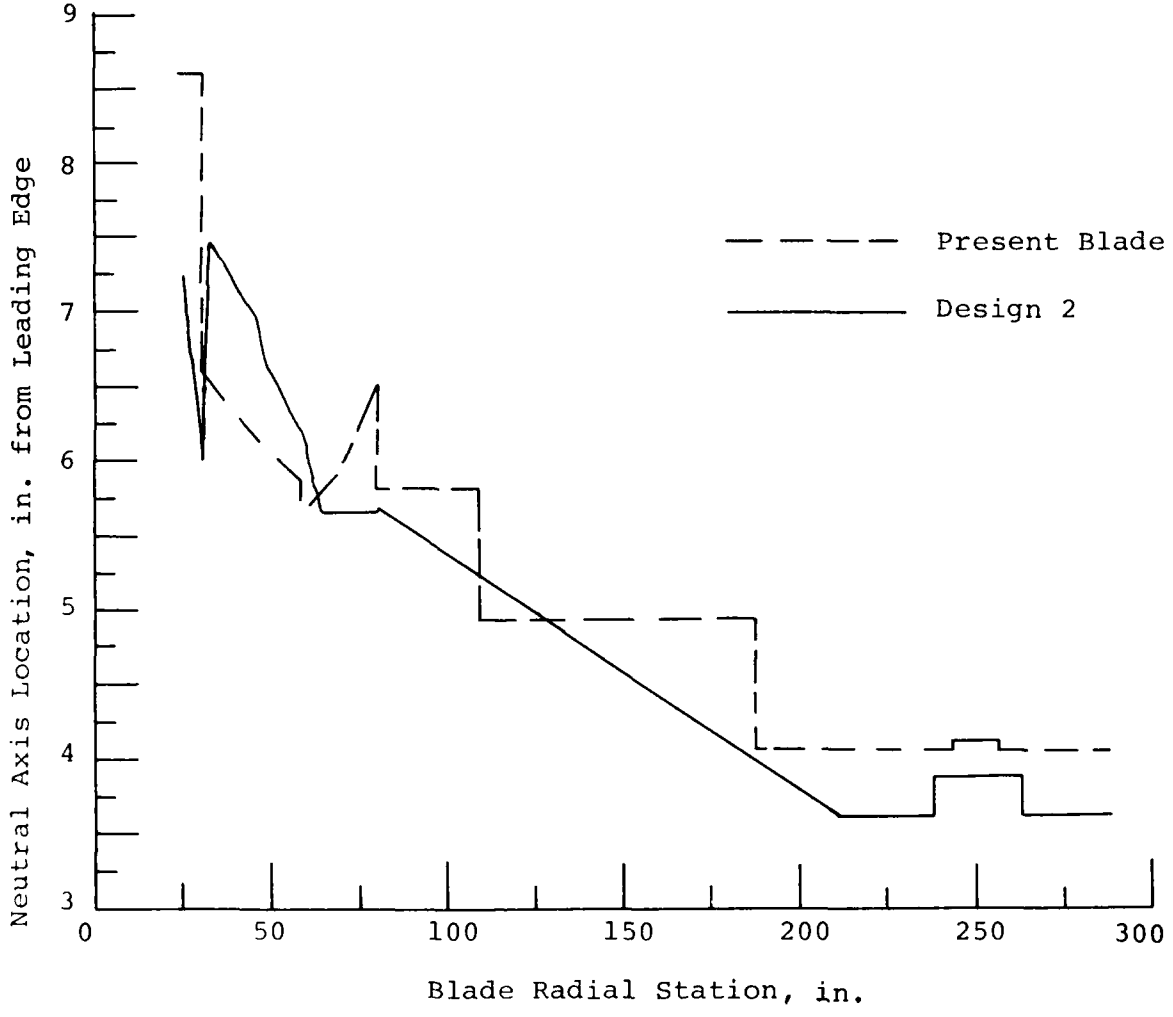

Figure 9. Concept 2, Current Blade Neutral Axis Location Distribution Comparison.

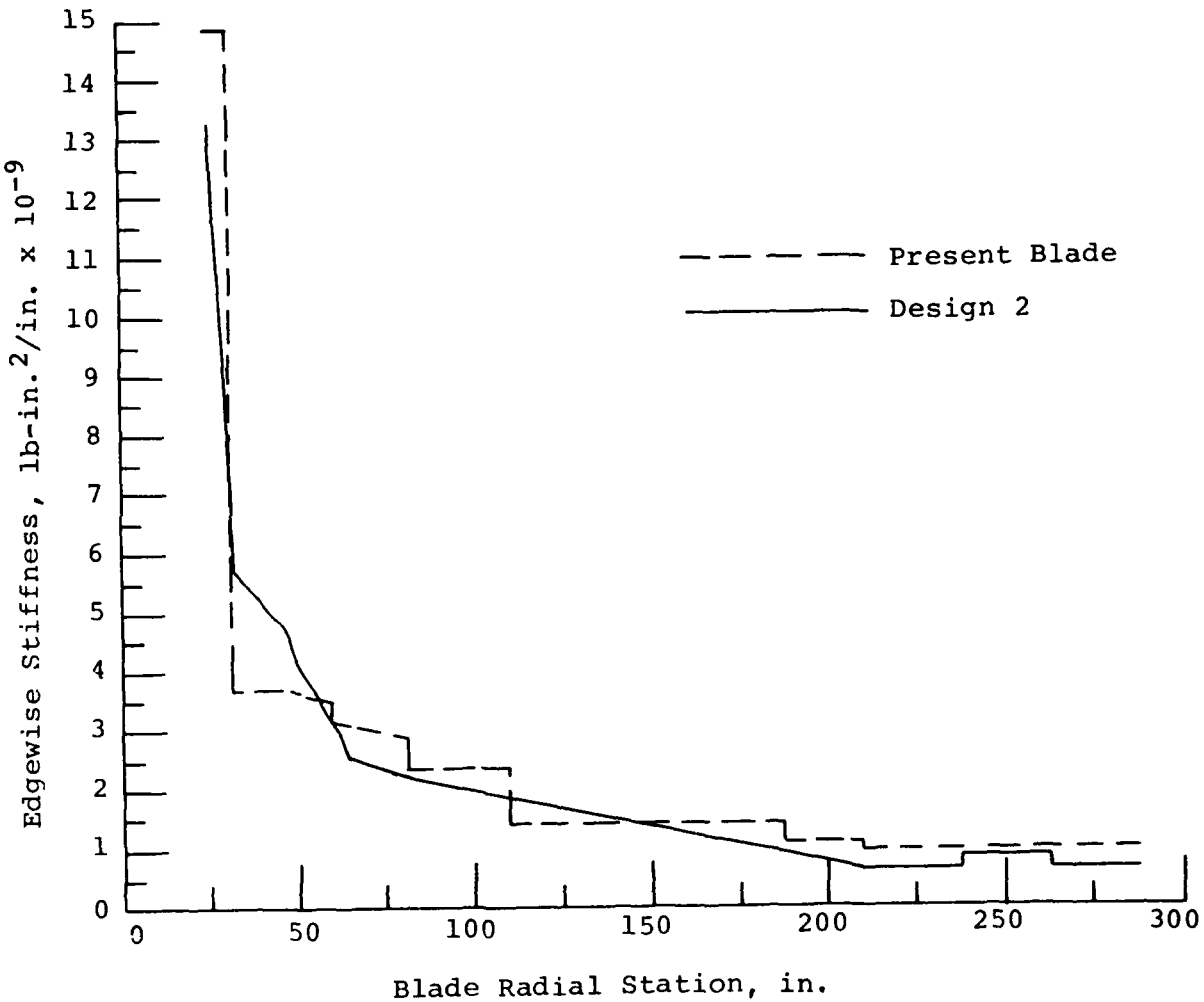

Figure 10. Concept 2, Current Blade Edgewise Stiffness Distribution Comparison.

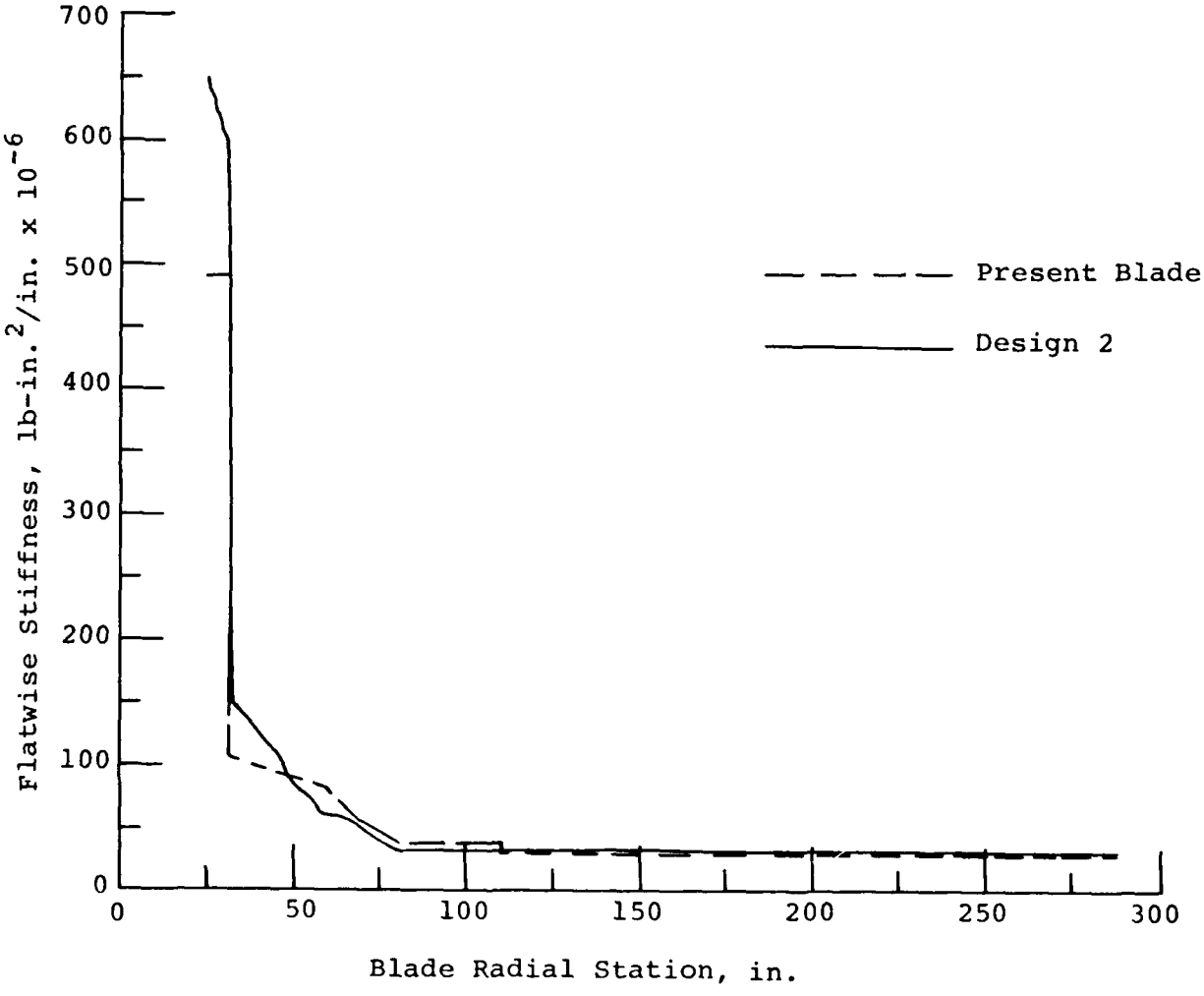

Figure 11. Concept 2, Current Blade Flatwise Stiffness Distribution Comparison.

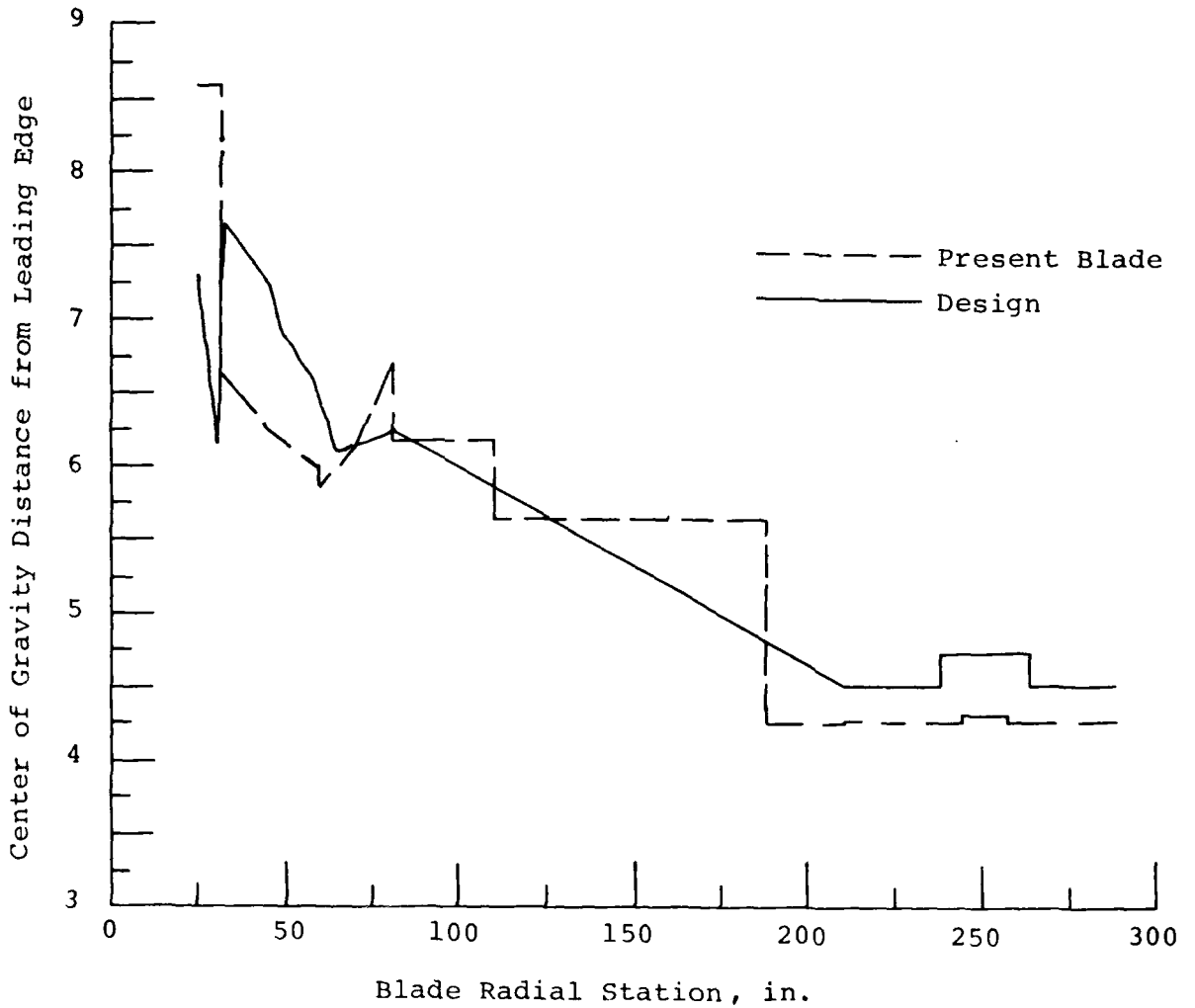

Figure 12. Concept 2, Current Blade Center of Gravity Distribution Comparison.

TABLE 3. WEIGHT AND BALANCE SUMMARY

CONCEPT	TOTAL BLADE WT (LB)	SPANWISE CG (IN. FROM C. ROT.)	CHORDWISE CG (IN. FROM LE)	DYNAMIC MASS AXIS (IN. FROM LE)
1	188.1	136.4	5.707	5.036
2	199.0	140.9	5.747	5.071
3	199.9	136.9	5.829	5.093
4	201.8	140.8	5.905	5.086
5	199.3	137.7	5.758	5.061
6	196.3	136.1	5.403	5.097
Current UH-1H	203.5	142.3	5.742	5.040

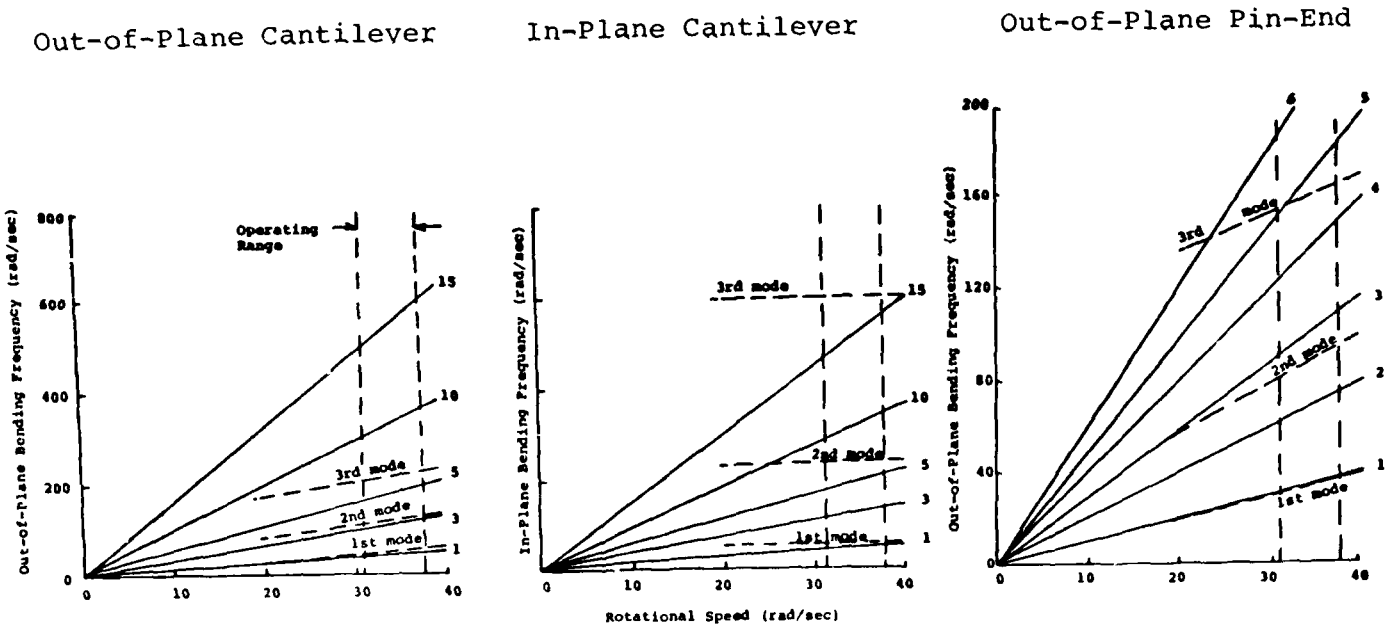

Figure 13. Natural Frequencies, Current UH-1H Blade.

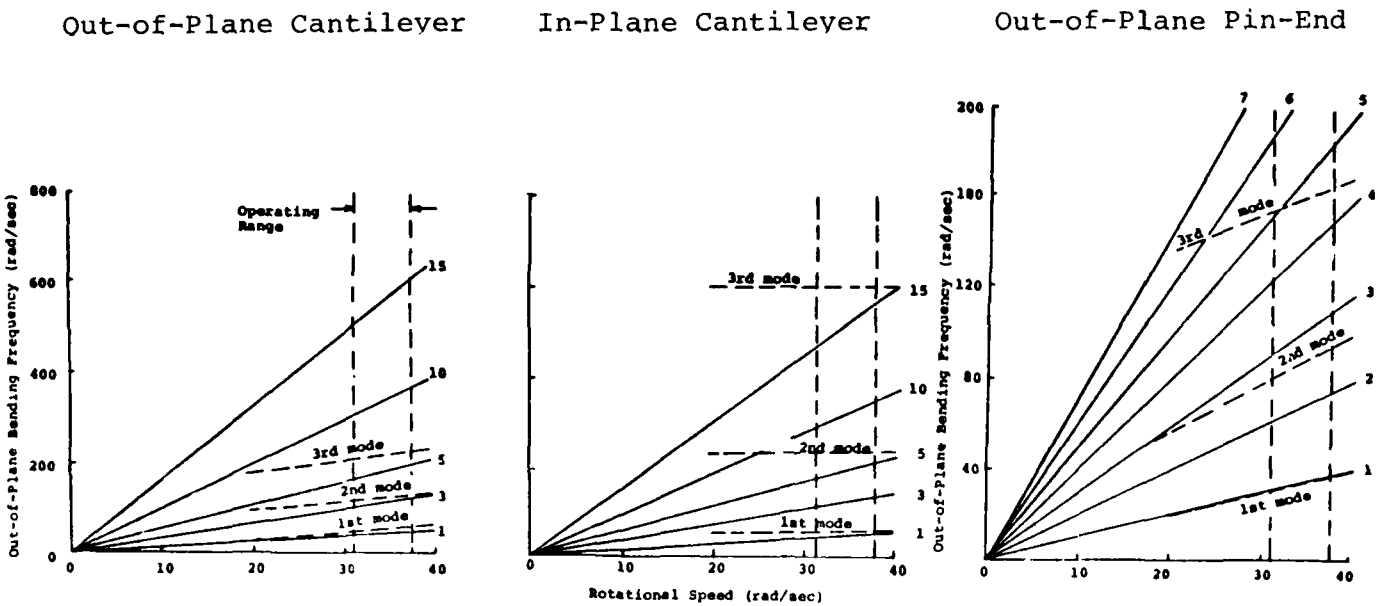

Figure 14. Natural Frequencies, Concept 2.

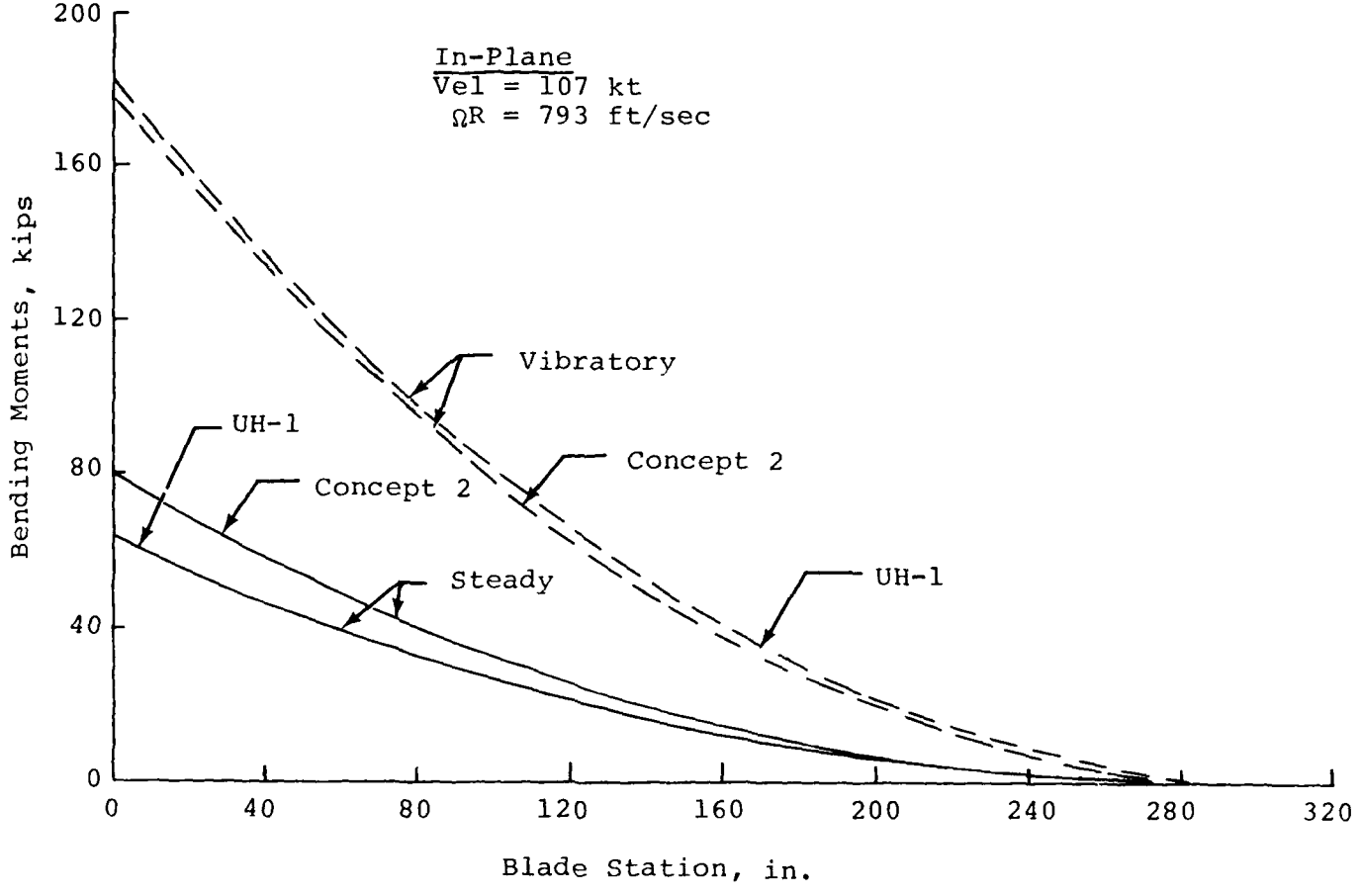

Figure 15. Concept 2, Current Blade Edgewise Bending Moment Distribution Comparison at 107 Knots.

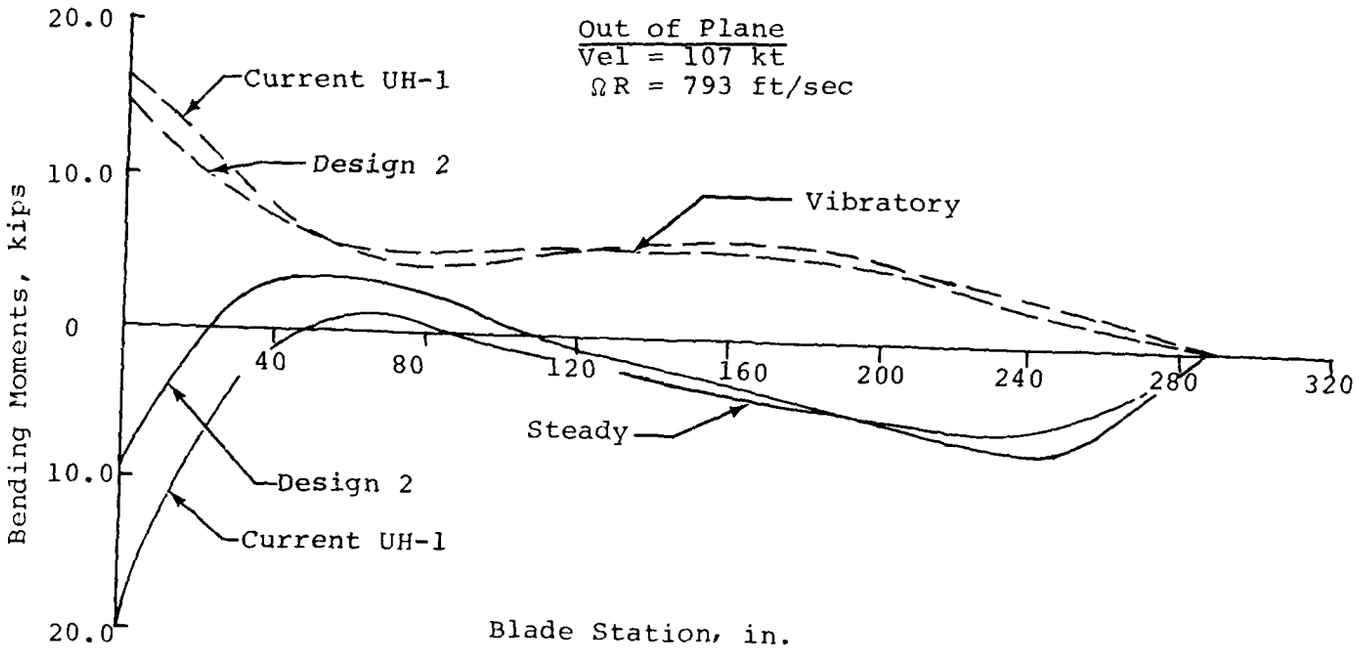

Figure 16. Concept 2, Current Blade Flatwise Bending Moment Distribution Comparison at 107 Knots.

TABLE 4. BASIC STRESS ANALYSIS SUMMARY

Configuration	Component (at station 81)	Coordinates (in.) x*	Coordinates (in.) y**	Fatigue Stress (ksi)			Margin of Safety
Current UH-1H	Abrasion Strip	0.000	0.000	32.89	±	7.11	+0.865
	Nose Weight	0.020	0.000	12.79	±	2.76	+0.748
	Spar	0.677	0.542	12.74	±	3.24	+0.491
	Skin	20.690	0.070	9.82	±	6.14	+0.170
	Spline	21.000	0.027	9.77	±	6.21	-0.179
Concept 1	Nose	0.000	0.000	11.80	±	2.15	+0.925
	Nose	5.500	-1.257	11.81	±	2.02	+1.051
	Nose	6.500	-1.205	11.63	±	2.26	+0.843
	Skin	5.500	-1.257	4.89	±	0.84	+3.269
	Skin	20.620	-0.043	3.68	±	2.43	+0.513
	Spline	20.620	-0.043	8.89	±	5.86	-0.216
	Spline	21.000	-0.005	8.81	±	5.95	-0.225
Concept 2	Nose	0.000	0.000	12.51	±	2.34	+0.717
	Nose	5.500	-1.253	12.51	±	1.85	+1.175
	Nose	6.500	-1.237	12.32	±	1.98	+1.044
	Skin	6.500	-1.237	5.10	±	0.82	+3.318
	Skin	5.500	-1.253	5.18	±	0.77	+3.618
	Spline	21.000	-0.005	8.86	±	6.14	-0.251
	Spline	20.620	-0.056	8.97	±	6.06	-0.243
Concept 3	Nose	0.000	0.000	31.03	±	7.13	+0.480
	Nose	4.940	-1.260	30.71	±	6.09	+0.747
	Skin	4.940	-1.260	4.66	±	0.92	+2.879
	Skin	21.000	-0.028	3.20	±	2.43	+0.528
	Spline	21.000	-0.005	6.04	±	4.57	+0.283

TABLE 4.- Continued

Configuration	Component (at station 81)	Coordinates (in.) x*	Coordinates (in.) y**	Fatigue Stress (ksi)	Margin of Safety
Concept 4	Nose	0.000	0.000	34.82 ± 7.88	+0.223
	Nose	4.940	-1.238	34.35 ± 6.72	+0.452
	Skin	4.940	-1.238	5.22 ± 1.02	+2.405
	Skin	21.000	-0.028	3.79 ± 2.30	+0.594
	Spline	21.000	-0.005	7.16 ± 4.32	+0.353
Concept 5	Nose	0.000	0.000	30.46 ± 6.91	+0.547
	Nose	4.940	-1.260	30.12 ± 5.69	+0.894
	Skin	4.940	-1.260	4.57 ± 0.86	+3.161
	Skin	21.000	-0.028	3.15 ± 2.39	+0.559
	Spline	21.000	+0.005	5.94 ± 4.54	+0.295
Concept 6	Nose	0.000	0.000	32.27 ± 7.65	+0.469
	Nose	4.940	-1.260	31.82 ± 6.38	+0.477
	Skin	4.940	-1.260	4.83 ± 0.97	+2.130
	Skin	21.000	-0.028	3.44 ± 2.26	+0.832
	Spline	21.000	+0.005	6.48 ± 4.29	+0.543

* X is measured from the leading edge parallel to the chord plane.

** Y is measured from the chord plane and perpendicular to it.

outboard doubler ends, proved to be the station at which the minimum margins occurred on all of the designs, including the present UH-1 blade. Designs 1 and 2 (extruded aluminum spar) had more negative margins of safety on the trailing-edge spline than the current UH-1H blade, while all of the other design concepts considered had higher margins in this area. The small difference between the current blade's margin of safety and those of Concepts 1 and 2 does not exclude them from further consideration. In the detail design phase, slight geometric changes could reduce stresses without compromising frequency requirements.

The Design Specification given in Appendix A requires that the FREB design provide no greater contribution to the UH-1 helicopter's aural detectability than does the present blade. The acoustic dipole strength of the UH-1 main rotor system is largely related to the drag-divergence Mach number of the airfoils used. The even-numbered concepts have the same airfoil as the present blade and will, therefore, have identical acoustic properties. In order to be a less efficient acoustic emitter than the present UH-1 blade, the modified airfoil must exhibit higher drag-divergence Mach number characteristics than the present airfoil. Airfoils such as the modified Wortmann series, which have high drag divergence Mach numbers, reach maximum thickness slowly and stay relatively thick over an appreciable part of the airfoil chord. The modified airfoil proposed for the even-numbered concepts is constructed by using an NACA 0015 airfoil up to a tangency point at 8.87 inches from the leading edge. As can be seen in Figure 17, this modified airfoil both gets thick more quickly than the standard airfoil and loses its thickness more quickly. These geometric changes act to decrease the drag-divergence Mach number. Figure 18 shows the results of decreasing the drag-divergence Mach number below that of the present airfoil. Figure 19 shows that the modified airfoil would have to be flown more slowly than the standard airfoil, to result in the same aural detectability.

The twelve concepts were lumped into several groups for purposes of radar cross section analysis. Concepts 7, 9 and 11 are the same from an RCS standpoint as Concept 1, while Concepts 8, 10 and 12 are the same as Concept 2. Concept 5 is the same as Concept 3, and Concept 6 is the same as Concept 4. Static measurements of the radar cross sections of the four concepts were made, while their dynamic radar cross section was predicted analytically. The aluminum and stainless steel spars of Concepts 1 and 2 are the same from an RCS standpoint as the stainless-steel spars of Concepts 3 and 4. The study showed that Concepts 3 and 4, with nonreflecting splines, would need some treatment in order to mask the aft wall of the spar. If this were accomplished, all of the designs would

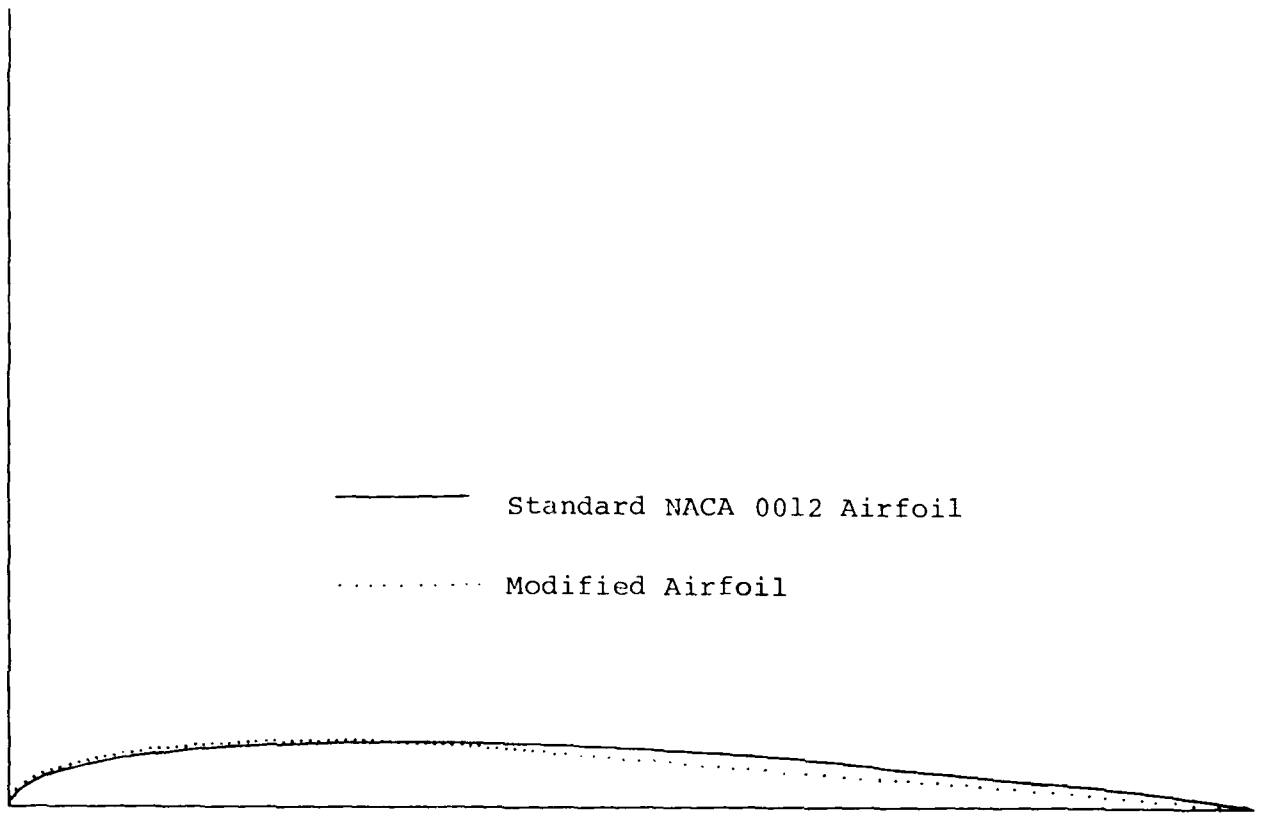

Figure 17. Standard and Modified Airfoil Comparison.

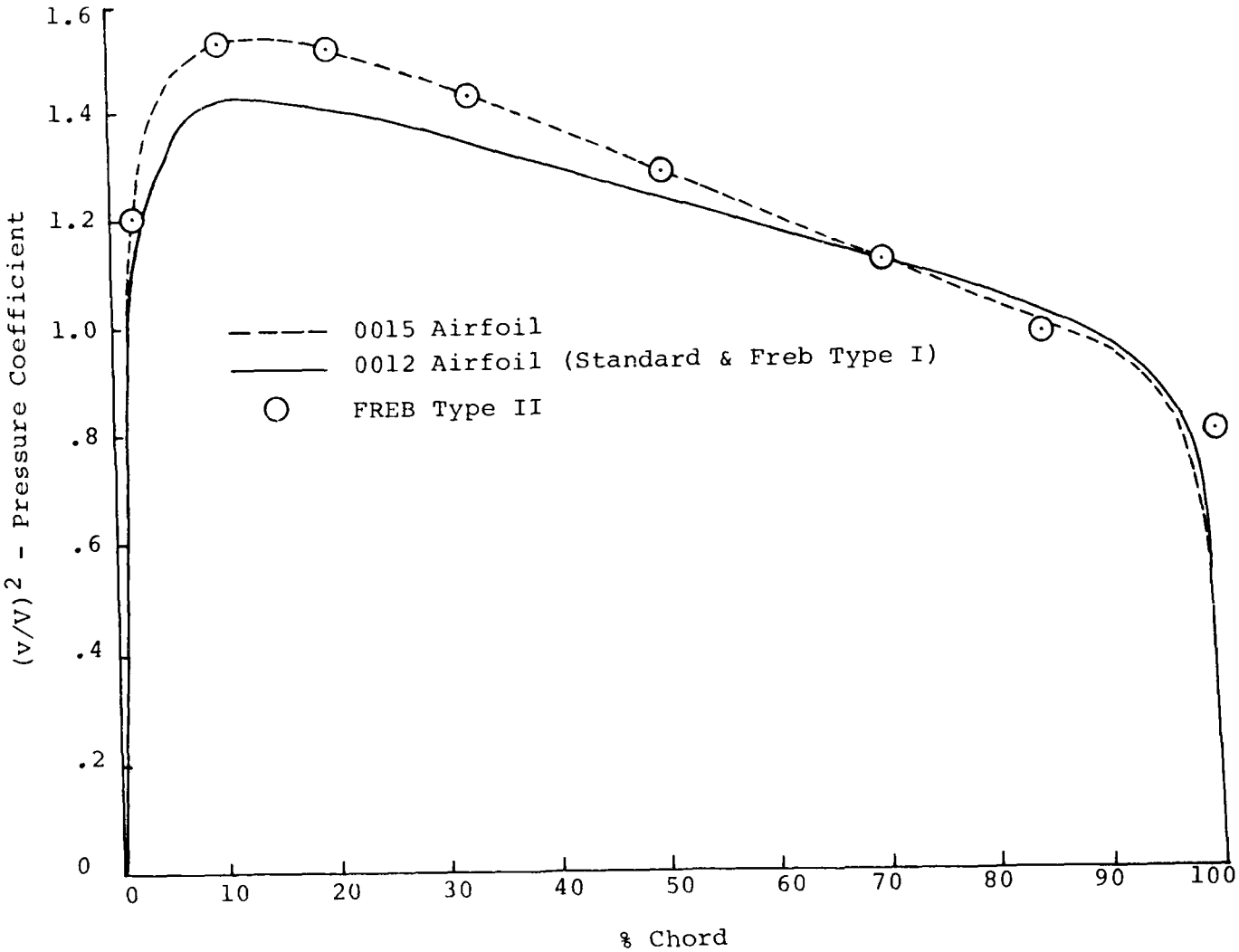

Figure 18. Airfoil Pressure Distribution for 0015, 0012 and FREB Type II Airfoils.

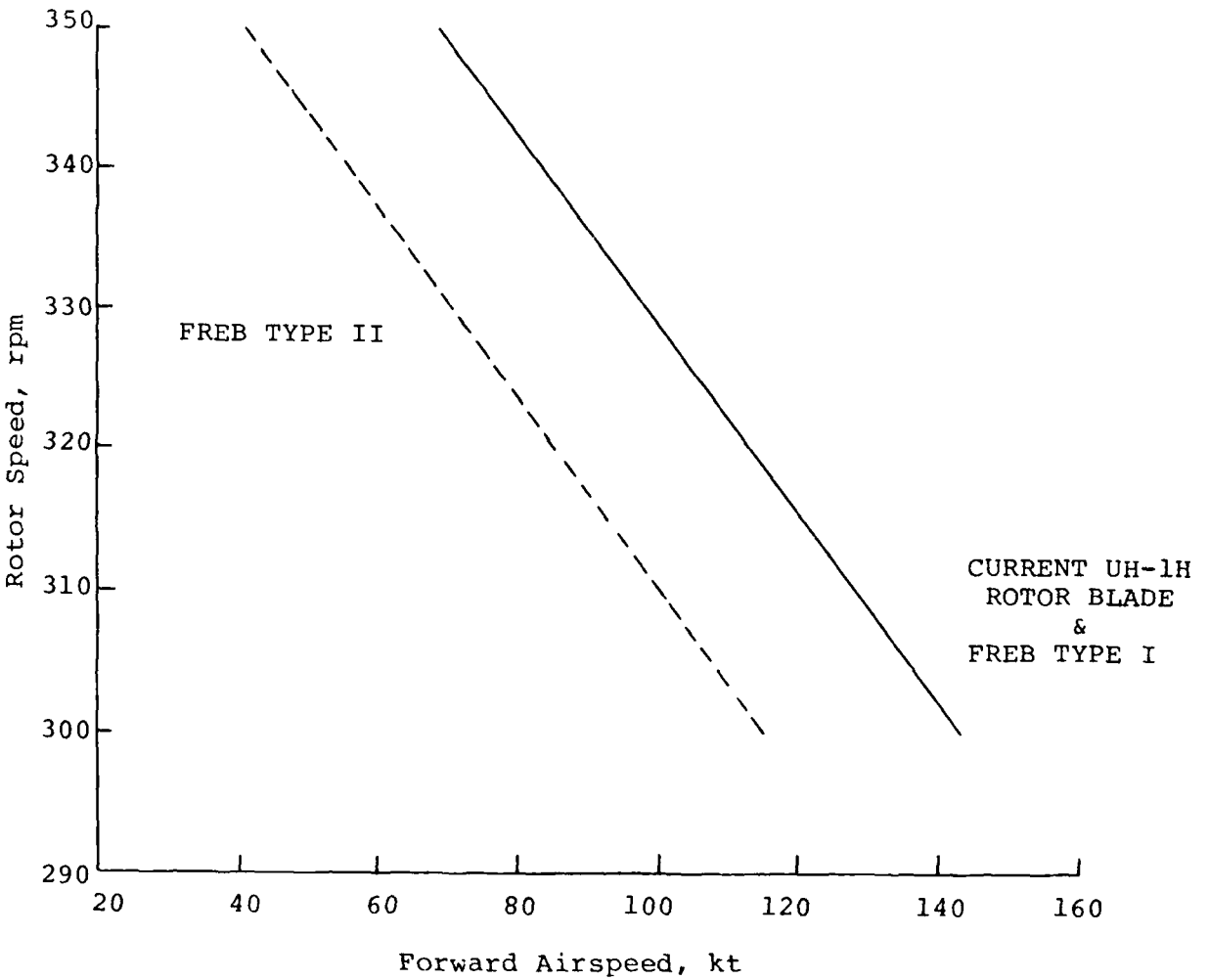

Figure 19. Rotor Speed vs. Forward Airspeed for Constant Aural Detection Range.

meet the requirement that RCS values be no greater than that of the current UH-1H blade. Additionally, it was concluded that proper repair of damaged blades would leave the radar cross section virtually unchanged.

LIFE-CYCLE COST ANALYSES

The use of the contractor's time-sharing computer programs to predict life-cycle costs of the candidate blade concepts on a real time basis allowed the study of life-cycle costs as a function of various blade parameters.

Table 5 compares the life-cycle costs for the present UH-1H blade to those of the various design candidates. Both 600- and 1000-hour MTBFs were used to cover the variation in MTBFs from various data sources. Concepts 1 and 2 are repeatedly the least expensive, while all of the concepts considered showed substantial improvements over the present blade.

Figures 20 through 25 compare the life-cycle costs of the various design concepts and the present blade as functions of initial procurement costs, MTBF, field repairability and fatigue life. Wherever possible, the candidates were lumped together to minimize the complexity of the curves. The trends on the curves show that there are no optimum points, but that the design concepts have various degrees of sensitivity to the independent variable.

It was initially intended that a value of 914 hours between failures, from Table E-1 of Reference 2, would be used as the basis for determining rates of failure and life-cycle costs. However, subsequent information has indicated that this may be an unconservative number, so the curves of Figures 21 and 23 are plotted for a range of failure rates. The other curves use 600 hours as the base MTBF.

Tables 6 through 9 give representative outputs of the life-cycle cost model for both Concept 2 and the current blade.

It should also be noted that incorporation of depot repair in the maintenance cycle of the current blades saves an almost negligible $700 (in $45,000) in the cost of each helicopter life cycle.

RELIABILITY AND MAINTAINABILITY ANALYSES

The basis for selection of candidate design concepts for the FREB, after determining that basic structural and performance criteria would be met, was each design's potential for achieving low life-cycle costs. Reliability and maintainability were the important factors in this assessment. As stated earlier,

TABLE 5. LIFE-CYCLE COST SUMMARY

Mean Time Between Failures (Current Blade Operations as Base) Concept	600 Hours	1000 Hours
	Life-Cycle Blade Costs, $K	
A. With Combat Damage		
Current UH-1D/H Blade	60.36	44.02
1	33.86	27.16
2	34.67	27.81
3	48.37	38.98
4	48.69	39.23
5	46.15	37.18
6	46.48	37.45
7	34.15	27.39
8	34.95	28.04
9	34.11	27.37
10	34.92	28.02
11	38.92	31.40
12	39.79	32.03
B. Without Combat Damage		
Current UH-1D/H Blade	54.32	40.86
1	31.15	25.47
2	31.89	26.08
3	44.48	36.08
4	45.03	35.80
5	42.43	36.22
6	42.89	34.57
7	31.41	26.68
8	32.15	26.29
9	31.39	25.66
10	32.13	26.27
11	35.89	29.45
12	36.63	30.06

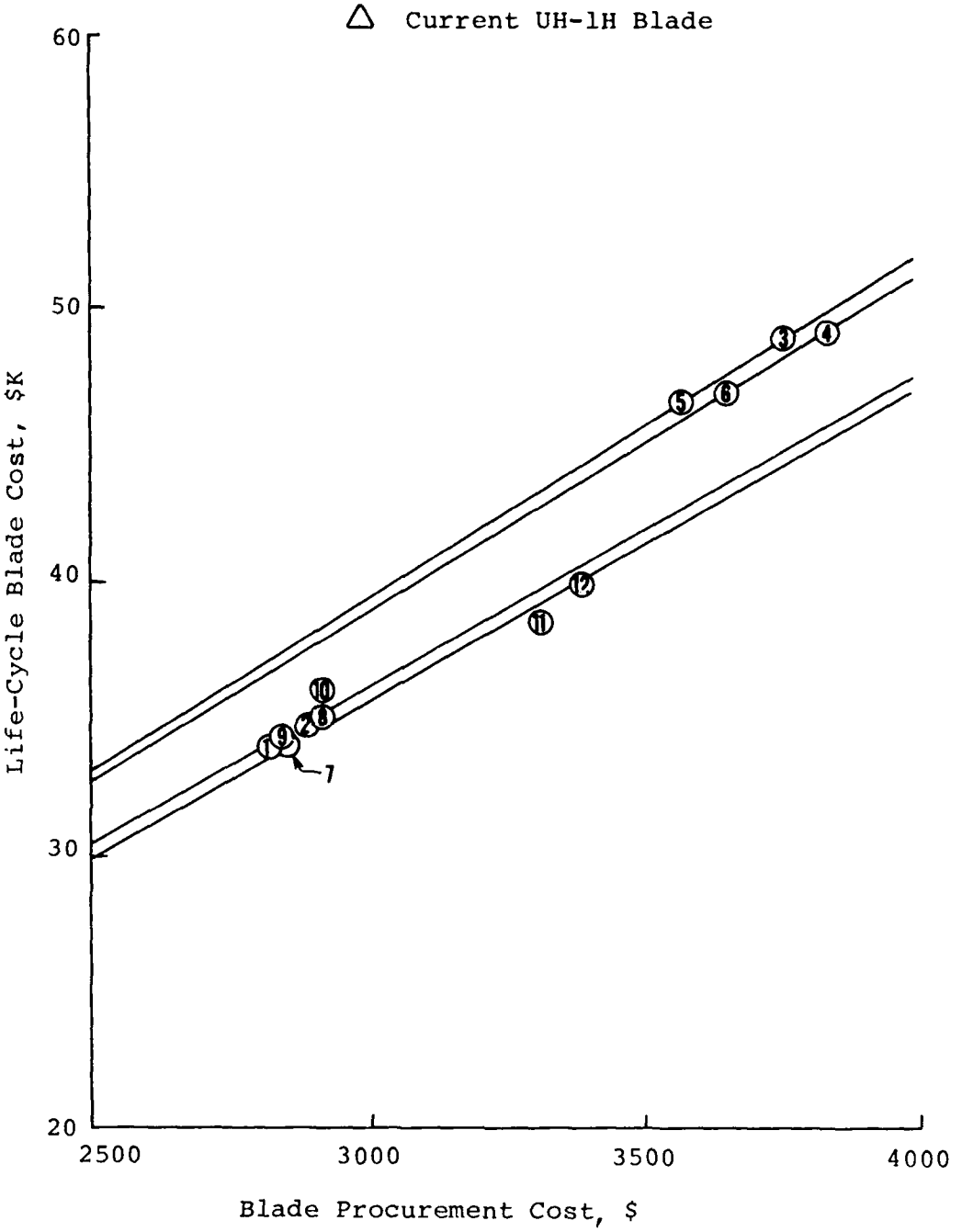

Figure 20. Life-Cycle Costs vs. Initial Procurement Costs.

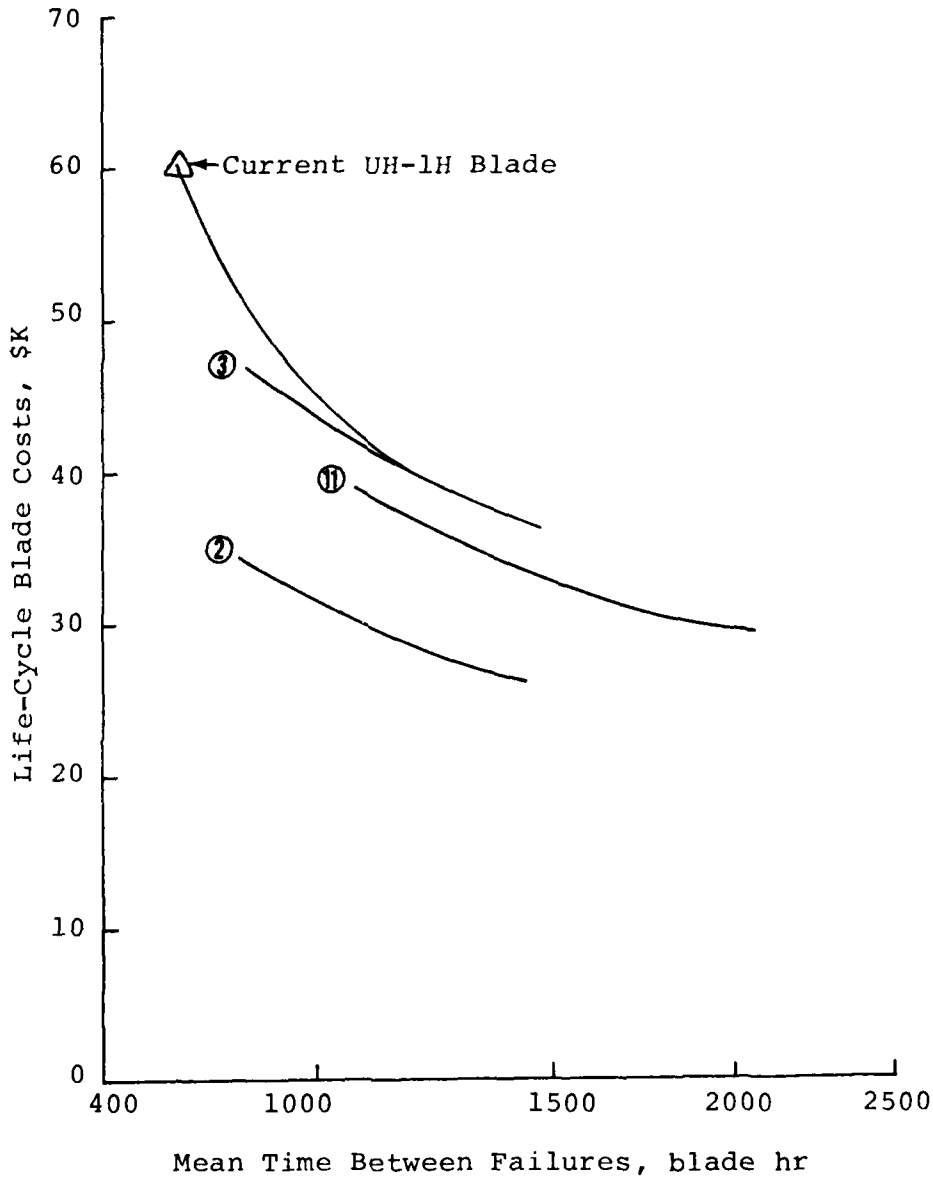

Figure 21. Life-Cycle Costs vs. Mean Time Between Failures, Combat Environment.

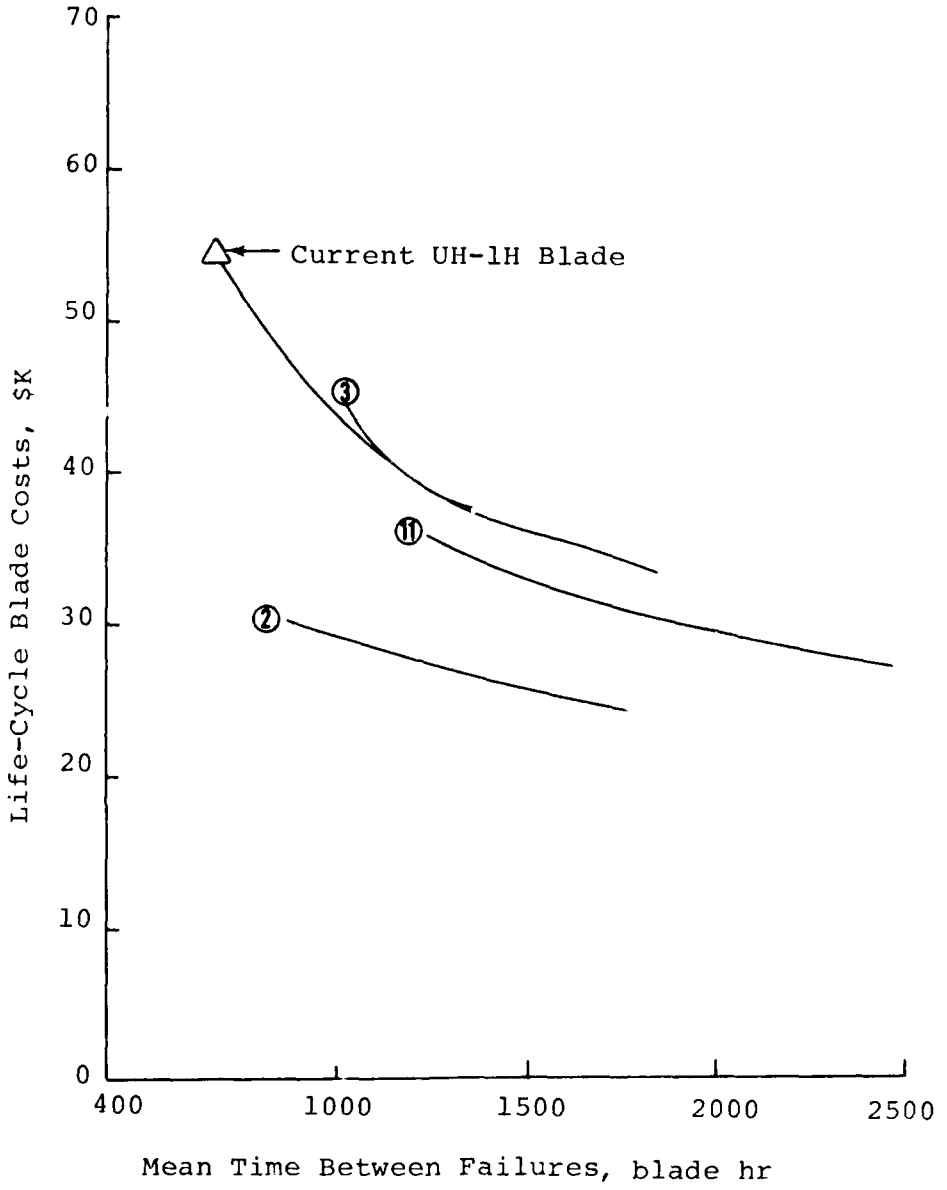

Figure 22. Life-Cycle Costs vs. Mean Time Between Failures, Noncombat Environment.

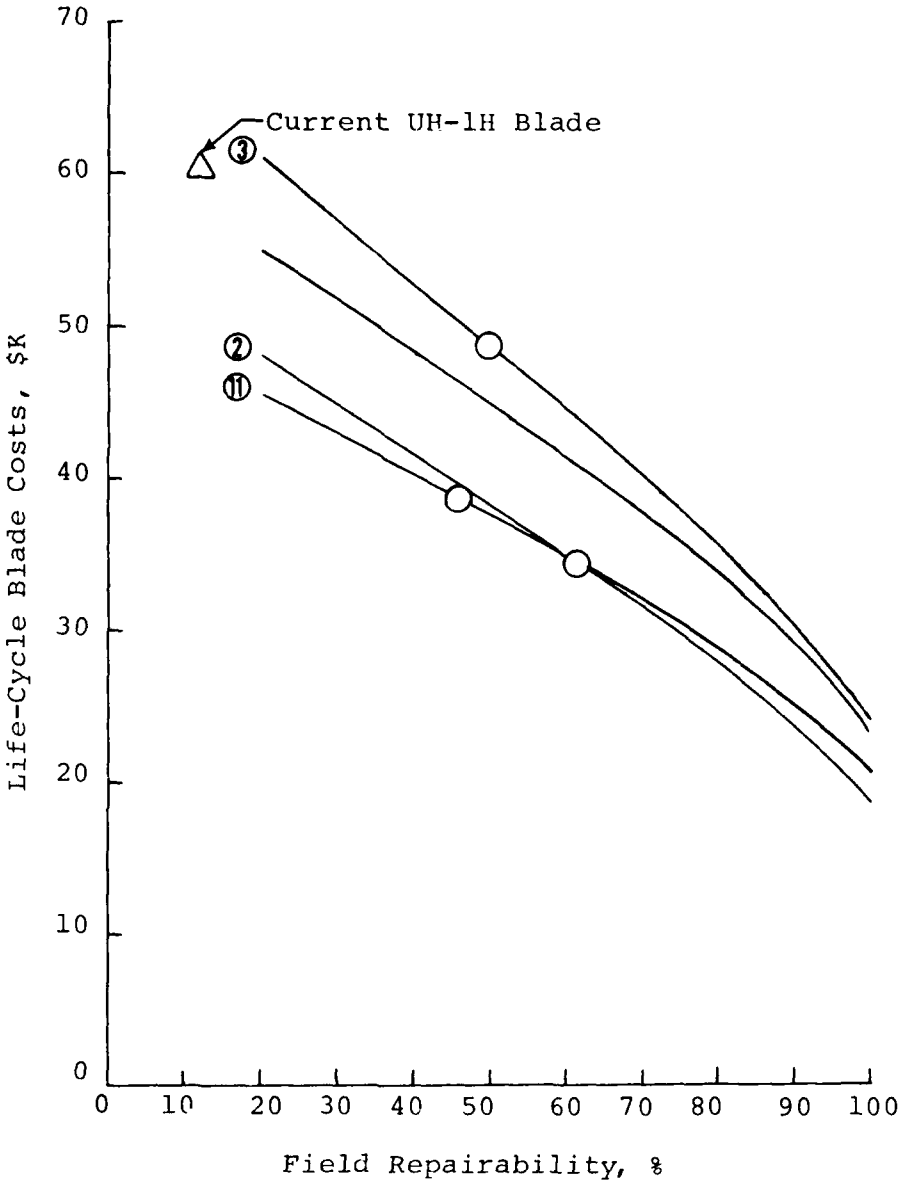

Figure 23. Life-Cycle Costs vs. Field Repairability, Combat Environment.

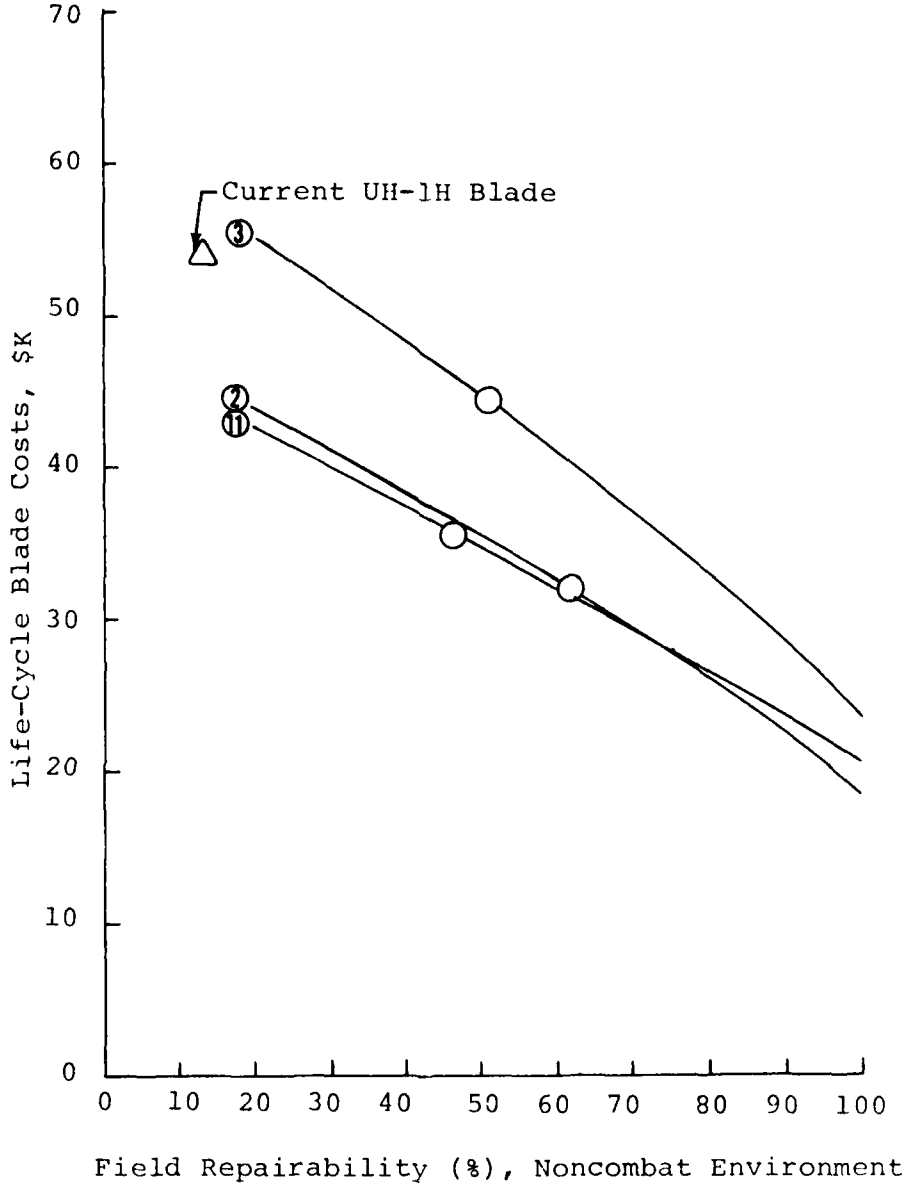

Figure 24. Life-Cycle Costs vs. Field Repairability, Noncombat Environment.

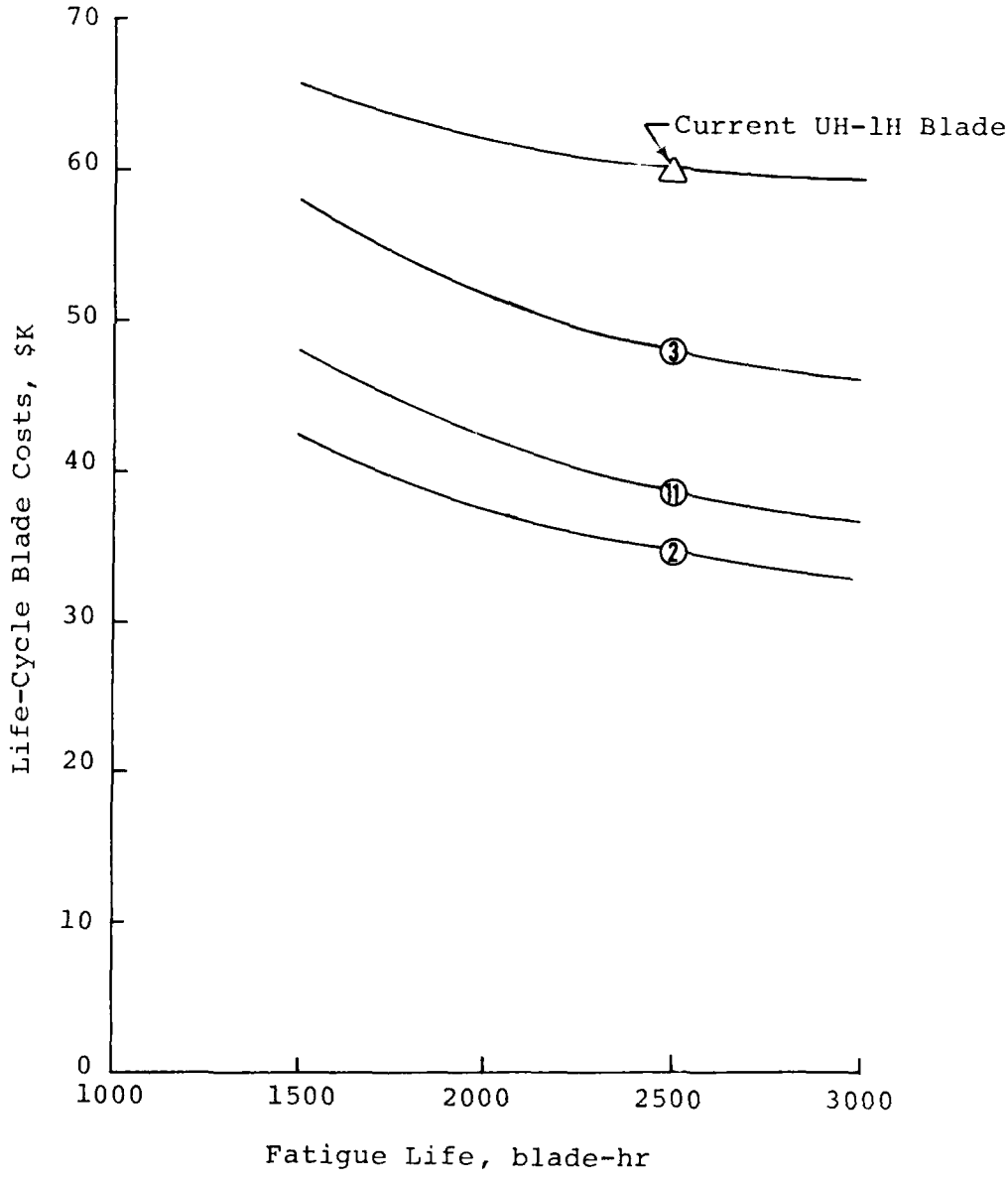

Figure 25. Life-Cycle Costs vs. Fatigue-Limited Service Life.

TABLE 6. LIFE-CYCLE COST PROGRAM OUTPUT, CURRENT BLADE WITHOUT COMBAT, 600-HOUR BASE MTBF

NEW BLADE PRICE	= $ 3,000	
MEAN TIME BETWEEN FAILURES	= 686.4 Blade Hours	
FIELD REPAIRABILITY	= 13.2 percent	
MEAN TIME BETWEEN MAINTENANCE ACTIONS (BLADE HOURS):		
Replacements	= 848.7	
Removals for Repair or Replacement	= 652.9	
Repairs	= 2,831.3	
Damage Replacements	= 906.1	
Unscheduled Maintenance	= 686.4	
Scheduled Maintenance (Retirement)	= 13,398.1	
All Maintenance Actions	= 652.9	
BLADE EVENTS PER AIRCRAFT LIFE CYCLE:		
Number Lost to Attrition	= 1.5000	
Number Fatigue Retired Undamaged	= 0.7464	
Number Repaired on Aircraft	= 0.0000	
Number Repaired off Aircraft in Field	= 1.9177	
Number Scrapped in Field	= 4.6781	
Number Damaged and Retired in Field	= 0.0406	
Number Repaired at Depot	= 1.6142	
Number Scrapped at Depot	= 3.7930	
Number Damaged and Retired at Depot	= 2.5251	
TOTAL Number Damaged and Not Repaired	= 11.0368	
TOTAL Number All Replacements	= 11.7832	
MAIN ROTOR BLADE COSTS PER AIRCRAFT LIFE CYCLE:		
COST OF INITIAL PROCUREMENT:		
New Aircraft Outfitting Cost	= $ 6,000.00	
Spares Cost, with Containers	= 2,016.00	
Spare Repair Materials	= 0.50	
Repair Support Equipment	= 160.00	
TOTAL Initial Procurement Cost	=	$ 8,176.50
COST OF REPLACEMENT BLADES FOR THOSE LOST AND UNSERVICEABLE (INCLUDING BLADE SHIPPING AND CONTAINER SHIPPING COSTS):		
Blades Lost to Attrition	= $ 4,762.50	
Damaged Blades Not Repaired	= 35,501.80	
Time-Expired Undamaged Blades	= 2,369.70	
TOTAL Replacement Cost	=	$ 42,634.00
COST OF MAINTENANCE ACTIONS (LABOR AND MATERIAL TO INSPECT, REMOVE, REPAIR, REPLACE, ALIGN AND TRACK):		
Field Repair on Aircraft	= $ 0.00	
Field Repair off Aircraft	= 85.10	
Field Scrap	= 168.40	
Field Retirement	= 23.60	
Depot Repair	= 1,971.00	
Depot Scrap	= 766.20	
Depot Retirement	= 494.90	
TOTAL Maintenance Cost		$ 3,509.20
TOTAL LIFE-CYCLE BLADE COST PER AIRCRAFT		$ 54,319.80
MAINTENANCE MAN-HOURS/FLIGHT HOUR	= 0.0279	
BLADE-RELATED AIRCRAFT DOWNTIME	= 33 Hours	

TABLE 7. LIFE-CYCLE COST PROGRAM OUTPUT, CONCEPT 2 WITHOUT COMBAT, 600-HOUR BASE MTBF

NEW BLADE PRICE	= $ 2,888	
MEAN TIME BETWEEN FAILURES	= 891.6 Blade Hours	
FIELD REPAIRABILITY	= 61.8 percent	
MEAN TIME BETWEEN MAINTENANCE ACTIONS (BLADE HOURS):		
Replacements	= 1,588.2	
Removals for Repair or Replacement	= 1,530.4	
Repairs	= 1,445.2	
Damage Replacements	= 2,327.5	
Unscheduled Maintenance	= 891.6	
Scheduled Maintenance (Retirement)	= 5,000.0	
All Maintenance Actions	= 756.7	
BLADE EVENTS PER AIRCRAFT LIFE CYCLE:		
Number Lost to Attrition	= 1.5000	
Number Fatigue Retired Undamaged	= 2.0000	
Number Repaired on Aircraft	= 6.6814	
Number Repaired off Aircraft in Field	= 0.2379	
Number Scrapped in Field	= 4.2770	
Number Damaged and Retired in Field	= 0.0195	
TOTAL Number Damaged and Not Repaired	= 4.2965	
TOTAL Number All Replacements	= 6.2965	
MAIN ROTOR BLADE COSTS PER AIRCRAFT LIFE CYCLE:		
COST OF INITIAL PROCUREMENT:		
New Aircraft Outfitting Cost	= $ 5,776.00	
Spares Cost, with Containers	= 1,948.80	
Spare Repair Materials	= 25.40	
Repair Support Equipment	= 160.00	
TOTAL Initial Procurement Cost	=	$ 7,910.20
COST OF REPLACEMENT BLADES FOR THOSE LOST AND UNSERVICEABLE (INCLUDING BLADE SHIPPING AND CONTAINER SHIPPING COSTS):		
Blades Lost to Attrition	= $ 4,594.50	
Damaged Blades Not Repaired	= 12,516.40	
Time-Expired Undamaged Blades	= 6,126.00	
TOTAL Replacement Cost	=	$ 23,236.90
COST OF MAINTENANCE ACTIONS (LABOR AND MATERIAL TO INSPECT, REMOVE, REPAIR, REPLACE, ALIGN AND TRACK):		
Field Repair on Aircraft	= $ 521.00	
Field Repair off Aircraft	= 11.50	
Field Scrap	= 154.00	
Field Retirement	= 60.60	
TOTAL Maintenance Cost	=	$ 747.10
TOTAL LIFE-CYCLE BLADE COST PER AIRCRAFT		$ 31,894.20
MAINTENANCE MAN-HOURS/FLIGHT HOUR	= 0.0148	
BLADE-RELATED AIRCRAFT DOWNTIME	= 55 Hours	

TABLE 8. LIFE-CYCLE COST PROGRAM OUTPUT, CURRENT BLADE WITH COMBAT, 600-HOUR BASE MTBF

NEW BLADE PRICE	= $ 3,000	
MEAN TIME BETWEEN FAILURES	= 600.0 Blade Hours	
FIELD REPAIRABILITY	= 12.4 percent	
MEAN TIME BETWEEN MAINTENANCE ACTIONS (BLADE HOURS):		
Replacements	= 739.6	
Removals for Repair or Replacement	= 581.7	
Repairs	= 2,725.0	
Damage Replacements	= 769.4	
Unscheduled Maintenance	= 600.0	
Scheduled Maintenance (Retirement)	= 19,058.9	
All Maintenance Actions	= 581.7	
BLADE EVENTS PER AIRCRAFT LIFE CYCLE:		
Number Lost to Attrition	= 1.5000	
Number Fatigue Retired Undamaged	= 0.5247	
Number Repaired on Aircraft	= 0.0000	
Number Repaired off Aircraft in Field	= 2.0609	
Number Scrapped in Field	= 5.5180	
Number Damaged and Retired in Field	= 0.0462	
Number Repaired at Depot	= 1.6088	
Number Scrapped at Depot	= 4.5545	
Number Damaged and Retired at Depot	= 2.8782	
TOTAL Number Damaged and Not Repaired	= 12.9969	
TOTAL Number All Replacements	= 1[illegible].5216	
MAIN ROTOR BLADE COSTS PER AIRCRAFT LIFE CYCLE:		
COST OF INITIAL PROCUREMENT:		
New Aircraft Outfitting Cost	= $ 6,000.00	
Spares Cost, with Containers	= 2,016.00	
Spare Repair Materials	= 0.60	
Repair Support Equipment	= 160.00	
TOTAL Initial Procurement Cost	=	$ 8,176.60
COST OF REPLACEMENT BLADES FOR THOSE LOST AND UNSERVICEABLE (INCLUDING BLADE SHIPPING AND CONTAINER SHIPPING COSTS):		
Blades Lost to Attrition	= $ 4,762.50	
Damaged Blades Not Repaired	= 42,000.40	
Time-Expired Undamaged Blades	= 1,665.90	
TOTAL Replacement Cost	=	$ 48,428.70
COST OF MAINTENANCE ACTIONS (LABOR AND MATERIAL TO INSPECT, REMOVE, REPAIR, REPLACE, ALIGN AND TRACK):		
Field Repair on Aircraft	= $ 0.00	
Field Repair off Aircraft	= 91.30	
Field Scrap	= 198.60	
Field Retirement	= 17.10	
Depot Repair	= 1,964.30	
Depot Scrap	= 920.00	
Depot Retirement	= 564.10	
TOTAL Maintenance Cost	=	$ 3,755.60
TOTAL LIFE-CYCLE BLADE COST PER AIRCRAFT		$ 60,360.90
MAINTENANCE MAN-HOURS/FLIGHT HOUR	= 0.0313	
BLADE-RELATED AIRCRAFT DOWNTIME	= 93 Hours	

TABLE 9. LIFE-CYCLE COST PROGRAM OUTPUT, CONCEPT 2 WITH COMBAT, 600-HOUR BASE MTBF

NEW BLADE PRICE	= $ 2,888	
MEAN TIME BETWEEN FAILURES	= 756.6 Blade Hours	
FIELD REPAIRABILITY	= 61.2 percent	
MEAN TIME BETWEEN MAINTENANCE ACTIONS (BLADE HOURS):		
Replacements	= 1,407.0	
Removals for Repair or Replacement	= 1,361.3	
Repairs	= 1,238.4	
Damage Replacements	= 1,944.6	
Unscheduled Maintenance	= 756.6	
Scheduled Maintenance (Retirement)	= 5,088.7	
All Maintenance Actions	= 658.7	
BLADE EVENTS PER AIRCRAFT LIFE CYCLE:		
Number Lost to Attrition	= 1.5000	
Number Fatigue Retired Undamaged	= 1.9651	
Number Repaired on Aircraft	= 7.8390	
Number Repaired off Aircraft in Field	= 0.2357	
Number Scrapped in Field	= 5.1192	
Number Damaged and Retired in Field	= 0.0232	
TOTAL Number Damaged and Not Repaired	= 5.1424	
TOTAL Number All Replacements	= 7.1075	
MAIN ROTOR BLADE COSTS PER AIRCRAFT LIFE CYCLE:		
COST OF INITIAL PROCUREMENT:		
New Aircraft Outfitting Cost	= $ 5,776.00	
Spares Cost, with Containers	= 1,948.80	
Spare Repair Materials	= 31.70	
Repair Support Equipment	= 160.00	
TOTAL Initial Procurement Cost	=	$ 7,916.50
COST OF REPLACEMENT BLADES FOR THOSE LOST AND UNSERVICEABLE (INCLUDING BLADE SHIPPING AND CONTAINER SHIPPING COSTS):		
Blades Lost to Attrition	= $ 4,594.50	
Damaged Blades Not Repaired	= 15,231.60	
Time-Expired Undamaged Blades	= 6,019.20	
TOTAL Replacement Cost	=	$ 25,345.20
COST OF MAINTENANCE ACTIONS (LABOR AND MATERIAL TO INSPECT, REMOVE, REPAIR, REPLACE, ALIGN AND TRACK):		
Field Repair on Aircraft	= $ 648.00	
Field Repair off Aircraft	= 11.40	
Field Scrap	= 184.30	
Field Retirement	= 59.60	
TOTAL Maintenance Cost	=	$ 903.40
TOTAL LIFE-CYCLE BLADE COST PER AIRCRAFT		$ 34,665.20
MAINTENANCE MAN-HOURS/FLIGHT HOUR	= 0.0169	
BLADE-RELATED AIRCRAFT DOWNTIME	= 63 Hours	

twenty-six concepts were proposed initially, and from these, twelve, showing particular promise, were selected for further study. While the twelve concepts chosen each represented a different combination of materials and construction methods, some differed only in details of the design. From the standpoint of reliability and maintainability, the twelve concepts were variations on two basic design approaches: blades with aluminum spars and blades with stainless-steel spars, both having afterbodies constructed of composite materials. The reliability and maintainability analyses were thus able to focus on two basic types of design, leaving detail variations for later consideration.

Reliability Analysis

The reliability analysis of new designs, such as the FREB, is predicated on past experience with similar designs under like conditions of environment and use. Failure modes and effects are studied and compared, and engineering analysis is used to estimate reliability improvements or degradations expected to occur as a result of design variations, changes in environment, operating stress, etc. This technique is effective when the new design is similar to designs for which data is available or employs common parts and components with known reliability characteristics.

Since the FREB concepts represented new approaches to rotor blade design, direct comparisons with rotor blades in current use were somewhat difficult. Although the existing UH-1D/H blade differed in significant respects from the FREB concepts being considered, the experience data on this blade was judged to be the best basis from which to make reliability projections, since the operating environment, at least, was directly comparable.

Data Sources

The best source of reliability data for the UH-1D/H rotor blade was found in the failure and scrap rate data analysis contained in Reference 2 and, used previously in the studies of repairable and expendable blade concepts, References 5 and 6. This data, which tabulates fleet-wide blade removals by cause, had been analyzed to apportion failures to major components of the blade on the basis of engineering judgement. This was done in order to put the data in a form that would allow comparisons to be made of new concepts and the existing blade. While the failure and scrap rate data on the UH-1D/H blade as reported in Reference 2 was the most useful reference available, the use of field data for reliability analysis and prediction was found to have some serious limitations.

Data collected via the standard military reporting systems, because it originates from diverse and widely scattered sources, suffers problems of accuracy and completeness, and provides, at best, a gross indication of reliability performance. For reliability work on structural components such as rotor blades, some particular difficulties are encountered in its use:

a. A new rotor blade, such as the FREB, frequently possesses design characteristics for which no directly comparable experience exists.

b. The field reliability data which comprise the bulk of the recorded experience on rotor blades do not identify failures with specific parts or components of the blade.

c. Field reports frequently report the symptom of failure (e.g., "excessive vibration") instead of the mode of failure (e.g., "cracked").

d. Field reports frequently contain illogical or obviously incorrect failure modes.

For these several reasons, field data provides only a very general indication of the modes and causes of failure and their frequency of occurrence. Recognizing the limitations of field data for reliability work, however, it is possible, with the aid of engineering judgement, to extrapolate from one design to another, at least in comparative terms. This approach had already been used successfully in the studies of repairable and expendable blade concepts and was carried forward to the FREB.

Another source of data for the reliability analysis of FREB concepts was the random damage scenario for rotor blades developed by USAAMRDL and originally provided to the contractor for the repairable blade concept study. This scenario, based on actual combat experience with helicopters in Southeast Asia, distributes 100 random damage events over a blade planform of 300-inch span and 30-inch chord. Use of the scenario overcomes some of the deficiencies inherent in the use of field statistics, alone, by providing specific damage types and locations upon which to base reliability and repairability estimates.

Analysis of Inherent Failure Modes

Inherent modes of failure for the rotor blade are basically of two origins: (1) stress or fatigue-generated failures, such as cracks and bond separations, and (2) environment-related failures, such as corrosion and erosion. Failures of the first type are related to the material composition of the rotor blade and its structural design, and also to manufacturing processes

and quality control. Failures of the second type are related mainly to material properties and the blade's exposure to hostile environment.

A Failure Modes and Effects Analysis (FMEA) was conducted for each of the two basic design concepts to identify, for each of the blade's major components (spar, root end, etc.), the possible modes and causes of inherent failure and the effect and criticality of each mode. For each of the inherent modes of failure, a failure rate prediction was made.

The basis for estimating rates of inherent failure is the statistical experience of other helicopter rotor blades used under similar conditions. While the FREB concepts possessed some characteristics in common with the existing UH-1D/H rotor blade (notably in the spar and root end areas), major dissimilarities also existed, and this made direct comparisons impractical in some cases. In areas where the experience data on the UH-1D/H blade was considered to be a reasonable base for comparison, failure rate estimates were developed by applying factors to this data. These factors, arrived at mainly through engineering judgement, attempted to account for differences in materials, construction techniques, etc., between the existing blade and the FREB concept being evaluated. In areas where no reasonable basis for comparison was found, other reference sources were examined. These included Navy and Marine Corps 3-M data and Army TAMMS data on many different helicopter models. Despite the availability of these rather extensive data files, however, in some cases no relevant experience base could be found, and it was necessary to rely mainly on engineering judgement to estimate failure rates. Where such judgements were necessary, Reliability consulted with the Materials Engineering and Stress groups to obtain guidance on such factors as material strength, environmental properties and stress levels.

Analysis of Induced Failure Modes

Induced modes of failure for a rotor blade emanate from handling damage, foreign object impacts and ballistic hits. The rate at which these events occur will vary considerably with the mission, the environment and maintenance operations.

In the analysis of induced failures, external damage events, i.e., dents, tears, punctures, etc., were projected to be of the same type, and to occur at the same frequency, as those reported in the UH-1D/H rotor blade failure data. Modes of induced failure and their overall rate of occurrence thus remain unchanged from concept to concept. However, the distribution of induced failures, i.e., the relative proportion of damage events incurred by various elements of the blade and their

disposition in terms of repair or scrap, were evaluated for each concept, separately. This was done by applying the random damage scenario to each concept.

An overlay of the FREB concept planforms was used to determine which of the 100 potential damage incidents portrayed by the scenario would intersect the blade and the components of the blade affected by each incident. (The incident locations on the blade planform and their dimensional description as to span, chord and depth were determined for the scenario via random number selection.) In general, the random damage scenario was used as supplied. Some modifications were necessary, however, when the damage event, as described by the scenario, was not compatible with the blade design and construction. This would happen, for example, if the scenario described a "tear" of a metal component. Based on prior analysis of the scenario and specific laboratory testing, the following modifications related to damage depth were employed:

1. All battle damage was considered to penetrate through full blade thickness.

2. All punctures were considered to have penetrated through half the blade thickness.

3. Depths of dents, tears and foreign object damage occurring in areas other than the spar are as defined by the random analysis.

4. Depths of dent, tears and foreign object damage occurring in the spar area were adjusted to reflect the relative strength of the spar.

Each of the damage events in the scenario was analyzed to determine the components of the blade affected and the extent of damage sustained. In each case, a decision was made to repair the described damage in the field, or to scrap the blade. Damage events outside the planform of the blade concept being evaluated were considered "misses".

The results of the random damage analysis were then translated into a reliability prediction for induced failure modes by apportioning the rate of induced damage (as derived from the UH-1D/H rotor blade failure and scrap rate analysis) on the basis of the distribution obtained from the scenario. The prediction, based as it was on a random selection of external damage events, is considered to be representative of the failure distribution that might be experienced in actual operation under combat conditions.

FMEA and Failure Rate Prediction

The results of the FMEA and failure rate predictions, for both inherent and induced failure modes, are given in Table 10. The table compares the predicted reliability of the two basic FREB concepts with that of the existing UH-1D/H blade, based on an assumed MTBF for the present blade of 1,000 hours. Predicted failure rates for the two FREB design concepts are approximately 15% lower than those reported for the current UH-1D/H blade. FREB Concept 3/4 has a predicted failure rate slightly lower than Concept 1/2.

Maintainability Analysis

The FREB program had, as its principal objective, the design of a rotor blade with significantly lower costs over its life cycle. The studies of repairable and expendable blade concepts preceding award of the FREB contract had shown that field repairability would be a major factor in the design of a lower cost rotor blade. Achieving significant improvements in repairability would require that maintainability have a large influence in design.

There were two important aspects to the maintainability program. One was an analytical effort involving the specification of design goals and the measurement and demonstration of maintainability. The other was an engineering effort involving the design and development of repair systems for the FREB, i.e., the repair methods, tools and equipment.

Maintainability Measurement and Specification

One aim of the FREB program was to demonstrate that R&M requirements could be specified as major design goals for a rotor blade and that progress toward achieving these goals could be monitored effectively during design. The one quantitative maintainability goal specified by the Army for design of the FREB was the 95th percentile field repair time of 3 hours. In order to provide meaningful criteria for the designer, it was necessary to translate this requirement into repair time goals for specific tasks, based on their expected frequency. This was done by performing a maintainability allocation.

The allocation of repair time necessarily required a prior definition of the design concept, since the basic configuration and materials employed would be influential in the allocation. In the area of external damage, for example, the frequency of events was fixed for all FREB concepts by the damage scenario supplied by the Army (modified only by variances in blade planform which avoid certain damage events). However, the severity

TABLE 10. FAILURE RATE* SUMMARY

FAILURE CLASS	UH-1D/H BLADE	FREB CONCEPT 1/2	FREB CONCEPT 3/4
Inherent	348.6	229.6	198.6
Induced	651.4	659.9	651.4
TOTAL	1000.0	889.5	850.0

*Failures per 10^6 blade hours.

of damage resulting from each of the events programmed in the scenario would be dependent upon the construction of the blade and the materials in the area of the damage.

The damage sustained by a stainless-steel spar, as a result of impact by a certain projectile, would expectedly be less than that sustained by a fiberglass or aluminum spar of equivalent construction. In one case the damage may be negligible and require no repair. In the other, serious damage requiring blade scrappage may result. Because of this, an allocation of repair times to the blade spar, without regard to the type of spar, would be quite meaningless and, perhaps, needlessly restrictive. The repair time allocation was based, therefore, on a broad definition of the blade design concept in which the proposed configuration and materials were tentatively identified, e.g., rolled and bonded stainless-steel spar with fiberglass aft section and skins. Table 11 shows the repair/scrap assignments by blade component and failure mode developed for the selected FREB concept.

Using the design concept definition, the frequency of damage or failure was apportioned to components of the blade, based on the damage scenario and the preliminary estimate of inherent failure rates. The nature of the anticipated damage or failure was tentatively identified on the basis of the cause and the proposed blade construction in the affected area. These preliminary determinations were subject to repeated modifications as the specific design characteristics of the blade evolved.

The estimated frequency of failure and damage provided the basis for allocating repair time to discrete elements of the blade (spar, skin, core, etc.). An initial decision was made in the case of each failure or damage incident either to scrap the blade or to provide for repair, either on or off the aircraft. In some cases, such as massive damage to the spar, the decision to scrap was obvious. In others, an engineering analysis was needed to assess the reliability, safety and economic implications of the contemplated repair. These analyses relied mainly on intuitive judgements in the early stages of the design definition and were refined as the design progressed.

The next step in the allocation process was to assign a repair time goal to each type of repair task. The repair time allocation reflected the initial engineering estimate of the average elapsed time required for the typical Army mechanic to perform specified types of repair on the blade. It encompassed the time required to isolate and correct the fault, including any adhesive curing time, and place the aircraft in an operational status. It attempted to reflect expected performance under field maintenance conditions and the resources available to

TABLE 11. REPAIR/SCRAP DISPOSITION ANALYSIS, FREB CONCEPTS 1/2

BLADE COMPONENT	FAILURE MODE/DAMAGE EVENT									
	CRACKED	BENT, DISTORTED	PUNCTURED, TORN	DELAMINATED	DENTED	CORRODED	ERODED	NICKED, SCRATCHED	WORN, OVERSIZE	LOOSE OR MISSING HARDWARE
Abrasion sheath (Polyurethane tape)			I	I			I	I		
Spar (Aluminum)	S	S	S	S	A	R	A	A R		
Skin (Fiberglass)	R		R	R	A			A R		
Core (Nomex)			R		A R					
T E Spline (Aluminum)	S	S	S	S	A R	R		R		
Trim tab (Aluminum)	I	R I	I	I	A I	R I		R I		
Root doublers (Aluminum)	S		S	S	S	R		R		
Grip and drag plates (Aluminum)	S		S	S	S	R		R		
Grip pad (Steel)	S		S	S		R		R		
Grip and drag bushings (Steel)	S					R		R	S	
Root closure (Aluminum)	S		S	S	A	R		R		
Tip closure (Fiberglass)	R		R	S	A			A R		
Root cap (Aluminum)	I		I		I	R I		R I		R
Tip cap (Aluminum)	I	I	I		I	R I	A	R I		R

CODES: A = Acceptable as is (if within limits)
R = Repair (if within limits)
I = Install replacement detail
S = Scrap rotor blade

the field mechanic. It was an estimate of productive maintenance time only, however, and did not account for supply delays, administrative time, etc.

After repair times had been allocated to each type of repair, the mean time to repair (MTTR) for the entire blade was calculated, using the frequency of occurrence obtained from the reliability analysis as the weighting factor. The 95th percentile repair time (M_{max}) for the overall blade was calculated next, using a regression equation which relates the mean repair time to the variance of the distributed repair times. (A discussion of this equation, and its derivation, is contained in Appendix III to Reference 1.) If the value of M_{max} exceeded the 3-hour specification, the repair time goals were tightened. The analyst would review the distribution of repair tasks and allocated goals and reduce repair times on those tasks for which a more stringent specification appeared feasible. After these adjustments had been completed, M_{max} for the overall blade was again calculated and compared with the 3-hour specification. If no combination of feasible repair time goals would satisfy the requirement, changes to the basic design concept would be pursued with the designer. Figure 26 shows the format in which data for the maintainability allocations were assembled. The allocated repair times became goals against which predictions were compared as the design work proceeded.

Analysis and prediction of maintainability was an extension of the allocation process, an iterative procedure of upgrading and refining the original allocations, as new design information became available. A computer program had been developed by the contractor for conducting maintainability predictions as part of the life-cycle cost analysis. Using individual task times and frequencies as the basic inputs, and the techniques discussed earlier for predicting parameters of the repair time distribution, the program calculates the following maintainability indices by component and level of maintenance:

a. Mean Time to Repair (MTTR)

b. Mean Preventive Action Time ($\bar{M}_{pt}$)

c. Mean Corrective Maintenance Time ($\bar{M}_{ct}$)

d. Maintenance Man-Hours Per Flight-Hour (MMH/FH)

e. 95th Percentile Corrective Maintenance Time (M_{max})

Use of the computer program facilitated the maintainability prediction task and permitted the impact of changes in

MAINTAINABILITY ALLOCATION

BLADE CONFIGURATION: _____ DATE PREPARED: _____ REV: ____

BLADE ELEMENT AND DAMAGE OR FAILURE DESCRIPTION	FMEA REFERENCE	INHERENT	EXTERNAL	EVENTS PER 10^6 FLIGHT-HOURS	MAINTENANCE ACTION	LEVEL	TIME - HOURS: ON A/C	OFF A/C	REMOVE AND INSTALL	REPAIR	TOTAL	95th PERCENTILE M_{max}	NO. MEN	MAN-HOURS PER FLIGHT HOUR x 10^4	EQUIPMENT REFERENCE	REPAIR KIT REFERENCE
SPAR																
Abraded or Erroded		X		20	Blend/Refinish	ORG	X			1.2	1.2		1	.24		1
Nicked or Scratched			X	5	Restore Profile	ORG	X			0.8	0.8		1	.04		1
Dented			X	85	Restore Profile	ORG	X			0.8	0.8		1	.68		1
Worn		X		20	Blend/Refinish	ORG	X			1.2	1.2		1	.24		1
Abrasion Sheath Loose		X		10	Restore Bond.	ORG	X			1.5	1.5		1	.15	2	2
SKIN AND CORE																
Cracked		X		50	Patch	ORG	X			1.6	1.6		1	.80		3
Puncture thru 1 Surface Skin & Core			X	5	Patch	ORG	X			1.8	1.8		1	.09		3
Delamination between Skin & Core		X		80	Patch	ORG	X			2.0	2.0		1	1.60		3
TOTAL				275										3.84		
WT. AVG.											1.26	3.1				

Figure 26. Maintainability Allocation Data Format.

maintenance functions, failure rates, task times, etc., to be analyzed easily. The maintainability predictions paralleled the allocation techniques described earlier and used the same format for documenting results. Table 12 shows, in abbreviated form, the maintainability prediction for the selected FREB design, Concept 2.

Repair Concept Evaluation

Necessary for the assignment and allocation of repair times was a conceptual definition of the repair procedures to be used. From the work accomplished in the study of repairable blade concepts, repair schemes had been developed for field repair of rotor blades employing afterbodies of Nomex core and glass skin construction, the type of contruction being proposed for the majority of the FREB candidate designs. Procedures for repairing skin and core in the blade afterbody had been defined, and required materials and equipment had been tentatively selected. Estimates for repair time and adhesive cure times had also been established.

After the choice of candidates had been narrowed to two basic design approaches (Concepts 1/2 and Concepts 3/4, both employing the Nomex core/glass skin construction), maintainability estimates were made on the basis of the repair schemes and techniques developed in the study of repairable blade concepts. Time estimates for other types of repairs, metal reworking for example, were also based on those developed under the repairable blade study except in cases where tasks were newly introduced with a concept, in which event an independent time estimate was made.

The repair systems developed for the FREB were basically conceived in the study of repairable blade concepts, although many refinements were made in the techniques, tools and materials during the FREB design and development program. A complete discussion of the repair concepts for the FREB is contained in a later section of this report.

TABLE 12. MAINTAINABILITY PREDICTION (REPAIRABLE FAILURE/DAMAGE)

BLADE ELEMENT	FAILURE OR DAMAGE DESCRIPTION	% OF TOTAL EVENTS	MAINTENANCE ACTION	TIME (HOURS) REPAIR	CURE/ DRY	TOTAL	REPAIR PROCED. NO.	REPAIR KIT NO.
SPAR	Corroded, Eroded, Nicked, Scratched, Abraded	15.6	Blend/Refinish	0.32	--	0.32	2-5	--
SKIN	Dented, Nicked, Scratched, Abraded	42.7	Skin Patch	1.10	0.25	1.35	2-1	1, 3, 5
SKIN/CORE	Punctured, Torn, Dented, Battle Damage	9.6	Skin Patch	1.10	0.25	1.35	2-1	1, 3, 5
		3.2	Double Skin Patch	2.03	0.50	2.53	2-1	1, 3, 5
		11.2	Plug Patch	1.42	0.25	1.67	2-2	7, 9, 101, 103, 105, 107
		8.0	Double Plug Patch	2.63	0.50	3.13	2-2	7, 9, 101, 103, 105, 107
GRIP AND DRAG PLATES	Corroded, Nicked, Scratched	3.3	Blend/Refinish	0.32	--	0.32	2-5	--
GRIP AND DRAG BUSHINGS	Nicked, Scratched	0.1	Polish	0.18	--	0.18	2-6	--
GRIP PAD	Corroded, Nicked, Scratched	0.5	Polish, Blend/ Refinish	0.32	--	0.32	2-6	--
GRIP DOUBLERS	Nicked, Scratched	0.7	Blend/Refinish	0.32	--	0.32	2-5	--

TABLE 12. MAINTAINABILITY PREDICTION (REPAIRABLE FAILURE/DAMAGE) (continued)

BLADE ELEMENT	FAILURE OR DAMAGE DESCRIPTION	% OF TOTAL EVENTS	MAINTENANCE ACTION	TIME (HOURS) REPAIR	CURE/ DRY	TOTAL	REPAIR PROCED. NO.	REPAIR KIT NO.
TIP CAP	Cracked, Bent, Distorted, Punctured, Dented, Battle Damage	0.5	Replace Tip Cap	0.20	--	0.20	2-3	--
	Corroded, Nicked, Scratched, Eroded, Abraded	0.3	Blend/Refinish	0.32	--	0.32	2-5	--
	Loose, Missing Hardware	0.2	Secure/Replace Hardware	0.10	--	0.10	2-3	--
TRAILING-EDGE SPLINE	Corroded, Nicked, Scratched, Dented	4.2	Blend/Refinish	0.32	--	0.32	2-5	--
TRIM TAB	Corroded, Nicked, Scratched	0.1	Blend/Refinish	0.32	--	0.32	2-5	--
	Bent, Distorted	0.1	Mech. Straighten	0.32	--	0.32	2-4	--
	TOTAL EVENTS	100.0	AVERAGES	1.09	0.22	1.30		

SELECTION OF FREB FINAL DESIGN

All of the concepts using the modified airfoil were eliminated from further consideration because of the unacceptable deterioration in acoustic signature. In addition, the methods used for carving the curved surfaces in blade afterbodies are well developed, and the fabrication cost reduction resulting from the straight-sided afterbody would be relatively small.

The remaining three candidate concepts, numbers 2, 4 and 6, exhibit similar degrees of afterbody repairability. The stainless steel spar sections of Concepts 4 and 6 are thought to be less susceptible to dents and dings than the heavy-walled section of Concept 2. However, Concept 2 offers fewer components and their resulting bond lines than the multi-piece stainless steel spars of Concepts 4 and 6. Additionally, Concept 2 offers the lowest life-cycle costs of the remaining three candidates. Therefore, Concept 2, as shown in Figure 27, was chosen as the candidate most likely to be able to meet the program requirements.

Schematics of the blade design are given in Figures 27, 28 and 29. The FREB has the same chord (21"), span (288" at tip) and airfoil (NACA 0012) as the existing blade. Its main features are the single-piece, extruded spar and spline and the composite afterbody. The spar is used in the as-extruded condition and is twisted prior to final blade assembly. The trailing edge spline is also extruded and is slab-cut prior to final blade assembly. The cut tapers the chordal dimension from 2.78" at station 81 to .78" at station 210, and then retains the .78" dimension out to the tip. The root reinforcement is very similar to that of the existing blade. For cost reduction the sheet aluminum doublers have the same shape and are staggered. The aluminum trim tab was lengthened and reduced in chordal dimension to provide increased bond area on the spline. In addition, the trim tab's reduced width makes it a stiffer "beam", less susceptible to handling damage. The tip weight retention is designed for ease of modification after blade repair. Removal of four screws on the tip cap allows ready access to the tip weight "washers" which are moved in accordance with a re-balancing chart.

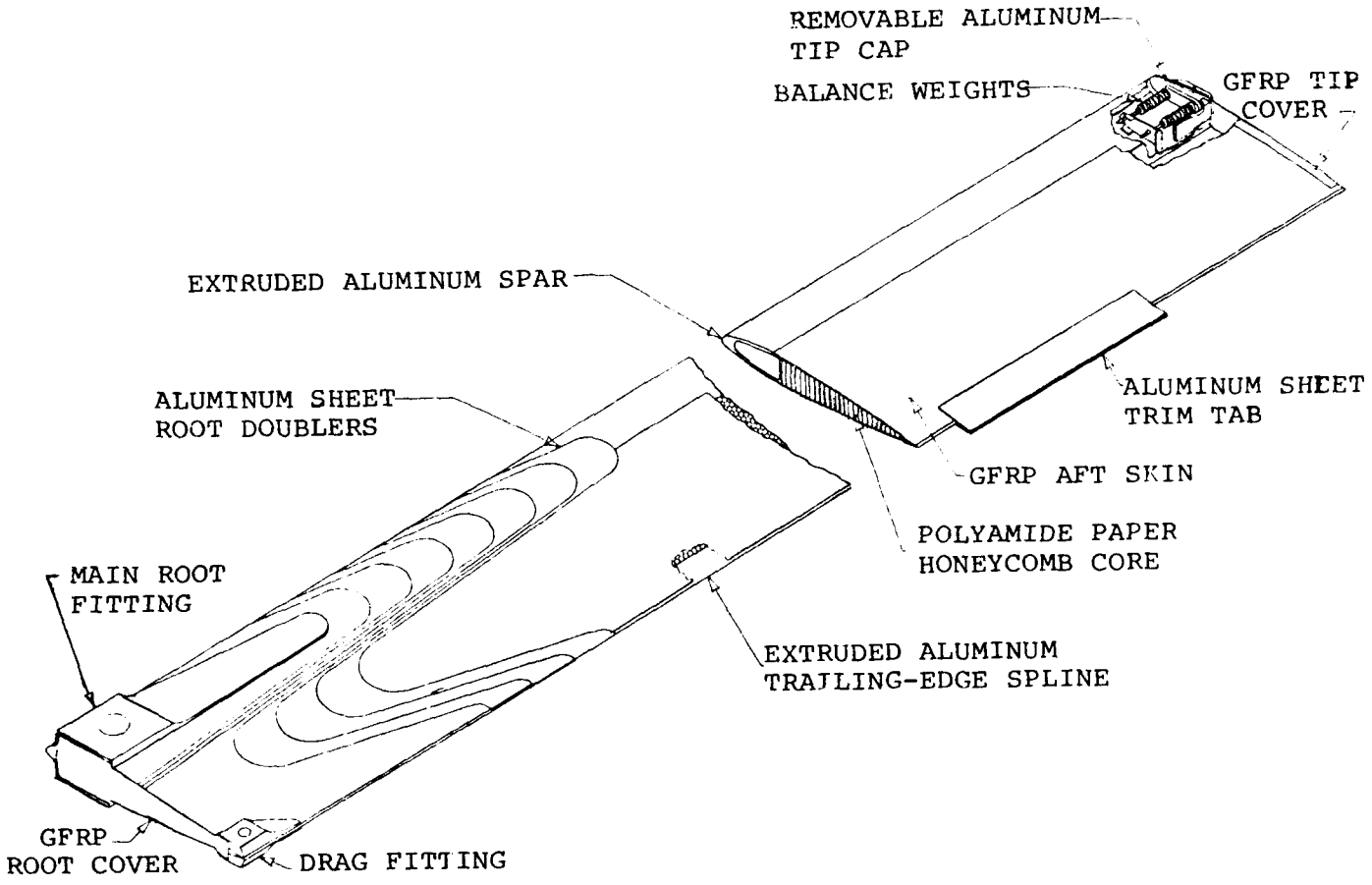

Figure 27. FREB Blade Schematic.

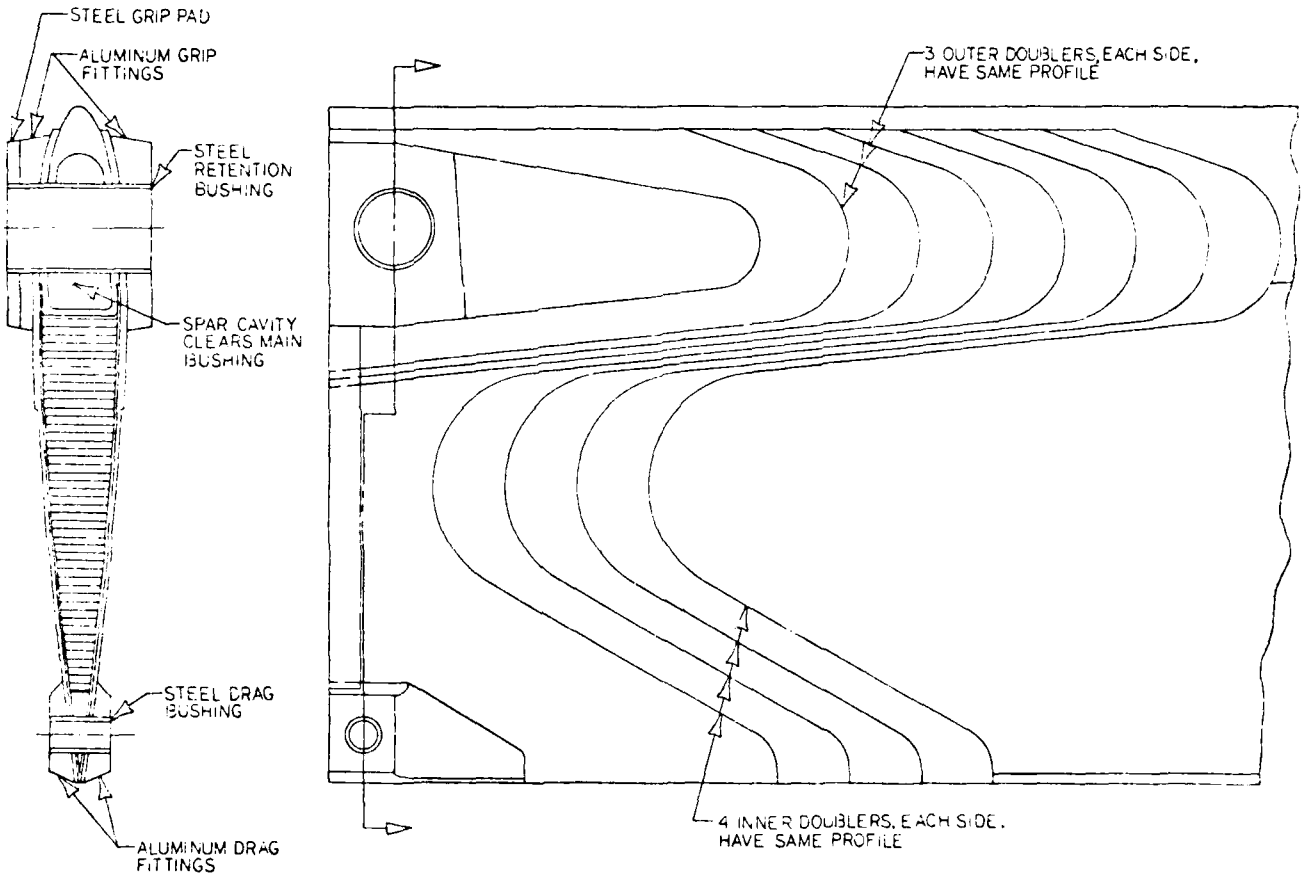

Figure 28. FREB Root End Schematic.

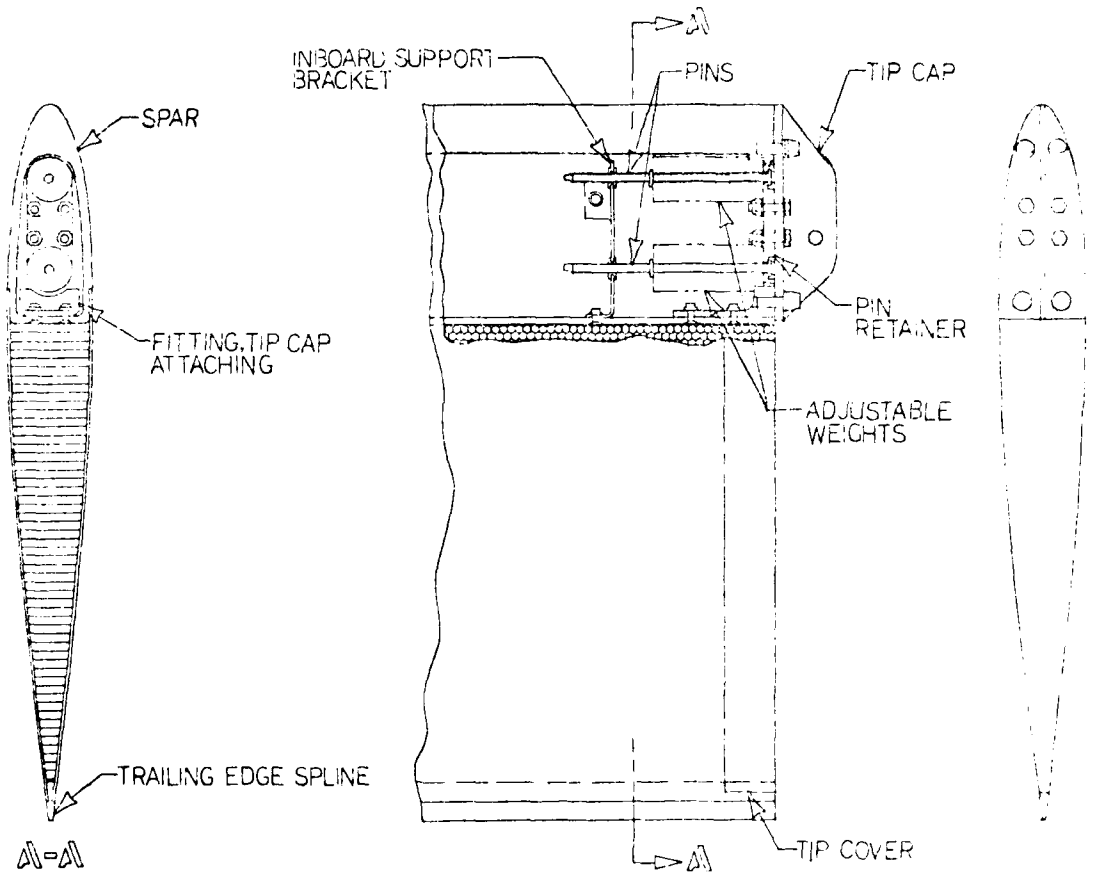

Figure 29. FREB Tip Weight Schematic.

TECHNICAL EVALUATION

The most direct method of insuring that the FREB will be compatible with the UH-1 helicopter system is to reproduce the characteristics of the present UH-1H blade as closely as possible. Wherever possible, the FREB design was evaluated by running similar analyses on both the FREB and the present UH-1 blade. Ideally, comparison of these analyses should not show the FREB design to be inferior to the present UH-1 blade.

SECTION PROPERTIES

The section properties for the FREB design are those shown for Concept 2 in Figures 7 through 12. A detailed numerical listing is given in Table 13. Figures 7 through 12 show good agreement between the section properties of the FREB and those of the existing UH-1 rotor blade.

WEIGHT AND BALANCE

The total blade weight, as given in Table 14, results from the integration of the values in Figure 7. The same compilation for the present blade is given in Table 15. The FREB mass properties are almost identical to those of the present blade.

NATURAL FREQUENCIES AND BENDING MOMENTS

The natural frequencies given in Figure 14, for Concept 2, are the same as those of the FREB final design. These frequencies were calculated using the contractor's standard computer programs. Again, the natural frequencies of the FREB are quite close to those of the present UH-1 blade. Figures 15 and 16, given previously, show the bending moment distribution along the FREB for a fatigue condition (107 kt, ΩR = 793 ft/sec). Figures 30 and 31 show the bending moment distribution along the blade at a limit condition at 1.544 gs.

STRESS ANALYSIS

The following stress analysis uses the moments and centrifugal force given previously to evaluate the structural integrity of the FREB. Wherever similarities between the FREB and the present blade allow, the margin of safety on the FREB will be compared to that of the present UH-1 blade. Wherever the structures differ, positive margins of safety, under both fatigue and ultimate loadings, will be required.

The analysis will be broken down into sections on the main and drag bushings, blade, trim tab, tip weight retention and repairs.

TABLE 13. SECTION PROPERTY SUMMARY, FREB

Sta. (IN.)	EA *1.0E-6	XNA (IN.)	WA (IN/IN.)	XCG (IN.)	EIXX *1.0E-6	EIYY *1.0E-9
25.00	319.400	7.225	3.163	7.301	647.638	13.238
31.00	275.770	5.995	2.746	6.138	595.678	7.754
32.70	147.160	7.461	1.505	7.642	150.770	5.676
46.00	115.930	6.960	1.201	7.196	106.060	4.731
49.50	102.400	6.629	1.068	6.912	88.400	4.200
58.50	82.810	6.200	0.876	6.567	62.300	3.279
65.00	75.913	5.658	0.806	6.096	57.920	2.566
79.00	58.677	5.649	0.636	6.214	34.046	2.271
81.00	56.811	5.668	0.618	6.248	31.718	2.234
210.00	49.410	3.633	0.545	4.514	31.580	0.661
230.86	49.410	3.633	0.545	4.514	31.580	0.661
237.66	49.410	3.633	0.545	4.514	31.580	0.661
237.66	50.152	3.890	0.553	4.745	31.590	0.881
262.80	50.152	3.890	0.553	4.745	31.590	0.881
262.80	49.410	3.633	0.545	4.514	31.580	0.661
288.00	49.410	3.633	0.545	4.514	31.580	0.661

NOTE: Neutral axis and center of gravity distances from chord plane are zero except inboard, where differences between top and bottom grip pads cause slight eccentricities.

TABLE 14. WEIGHT, BALANCE, CF AND DROOP VALUES FOR THE FREB

BLADE WEIGHT AND BALANCE:

TOTAL BLADE WEIGHT	= 198.989	POUNDS
MOMENT ABOUT CENTER OF ROTATION	= 28041.9	LB-IN.
SPANWISE CENTER OF GRAVITY	= 140.922	IN. FROM C. ROT.
CHORDWISE CENTER OF GRAVITY	= 5.74741	IN. FROM L.E.
DYNAMIC MASS AXIS	= 5.07104	IN. FROM L.E.
(I.E. SPAN-WEIGHTED CHORDWISE CENTER OF GRAVITY)		
INERTIA ABOUT CENTER OF ROTATION	= 1179.21	SLUGS-FT. SQ.

CENTRIFUGAL LOADING AT ONE (1.0) RADIAN/SECOND:

SPAN STATION (RADIUS) (INCHES)	CENTRIFUGAL FORCE (POUNDS)	IN-PLANE BENDING MOMENT ABOUT N.A. (LB-IN., + FOR L.E. IN TENSION)
24.50	72.57	255.45
31.80	71.00	112.74
45.90	69.38	82.10
60.00	67.34	46.61
81.00	64.34	60.29
97.12	62.07	47.11
113.25	59.42	34.77
129.37	56.42	23.38
145.50	53.06	13.04
161.62	49.37	3.83
177.75	45.34	-4.16
193.87	41.00	-10.84
210.00	36.36	-16.13
226.50	31.26	-0.18
241.25	26.27	3.48
256.00	20.96	-0.65
282.00	11.06	7.06
288.00	0.00	0.00

STATIC BENDING (DROOP) AT 1.0G:

SPAN STATION (INCHES)	BENDING MOM. (LB-IN.)	DEFLECTION (INCHES)
24.50	23184.08	0.00
31.80	21810.27	0.00
45.90	19422.87	0.03
60.00	17254.55	0.09
81.00	14356.48	0.29
97.12	12344.68	0.56
113.25	10490.58	0.92
129.37	8791.96	1.37
145.50	7246.63	1.89
161.62	5852.37	2.47
177.75	4606.96	3.09
193.87	3508.21	3.76
210.00	2553.89	4.45
226.50	1725.17	5.18
241.25	1111.72	5.84
256.00	619.89	6.51
282.00	45.00	7.71
288.00	0.00	7.98

TABLE 15. WEIGHT, BALANCE, CF AND DROOP VALUES FOR THE CURRENT UH-1H BLADE

BLADE WEIGHT AND BALANCE:

TOTAL BLADE WEIGHT	=	203.495	POUNDS
MOMENT ABOUT CENTER OF ROTATION	=	28959.5	LB-IN.
SPANWISE CENTER OF GRAVITY	=	142.31	IN. FROM C. ROT.
CHORDWISE CENTER OF GRAVITY	=	5.74233	IN. FROM L.E.
DYNAMIC MASS AXIS	=	5.03968	IN. FROM L.E.
(I.E. SPAN-WEIGHTED CHORDWISE CENTER OF GRAVITY)			
INERTIA ABOUT CENTER OF ROTATION	=	1228.84	

CENTRIFUGAL LOADING AT ONE (1.0) RADIAN/SECOND:

SPAN STATION (RADIUS) (INCHES)	CENTRIFUGAL FORCE (POUNDS)	IN-PLANE BENDING MOMENT ABOUT N.A. (LB-IN., + FOR L.E. IN TENSION)
24.50	74.95	15.76
25.00	74.81	266.51
31.80	73.35	119.11
45.90	71.70	87.46
60.00	69.65	50.75
70.50	68.06	71.58
81.00	66.50	65.06
95.50	64.33	65.88
110.00	61.80	13.13
125.60	59.31	14.86
141.20	56.49	16.83
156.80	53.34	19.03
172.40	49.86	21.45
192.00	46.04	-16.09
210.00	38.95	-14.90
227.00	33.07	-13.57
244.00	26.73	16.73
256.57	21.47	-6.78
272.50	14.77	-5.51
282.50	9.18	-4.42
288.00	0.00	0.00

STATIC BENDING (DROOP) AT 1.0G:

SPAN STATION (INCHES)	BENDING MOM. (LB-IN.)	DEFLECTION (INCHES)
24.50	2397.18	0.00
25.00	23877.98	0.00
31.80	22577.30	0.00
45.90	20136.67	0.03
60.00	17916.32	0.10
70.50	16391.36	0.18
81.00	14957.15	0.29
95.50	13103.76	0.52
110.00	11388.09	0.81
125.60	9680.11	1.21
141.20	8099.65	1.68
156.80	6646.71	2.22
172.40	5321.28	2.28
192.00	4123.38	3.46
210.00	2675.45	4.41
227.00	1762.09	5.18
244.00	1025.59	5.96
256.57	597.44	6.55
272.50	197.43	7.30
282.50	34.18	7.77
288.00	0.00	8.03

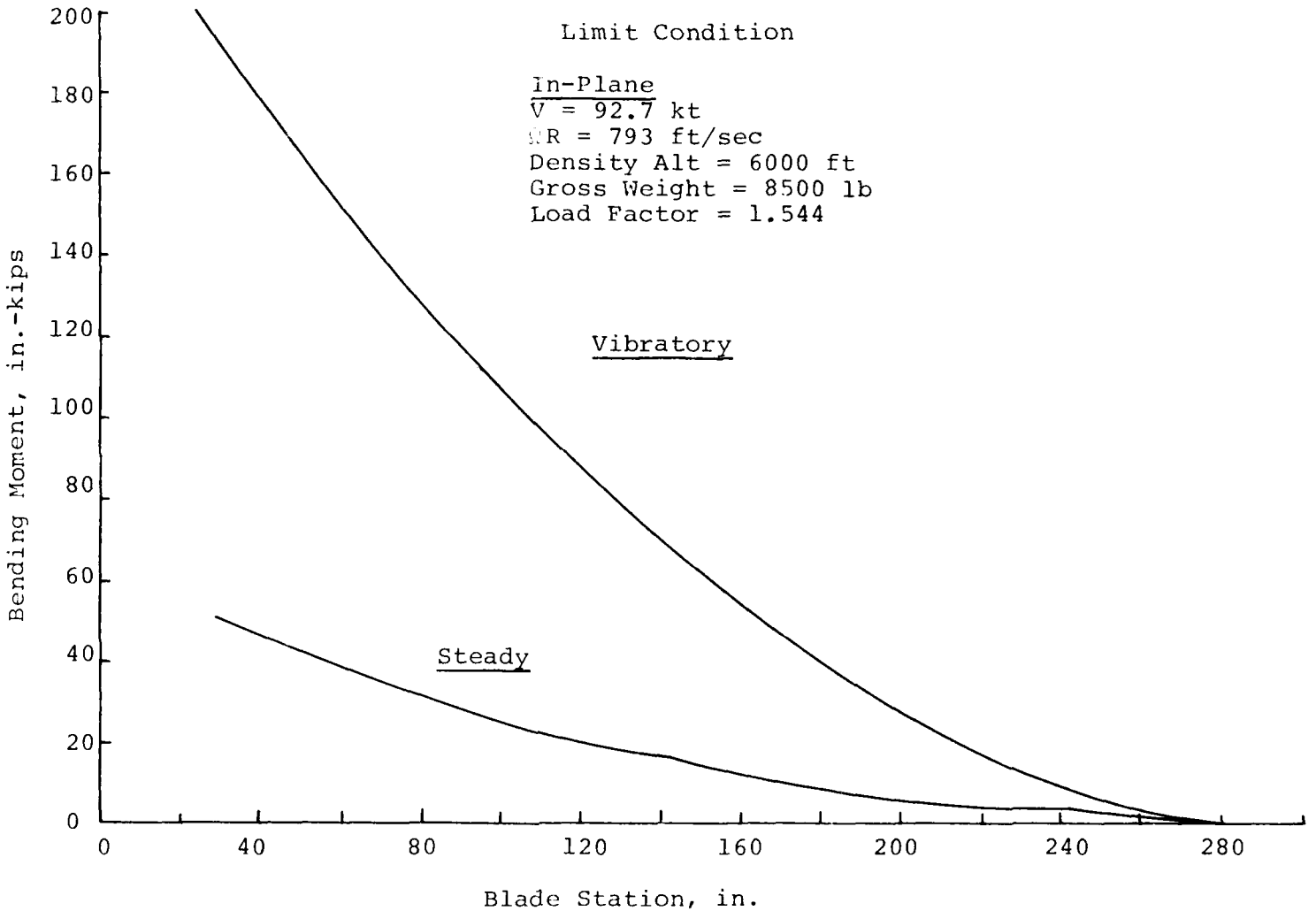

Figure 30. FREB In-Plane Bending Moment Distribution for Limit Condition.

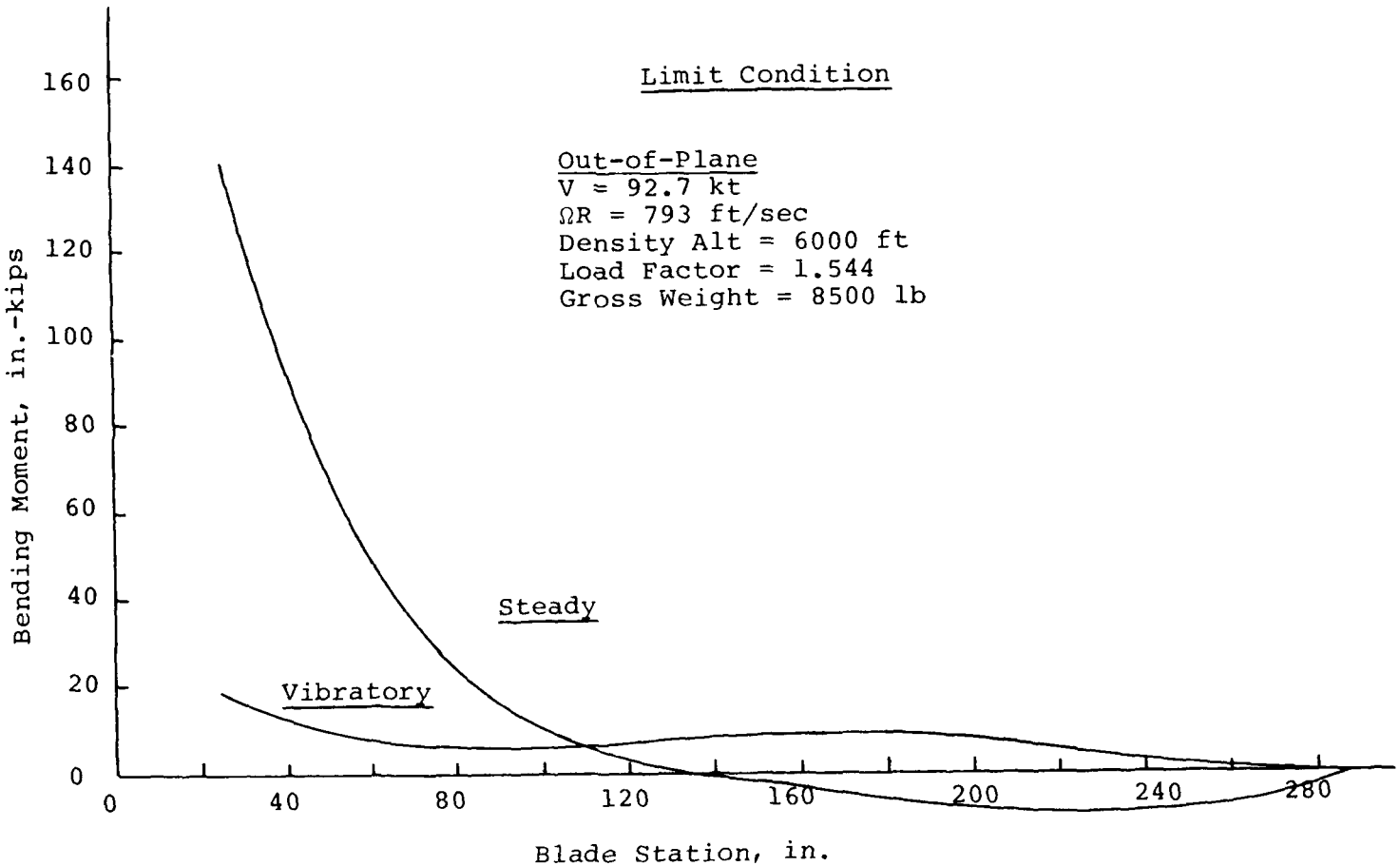

Figure 31. FREB Out-of-Plane Bending Moment Distribution for Limit Condition.

Main and Drag Bushings

The following analysis conservatively assumes that the main pin reacts all the flatwise moment, while the main and drag pins together react the edgewise moment and centrifugal force. The following equations will be used, based upon the geometry shown in Figures 32 and 33:

$$(\sigma_{bru})_{\text{main pin}} = \left(\frac{CF}{2} + \frac{M_{EW}}{14.97}\right) \frac{E}{EA_{TOT}} + \frac{M_{FW} \times C \times E}{EI_{FW}} \qquad (1)$$

$$(\sigma_{bru})_{\text{DRAG PIN}} = \left(\frac{CF}{2} + \frac{M_{EW}}{14.97}\right) \frac{E}{EA_{TOT}} \qquad (2)$$

for the present blade:

$EA_{TOT} = 102.44 \times 10^6$ (main pin)
$EI_{FW} = 299.62 \times 10^6$
$M_{FW_{LIM}} = 270000$
$M_{EW_{LIM}} = 214000$
$CF_{LIM} = 100000$ @ 356 rpm
$Y_{NA} = 1.823$
$EA_{TOT} = 21.25 \times 10^6$ (drag pin)

Reference 3

$$\sigma_{bru\ \text{main pin}} = \left(\frac{100000}{2} + \frac{214000}{14.97}\right) \times \frac{30 \times 10^6}{102.44 \times 10^6} + \frac{270000 \times 1.823 \times 30 \times 10^6}{299.62 \times 10^6}$$

$$= 68112 \text{ psi}$$

$$M.S._{ULT} = \frac{190000}{68112 \times 1.5} - 1 = .86$$

$$\sigma_{bru\ \text{DRAG PIN}} = \left(\frac{100000}{2} + \frac{214000}{14.97}\right) \frac{10 \times 10^6}{21.25 \times 10^6} = 30256 \text{ psi}$$

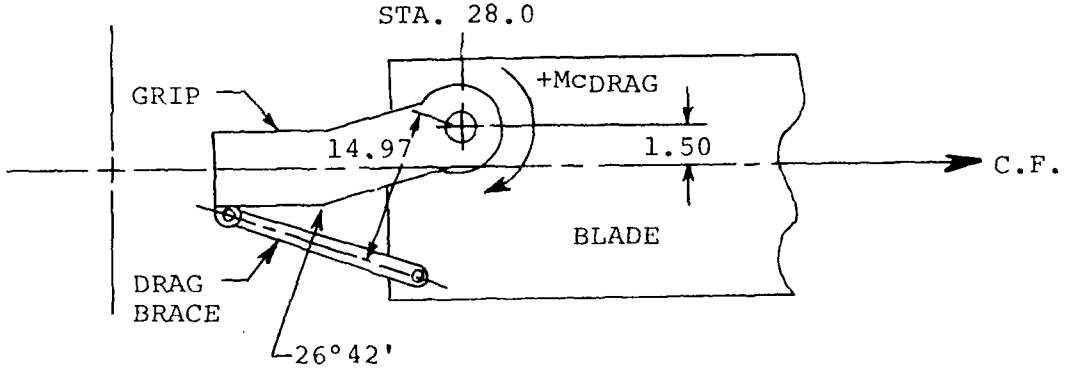

Figure 32. FREB Blade Root Geometry.

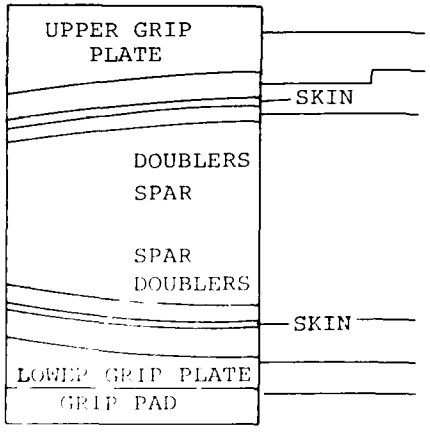

	Proposed Blade		Present Blade	
	MAT'L	F_{BRU}	MAT'L	F_{BRU}
UPPER GRIP PLATE	7075-T73511	101 Ksi	2014 T6	93 Ksi
SKIN	2024 T3	101	18-8 CRES	244
SKIN	6061 T6511	67	2014 T6	93
DOUBLERS				
SPAR				
SPAR DOUBLERS				
SKIN	F/G LAM	8.7*	2024-T3	101
LOWER GRIP PLATE	2024 T3	101	2025-T3	101
GRIP PAD	4130	190	4130	190

* F_{cu}

The drag plate material is 2024-T4, F_{bru} = 93 Ksi

$$M.S._{ULT} = \frac{93000}{30256 \times 1.5} - 1 = 1.05$$

for the FREB:

$EA_{TOT} = 93.4 \times 10^6$ (main pin)

$EI_{FW} = 259.8 \times 10^6$

$M_{FW_{LIM}} = 246000$

$M_{EW_{LIM}} = 214000$

$CF_{LIM} = 96600$ @ 356 rpm

$Y_{NA} = 1.740$

$EA_{TOT} = 21.25 \times 10^6$ (drag pin)

$$(\sigma_{bru})_{\text{main pin}} = \left(\frac{96600}{2} + \frac{214000}{14.97}\right) \times \frac{10}{93.4} + \frac{246000 \times 1.74 \times 30 \times 10^6}{259.8 \times 10^6} = 56129 \text{ psi}$$

$$M.S._{ULT} = \frac{190000}{56129 \times 1.5} - 1 = 1.26$$

$$(\sigma_{bru})_{\text{DRAG PIN}} = \left(\frac{96600}{2} + \frac{214000}{14.97}\right) \times \frac{10 \times 10^6}{21.25 \times 10^6} = 29456 \text{ psi}$$

$$M.S._{ULT} = \frac{93000}{1.5 \times 29456} - 1 = 1.10$$

Therefore, in the area of the grip and drag bushings, the FREB has higher ultimate margins of safety than the present UH-1 blade.

Blade

The blade has been analyzed at stations 60, 81 and 210, under fatigue and ultimate loads. These loads and conditions are defined by Figures 15, 16, 30 and 31. The material properties

used in the blade analysis are given in Table 16. The analysis results are shown in Tables 17 and 18. Based upon conservative values of the fatigue strength of aluminum, the spline and aft doublers are predicted to have a negative margin of safety for infinite life. The current blade was then analyzed to determine its margin of safety in fatigue. Table 19 shows that the current blade has even more negative margins based upon fatigue loading using the same conservative fatigue allowables. It can, therefore, be concluded that the FREB will have a fatigue life in excess of that of the current blade. The FREB has positive margins of safety when analyzed under ultimate loading, as shown in Table 18.

Trim Tab

The trim tab on the present blade has 50.28 square inches of bond area attaching it to the blade. The trim tab on the FREB has 100.56 square inches of bond area. The FREB's trim tab installation is, therefore, adequate by comparison to the present blade's trim tab installation.

Tip Weight Retention

The tip weight retention for the FREB is shown in Figure 29. The following weights contribute to the centrifugal force on the four retainer bolts:

Qty.	Description	Wt, Lb	Span CG	WS
2	K30-115 Pins	.18	285.3	51.354
*	K30-119 Wts	3.36	286.0	960.960
1	K30-113 Retainer	.14	287.8	40.292
4	MS20005 Bolts	.12	287.9	34.548
4	NAS1104-9 Bolts	.07	288.0	20.160
4	MS21042 Nuts	.01	288.0	2.880
1	K30-116-11 Cap	.44	288.7	127.028
				1237.222

$$\text{Limit CF} = Mr\omega^2 = \frac{1237.22}{386} = \frac{324 \times 1.1 \times 2}{60} = 4464.7 \text{ lb}$$

The tip cap will be analyzed using the free-body diagram shown in Figure 34.

TABLE 16. BLADE MATERIALS AND ALLOWABLES

ITEM	MAT'L	F_{Tu}	F_{cu}	F_E	E
Spar (K30-102)	6061-T6511	42 Ksi	-42 Ksi	6 Ksi	9900 Ksi
Spline (K30-106)	6061-T6511	42	-42	6	9900
Skins (K30-104)	*	35	-17.4	4	2080
Doublers (K30-108)	2024-T3	60	-60	6	1050
Grip Plates (K30-103)	7075-T7351	68	-68	6	1040
Drag Plates (K30-107)	7075-T7351	68	-68	6	1040
Grip Pad (K30-104)	4130 Cond N	125	-125	18	2900

*2 Plies XP114 laid up at $\pm$ 45° between two plies of 120 glass cloth

TABLE 17. FREB STRESS ANALYSIS SUMMARY, FATIGUE LOADING

STATION 60.00

STRESSES BELOW ARE BASED ON THE FOLLOWING BLADE SECTION PROPERTIES AND LOADS. FUNCTIONS OF MODULUS ARE IN MILLIONS.

EA= 81.2 XNA= 6.075 YNA=+0.000 EIXX= 61.3 EIYY=3114.5

STRESSES WILL BE CALCULATED ACCORDING TO THE FORMULA:
STRESS= (CF*E/EA) + (MX*Y*E/EIXX) + (MY*X*E/EIYY)

FOR FATIGUE CONDITION:
MX= +4.5 +/- 6.0 IN-KIPS MY= +34.0 +/- 99.0 IN-KIPS
CF= +74.00 KIPS

COMPONENT	COORDINATES X	COORDINATES Y	CF STRESS (KSI)	MX STRESS (KSI) STEADY	MX STRESS (KSI) ALT'NG	MY STRESS (KSI) STEADY	MY STRESS (KSI) ALT'NG	TOTAL STRESS (KSI) STEADY	TOTAL STRESS (KSI) ALT'NG	MARGIN OF SAFETY
DOUBLERS	2.700	-1.240	+9.57	+0.96	1.27	+0.39	1.13	+10.91	+2.40	+1.045
DOUBLERS	7.160	-1.420	+9.57	+1.09	1.46	-0.12	0.36	+10.54	+1.82	+1.715
DOUBLERS	19.160	-0.310	+9.57	+0.24	0.32	-1.50	4.37	+8.31	+4.69	+0.103
DOUBLERS	20.620	-0.950	+9.57	+0.73	0.98	-1.67	4.85	+8.63	+5.83	-0.119
SPAR	0.000	+0.000	+9.02	+0.00	0.00	+0.66	1.91	+9.69	+1.91	+1.415

STATION 91.00
EA= 56.8 XNA= 5.669 YNA=+0.000 EIXX= 31.7 EIYY=2233.5
FOR FATIGUE CONDITION:
MX= +2.0 +/- 5.5 IN-KIPS MY= +28.0 +/- 32.0 IN-KIPS
CF= +70.60 KIPS

COMPONENT	COORDINATES X	COORDINATES Y	CF STRESS (KSI)	MX STRESS (KSI) STEADY	MX STRESS (KSI) ALT'NG	MY STRESS (KSI) STEADY	MY STRESS (KSI) ALT'NG	TOTAL STRESS (KSI) STEADY	TOTAL STRESS (KSI) ALT'NG	MARGIN OF SAFETY
DOUBLER	5.000	-1.400	+13.05	+0.93	2.55	+0.09	0.26	+14.06	+2.81	+0.637
SPAR	0.000	+0.000	+12.30	+0.00	0.00	+0.70	2.06	+13.01	+2.06	+1.011
SPLINE	21.000	-0.023	+12.30	+0.01	0.04	-1.90	5.57	+10.41	+5.61	-0.196

STATION 210.00
EA= 49.4 XNA= 3.663 YNA=+0.000 EIXX= 31.6 EIYY= 660.8
FOR FATIGUE CONDITION:
MX= -5.0 +/- 6.0 IN-KIPS MY= +5.0 +/- 15.0 IN-KIPS
CF= +36.75 KIPS

COMPONENT	COORDINATES X	COORDINATES Y	CF STRESS (KSI)	MX STRESS (KSI) STEADY	MX STRESS (KSI) ALT'NG	MY STRESS (KSI) STEADY	MY STRESS (KSI) ALT'NG	TOTAL STRESS (KSI) STEADY	TOTAL STRESS (KSI) ALT'NG	MARGIN OF SAFETY
SPAR	0.000	+0.000	+7.36	+0.00	0.00	+0.27	0.92	+7.64	+0.92	+4.964
SPAR	5.500	+1.257	+7.36	+1.97	2.36	-0.14	0.41	+9.20	+2.78	+0.647
SKIN	5.500	+1.257	+1.55	+0.41	0.50	-0.03	0.09	+1.93	+0.59	+5.477
SKIN	20.620	+0.043	+1.55	+0.01	0.02	-0.27	0.80	+1.29	+0.82	+3.712
SPLINE	20.620	+0.043	+7.36	+0.07	0.08	-1.27	3.81	+6.16	+3.89	+0.316
SPLINE	21.000	+0.005	+7.36	+0.01	0.01	-1.30	3.90	+6.07	+3.91	+0.314

TABLE 18. FREB STRESS ANALYSIS SUMMARY, ULTIMATE LOADING

STATION 60.00

STRESSES BELOW ARE BASED ON THE FOLLOWING BLADE SECTION PROPERTIES AND LOADS. FUNCTIONS OF MODULUS ARE IN MILLIONS.

EA= 51.2 XNA= 6.075 YNA=+0.000 EIXX= 61.3 EIYY=3114.5

STRESSES WILL BE CALCULATED ACCORDING TO THE FORMULA:
STRESS= (CF*E/EA) + (MX*Y*E/EIXX) + (MY*X*E/EIYY)

FOR ULTIMATE CONDITION:
(MOMENTS GIVEN BELOW ARE 150% OF LIMIT MOMENTS
CF LOADS ARE BASED ON 10% OVERSPEED)

MX= +87.0 +/- 0.0 IN-KIPS MY= +256.0 +/- 0.0 IN-KIPS
CF= +89.54 KIPS

COMPONENT	COORDINATES X	COORDINATES Y	CF STRESS (KSI)	MX STRESS (KSI) STEADY	MX STRESS (KSI) ALT'NG	MY STRESS (KSI) STEADY	MY STRESS (KSI) ALT'NG	TOTAL STRESS (KSI) STEADY	TOTAL STRESS (KSI) ALT'NG	MARGIN OF SAFETY
SPAR	0.000	+0.000	+10.91	+0.00	0.00	+5.56	0.00	+16.48	+0.00	+1.549
SPAR	5.500	-1.257	+10.91	+17.66	0.00	+0.53	0.00	+29.10	+0.00	+0.443
SKIN	5.500	-1.257	+2.29	+3.71	0.00	+0.11	0.00	+6.11	+0.00	+4.724
SKIN	20.620	+0.043	+2.29	-0.13	0.00	-2.80	0.00	-0.63	+0.00	+26.555
SPLINE	20.620	+0.043	+10.91	-0.60	0.00	-13.38	0.00	-3.01	+0.00	+12.974
SPLINE	21.000	+0.005	+10.91	-0.07	0.00	-13.66	0.00	-2.82	+0.00	+13.899

STATION 81.00
EA= 56.8 XNA= 5.668 YNA=+0.000 EIXX= 31.7 EIYY=2833.5
FOR ULTIMATE CONDITION:
(MOMENTS GIVEN BELOW ARE 150% OF LIMIT MOMENTS
CF LOADS ARE BASED ON 10% OVERSPEED)

MX= +42.0 +/- 0.0 IN-KIPS MY= +238.5 +/- 0.0 IN-KIPS
CF= +85.40 KIPS

COMPONENT	COORDINATES X	COORDINATES Y	CF STRESS (KSI)	MX STRESS (KSI) STEADY	MX STRESS (KSI) ALT'NG	MY STRESS (KSI) STEADY	MY STRESS (KSI) ALT'NG	TOTAL STRESS (KSI) STEADY	TOTAL STRESS (KSI) ALT'NG	MARGIN OF SAFETY
SPAR	0.000	+0.000	+14.58	+0.00	0.00	+5.99	0.00	+20.57	+0.00	+1.012
SPAR	5.500	-1.257	+14.58	+16.48	0.00	+0.18	0.00	+31.54	+0.00	+0.332
SKIN	5.500	-1.257	+3.13	+3.46	0.00	+0.04	0.00	+6.63	+0.00	+4.282
SKIN	20.620	+0.043	+3.13	-0.12	0.00	-3.32	0.00	-0.31	+0.00	+54.647
SPLINE	20.620	+0.043	+14.58	-0.56	0.00	-15.81	0.00	-1.49	+0.00	+27.221
SPLINE	21.000	+0.005	+14.58	-0.07	0.00	-16.21	0.00	-1.39	+0.00	+29.176

STATION 210.00
EA= 49.4 XNA= 3.633 YNA=+0.000 EIXX= 31.6 EIYY= 660.8
FOR ULTIMATE CONDITION:
(MOMENTS GIVEN BELOW ARE 150% OF LIMIT MOMENTS
CF LOADS ARE BASED ON 10% OVERSPEED)

MX= -24.0 +/- 0.0 IN-KIPS MY= +40.5 +/- 0.0 IN-KIPS
CF= +44.47 KIPS

COMPONENT	COORDINATES X	COORDINATES Y	CF STRESS (KSI)	MX STRESS (KSI) STEADY	MX STRESS (KSI) ALT'NG	MY STRESS (KSI) STEADY	MY STRESS (KSI) ALT'NG	TOTAL STRESS (KSI) STEADY	TOTAL STRESS (KSI) ALT'NG	MARGIN OF SAFETY
SPAR	0.000	+0.000	+8.91	+0.00	0.00	+2.20	0.00	+11.11	+0.00	+2.779
SPAR	5.500	+1.257	+8.91	+9.46	0.00	-1.13	0.00	+17.23	+0.00	+1.437
SKIN	5.500	+1.257	+1.87	+1.99	0.00	-0.24	0.00	+3.62	+0.00	+8.466
SKIN	20.620	+0.043	+1.87	+0.07	0.00	-2.17	0.00	-0.23	+0.00	+74.436
SPLINE	20.620	+0.043	+8.91	+0.38	0.00	-10.31	0.00	-1.07	+0.00	+38.157
SPLINE	21.000	+0.005	+8.91	+0.04	0.00	-10.54	0.00	-1.59	+0.00	+25.431

TABLE 19. CURRENT UH-1 BLADE STRESS ANALYSIS SUMMARY, FATIGUE LOADING

STATION 60.00

STRESSES BELOW ARE BASED ON THE FOLLOWING BLADE SECTION PROPERTIES AND LOADS. FUNCTIONS OF MODULUS ARE IN MILLIONS.

EA= 95.0 XNA= 5.620 YNA=+0.000 EIXX= 81.0 EIYY=3000.0

STRESSES WILL BE CALCULATED ACCORDING TO THE FORMULA:
STRESS= (CF*E/EA) + (MX*Y*E/EIXX) + (MY*X*E/EIYY)

FOR FATIGUE CONDITION:
MX= +1.0 +/- 5.5 IN-KIPS MY= +38.0 +/- 113.0 IN-KIPS
CF= +73.00 KIPS

COMPONENT	COORDINATES X	COORDINATES Y	CF STRESS (KSI)	MX STRESS (KSI) STEADY	MX STRESS (KSI) ALT'NG	MY STRESS (KSI) STEADY	MY STRESS (KSI) ALT'NG	TOTAL STRESS (KSI) STEADY	TOTAL STRESS (KSI) ALT'NG	MARGIN OF SAFETY
OUTER DBLR	1.245	-0.970	+8.07	+0.13	0.69	+0.58	1.73	+8.79	+2.42	+1.115
OUTER DBLR	5.940	-1.420	+8.07	+0.16	1.01	-0.04	0.13	+8.21	+1.14	+3.547
OUTER DBLR	19.960	-0.200	+8.07	+0.03	0.14	-1.91	5.67	+6.19	+5.81	-0.074
OUTER DBLR	20.620	-0.950	+8.07	+0.12	0.68	-1.99	5.93	+6.20	+6.61	-0.156
ABR STRIP	0.000	+0.000	+20.75	+0.00	0.00	+1.92	5.72	+22.67	+5.72	+1.575

STATION 81.00
EA= 53.0 XNA= 5.900 YNA=+0.000 EIXX= 40.0 EIYY=2400.0
FOR FATIGUE CONDITION:
MX= +0.5 +/- 5.2 IN-KIPS MY= +32.0 +/- 96.0 IN-KIPS
CF= +70.00 KIPS

COMPONENT	COORDINATES X	COORDINATES Y	CF STRESS (KSI)	MX STRESS (KSI) STEADY	MX STRESS (KSI) ALT'NG	MY STRESS (KSI) STEADY	MY STRESS (KSI) ALT'NG	TOTAL STRESS (KSI) STEADY	TOTAL STRESS (KSI) ALT'NG	MARGIN OF SAFETY
OUTER DBLR	0.650	-0.790	+13.87	+0.10	1.08	+0.72	2.15	+14.69	+3.23	+0.403
ABR STRIP	0.000	+0.000	+35.66	+0.00	0.00	+2.09	6.26	+37.75	+6.26	+1.006
SPLINE	21.000	-0.022	+14.26	+0.00	0.03	-2.19	6.57	+12.09	+6.60	-0.274

STATION 210.00
EA= 47.4 XNA= 4.062 YNA=+0.000 EIXX= 30.3 EIYY=1086.1
FOR FATIGUE CONDITION:
MX= -5.5 +/- 4.2 IN-KIPS MY= +5.0 +/- 16.0 IN-KIPS
CF= +45.10 KIPS

COMPONENT	COORDINATES X	COORDINATES Y	CF STRESS (KSI)	MX STRESS (KSI) STEADY	MX STRESS (KSI) ALT'NG	MY STRESS (KSI) STEADY	MY STRESS (KSI) ALT'NG	TOTAL STRESS (KSI) STEADY	TOTAL STRESS (KSI) ALT'NG	MARGIN OF SAFETY
ABR STRIP	0.000	+0.000	+25.66	+0.00	0.00	+0.50	1.52	+26.17	+1.52	+6.830
ABR STRIP	5.500	+1.257	+25.66	+6.15	4.70	-0.18	0.64	+31.64	+5.34	+1.516
SPLINE	21.000	+0.022	+10.27	+0.04	0.03	-0.84	3.03	+9.47	+3.06	+0.649

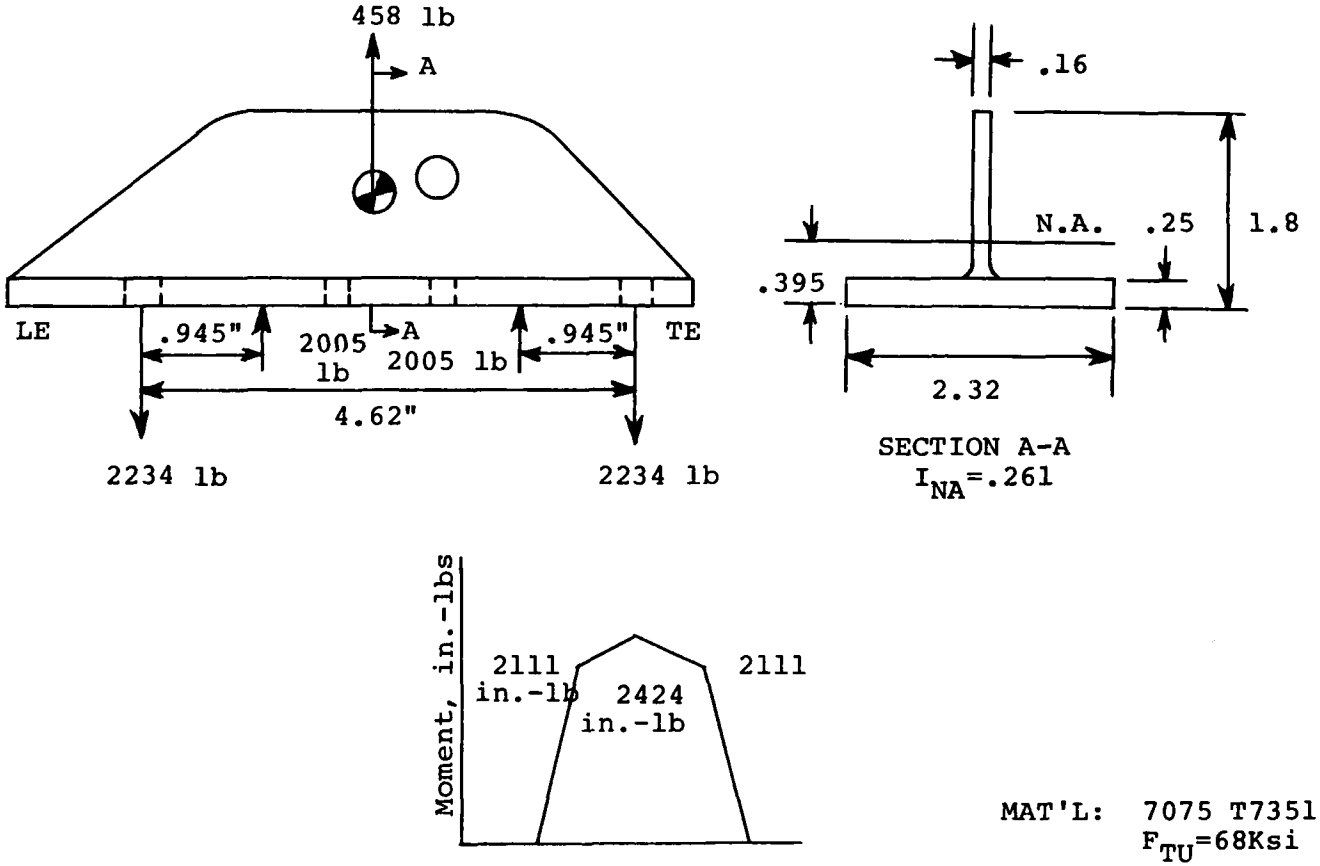

Figure 34. Tip Cap Free-Body Diagram.

Checking stress at section A-A:

$$\sigma_{LIM} = \frac{MC}{I} = \frac{2424 \times .9}{.261} = 8.36 \text{ Ksi}$$

$$M.S._{ULT} = \frac{68}{1.5 \times 8.36} - 1 = 4.42$$

The tip cap is fastened to the blade spar by four MS 20005 bolts. The margin on these bolts is calculated as follows:

$$M.S._{ULT} = \frac{9820}{1.5 \times \frac{4464.7}{4}} - 1 = 4.86$$

The MS 20005 bolts thread into four SR314 fasteners. Per Reference 4, the ultimate pullout strength is 12600 pounds. These inserts have adequate ultimate margin, based on comparison to the MS 20005 bolts.

The aft end of the tip cap is held to the spar by the K30-118 fitting. The critical area on this fitting is the rivet attachment to the aft spar wall. The fitting is attached to the spar by four MS 21140-0606 rivets. The margin of safety on these rivets will be computed as shown in Figure 35 and as follows:

$$\text{Shear load on rivets} = \frac{4464.7}{4} = 1116.18 \text{ lb/rivet}$$

$$\text{Tensile load on rivets} = \frac{R}{2} \times \frac{.450}{1.32} = .1705 \text{ P} = .1705 \times \frac{4464.7}{2}$$

$$= 380 \text{ lb/rivet}$$

The ultimate tensile strength of the rivet is 1690 pounds, while the ultimate shear strength is 2925 pounds, assuming a linear deterioration of shear strength with applied tensile load:

$$M.S._{ULT} = \frac{2925}{1116.18 \times 1.5} - 1 = .16$$

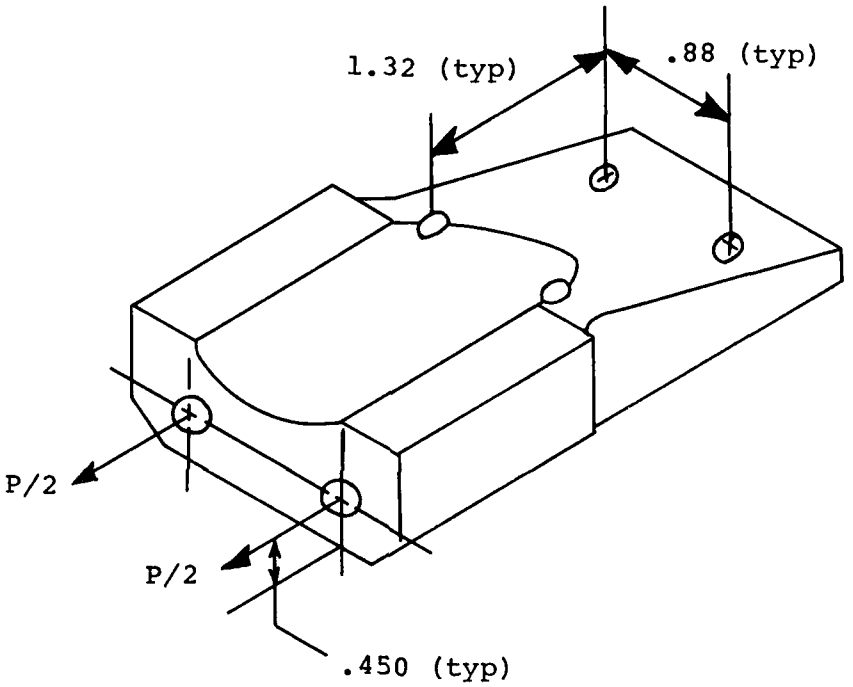

Figure 35. K30-118 Tip Weight Retention Fitting Free-Body Diagram.

REPAIR SYSTEMS

Concepts for repair of rotor blade aft structures comprised of polyamide paper (Nomex) core and glass skins had been conceived in the study of repairable blade concepts for USAAMRDL (Reference 5). It was from these basic concepts that development of the FREB repair system evolved. In formulating concepts for field repair of rotor blades, initially as part of the repairable blade study, and later for design of the FREB, a number of objectives were pursued, some of which were mentioned in the opening section of this report.

First, and most important, was the recognition that repairs would have to be performed on the installed rotor blade and would have to be simple enough to accomplish so that making a repair would be a more attractive alternative, in terms of time and effort, than replacing the blade. Having to remove the rotor blade for repair, despite the capability of performing the repair locally rather than at depot, would greatly diminish the cost effectiveness of a repairable blade, since it would not reduce on-aircraft maintenance time nor improve readiness. Something would be saved in transportation and depot maintenance costs, but the major benefit of improved repairability would be lost. There was also some concern that damaged blades, once removed from the aircraft, might be scrapped rather than repaired if the extent of damage approached allowable limits. A goal was established that no more than 5% of the repairable damage to the FREB require its removal from the aircraft.

While the maximum amount of on-aircraft field repairability was desired in design of the FREB, the ability to repair under extremely adverse ("boondocks") conditions was thought to be unnecessary. It was reasoned that any blade damage repairable on the aircraft would also, via some temporary fix such as wrapping the blade with tape, allow the aircraft to be flown for sufficient time to return to a fixed base. To attempt to provide a repair capability for the most primitive field conditions (no electrical power, work stands, etc.) would impose very difficult and unnecessary constraints on the design.

Simplicity was considered vital to obtaining a successful repair system. One of the Army's requirements was that repairs be within the capability of an UH-1 helicopter repairman, MOS 67N20. Since the MOS 67N20 rate is found at both Organizational and DS/GS maintenance levels, this could represent a wide range of skills and experience. It was decided to tailor the design of the repair system to the skill level of the average flight line repairman or crew chief who, while possessing no specific experience in the repair of composite structures, would be expected to acquire some minimal training

in repair of the FREB. The repair system would have to be simple enough to allow someone of limited skill and experience to make proper repairs after acquiring only a brief course of instruction, i.e., to avoid the need for specialist training.

Aside from the major objectives of simplicity and maximum on-aircraft repairability, a number of secondary objectives relating to the design of the repair methods, kits and tools were established. These are enumerated in the FREB Detail Specification contained in Appendix A of this report and are discussed in the remaining text of this section, which describes the development of the repair kits and tools.

Repair Kits

Objectives in design of the repair kits were to provide the fewest number of kits, consistent with the goal of maximum field repairability, and to provide the repair materials in pre-measured and prefabricated form to avoid the need for custom fabrication at the site. For convenience, all of the consumable materials required for a repair, except hazardous substances and materials with limited shelf life, would be packaged together, including such items as disposable gloves, templates and mixing utensils. Epoxy adhesive would be provided in a separate kit in two-part, premeasured packages. Bulk items, such as cleaning solvents and paint, would be drawn from supply as needed.

Two types of repair kits were devised. One was a skin patch for repair of superficial damage not affecting the core of the blade, and for core damages less than 1-inch in diameter. The other was a combination skin patch and core plug to be used when core damage exceeded 1-inch in diameter. Square and rectangular patches and plugs were considered initially, but it was quickly concluded that round patches offered several significant advantages, including ease of damage cleanup and the need to remove the least amount of material for a given amount of damage.

Skin Patch

The skin patch, shown schematically in Figure 36, is a buildup of three doublers of impregnated glass fabric and scotchply material. After bonding, a molded patch is formed, sized to permit a 1-inch overlap around the damaged area after cleanup. Originally, the patch was supplied with two peel plies to protect the inner and outer surfaces from contamination. The peel plies were the same diameter as the patch, which made removal difficult and required the use of a parting cloth over the patch to prevent the adhesive squeeze-out from coming in contact with the bladder of the pressure/heat pack during curing. The final configuration eliminated the inner peel ply and made the outer ply larger in diameter than the patch, eliminating the

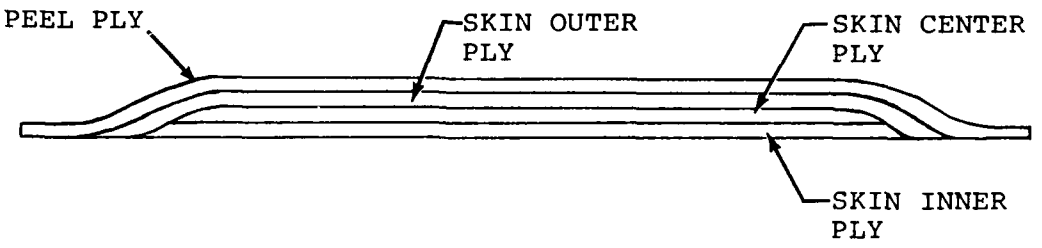

(PLY THICKNESSES DRAWN OVERSIZE FOR CLARITY)

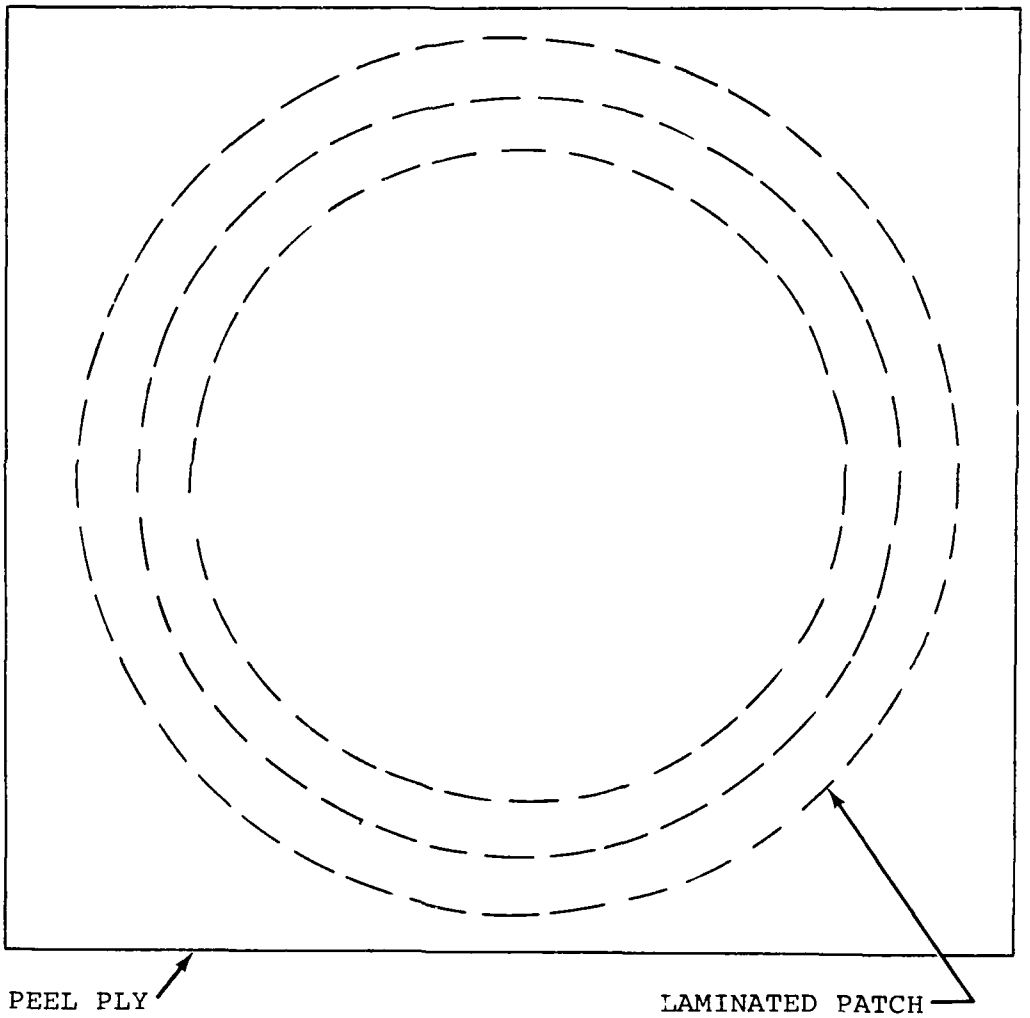

Figure 36. Typical Skin Patch Construction.

need for a parting cloth and facilitating removal. The patch is packaged in a plastic bag to prevent contamination of the inner surface.

Application of the skin patch, the specific procedure for which is explained in Appendix B, essentially involves cleaning and abrading the blade surface and applying the patch under heat and pressure using an epoxy adhesive. Skin damage as large as 7-inches in diameter can be patched with one of the standard kits. Core damage, not exceeding 1-inch in diameter, can be repaired with a skin patch without replacing the damaged core (two patches being used for through-damage). Selection of patch sizes for the repair kits was based on an analysis of the damage events presented by the Army's random damage scenario. All of the damage events which could be repaired with a skin patch (surface damage and confined core damage) were ranked in order of size. Patch sizes were selected to provide the maximum repairability with the fewest number of kits. This selection resulted in patch sizes of 3 inches, 5 inches and 7 inches in diameter.

Plug Patch

The plug patch, shown schematically in Figure 37, is a skin patch to which a cylindrical section of core material, smaller in diameter, is bonded. Installation of a plug patch, the specific procedure for which is explained in Appendix B, essentially involves removing the damaged core, cleaning and abrading the surface surrounding the cavity, and bonding the plug into place under heat and pressure using an epoxy adhesive. Like the skin patch, the first plug patch used two peel plies of the same diameter as the patch and were later modified to use only an outer ply, larger than the patch, to accommodate the adhesive squeeze-out and to facilitate removal. The plug patch is also packaged in a plastic bag.

Selection of plug patch sizes for the repair kits was based on the same analysis used for the selection of skin patch sizes. Plug sizes were selected, based on the damage events portrayed in the random damage scenario, to provide the maximum repairability with the fewest number of kits. This resulted in the selection of two plug diameters, 3 inches and 7 inches, and three plug depths, 1/4 inch, 1/2 inch and 1-1/4 inches, a total of six plug patch kits. The 7-inch-diameter core plug is the largest which can be accommodated by the pressure heat pack, the skin section of the patch being 9 inches in diameter. 3 inches in diameter was found to be the optimum size for a small plug, based on the analysis of typical damage events.

The 7-inch diameter of the largest plug is smaller than that required to repair the largest damage events represented in the

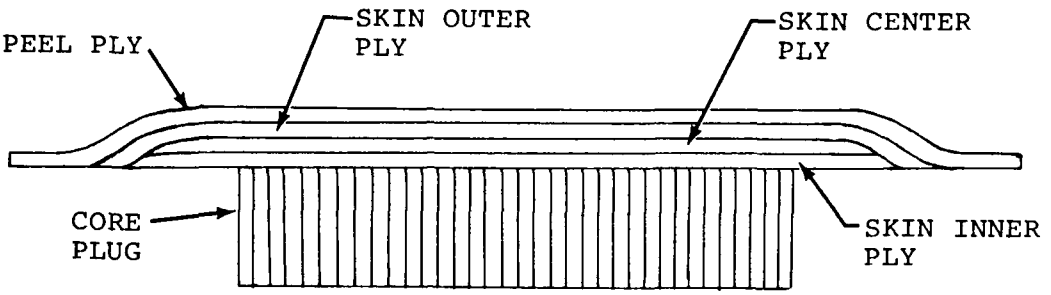

(PLY THICKNESSES DRAWN OVERSIZE FOR CLARITY)

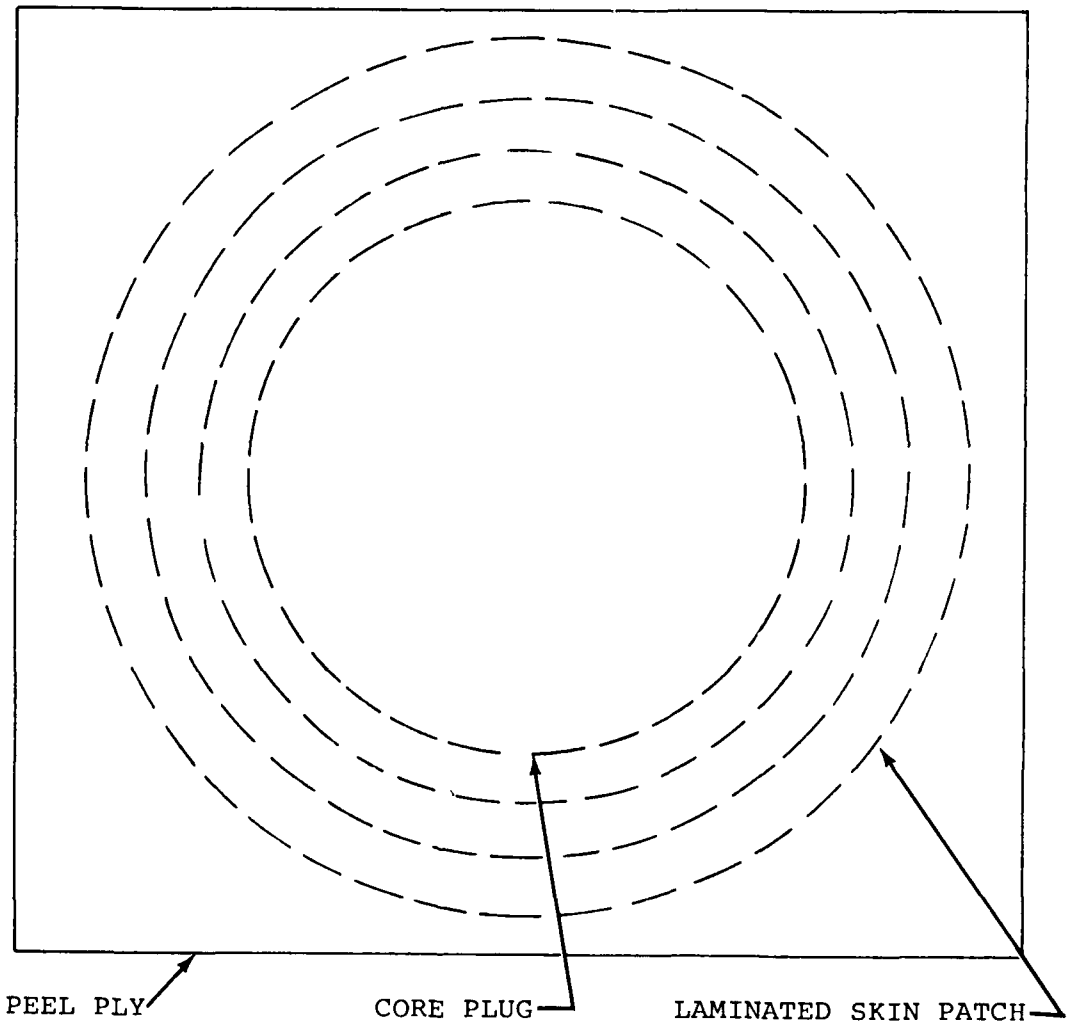

Figure 37. Typical Plug Patch Construction.

scenario. It was decided to opt for scrapping the blade in the event of very large damage rather than to bear the cost and complexity of enlarging the pressure/heat pack and provisioning three more repair kits. It is expected that repairable damage exceeding the size of the largest plug will represent only a small fraction of the total damage events to the blade.

The choice of three plug depths was prompted by the need to repair as close as possible to the trailing-edge spline, where the core section is thin, and to repair through-damage in the area of largest section near the spar. This dictated the choice of 1/4-inch and 1-1/4-inch deep plugs, respectively, the latter being one-half the largest section thickness. The 1/2-inch-deep plug was judged to be a desirable intermediate size.

Repair of through-damage to the core is accomplished by installing two plugs from opposite surfaces of the blades. The first plug is installed and allowed to cure, whereupon the second plug is installed from the other side, routing away portions of the first plug along with original structure. Figure B-11 shows a cross section through a double plug patch.

Repair Kit Makeup

The repair kits, as mentioned, were designed to include all of the consumable materials needed for a repair, except for hazardous and limited-life substances. Table B-10 of Appendix B lists the contents of the nine repair kits developed under the program: three skin patch kits and six plug patch kits. In addition to the patch or plug, each kit contains disposable templates for drawing circles on the blade which denote the area of the repair. It also includes gloves, a paint brush, wooden spatula, tape, cheesecloth and abrasive paper--all of the consumable materials, except the adhesive kit and bulk items, needed for the repair. After evaluating the blade damage, the repairman will draw from supply the required repair kit and as many adhesive kits as the instructions state are needed for that size repair. Such items as solvents and cleaning agents are drawn from bulk supply.

Adhesive Kits

Major objectives in design of the adhesive system were to obtain a low-temperature, fast-curing adhesive suitable for making rapid repairs which would remain structurally sound for the life of the blade. Initially, film adhesives were considered but were, after testing, found lacking in required properties. It was then that various epoxies were evaluated. A two-part thixotropic adhesive, Number AS-401-1, was finally selected as best meeting the requirements for FREB repair. AS-401-1, widely used by commercial airlines for repair of honeycomb panels having either

metal or fiberglass facings, is marketed by Airline Systems, a Division of Adhesive Engineering Company of San Carlos, Calif. Airline Systems, as subcontractor to Kaman in the FREB program, in addition to supplying adhesives, also did much of the inital work which led to the development of the pressure/heat pack discussed in the section of this report entitled "Repair Tools and Equipment".

Having selected a two-part adhesive for repair of the blade, various packaging methods were evaluated. It was decided that stocking the resin and curing agent in bulk would be unsatisfactory since it would complicate the repair process by requiring the repairman to measure quantities in the field, and could lead to improper mixes and faulty bonds. A simple kit containing the resin and curing agent in separate, premeasured amounts was judged to be the preferable approach. Different size kits were deemed to be unnecessary since the amount of adhesive needed for any repair could be obtained by adding together the contents of several kits. A kit containing 32 grams of adhesive, the amount needed to make one shallow plug patch, was chosen. A table indicating the number of kits, or fractions thereof, needed to make various types of repairs was prepared.

Several schemes for packaging the two-part adhesive so as to facilitate mixing in the field were evaluated. These included a pouch containing the two agents in separate compartments, which when unseparated would allow the adhesive to be mixed by kneading the pouch. A scheme using a tube and plunger to mix the two agents was also considered. The method found to be most satisfactory places the resin in an oversized wide-mouth jar and the curing agent in a toothpaste-type tube. The curing agent is squeezed into the jar, which serves as the mixing container.

Repair Tools and Equipment

The installation of skin patch and plug patch repairs created the need for two kinds of tools. First, removal of damaged core and preparation of the blade to receive fixed-size plugs required some type of powered cutting tool. (Hand tools were ruled out as being too difficult and time-consuming.) Equipment was also required to cure the patches and plugs under heat and pressure. Both kinds of equipment would have to be suited to the Army's field environment and to repair of the installed rotor blade (from either the top or the underside of the blade). Simplicity, ease of handling and ruggedness were essential in the design.

Router

In order to install plug patches in the blade, it was necessary to remove the damaged core material and to create a cavity which would accept the plug. A round cavity with smooth walls and a flat floor, held to relatively close dimensions, would be required. The time required to prepare the cavity would be an important factor in achieving the repair time goals for the FREB.

Before deciding on a high-speed router, two alternatives were considered. One was to use a battery-powered drill motor and a special drill bit to machine the walls of the cavity. The drill bit had a fluted tip for drilling the initial hole in the core and a coarse rasp surface which acted as a router for tracing the walls of the cavity. There were serious disadvantages with this approach. It was difficult to control the depth and evenness of the cut, and it was both tiring and time-consuming to work. Once the walls were cut, it was necessary to carve out the cavity by hand, another difficult and time-consuming operation. A second approach was to use a circular saw to cut the walls of the cavity. However, the largest saw of this type was only 2-1/2 inches in diameter, a size too small to be practical, and the need to hand carve the core was also present here. Saber saws were ruled out immediately, as they would tend to tear the skin away from the core, creating a ragged and uneven cut.

A high-speed router was found to be the only feasible approach. Modifications were required to the base plate and cutting bit to adapt a standard router to the requirements, however. The base plate of standard off-the-shelf routers was found to be too short to bridge the 7-inch-diameter cavity. A larger base was fabricated. Several router bit types were tested. The first, a 1/4-inch, high-speed, steel, two-lip bit was found to wear very rapidly. The same type of bit made of carbide held up better, but still was not durable enough. The type of bit finally selected was a solid carbide, rasp type, one which demonstrated satisfactory wear performance. A flute length of 1-1/2 inches was selected, the length needed for the deepest plug.

The use of a router for preparing the plug cavity is described in detail in Appendix B. After the surface area has been cleaned and the outline of the cavity has been drawn with the template provided in the repair kit, the procedure calls for making a circular cut along the drawn line to form the wall of the cavity. (The plug patch is used as a gage to adjust the depth of the router cut.) The skin is peeled from the center of the cavity, and the router is used to remove the underlying core material. The routing operation is quick to accomplish and, from the experience of many trials, is not prone to error.

Routing the lower surface of the blade (router held overhead) is not particularly troublesome, and little practice is required to attain proficiency.

Pressure/Heat Pack

At the outset of the program, the Contractor reviewed, with Airline Systems, the metal and composite structure repair systems they had been designing and producing for aircraft maintenance use. Designed primarily for the airlines and commercial aircraft operators, most of these systems were found to be somewhat too complex for Army field use, involving, in some cases, the use of equipment lacking the durability needed for that environment. Unlike the airline maintenance environment, where facilities and skills are conducive to the use of sophisticated equipment, the Army's field environment would demand the utmost in simplicity and durability. None of Airline Systems' existing repair equipment was found to be entirely satisfactory in this regard. A basic design they had developed for heat and pressure bonding of structural repairs was selected for modification, however.

The initial prototype of the pressure/heat pack consisted of a rigid metal frame to which a pressure bladder, containing a heat blanket, was attached. Pressure was supplied via a hand pump afixed to the frame. A pressure relief valve was provided to control pressure in the bladder, but the unit had no pressure gage. An aircraft-type electrical connector was used to connect the unit to a power supply. A rheostat controlled the temperature of the heat blanket. The unit was secured to the blade with straps, and suction cups were provided at the four corners of the frame to hold the unit temporarily until the straps were in place. The unit measured 12-1/2 inches square and had a bladder surface area of 12 inches by 12-1/2 inches.

Early trials of the unit revealed a number of faults which were subsequently corrected. Without a pressure gage, it was impossible to tell whether the required pressure was being held; a pressure gage was added. The rheostat used to make the temperature setting was found to be unreliable and was replaced with a better quality unit. The suction cups worked poorly and were more of a hindrance than an aid; they were removed. The largest problem had to do with the web straps used to secure the device to the blade.

One drawback to the use of straps was their tendency to stretch, causing the lower surface of the inflated bladder to become convex and lose contact with the edges of the patch. Another problem was the need to use wooden blocks on the blade trailing edge to avoid having the straps exert bending forces on the spline. While this approach worked, it could not be used in

the area where the trim tab attached to the blade, which sacrificed repairability along a significant section of the blade. (No effective way of bridging the trim tab was conceived.) To overcome this problem, it was necessary to add channels to the pressure/heat pack which would carry the straps over the trim tab. But, having added these channels, it became apparent that another set of channels on the opposite side of the blade would obviate the need for straps altogether. The unit was thus modified to eliminate the straps by providing metal channels, hinged at the trailing edge, and secured to the blade with swing-up draw bars at the leading edge. The final configuration is shown in Figure 38. Views of the installed heat and pressure pack are shown in Figures 39 through 42.

With these various modifications, the pressure/heat pack worked well and produced consistently good bonds, except for the deep, 1-1/4-inch plugs, whose installation tended to produce slight bulges in the skin on the opposite side of the blade. Upon investigation, it was determined that the expansion of air within the core, due to the application of heat, exerted an outward force on the skins. This force was reacted by the bladder on the side of the repair; but on the opposite side of the blade, where no restraint was present, the skin bulged. Since this occurred before the adhesive was completely cured, the adhesive became redistributed along the floor of the cavity and, after hardening, prevented the skin from returning to its natural shape. This problem was corrected by adding a backing plate to the pressure/heat pack which kept pressure against the opposite skin during the cure cycle.

The problem was not entirely eliminated with this modification, however. Some bulging of the skin persisted with deep plugs after the backing plate was added. It was determined that insufficient cure time was the cause. Removing the pressure/heat pack from the blade before the bond at the bottom of the plug was completely cured allowed the heated air to bulge the skin slightly as before and, when the cure was complete, caused a permanent deformation. This was corrected by increasing the cure cycle from 15 minutes to 30 minutes for the deep plugs.

There occurred one other problem of this type with the installation of large-diameter deep plugs, although unrelated to the design of the pressure/heat pack and the cure cycle. The FREB employs flat layup glass skins which assume the shape of the airfoil when bonded to the carved core. When a deep cavity is routed in the core, leaving only a small layer of core on the opposite skin, the skin tends to resume its original flat shape, creating a dimple where it contracts toward the cavity. Since this takes place as the cavity is being routed, additional core is removed; and the plug, when installed, fits the cavity exactly, leaving a slight flat spot on the opposite skin. Where

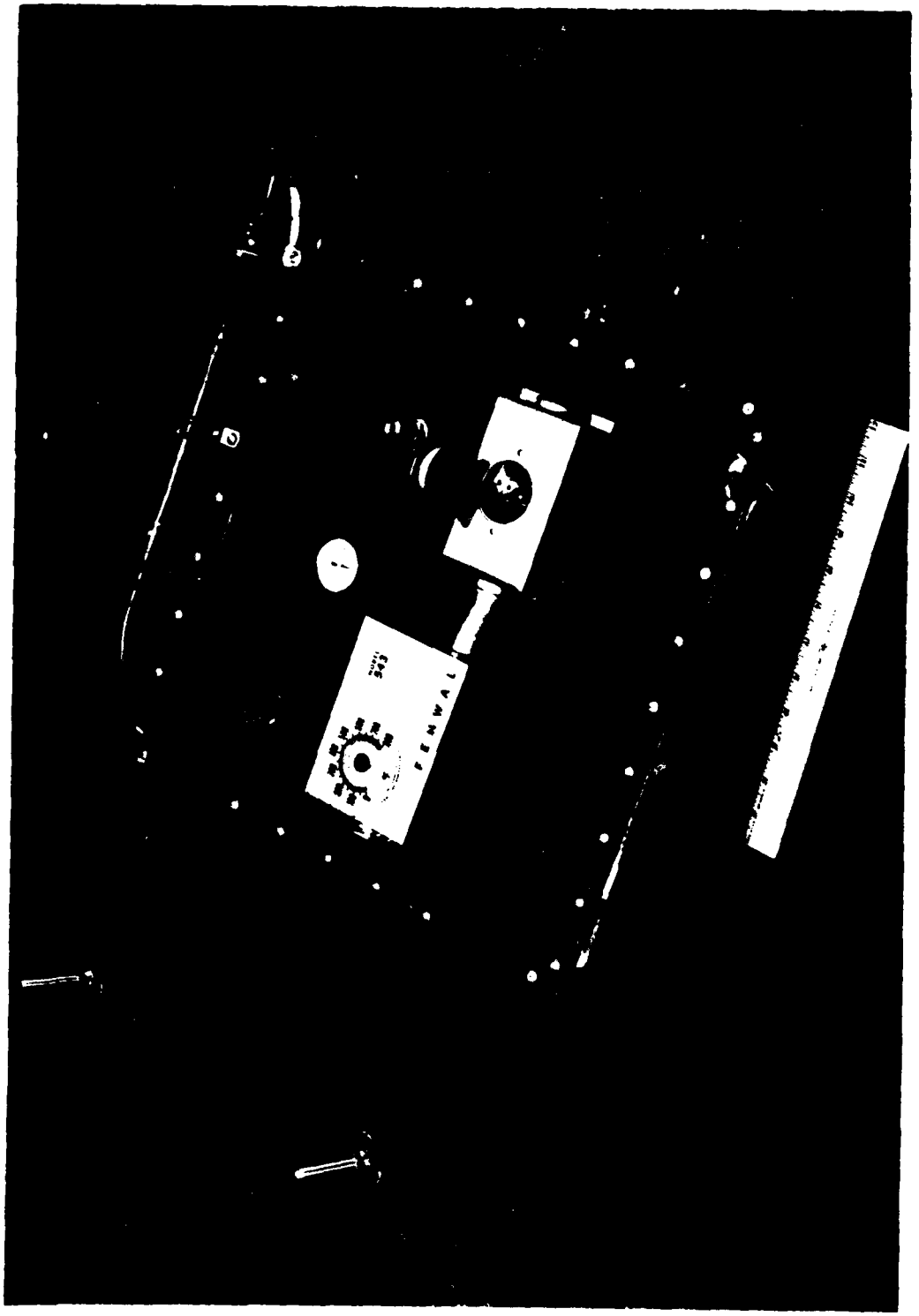

Figure 38. Pressure/Heat Pack.

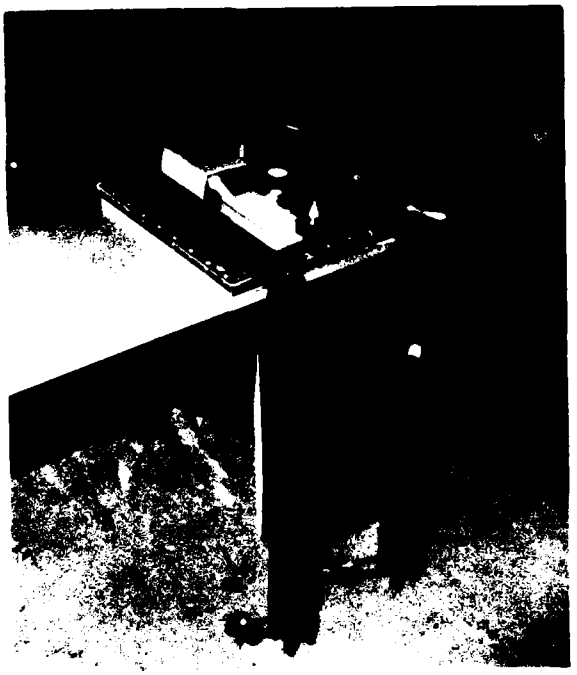

Figure 39. Pressure/Heat Pack in Place on Blade Prior to Securing.

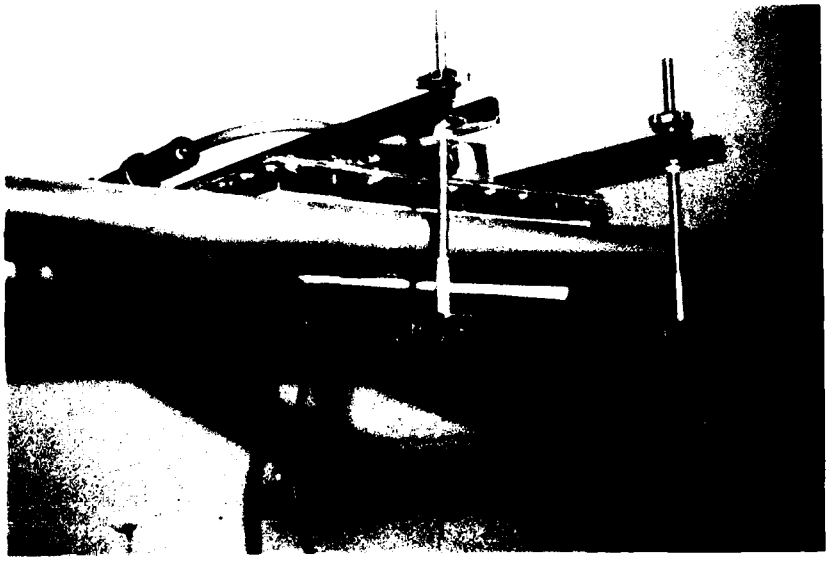

Figure 40. Pressure/Heat Pack Installed, Leading-Edge View.

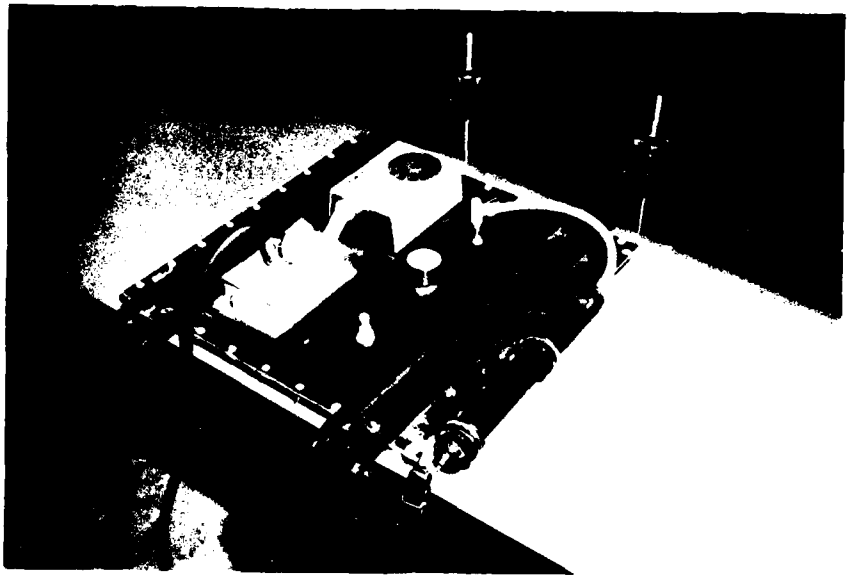

Figure 41. Pressure/Heat Pack Installed, Top View.

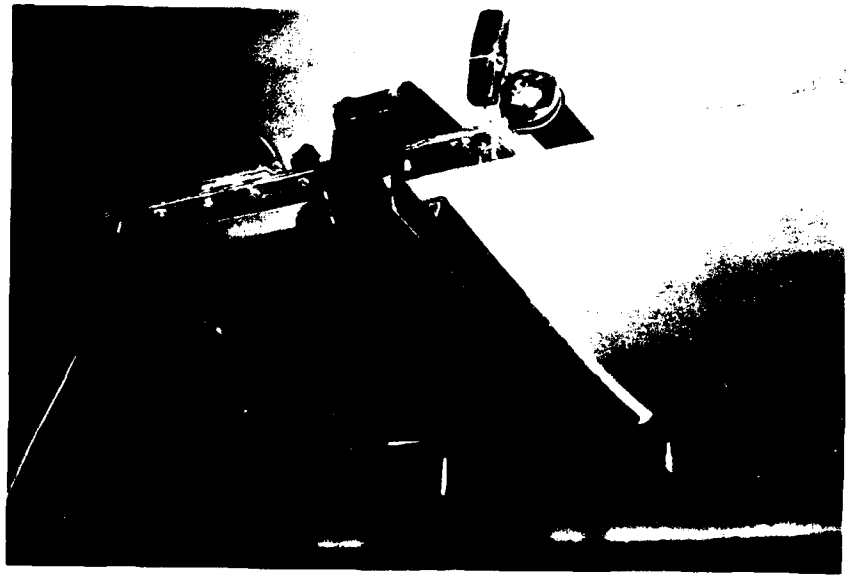

Figure 42. Pressure/Heat Pack Installed, Bottom View.

maintenance of the blade airfoil is critical to performance, a slight depression in the skin such as this could be detrimental. The use of contoured skins would avoid this problem entirely.

MAINTAINABILITY ANALYSIS AND PREDICTION

As the design of the FREB and its repair system evolved, the maintainability analysis and prediction, originally done for the winning FREB concept during the preliminary design evaluations, was modified and updated. In the previous section of this report, discussing development of the repair systems, it was explained how the kits and tools underwent a number of modifications in the course of perfecting the repair techniques. When significant changes in repair methods or materials were made, they were evaluated for their impact on repair time and the quantitative maintainability analysis was modified. A number of such modifications took place in the course of final design effort.

Maintenance Requirements Analysis

The methods used to perform the numerical analyses of maintainability were described earlier in the section of this report covering R&M analysis during preliminary design. One additional task, not required for the preliminary design evaluations, was performed for the final design: a maintenance requirements analysis. The purpose of this analysis was to define the specific maintenance functions and support requirements for the FREB. It also included development of criteria for support equipment and personnel training, based on the plan for maintenance.

The maintenance requirements analysis involved three types of activity:

1. Preparation of a maintenance plan, which identified all of the preventive and corrective maintenance functions for the FREB and provided the rationale for the selected maintenance concepts.

2. Identification of the basic support requirements for each of the preventive and corrective maintenance functions, to include personnel skills, task time, repair parts and materials, special tools, and support equipment.

3. Detailed task descriptions and illustrations for each of the defined maintenance functions, to be assembled into a repair instruction manual for the FREB.

The completed maintenance requirements analysis, together with the numerical predictions, provided the information needed to structure the maintainability demonstration.

MATERIALS EVALUATION

In order to choose and prove prospective materials and processes for use in the FREB, extensive coupon testing was performed under a variety of ambient conditions. The coupon testing was broken into four sections:

- Root doubler bond environmental fatigue: evaluated any reduction in fatigue life of doubler bonds resulting from extremes of heat and humidity.
- Environmental resistance of representative FREB skins and skin/core bonds: evaluated changes in skin strength and skin core bond strength under extremes of heat and humidity.
- Comparison of adhesives for use in blade repairs: evaluated several candidate repair adhesives under extremes of heat and humidity.
- Structural integrity of repaired ballistically damaged specimens: evaluated both the ballistic tolerance of representative FREB components and the structural integrity of typical repairs.

Pertinent details of the tests and test results are given below.

ROOT DOUBLER BOND ENVIRONMENTAL FATIGUE TEST

The specimens described in Figure 43 were representative of the FREB root doubler bond. The specimens were made by acid etching the aluminum, and then priming it (250°F for 40 min., t = .0001 - .0003) with Plastilock 718-2 primer. The representative skins were precured with a peel-ply on the exterior surfaces. The peel-ply was removed, and the "skins" were bonded to the primed aluminum with Plastilock 717 adhesive film. The specimens were cycled from 500 pounds to 23,500 pounds axial load. This load produced a stress of 14.08 Ksi at the doubler tip, equivalent to the limit stress in the blade at the doubler tip during normal operation. Each specimen was intended to be run to 3000 cycles, but several specimens were run considerably longer in an attempt to produce failures. Three-thousand cycles at this load level is in excess of all the ground-air-ground cycles that a blade is likely to experience on the UH-1 helicopter.

The results of this testing, summarized in Table 20, show that the root doubler bond on the FREB should remain unaffected by the extremes of heat and humidity encountered in the Army's operating environment. Figure 44 shows a close-up of the specimen and a view of the specimen mounted in the environmental test chamber.

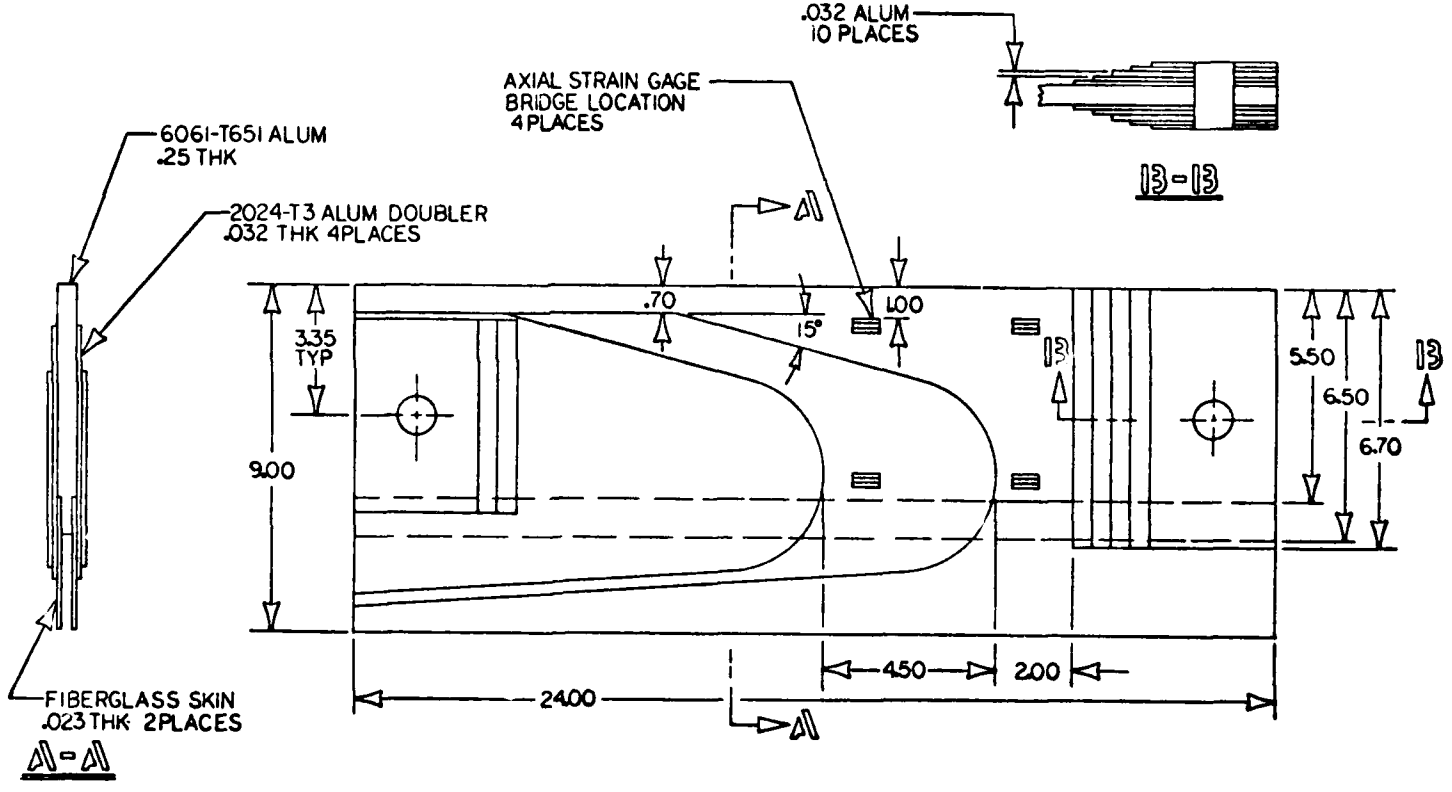

Figure 43. Root Doubler Bond Fatigue Test Specimen Schematic.

TABLE 20. ROOT END DOUBLER SPECIMEN BOND ENVIRONMENTAL TEST RESULTS.

SPEC. NO.	EXPOSURE	TEST COND.	TOTAL CYCLES	REMARKS
1	Room Temp.	Room Temp.	3000	This specimen was instrumented with strain gages.
2	Room Temp.	Room Temp.	12633	
3	90 days 95% RH @ 120°F	90 - 95% RH 120 - 130°F	4894	Instrumented with strain gages. Tested to 3000 cycles after 6 days. Replaced in exposure chamber for 3 more days and tested to another 1894, cycles when a grip bolt broke.
4	63 days 95% RH @ 120°F	90 - 95% RH 120 - 130°F	7458	Tested to 2468 cycles, when grip bolt broke. Replaced in exposure for 2 more days and tested to the total of 3000 cycles. Replaced in chamber for another 57 days of intermittent exposure, when chamber was shut down for 4-day holiday between 23 December and 2 January.
5	6 days 95% RH @ 120°F	90 - 95% RH 120 - 130°F	3000	

NOTE: All specimens cycled from 500 lb to 23500 lb at approximately 3 cycles per minute. No failure noted in any specimen after testing.

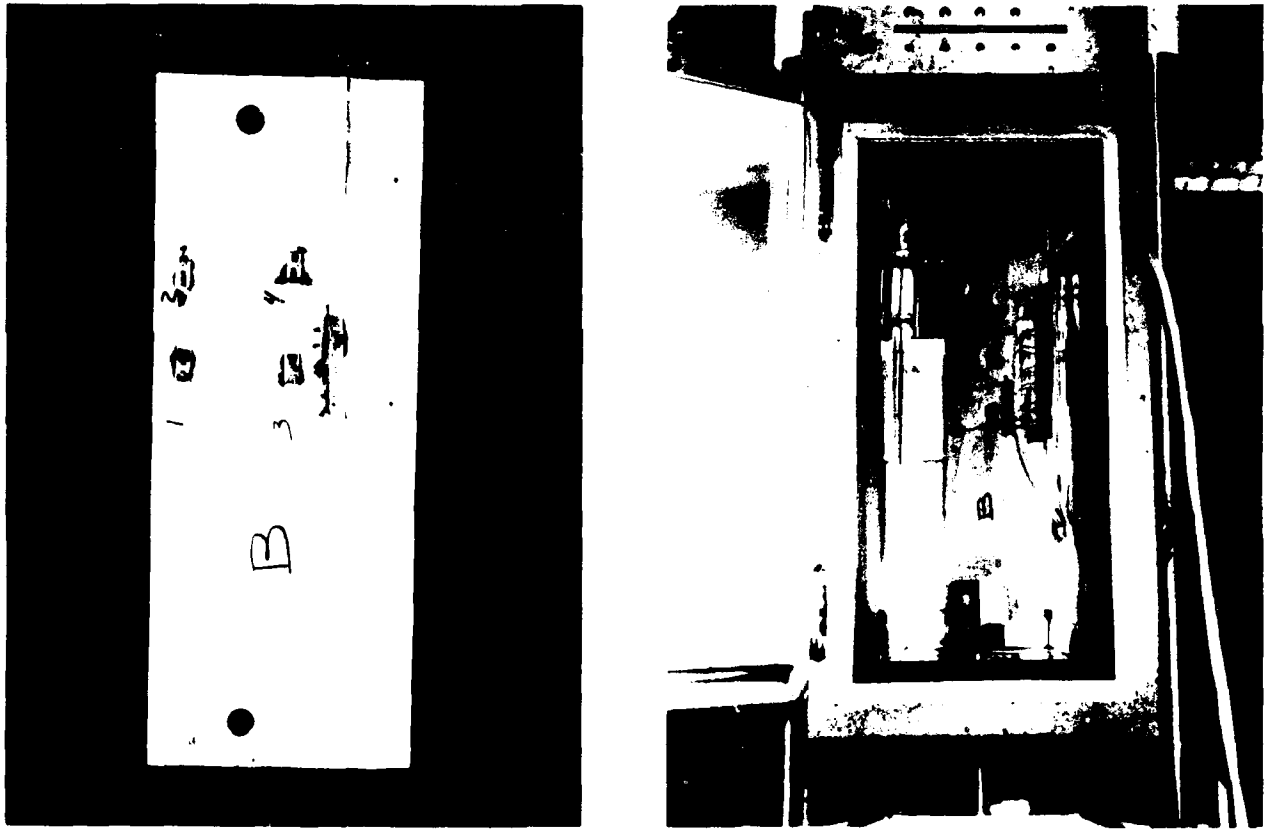

Figure 44. Root Doubler Bond Fatigue Specimen and Specimen Installed in Environmental Chamber.

ENVIRONMENTAL RESISTANCE OF REPRESENTATIVE FREB SKINS AND SKIN/CORE BONDS

Skins

The composite layup used for the FREB skins is shown schematically in Figure 45. A representative skin laminate, the same as that shown in Figure 45, but with .005-inch thick cloth, (total laminate thickness of .025-inch) was tested for tensile strength and modulus variations with changes in environment. Tensile specimens were cut out of a large sheet of laminate. Specimens were 1 inch wide and 8 inches long by .025-inch thick. Reinforcing plates were bonded to the ends of the specimens for ease of load introduction, and the specimens were cut so that the uni-directional plies were at $\pm$ 45° to the load axis. The specimens were tested in a Tinius-Olsen testing machine at a strain rate of .05 inch/minute. Environmental exposure consisted of both soaking the specimens at constant heat and humidity, and putting the specimens through a "weather cycle exposure" consisting of 48 hours of 95% RH and 120°, 8 hours direct sunlight, 8 hours of - 65°, 8 hours of 130°, and then tested after 6 cycles.

The results of this testing, given in Table 21, show variations of tensile strength and stiffness of approximately 10% and 13%, respectively, from room temperature to high heat and humidity to 20% in strength from room temperature of - 65°F. These variations, however, are expected and do not represent deficiencies in the structural integrity of the FREB.

Short-beam flexural strength and core shear strength testing was performed to evaluate the shear strength variation in the core shear strength and the core/skin bond strength under variations in temperature and humidity. Specimens were fabricated by bonding the representative skins to either side of a "web" of Nomex core (1/8-inch cells, 1.8 pcf) using Plastiloc 717 adhesive. Specimens were loaded as shown in the diagram accompanying Table 22. In all of the test cases the core failed, and the failing shear loads were unaffected by variations in heat and humidity.

ASTM STD 1781, Climbing Drum Peel Strength Tests, were also performed to evaluate the peel strength variation of the skin-core bond with changes in heat and humidity. Table 23 summarizes these test results. Again, variation in strength with environmental exposure is considered small.

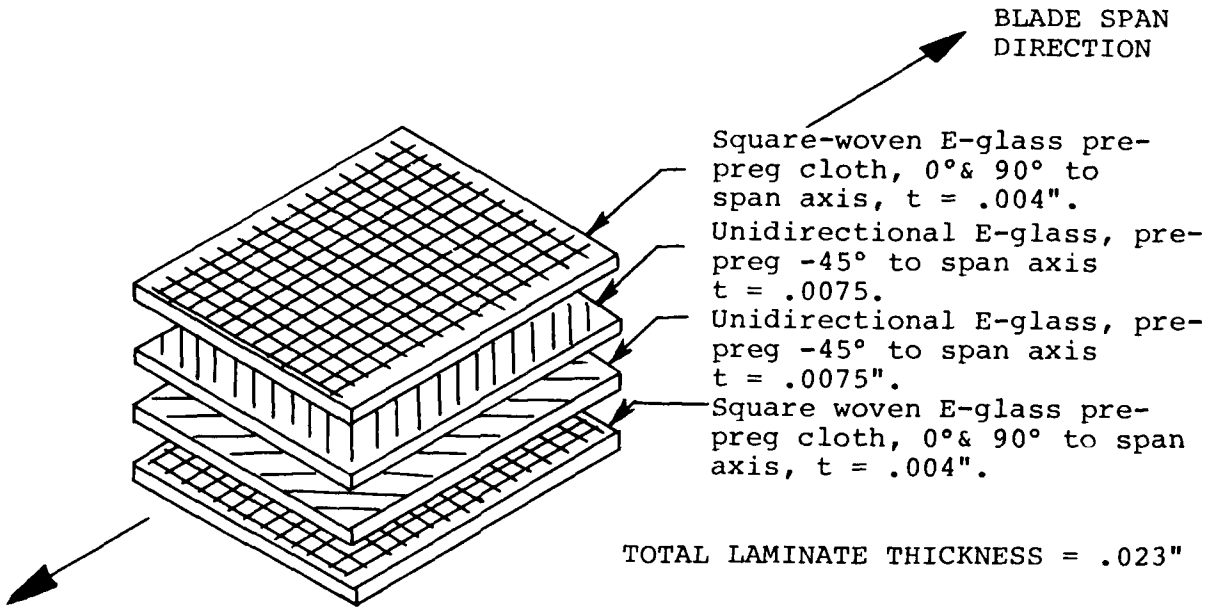

Figure 45. FREB Skin Laminate Schematic.

TABLE 21. TENSILE STRENGTH AND MODULUS COMPARISON AT VARIOUS ENVIRONMENTAL EXPOSURES OF REPRESENTATIVE FREB SKINS.

TEST CONDITIONS AFTER *ENVIRONMENTAL* EXPOSURE	ROOM TEMPERATURE		ROOM TEMPERATURE WEATHER CYCLE EXPOSURE		ROOM TEMPERATURE 30 DAYS AT 95% RH & 120°F		160°F 10 MIN. @ 160°F		- 65°F 10 MIN. @ - 65°F	
SPECIMEN NUMBER	F_{TU} Ksi	$E*10^{-6}$	F_{TU} Ksi	$E*10^{-6}$	F_{TU} Ksi	$E*10^{-6}$	F_{TU} Ksi	$E*10^{-6}$	F_{TU} Ksi	$E*10^{-6}$
1	40.6	2.06	51.1	1.99	41.0	1.84	43.3	-	51.7	-
2	45.9	1.62	48.0	2.09	46.4	2.05	40.2	-	56.3	-
3	48.5	1.65	50.0	1.99	44.3	1.98	39.6	-	57.6	-
AVERAGE	45	1.78	49.7	2.02	43.9	1.96	41.0	-	55.2	-

TABLE 22. SHORT BEAM FLEXURAL STRENGTH AND CORE SHEAR STRENGTH TEST RESULTS.

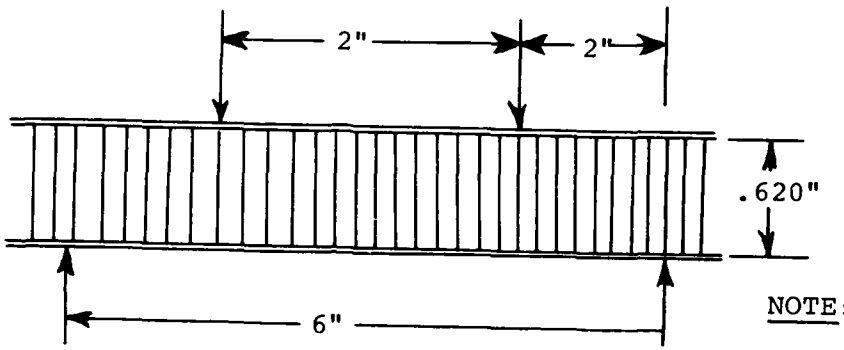

Loading Configuration

NOTE: All failures were in the core

TEST CONDITIONS AFTER ENV'MTL. EXPOS.	ROOM TEMPERATURE		ROOM TEMPERATURE 6 WEATHER CYCLES		160°F 10 MIN. @ 160°F		ROOM TEMPERATURE 30 DAYS @ 95% R.H. & 120°F	
Specimen Number	Skin Tensile Load, Psi	Core & Adhesive Bond Shear Strength, Psi	Skin Tensile Load, Psi	Core & Adhesive Bond Shear Strength, Psi	Skin Tensile Load, Psi	Core & Adhesive Bond Shear Strength, Psi	Skin Tensile Load, Psi	Core & Adhesive Bond Shear Strength, Psi
1	8290	100	8860	106	7490	90.2	7760	94
2	8060	97	8050	97	7050	85	8040	97
3	8190	98	8100	97	7540	90.7	8020	97
AVERAGE	8180	98.3	8337	100	7360	88.6	7940	96

TABLE 23. CLIMBING DRUM PEEL STRENGTH OF PLASTILOCK 717 ADHESIVE.		
TEST CONDITIONS AFTER ENVIRONMENTAL EXPOSURE	ROOM TEMPERATURE	ROOM TEMPERATURE WEATHER CYCLE EXPOSURE
SPECIMEN NUMBER	CORE FAILING LOAD, POUNDS PER 3" WIDTH	CORE FAILING LOAD POUNDS PER 3" WIDTH
1	20	20
2	19	22
3	19	23
AVERAGE	19.3	21.7

COMPARISON OF ADHESIVES FOR USE IN BLADE REPAIRS

The results of studies made early in the program of available adhesives showed that AS401, manufactured by Adhesive Engineering Company, San Carlos, California, Versalon 1140, manufactured by General Mills, and EC2216, manufactured by Minnesota Mining and Manufacturing Company, would all be candidates for use in bonding repair patches onto the FREB.

Preliminary testing with the hot-melt type of adhesive, Versalon 1140, showed that satisfactory shear strength could not be developed; in addition, the heat transfer properties of the repairs made melting of the adhesives deep in the blade afterbody difficult. Therefore, it was decided that if the AS401 was shown to be as acceptable as EC2216, efforts would be concentrated on developing the AS401 adhesive system because the AS401 cures faster than the EC2216. Specimens were made by bonding the .025-inch representative skin described previously to either side of 1.8 pcf polyamide paper core with 1/8-inch cells. Total specimen thickness was 1 inch. Core ribbon direction was perpendicular to the long dimension of the specimens, while the unidirectional skin fibers were laid up at $\pm$ 45° to the long dimension. Specimens were 6 x 18 inches and were repaired as shown in Figure 46. Holes were routed in the specimens to a depth of 1/2 inch, and a plug-patch was applied. Loads were applied as shown in the diagram accompanying Table 24. Testing was accomplished with the patches in both tension and compression and under a variety of conditions simulating both good and poor quality repairs.

In general, the test results given in Table 24 showed the AS401 to be no less strong than the EC2216. Absolute comparisons of the two adhesives from this test are not possible because, in all cases, the core failed in shear without failing the patch-core or core-core bonds made with either AS401 or EC2216. Because of this comparison of AS401 and EC2216, AS401 was chosen to be used as the repair adhesive for the remainder of the program.

STRUCTURAL INTEGRITY OF REPAIRED BALLISTICALLY DAMAGED SPECIMENS

In order to evaluate the effect of ballistic damage on the FREB afterbody and repairs to typical ballistic damage, specimens were tested at the Army's Ballistic Research Laboratories, Aberdeen, Maryland, with .30 caliber, .50 caliber and 23-millimeter ammunition and then were repaired and tested to destruction at the Contractor's Materials Laboratory.

Six of the seven specimens tested were 10 x 30 x 2 inches thick and consisted of the representative skin layup described earlier bonded to either side of a 2-inch piece of 1/8-inch cell, 1.8 pcf

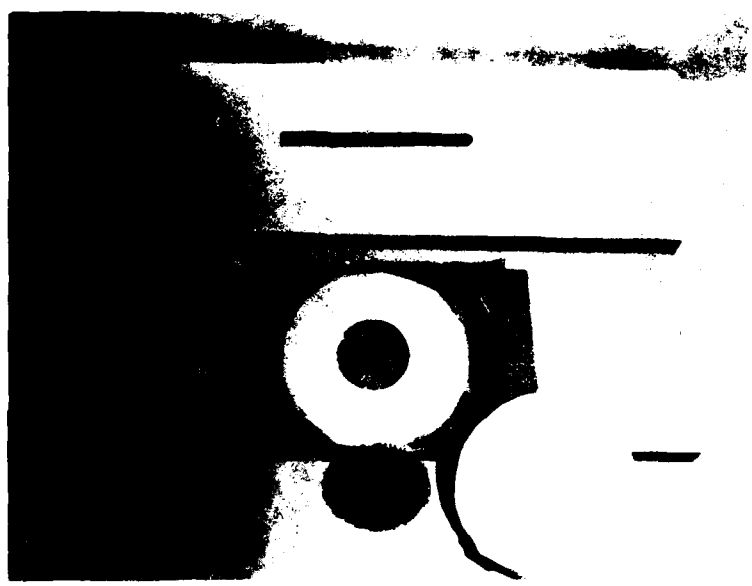

Figure 46. Blade Repair Specimen for Preliminary Adhesive Evaluation.

TABLE 24. REPAIR ADHESIVE COMPARISON

SPEC. NO.	TYPE OF REPAIR AND TEST CONDITION	AS 401		EC 2216	
		SKIN STRESS	CORE SHEAR	SKIN STRESS	CORE SHEAR
	Control - Test at R.T.				
1	No Patch	11500	61	-	-
2	No Patch	11650	62		
	Good Repair - R.T.				
3	Patch Up	12200	65	9590	51
4	Patch Down	12410	66	10050	54
	Good Repair - Test at R.T. After 30 Days 95% R.H. & 120°F				
5	Patch Up	10900	58	7060	38
6	Patch Down	10470	55	8750	46
	Good Repair - Test at R.T. After Weather Cycle				
7	Patch Up	8150	43	-	-
8	Patch Down	8300	44	-	-
	Good Repair - Test at 120°F After 10 Min. at 120°F				
9	Patch Up	9840	52	-	-
10	Patch Down	10150	54	-	-
	No Adh. in Bottom of Plug				
11	Patch Up	10730	57	11670	62
12	Patch Down	8080	43	9220	59
	No Adh. Over ½ Circumference				
13	Patch Up	12120	65	10520	56
14	Patch Down	8660	46	8150	43

NOTE: All failures for both adhesives were core shear either under one of the loading plates or between a plate and a reacting support.

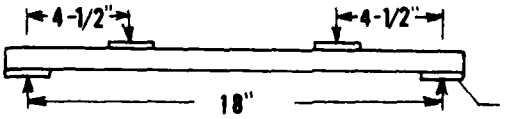

1/4 x 2 x 6 Al. Plates
4 Places

density polyamide paper honeycomb. Again, aluminum plates were bonded in place for local load introduction, and the unidirectional glass fibers in the skin and the ribbon direction in the core were at $\pm$ 45° and at 90° to the specimen's long dimension, respectively. The eighth specimen had the same fiber and core ribbon direction as the others, but was larger and had .050-inch channels bonded to its sides. This last specimen was the target for a 23-mm tumbled explosive round. Table 25 summarizes specimen loading, size and incidence of the projectiles.

Figures 47 through 50 show the entry and exit holes made in the specimens. With the exception of specimen 7, hit by a 23-mm HEI shell, all damaged specimens were repairable using the patch components shown in Figures 51 and 52. Specimen 7 showed that the 23-mm HEI round could remove a large percentage of the skin and core by a direct hit near the center of the afterbody. The .050-inch channels used on specimen 7 were severely distorted but not severed. Additional chordal thicknesses of metal bounding the afterbody, as in the spar aft wall and the trailing-edge spline, could limit severe damage to the metal components, preserving a large percentage of edgewise, flatwise and spanwise blade stiffnesses. Thus, with a 23-mm HEI round, blade scrappage would probably result, but catastrophic blade failure would not necessarily occur. Table 26 shows that the repaired specimens (numbers 1 through 6) showed no deterioration in static bending strength as a result of damage and patch repair. Figures 53 through 55 show the repaired specimens after test to destruction.

TABLE 25. BALLISTIC SPECIMEN SUMMARY

Specimen No.	Caliber Ball	Loading	Hit
1	.30	No CF	Perpendicular to surface
2	.30	No CF	45° to surface
3	.30	No CF	Tumbled perpendicular to surface
4	.30	No CF	Tumbled 45° to surface
5	.50	CF	Tumbled 45° to surface
6	.50	CF	Tumbled perpendicular to surface
7*	23mm	No CF	

* This was 60 inches long with aluminum channels on the sides.

#1 #2 #1 #2

ENTRANCE EXIT

Figure 47. Specimens 1 and 2 After Ballistic Damage.

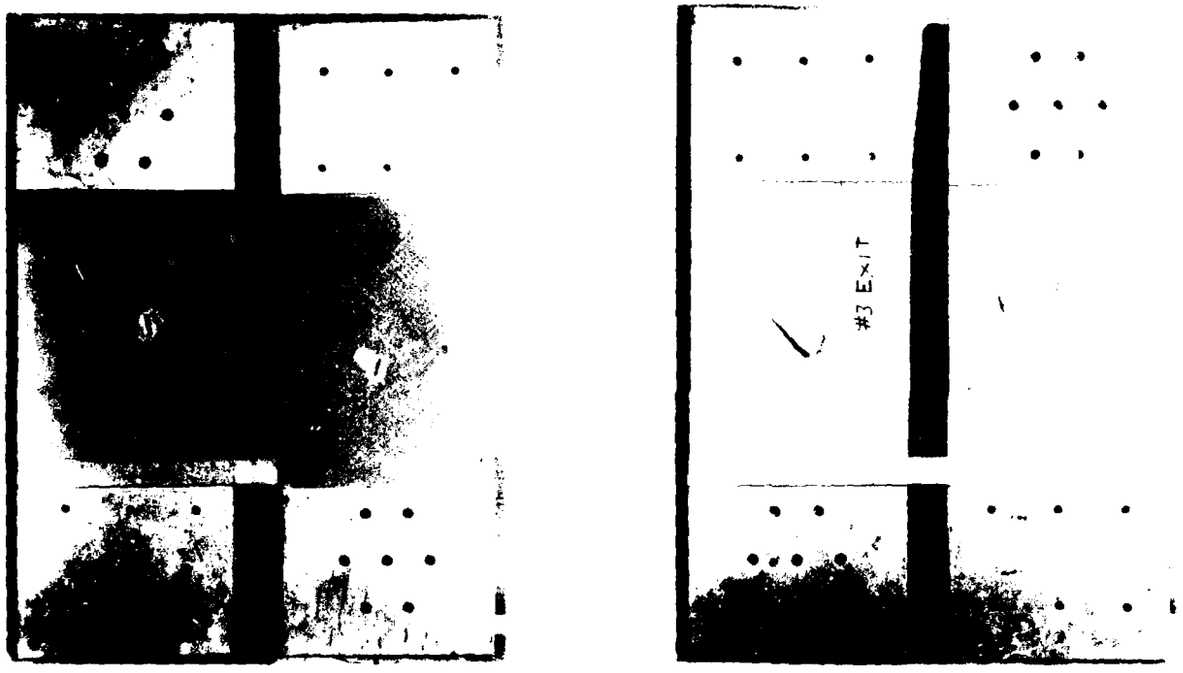

Figure 48. Specimens 3 and 4 After Ballistic Damage.

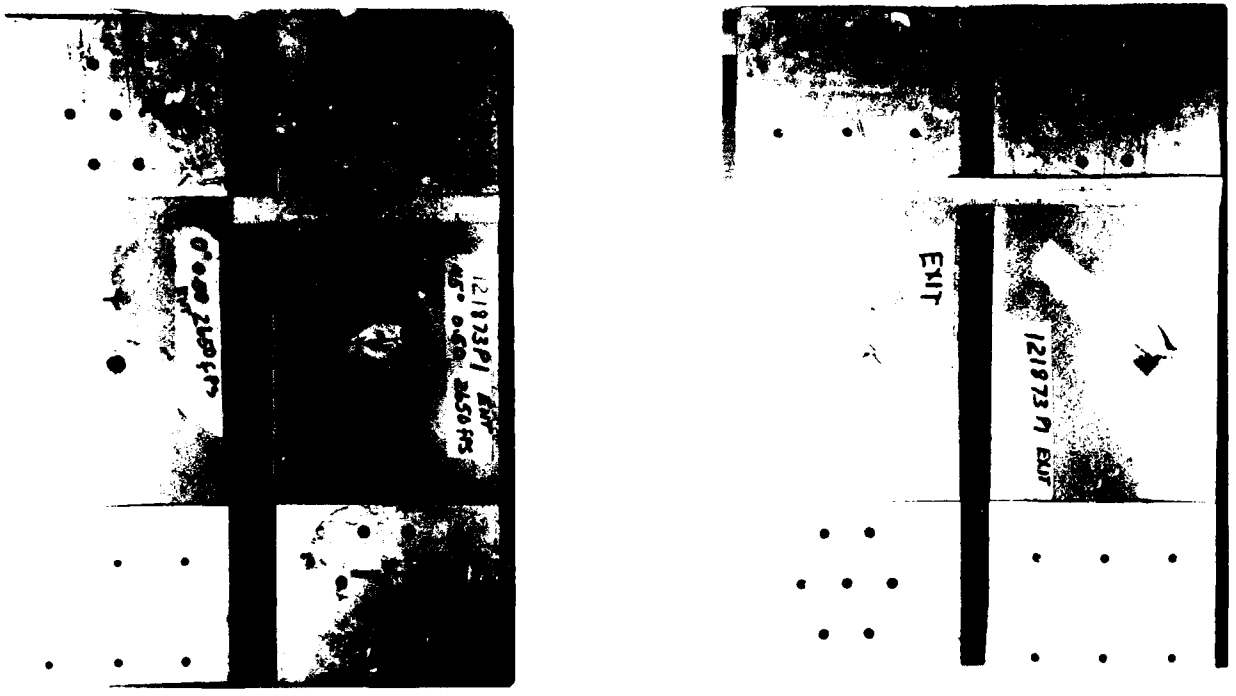

#5 #6 #5 #6

ENTRANCE EXIT

Figure 49. Specimens 5 and 6 After Ballistic Damage.

Figure 50. Specimen 7 After Ballistic Damage.

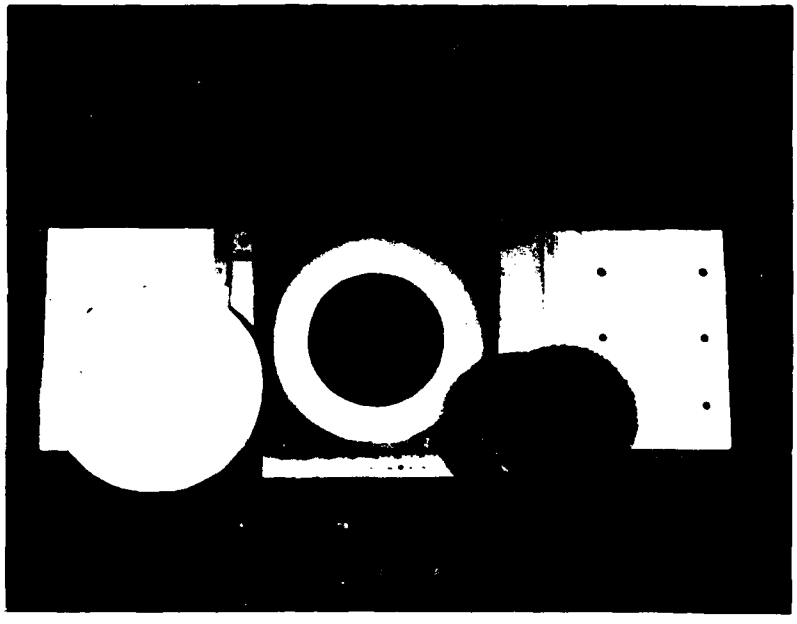

Figure 51. Repair Pieces.

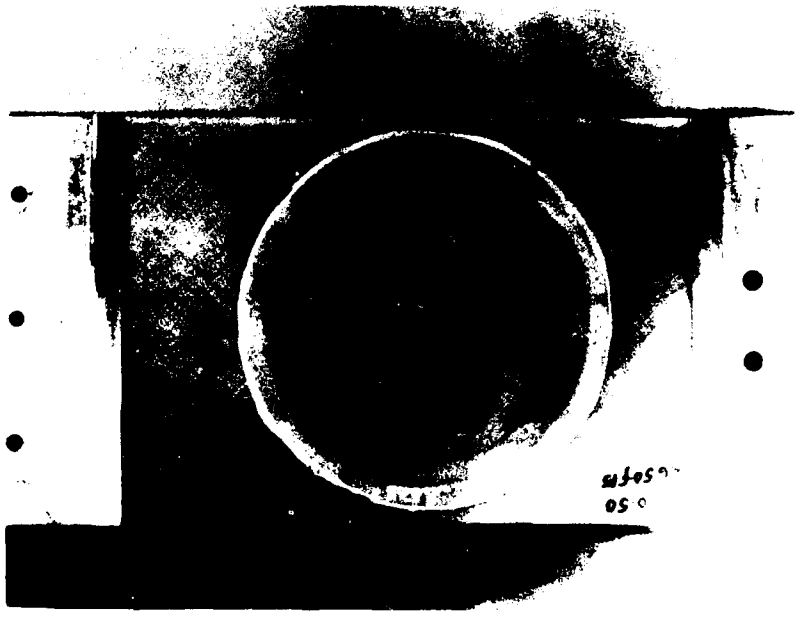

Figure 52. Completed Repair.

TABLE 26. TEST RESULTS OF BALLISTICALLY DAMAGED SPECIMENS AFTER PATCH REPAIR

SPECIMEN NUMBER	HOLE DIA. (IN.)	PATCH DIA. (IN.)	WEIGHT INCREASE (LB)	TYPE OF TEST	ULT. SKIN STRESS (psi)	FAILURE AND REMARKS
1	2.5	5.5	.16	Flexure	42300	Compression skin to core delamination outside of patch area. Distance of 16-1/2" between loading bars.
2	4.5	7.5	.21	Flexure	24700	Compression skin wrinkle into core just inside of loading plate. Distance of 14" between loading bars.
3	3.0	6.0	.20	Tension	22500	Skin on both sides at 45° (in direction of fibers) from edge to patch.
4	2.5	5.5	.20	Flexure	30200	Holes in skins approximately 2" off center from each other.
5	6	9	.31	Tension	27600	Skin on both sides at 45° through center of patch 14" between loading bars.
6	5	8	.23	Tension	23000	Skin on both sides at 45° through center of patch.
Control	---	---	---	Tension	22100	Skin on both sides at 45°

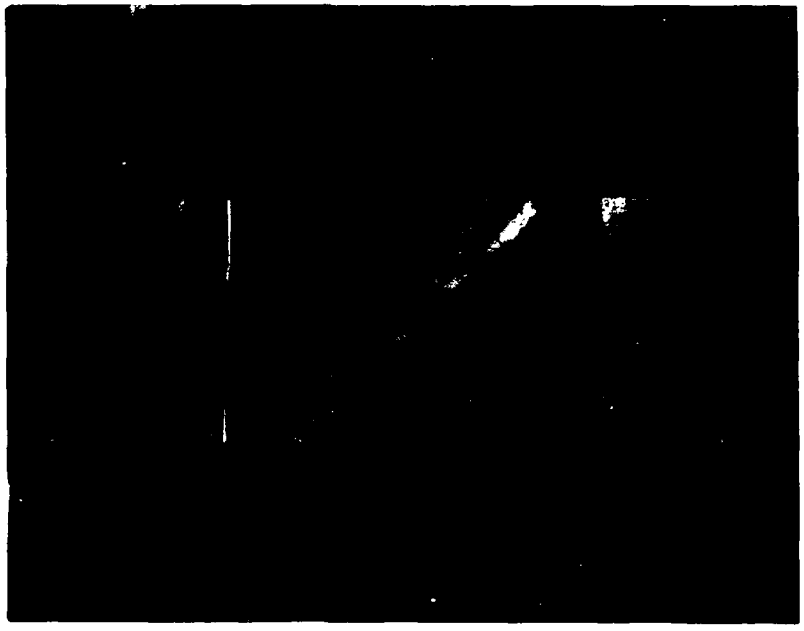

Figure 53. Undamaged Specimen Tested in Flatwise Flexure.

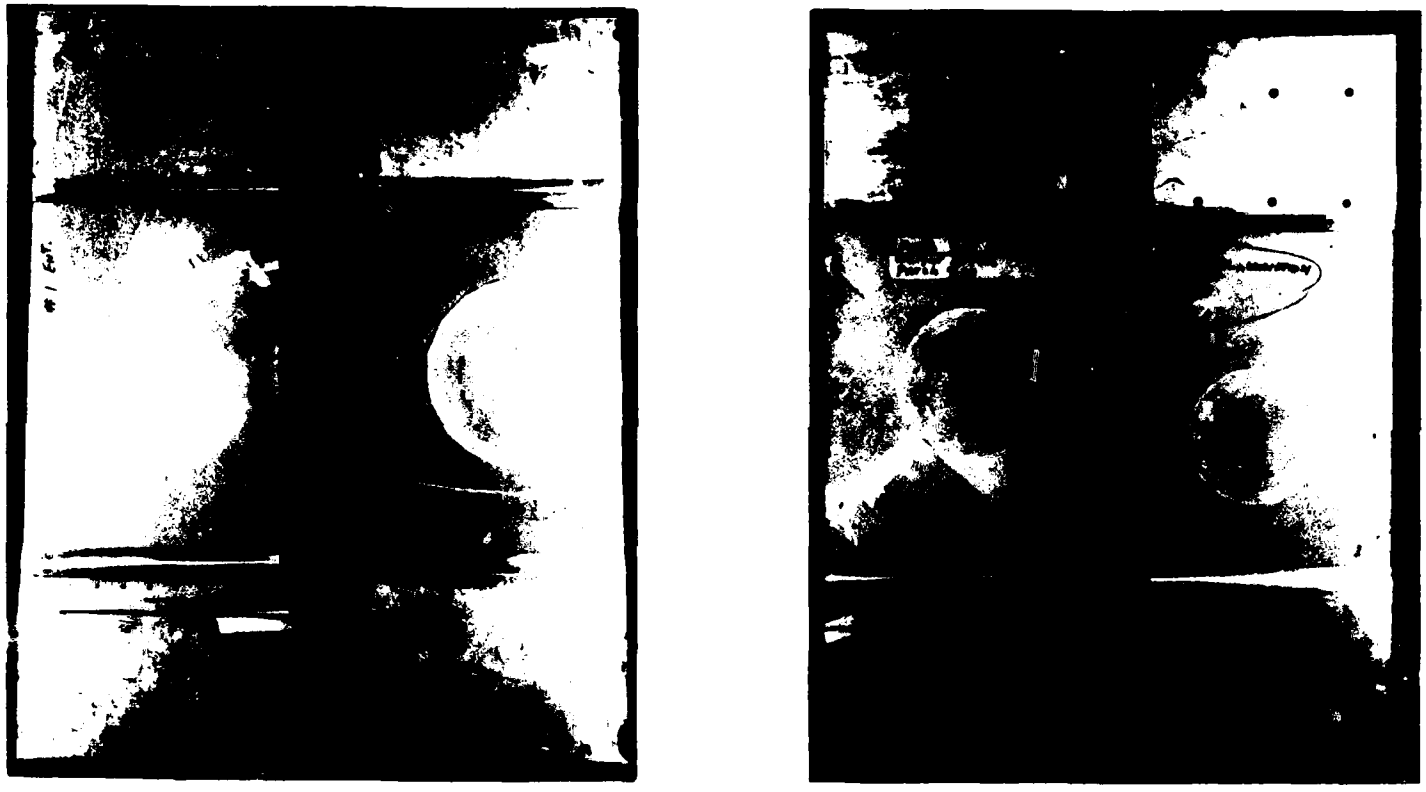

#1 #2 #3 #4

Figure 54. Failure Locations of Specimens 1 Through 4 After Repairs and Testing in Flatwise Flexure.

#5 #6

Figure 55. Failure Locations of Specimens 5 and 6 After Repairs and Testing in Flatwise Flexure.

MAINTAINABILITY DEMONSTRATION

One of the final tasks of the program was to conduct a maintainability demonstration of the FREB repair system. Prior sections of this report described the repair system development effort and the verification of processes and procedures that took place at various stages of the program. Numerous repairs of complete blades and blade sections had been performed by Maintainability personnel and by technicians from Kaman's Test and Development and Materials Engineering groups. The quality of the repairs had been verified via materials tests, static and fatigue tests, and whirl tower tests. When the program reached the point of the maintainability demonstration, the ability to make efficient and structurally reliable repairs of the FREB, within the time goals established, had already been substantiated.

The purpose of the maintainability demonstration was to verify that the Army's requirements for field repairability had been achieved and that the repair time specifications could be met by Army personnel working in a field environment. The demonstration was to be conducted under conditions representative of the Army's maintenance environment using the material, tools and data which would normally be available to the mechanic in the field.

DEMONSTRATION OBJECTIVES

The maintainability demonstration was to include a sample of repair tasks selected statistically from the population of tasks expected to occur over the life of the blade. The task sample was to be representative of the population in terms of frequency and maintenance time, and was to include at least one task of each significantly occurring type. Defects introduced into the test blades were to be dimensionally representative of the failure and damage events expected to be sustained in actual use. A maintainability demonstration plan was submitted to and approved by the Army prior to the demonstration.

DEMONSTRATION CONDITIONS

It was desired, insofar as was practicable, to reproduce the conditions and resources that would prevail in the Army's field maintenance environment. That environment presents an array of climatic and logistical conditions, however, which a demonstration such as this could not attempt to duplicate or simulate economically. It was necessary, therefore, to create a typical or average environment in which to conduct the demonstration. The conditions under which the demonstration was conducted represented those of a fixed-base Army facility with sheltered, temperature-controlled maintenance areas. Throughout the

demonstration, however, an attempt was made to assess the effect that adverse environmental conditions (cold, heat, high wind, etc.) might have on repair techniques, materials, tools and personnel efficiency. Figures 56 and 57 are views of the demonstration area.

TEST SITE AND FACILITIES

The demonstration took place at Kaman's Bloomfield, Connecticut, Test and Development facility. At this facility are flight, hangar and maintenance areas which are generally representative of fixed-base Army helicopter installations. The demonstration was conducted in one of the flight test hangars, with the test blades installed on a bailed UH-1H aircraft. Mobile maintenance stands were used, as necessary, to provide test personnel with working access to the installed rotor blades.

TEST BLADES

The demonstration was conducted with two sets of rotor blades, serial numbers 8 and 9, and serial numbers 12 and 13. All repairs performed for the maintainability demonstration except two were made on blades 8 and 9. The other two demonstrated repairs were made to blades 12 and 13. Each of the latter blades was damaged in one location, the type of damage inflicted being the most severe repairable. Repairs were made to the blades as part of the demonstration, and the blades were subsequently whirl tested.

REPAIR KITS, TOOLS AND DATA

The maintainability demonstration was conducted using the repair kits, tools and instructions developed under the program, as listed and described in Appendix B. Standard tools and bulk items not included in the repair kits were drawn from the Contractor's supply crib, as needed.

PARTICIPATING PERSONNEL

The Army supplied two helicopter repairmen for the demonstration. Both had primary MOSs 67N20, Utility Helicopter Repairman. One was a PFC, pay grade E3, and the other an SP6, pay grade E6. The PFC had just recently graduated from training school and had been working as a mechanic for only a short time. The SP6 was working as a Rotary Wing Technical Inspector. Neither had specialist experience in rotor maintenance nor experience with the repair of composite structures.

The two Army repairmen underwent five days of training in repair of the FREB in preparation for the demonstration. This training included, in addition to a basic familiarization with the

Figure 56. View of the Demonstration Area.

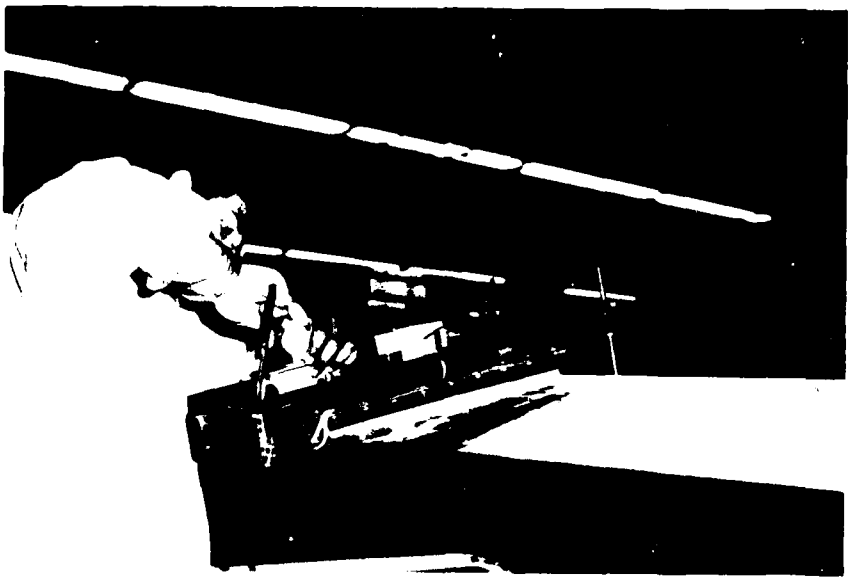

Figure 57. Army Repairman Installing Pressure/Heat Pack.

construction and material characteristics of the blade, instruction and practice in making each of the different types of repair. Blade sections, salvaged from the bench tests, were used to conduct this training. Each of the two repairmen performed each type of repair two to three times during training. All of the repairs performed for the demonstration were made by the two Army repairmen, approximately an equal number by each.

The Government's test observer was an inspector from the Quality Assurance Division of the DCASO at Kaman. His responsibilities were to oversee the demonstration, to verify that the approved demonstration plan was followed, and to assist with and approve the recording of test data. The test observer was given a brief indoctrination prior to the start of the demonstration to review the test schedule and procedures, data collection methods, etc.

The test coordinator was a member of the Contractor's Maintainability Engineering staff. His responsibilities included:

1. Assembling all of the required materials, tools and equipment at the demonstration site.

2. Scheduling facilities and personnel.

3. Conducting the training of Army repairmen and indoctrination of the Government test observer.

4. Scheduling the demonstration tasks and making necessary preparations, including the introduction of simulated blade failures or damage.

5. Supervising the demonstration and recording test data.

6. Working with the Government test observer to resolve problems encountered during the demonstration, reschedule tasks which were not successfully completed, etc.

ATTENDEES

The demonstration was attended by the USAAMRDL Project Engineer and, at the invitation of the Army, six industry representatives from the following four companies:

Bell Helicopter Company	Sikorsky Aircraft
Hughes Helicopters	Boeing Vertol Company

TEST DESIGN AND SAMPLE SIZE

MIL-STD-471A, Test Method 2, contains a maintainability demonstration procedure for a test involving the critical percentile of the repair time distribution. The procedure employs a fixed sample size test and decision criteria based upon the asymptotic normality of the maximum likelihood estimate of the percentile value.

The test hypotheses are stated in terms of:

H_0: 95th percentile, $M_{max} = t_0$

H_1: 95th percentile, $M_{max} = t_1 (t_1 > t_0)$

The test requires assignment of a producer's risk, α, and a consumer's risk, β (Figure 58).

The sample size is determined from:

$$n = \left[\frac{2 + Z_p^2}{2}\right] \tilde{\sigma}_x^2 \left[\frac{Z_{(1-\alpha)} + Z_{(1-\beta)}}{\log_{10} t_1 - \log_{10} t_0}\right]^2$$

where Z_p = standardized normal deviate corresponding to the M_{max} percentile (for 95th percentile, $Z_p = 1.645$)

$\tilde{\sigma}_x^2$ = prior estimate of σ_x^2, the true variance of the logarithms of maintenance time

$Z_{(1-\alpha)}$ = standardized normal deviate corresponding to $(1-\alpha)$

$Z_{(1-\beta)}$ = standardized normal deviate corresponding to $(1-\beta)$

The sample size is thus a function of the discrimination ratio: t_1/t_0 and the specified α and β risks. In designing a maintainability demonstration for the rotor blade, the hypotheses to be tested were:

H_0: $M_{max} = t_0 = 3.0$

H_1: $M_{max} - t_1 > 3.0$

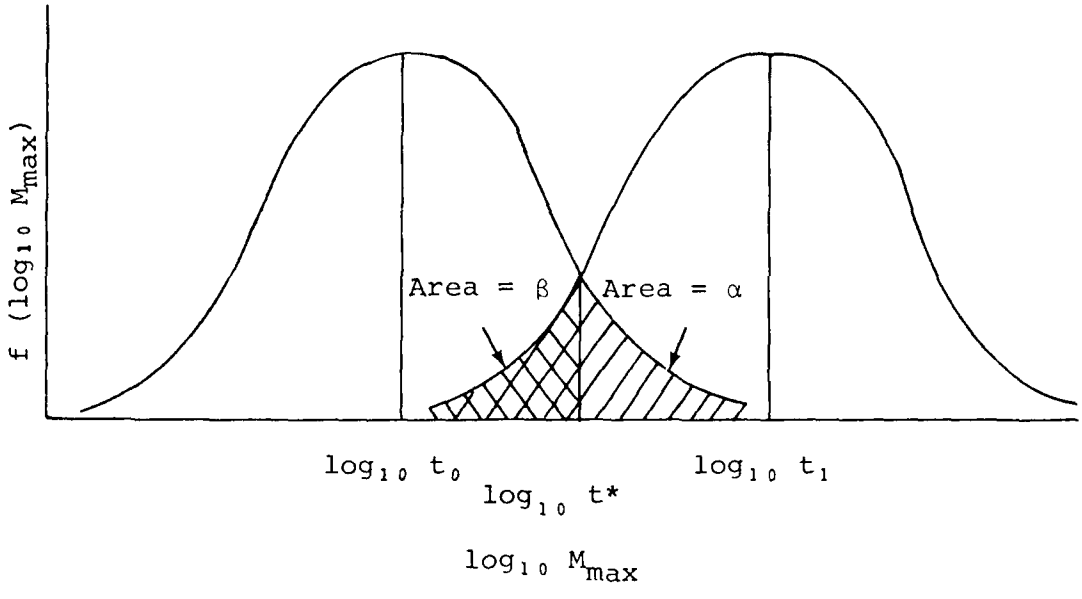

Figure 58. Producer's Risk, α, and Consumer's Risk, β, Illustrated.

Figure 59 shows the relationship of the α and β risks to task sample size (assuming equal risks) for several values of t_1 and an estimated value of $\sigma_x^2 = .0805$.

The contract work statement called for a sample of approximately twenty tasks and two additional tasks for whirl testing. From the curves of Figure 59, a sample of this size was found to be adequate for an H_1 hypothesis: $t_1 = 4.5$, and assigned risks: $\alpha = \beta = .18$. Better discrimination and/or lower risk values would require a larger task sample.

DECISION CRITERIA

Each demonstration task was monitored and timed. The recorded task times were used to compute the following statistics:

The mean of the logarithms of sample task times:

$$\hat{\bar{X}} = \frac{1}{n} \sum_{i=1}^{n} \log_{10} t_i$$

where t_i = elapsed time to perform the ith task.

The variance of the logarithms of the sample task times:

$$s^2 = \frac{1}{n-1} \left(\sum_{i=1}^{n} (\log_{10} t_i)^2 - n\hat{\bar{X}}^2 \right)$$

The critical value of t:

$$\log_{10} t^* = \log_{10} t_0 + Z_{(1-\alpha)} s \left(\frac{1}{n} + \frac{Z_p^2}{2(n-1)} \right)^{1/2}$$

where $Z_p = 1.645$

$Z_{(1-\alpha)} = .92$ (for $\alpha = .18$)

The accept/reject criteria was:

Accept H_0 if $\log_{10}^{-1} \left(\hat{\bar{X}} + 1.645\ s \right) \leq t^*$

Reject H_0 otherwise.

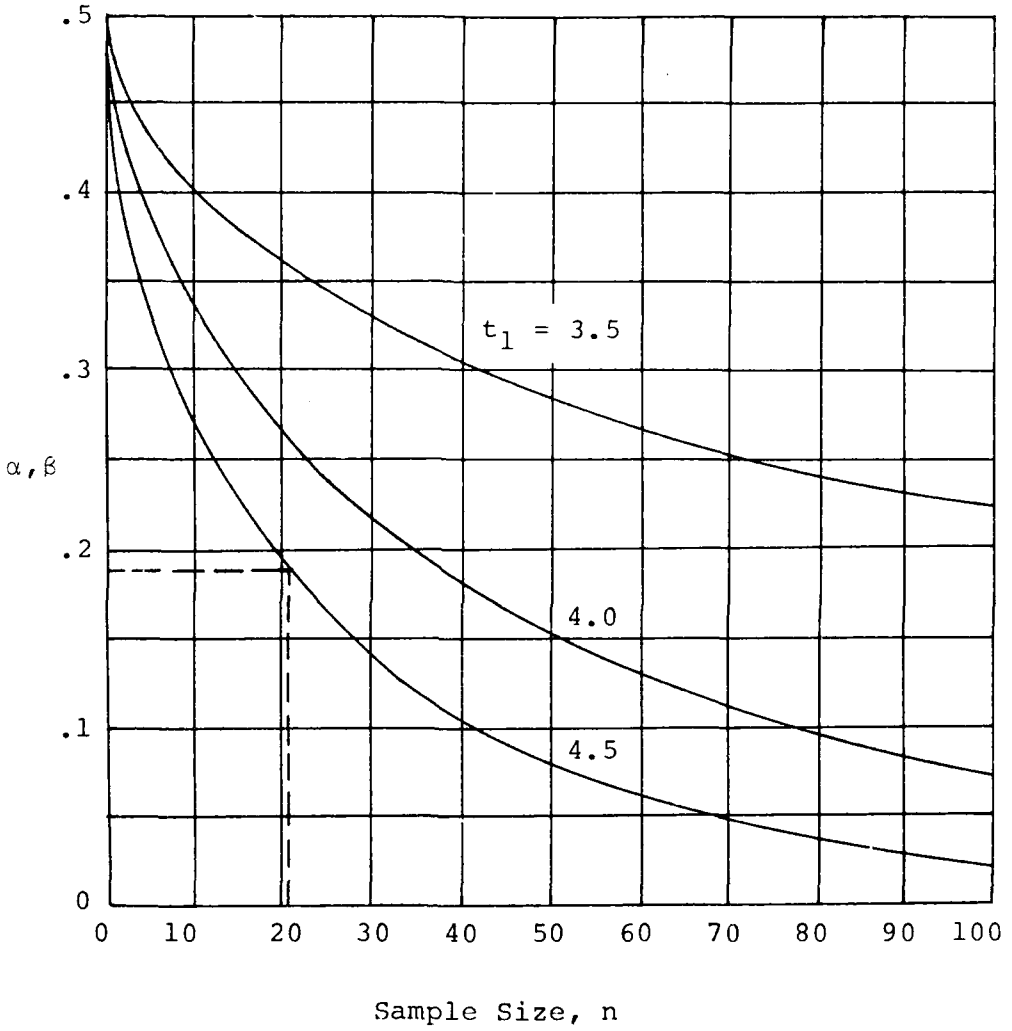

Figure 59. Producer's and Consumer's Risk Versus Sample Size.

Operating Characteristic Curve

The operating characteristic curve for this test, shown in Figure 60, is derived from

$$Z(A) = (\log_{10} t^* - \log_{10} t_p)/\sigma_x \left[\frac{1}{n} + \frac{Z_p^2}{2(n-1)}\right]^{1/2}$$

where $Z(A)$ = the standardized normal deviate corresponding to the probability of accepting H_0 when the true $M_{max} = t_p$

Task Sample Selection

Appendix A of MIL-STD-471A prescribes a procedure for selecting maintainability demonstration tasks using the method of proportional stratified sampling. With this method, the total population is divided into subpopulations or strata so that the sample drawn from each stratum is proportional to its contribution to the population. A minimum of one demonstration task is to be selected from each stratum.

The procedure of MIL-STD-471A establishes the sample strata on the basis of a hardware breakdown, i.e., parts, modules and assemblies of the article undergoing demonstration testing. Each hardware item whose repair or replacement constitutes a corrective maintenance action is assigned to a category, singly or in combination with like items. The hardware categories, after appropriate regrouping on the basis of similar actions and maintenance times, form the strata from which sample tasks are selected according to their proportional contribution to the total population of maintenance actions (failures).

Selecting a demonstration task sample on the basis of relative failure rates is a logical approach for most systems where each hardware failure generates, usually, one discrete corrective action. This is especially true with systems for which the only corrective maintenance is the replacement of failed units. There is no "repair" as such, and each failure dictates, more or less, one specific maintenance action. Selecting tasks on the basis of failure contribution is, then, equivalent to selecting on the basis of maintenance action rate.

Such is not the case with a structural type of component such as a rotor blade, however, whose elements or parts are, for the most part, inseparable from the main structure, i.e., not replaceable. Failure of an element is usually not corrected by replacing the element, but rather through in-place repair of the element. Several different repairs may be allowed to a single blade element, depending on the mode and extent of

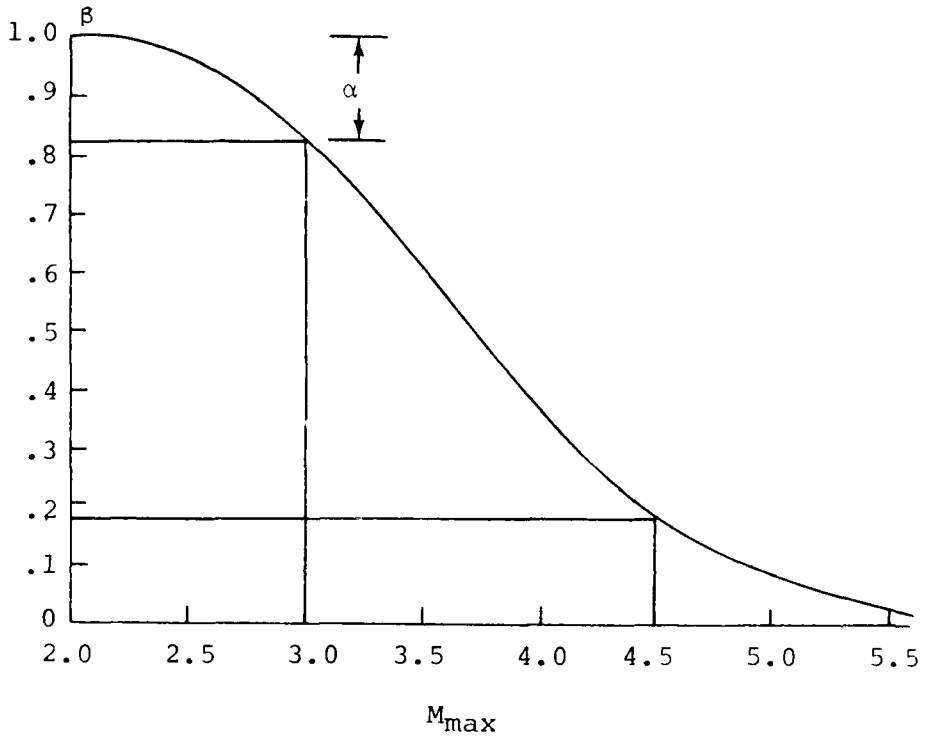

Figure 60. Operating Characteristic Curve.

failure or damage, and more than one element may be involved in a single repair action. Thus, to stratify the population of maintenance actions on the basis of blade element failure rates would not, in itself, yield a representative sample.

For the rotor blade, therefore, logical classifications of the population had to include combinations of blade element and repair method and provide for cases wherein multiple blade elements are involved in a single repair. Table 27 shows the demonstration task selection. All of the repairable blade elements are listed, together with the allowable repairs for each element. In addition to individual blade elements, combinations of elements found to sustain a significant incidence of simultaneous, repairable damage via the damage scenario are listed with the combined repairs that would be required. The number of tasks of each type were selected on the basis of the approximate contribution of each task to the total task population. The sample contains, beyond the 21 tasks required for the demonstration, two additional plug patch repairs which were made to the two blades later whirl tested.

Damage Simulation

The tasks demonstrated involved repair of failures or damage to various elements of the rotor blade. In order to establish realistic conditions for the demonstration, it was necessary to introduce, or simulate, the various defects or damage events.

The most complex repairs made to the rotor blade are those involving damage to the aft section, such as skin cracks and core punctures. In most cases, such factors as the damage location, angle of penetration, and size and shape of the hole have no effect on the repair to be made, other than to dictate the choice of patch or plug size. For a given damage event, core puncture, for example, there may be some slight task time increase for very large repairs or repairs made in proximity to critical blade elements, such as the trailing-edge spline or spar. In this latter case, the need to work more cautiously may add to the time of the task.

The second most prevalent type of repairable damage is surface defects, such as nicks, scratches, abrasions and corrosion. Within established repair limits for a given element of the blade, the nature of the defect, and its magnitude and location, again, have little impact on the repair procedure and task time. The time to blend out and refinish a 1-inch scratch will, for example, not differ significantly from that required for a similar repair of a 1/4-inch nick. Some time differential could be involved in assessing whether the damage is repairable, however, when it appears close to allowable limits.

TABLE 27. DEMONSTRATION TASK SAMPLE SELECTION

BLADE ELEMENT	MAINTENANCE ACTION	NUMBER DEMO. TASKS
Spar	Blend/Refinish	3
Skin	Skin Patch	8
Skin/Core	Skin Patch	2
Skin/Core	Plug Patch	4
Skin/Core	Double Plug Patch	4
Skin/Core	Double Skin Patch	
Grip and Drag Plates	Blend/Refinish	1
Grip and Drag Bushings	Polish	
Grip Pad	Polish, Blend/Refinish	
Grip Doublers	Blend/Refinish	
Tip Cap	Blend/Refinish	
Tip Cap	Secure/Replace Hardware	
Tip Cap	Remove/Replace	
Trim Tab	Blend/Refinish	
Trim Tab	Straighten	
Trailing-Edge Spline	Blend/Refinish	1
		23

The third general type of blade repair is that involving replacement of a separable blade part, the tip cap being the only item of this type. Again, the type of damage necessitating the replacement does not influence the repair procedure or time significantly. That is, it matters little whether a tip cap is dented, cracked or crushed, insofar as its replacement is concerned.

For each of the three general types of repairs to be demonstrated, therefore, the manner in which the defect was introduced was not overly important. To demonstrate a 3-inch-diameter skin patch, for example, it was immaterial whether the inflicted damage was a clean hole made with a screwdriver or a ragged hole made with a hammer, so long as a 3-inch patch was adequate. For a surface defect, a screwdriver scratch or file abrasion would produce essentially the same repair requirement.

In simulating blade damage for the demonstration, therefore, defects were introduced which were appropriate for the type of repair to be made without attempting to simulate all the different defects which a given repair might correct. If, for example, a given repair is applicable uniformly to cracks, punctures, tears or delaminations within established limits and two repairs of this type were to be demonstrated, the inflicted damage could be the same for both (screwdriver puncture, for example).

As pointed out previously, the location of damage may have some effect on the time required to effect a repair, especially if it is to be made in proximity to a critical blade element. In selecting damage events for the demonstration, locations were distributed so as to include some of those requiring special precautions or more exacting work.

Table 28 describes the characteristic failure or damage event selected for each of the 23 demonstrated tasks. Each failure or damage event is identified in terms of its physical description and blade location. For external damage causes, events were selected, wherever possible, from the damage scenario. Where the task selection called for multiple events of some general type, either externally caused or inherent failure, the physical dimensions and location of the several events were chosen to provide a sample representative of the distribution which might be experienced in actual use. Damage types and locations which are physically more difficult (underside of blade) or require special skills or precautions (repairs in proximity to the blade spar or spline) were included in the sample.

TABLE 28. MAINTENANCE TASK SAMPLE DESCRIPTION

TASK NO.	BLADE SERIAL NO.	BLADE ELEMENT/MAINTENANCE ACTION	REPAIR PROCEDURE NUMBER	Damage Description					Damage Location		
				TYPE	SPAN	CHORD	DEPTH	NO.	BLADE SPAN	BLADE CHORD	BLADE SIDE
1	8	Spar/Blend Repair	2-5	Nick	1.225	1.005	.003	87	69.1	1.6	Top
2	8	Skin-Core/7-Inch-Dia. Plug, 1-1/4 Inch Deep	2-2	Tear	.479	5.071	.558	56	70.9	10.6	Top
3	8	Skin-Core/3-Inch-Dia. Patch	2-1	Puncture	.782	.585	.821	44	77.8	10.3	Bot.
4	8	Skin-Core/3-Inch-Dia. Patch	2-1	Puncture	.396	.709	1.093	67	93.1	13.6	Bot.
5	8	T. E. Spline/Blend Repair	2-5	Nick	.250	.015	Thru	*	135.0	21.0	Both
6	8	Skin/5-Inch-Dia. Patch	2-1	Dent	.250	2.500	.030	*	141.5	12.7	Top
7	8	Skin-Core/7-Inch-Dia. Plug, 1/2 Inch Deep	2-2	Tear	.793	6.681	.418	*	170.7	11.5	Top
8	8	Skin-Core/3-Inch-Dia. Patch	2-1	Dent	.125	.875	.030	*	182.8	13.2	Bot.
9	8	Spar/Blend Repair	2-5	Nick	1.580	.005	.003	75	204.4	4.6	Bot.
10	8	Skin-Core/Double 3-Inch-Dia. Plug, 1/2 Inch Deep	2-2	Battle Damage	.700	1.999	Thru	84	216.7	15.1	Both
11	8	Skin-Core/3-Inch-Dia. Patch	2-1	Puncture	.663	.774	1/2 Thru	*	259.0	11.2	Top

TABLE 28 - Continued

TASK NO.	BLADE SERIAL NO.	BLADE ELEMENT/MAINTENANCE ACTION	REPAIR PROCEDURE NUMBER	Damage Description					Damage Location		
				TYPE	SPAN	CHORD	DEPTH	NO.	BLADE SPAN	BLADE CHORD	BLADE SIDE
12	9	Doubler/Blend Repair	2-5	Nick	.060	.250	.015	*	8.2	2.2	Bot.
13	9	Skin-Core/3-Inch-Dia. Patch	2-1	Puncture	.341	.601	.782	21	79.1	11.5	Bot.
14	9	Skin-Core/3-Inch-Dia. Patch	2-1	Puncture	.583	.862	.341	27	87.4	14.2	Top
15	9	Skin-Core/3-Inch-Dia. Plug, 1/2 Inch Deep	2-2	Puncture	.958	1.877	.334	*	89.8	9.0	Bot.
16	9	Skin-Core/Double 3-Inch-Dia. Plug, 1-1/4 Inch Deep	2-2	Battle Damage	1.149	1.215	Thru	20	123.7	10.6	Both
17	9	Spar/Blend Repair	2-5	Nick	1.164	1.832	.003	13	127.3	3.7	Top
18	9	Skin-Core/3-Inch-Dia. Plug, 1/2 Inch Deep	2-2	Puncture	.717	2.047	.329	63	151.9	10.6	Top
19	9	Skin-Core/3-Inch-Dia. Patch	2-1	Puncture	.322	.773	.489	51	171.4	18.7	Top
20	9	Skin-Core/3-Inch-Dia. Patch	2-1	Tear	.125	.875	.303	*	229.0	10.2	Top
21	9	Skin-Core/9-Inch-Dia. Patch	2-1	Tear	1.250	6.500	.030	*	244.5	13.5	Bot.
22	12	Skin-Core/Double 7-Inch-Dia. Plug, 1-1/4 Inch & 1/2 Inch Deep	2-2	Battle Damage	1.500	6.500	Thru	*	112.0	11.8	Both
23	13	Skin-Core/Double 7-Inch-Dia. Plug, 1-1/4 Inch & 1/4 Inch Deep	2-2	Tear	1.093	6.500	Thru	*	197.2	15.4	Both

* Supplementary Damage - Not Included in 100 Random Damage Scenerio.

DEMONSTRATION PROCEDURE

Each repair task was observed and timed by the contractor's test coordinator and Government test observer. The procedure was, generally, as follows:

1. The contractor's test coordinator scheduled the task and assembled the required materials, tools and data at the aircraft.

2. The failure or damage to be simulated was made to the blade by the test coordinator, usually in the presence of the Government test observer.

3. The Army repairman was summoned and instructed to assess the damage and make the repair. A stop watch was started and the time to perform each step of the repair was measured and recorded. Neither the test coordinator nor the test observer offered advice to the repairman either before or during the test.

4. If it was necessary to interrupt the test for any reason, such as to examine the repair in process or to allow the repairman or the observers personal time, the clock was stopped and restarted when the repairman actively resumed work.

5. At the conclusion of the test, a data sheet was filled out by the test coordinator and test observer to record the nature and conditions of the test, the time required, a statement of any problems or deficiencies encountered, and recommendations concerning the repair procedures, instructions, repair kits, tools, etc.

DEMONSTRATION RESULTS

All twenty-three repairs were demonstrated over a period of six days. Repairs were demonstrated one at a time, and a maximum of five repairs were made in a single day. All of the demonstrated repairs were made by the two Army repairmen, approximately an equal number of each type.

Analysis of Demonstrated Repair Times

All of the demonstrated repair tasks were observed and timed as explained in the discussion of the demonstration procedure. The time was recorded for each step of a repair task. Individual step times were later regrouped into the following eight sub-tasks, not all of which occur with every repair procedure:

1. Task Preparation
2. Balance Weight Adjustment
3. Damage Cleanup
4. In-Process Inspection
5. Patch/Plug Installation
6. Adhesive Curing
7. Post-Cure Cleanup
8. Surface Treatment

Tables have been prepared to show the results of the demonstration task analysis and to compare these results with predicted values. These tables are analyzed and discussed in the following paragraphs.

Skin Patch Task Demonstrations

Table 29 shows the recorded task times for the ten demonstrated skin patch repairs. Table 30 summarizes the ten demonstrations, showing the minimum, maximum and average time by subtask. As the tabulated data indicates, there was little variation in the time required to perform skin patch repairs and no appreciable difference between repairs made in the top and bottom surfaces of the blade. Slightly more time was expended on the two larger skin patches, primarily because of the greater area of damage cleanup involved.

Single Plug Patch Task Demonstration

Tables 31 and 32 show the detailed and summarized task times for the four demonstrated single plug patch repairs. Here, also, there exists no significant variation in total task time, although the one plug repair in the bottom surface of the blade did consume more time for cleanup and plug installation, indicative of the somewhat greater difficulty of working overhead. The two 7-inch plugs required, on the average, more time than did the 3-inch plugs, due primarily to added damage cleanup.

Double Plug Patch Task Demonstrations

Demonstrated task times for four double plug patch repairs are detailed and summarized in Tables 33 and 34. With the exception of the longer time, on the average, expended on damage cleanup and installation of the two larger plugs, no significant variations between tasks are apparent, even between upper and lower

TABLE 29. DEMONSTRATION TASK TIMES*, SKIN PATCHES.

PATCH SIZE →	3-INCH								5-IN.	9-IN.
BLADE SURFACE →	TOP				BOTTOM				TOP	BOT
TASK NUMBER →	11	14	19	20	3	4	8	13	6	21
Task Preparation	0.3	2.0	3.8	5.4	1.0	1.8	2.8	6.2	4.5	2.4
Balance Weight Adjustment	7.2	4.3	4.8	3.8	4.3	4.4	4.2	4.3	6.1	6.2
Damage Cleanup	9.4	8.3	8.6	8.4	11.1	8.4	11.1	7.9	11.0	18.0
Patch Application	6.6	6.9	5.5	5.8	5.4	6.7	6.4	6.6	8.5	7.4
Adhesive Curing	19.4	19.1	19.9	19.3	19.7	19.8	20.9	19.7	19.4	20.0
Post-Cure Cleanup	3.7	2.4	4.6	2.9	2.8	2.7	2.6	3.2	2.6	4.8
TOTAL TASK TIME	46.6	43.0	47.2	45.6	44.3	43.8	48.0	47.9	52.1	58.8

*Man Minutes

TABLE 30. DEMONSTRATION TASK TIME SUMMARY, SKIN PATCHES

TASK ELEMENT	MAN-MINUTES		
	AVERAGE VALUE	MINIMUM OBSERVED VALUE	MAXIMUM OBSERVED VALUE
Task Preparation	3.0	0.3	6.2
Balance Weight Adjustment	4.9	3.8	7.2
Damage Cleanup	10.2	7.9	18.0
Patch Application	6.6	5.4	8.5
Adhesive Curing	19.7	19.1	20.9
Post-Cure Cleanup	3.2	2.4	4.8
Complete Task	47.6	43.0	58.8

TABLE 31. DEMONSTRATION TASK TIMES*, SINGLE PLUG PATCHES

PLUG SIZE →	3-INCH		7-INCH	
BLADE SURFACE →	TOP	BOT	TOP	BOT
TASK NUMBER →	18	15	2	7
Task Preparation	5.9	3.8	1.5	5.5
Balance Weight Adjustment	4.5	4.9	5.3	5.4
Damage Cleanup	12.3	17.6	26.9	26.6
Plug Installation	7.4	11.1	12.5	11.2
Adhesive Curing	19.1	21.2	28.5	20.3
Post-Cure Cleanup	3.4	3.5	3.4	2.2
TOTAL TASK TIME	52.6	62.1	78.1	71.2

* Man-Minutes

TABLE 32. DEMONSTRATION TASK TIME SUMMARY, SINGLE PLUG PATCHES

TASK ELEMENT	MAN-MINUTES		
	AVERAGE VALUE	MINIMUM OBSERVED VALUE	MAXIMUM OBSERVED VALUE
Task Preparation	4.2	1.5	5.9
Balance Weight Adjustment	5.0	4.5	5.4
Damage Cleanup	20.9	12.3	26.9
Plug Installation	10.6	7.4	12.5
Adhesive Curing	22.3	19.1	28.5
Post-Cure Cleanup	3.1	2.2	3.5
Complete Task	66.0	52.5	78.2

TABLE 33. DEMONSTRATION TASK TIMES*, DOUBLE PLUG PATCHES

PLUG SIZE →	3-INCH						7-INCH					
TASK NUMBER →	10			16			22			23		
BLADE SURFACE→	TOP	BOT	BOTH	TOP	BOT	BOTH	TOP	BOT	BOTH	TOP	BOT	BOTH
Task Preparation	--	--	4.8	--	--	4.9	--	--	1.7	--	--	1.1
Balance Weight Adjustment	--	--	6.1	--	--	4.5	--	--	6.5	--	--	5.3
Damage Cleanup	19.5	15.5	35.0	13.2	16.8	30.0	24.9	28.4	53.3	20.1	23.7	43.8
Plug Installation	8.2	7.1	15.3	5.5	8.1	13.6	12.6	12.0	24.6	10.3	8.7	19.0
Adhesive Curing	20.0	21.2	41.2	23.0	29.3	52.3	30.7	23.6	54.3	29.2	19.8	49.0
Post-Cure Cleanup	1.5	1.5	3.0	2.7	1.2	3.9	4.9	5.7	10.6	3.5	5.4	8.9
TOTAL TASK TIME	49.2	45.3	105.4	44.4	55.4	109.2	73.1	69.7	151.0	63.1	57.6	127.1

*Man-Minutes

TABLE 34. DEMONSTRATION TASK TIME SUMMARY, DOUBLE PLUG PATCHES

TASK ELEMENT	MAN-MINUTES		
	AVERAGE VALUE	MINIMUM OBSERVED VALUE	MAXIMUM OBSERVED VALUE
Task Preparation	3.1	1.1	4.9
Balance Weight Adjustment	5.6	4.5	6.5
Damage Cleanup	40.5	30.0	53.3
Plug Installation	18.1	13.6	24.6
Adhesive Curing	49.2	41.2	54.3
Post-Cure Cleanup	6.6	3.0	10.6
Complete Task	123.1	109.2	151.0

plug installations. Post-cure cleanup, as expected, also requires more time for the larger diameter plugs.

Metal Reworking Task Demonstrations

Five metal reworking tasks were demonstrated, the results of which are given in Tables 35 and 36. The time required to perform these kinds of tasks is related mainly to the area of the damage, and appears to be longer for underside repairs. The task of this type requiring the most time was a repair on the doublers on the underside of the blade in a fillet which hampered cleanup and inspection of the rework.

Comparison With Predicted Values

Table 37 compares the demonstrated task times with those predicted for the maintainability analysis. For all of the tasks included in the sample, the demonstrated time is less than the predicted value. The mean time to repair calculated from the sample is much closer to the predicted value than would be indicated by differences between predicted and demonstrated values for the individual tasks. This is due to inclusion in the sample of the two double plug repairs (repairs numbers 22 and 23), made to the second set of blades for whirl testing. Inclusion of these two long-duration tasks, as specified by the Army, caused the demonstrated mean repair time to be larger than a sample based strictly on population would have produced.

The statistical variance of the sample is larger than that predicted, also influenced, however, by inclusion of the extra two double plug repairs. The 95th percentile maximum repair time calculated from the sample data is larger than the predicted value, but below the 3-hour requirement specified by the Army. Figure 61 is a plot of the demonstration sample data points and the repair time functions predicted and demonstrated.

Conclusion on Test of M_{max}

Earlier, the decision criteria for the test of the maximum repair time (M_{max}) were described. The test involves determination of a critical value for the M_{max} of the sample of demonstrated tasks and comparison of the observed M_{max} to that value. Based on the sample size, assigned risk value and sample variance, the critical value was calculated to be 3.85 hours. The observed M_{max} from the sample of demonstrated tasks is 2.86 hours, less than the critical value. From the results of this test, it is concluded that the Army's requirement for an M_{max} of 3 hours or less has been achieved in design of the FREB.

TABLE 35. DEMONSTRATION TASK TIMES*, METAL REWORKING TASKS

BLADE COMPONENT →	SPAR			SPLINE	DOUBLER
BLADE SURFACE →	TOP	TOP	BOT	THRU	BOT
TASK NUMBER →	1	17	9	5	12
Damage Cleanup	4.0	3.5	6.3	4.3	21.2
In-Process Inspection	0.8	0.5	1.0	0.7	2.3
Surface Treatment	3.3	4.2	5.0	2.9	2.8
TOTAL TASK TIME	8.1	8.2	12.3	7.9	26.3

* Man-Minutes

TABLE 36. DEMONSTRATION TASK TIME SUMMARY, METAL REWORKING TASKS

	MAN-MINUTES		
TASK ELEMENT	AVERAGE VALUE	MINIMUM OBSERVED VALUE	MAXIMUM OBSERVED VALUE
Damage Cleanup	7.9	3.5	21.2
In-Process Inspection	1.1	0.5	2.3
Surface Treatment	3.6	2.8	5.0
Complete Task	12.6	7.9	26.3

TABLE 37. COMPARISON OF PREDICTED AND DEMONSTRATED MAINTAINABILITY VALUES

	PREDICTED	DEMONSTRATED
TASK TIMES		
Skin Patch	1.35	0.78
Double Skin Patch	2.53	----
Plug Patch	1.67	1.10
Double Plug Patch	3.13	2.05
Metal Reworking (typ)	0.32	0.21
Tip Cap Replacement	0.20	----
Tip Cap Hardware Replacement	0.10	----
Trim Tab Straightening	0.32	----
Mean Time To Repair (MTTR)	1.30	0.94
Mean of Logarithms ($\bar{X}$)	- 0.0501	- 0.1420
Variance of Logarithms (σ_x^2)	0.0760	0.1322
Maximum Repair Time (M_{max})	2.75	2.86

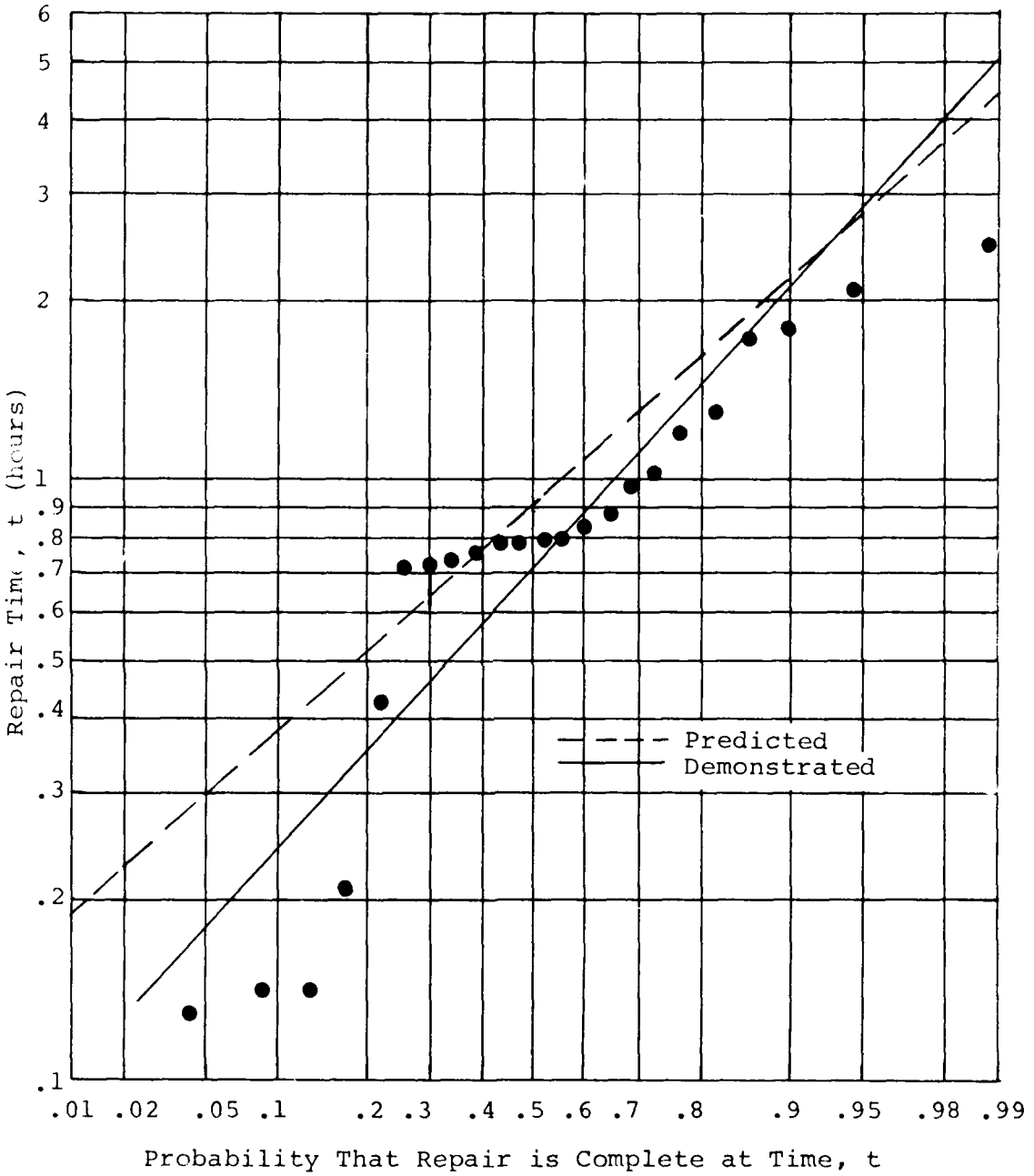

Figure 61. Maintainability Demonstration Task Times and Cumulative Repair Time Functions.

Qualitative Review of the Demonstration

The Army repairmen experienced no difficulty making any of the repairs during the demonstration, and all of the repairs were made successfully on the first attempt. At no time was it necessary to coach or instruct the repairmen while a task was being demonstrated, nor did they have a need to ask questions. The demonstration has shown, very convincingly, that average Army repairmen can, with minimal training, make structurally reliable repairs of the FREB on the aircraft in the field.

After the demonstration, blades 8 and 9, containing a total of 21 repairs, 16 of them patch or plug repairs, were whirl tested for a total of 35.7 hours. The blades were first whirled for 8.47 hours, as received from the demonstration. (The number of repairs made to the blades was so much beyond the allowable limits that it was necessary to use lead tape to adjust blade balance.) Subsequent to this, the blades were damaged and repaired four additional times and whirled. The damages were inflicted sequentially, and the blades were whirled in the damaged state for approximately two hours before each repair was made; a total of 10.5 whirl test hours was put on the blades during phase. The blades were then whirled for another 16.7 hours in that condition (a total of 25 repairs, 20 of them structural repairs). The final 20 minutes of this testing was made at 10% rotor overspeed. Figure 62 shows the blades installed on the whirl tower.

Throughout the whirl testing, none of the repairs showed any evidence of deterioration (despite the fact that the blades had been damaged and repaired much beyond the number of repairs that would be allowed in the field). Blade track remained within allowable limits.

Blades 12 and 13, which had the two most severe repairs made to them by the Army repairmen as part of the demonstration, were also whirled for 8.32 hours. No deterioration of the repairs occurred.

Demonstration Critique

At the conclusion of the demonstration, a critique was held to discuss the results and to obtain comments and recommendations from the participants. The critique was attended by the two Army repairmen, the Army's project engineer, the Contractor's Program Manager, and members of the Contractor's Maintainability and Materials Engineering groups. A number of comments and recommendations were made for refining the repair methods, kits and tools for future applications.

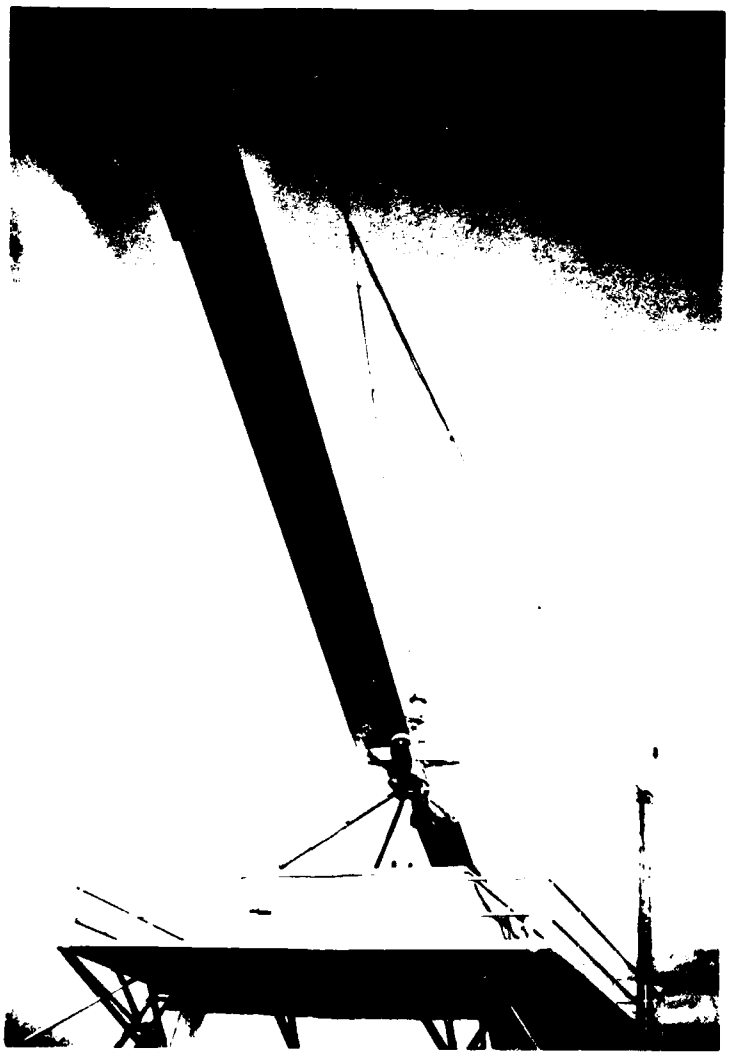

Figure 62. Repaired FREB on Whirl Rig.

FREB COMPONENT TEST

In order to evaluate the structural integrity of the FREB, a number of component tests were performed on virgin specimens, damaged specimens and repaired specimens. These tests included:

- Static strength and stiffness tests of whole blades and blade components
- Nonrotating natural frequency tests of whole blades
- Fatigue tests of blade components
- Whirl tests of full blades.

Table 38 summarizes the tests performed and the test results.

STATIC STRENGTH AND STIFFNESS TESTS

In order to check the accuracy of analytical predictions of FREB stiffnesses, measurements of blade spring rate were taken using the test setup shown in Figure 63. For the flatwise stiffness measurements, loads were applied at station 280 through the quarter chord. Deflections and strains were measured at various stations in order to experimentally determine blade stiffnesses and deflected mode shapes. Table 39 shows that the analytical predictions are within experimental accuracy of the measured values. The same basic setup was used to measure edgewise and torsional stiffnesses.

Subsequent to the deflection tests, the blade was loaded to ultimate load in the flatwise direction (4-G ground handling loads) without failure. The blade was then loaded to failure in edgewise bending. Failure occurred at 280% of limit load (290% of hard start loads) when the trailing-edge spline buckled, as shown in Figure 64. After failure, it was obvious that neither the spline nor the skins could carry edgewise load. The spar, however, was able to still carry 140% design limit load.

Specimens consisting of the first 100 inches of the blade with reinforcement at the outboard end were used to evaluate the static strength of the blade root end. A test specimen is shown mounted in the test fixture in Figure 65. This fixture allows simultaneous application of static and/or dynamic edgewise and flatwise loads and CF loads. For the static test, limit stresses were those peak stresses predicted to occur on the blade during flight at 92.7 knots, 6000 ft, N = 1.544 with a gross weight of 8500 pounds. At the maximum test condition, loads to the undamaged specimen were as given in Table 40. This

TABLE 38. FREB COMPONENT TEST SUMMARY

STATIC STRENGTH AND STIFFNESS		NONROTATING NATURAL FREQUENCY		FATIGUE		WHIRL
FULL BLADE VIRGIN SPECIMENS		FULL BLADE VIRGIN SPECIMENS		BLADE ROOT END		FULL BLADE
F/W Stiffness & Static Droop	Tests showed good agreement with analytical predictions	PIN-END		Combined E/W, F/W & CF, Virgin specimen	Specimens withstood max vibratory strains mixed with G-A-G for loads up to 2×10^6 cycles. Blade sections survived while standard UH-1 drag braces failed	Virgin, damaged and damaged/repaired blades whirled at both overspeed and 9900 lb, 315 rpm. No failures, damage progression, excessive vibration or out-of-track occurred.
E/W Stiffness		Edgewise	Modal frequencies within experimental accuracy of those obtained by similar test on present blade	Combined E/W, F/W & CF, Damaged and Repaired specimen		
Torsional Stiffness		Flatwise				
F/W Strength	Specimen withstood 150% of limit load	CANTILEVER				Thrust vs HP data matched that of present UH-1 blade
E/W Strength	Specimen withstood 280% of limit load. At 290%, spline buckled	Edgewise				
		Flatwise				
ROOT END VIRGIN SPECIMENS				FREE-FREE BEAMS (OUTBD SECTIONS)		
Combined E/W, F/W & C/F	Specimen withstood combined CF, F/W & E/W ultimate loads without failure			VIRGIN SPECIMENS F/W - Valid spar failure forced at high load level E/W - Valid spline failure forced at high load level		
				DAMAGED & REPAIRED SPECIMENS *F/W - Had to be dented beyond repair limits to produce failure *E/W - Valid spline failure forced at high load level *No failures originating in repairs		
				TIP WEIGHT RETENTION Withstood 2400 G-A-G cycles. Last 400 cycles were at 150% of G-A-G normal loading.		

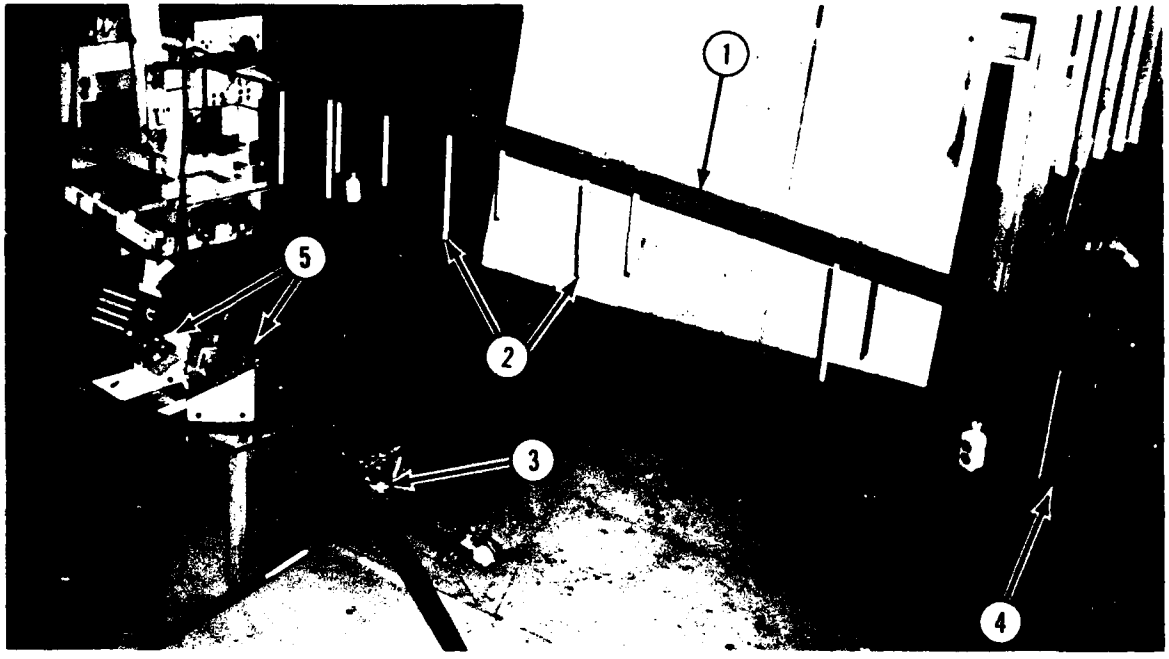

FLATWISE BENDING DEFLECTION TEST

1. K30-100 blade.
2. Deflection scales.
3. Surveyor's level.
4. Applied load (50-pound maximum load in position).
5. Strain gage read-out equipment.

Figure 63. Flatwise Bending Deflection Test Setup.

TABLE 39. COMPARISON OF ANALYTICALLY PREDICTED AND EXPERIMENTALLY MEASURED TEST VALUES

BLADE STATION (IN.)	FLATWISE EI ($LB\text{-}IN.^2 \times 10^6$)		EDGEWISE EI ($LB\text{-}IN.^2 \times 10^9$)	
	FROM STRAIN GAGE DATA	FROM COMPUTER PROGRAM	FROM STRAIN GAGE DATA	FROM COMPUTER PROGRAM
33			6.2	5.7
34	164	151		
64	64.9	57.9	3.02	2.57
82	31.9	31.70	2.22	2.23
123	32.4	31.67	1.62	1.722
165	32.7	31.63	1.11	1.21
230	33.2	31.6	.64	.661

Figure 64. Top View of Edgewise Static Load Specimen After Failure.

Figure 65. View of FREB Root End Specimen Mounted in Test Rig (View Looking Inboard).

TABLE 40. ROOT END SPECIMEN STATIC LOADS AND PERCENTAGES OF LIMIT LOADS

	STATION		
	34	64	82
Flatwise Moment, in.-kips	197.33	53.18	28.0
Edgewise Moment, in.-kips	366.2	344.65	230.47
Centrifugal Force, kips	153.76	153.76	153.76
Percentage of Limit Stress at Critical Location	171% Spar, max t	156% Spar, max t	166% Spar, max t

table also shows the percentage of the limit load condition described above. The stresses achieved in the parts were in excess of the 150% of limit load defining ultimate load. No deterioration of the specimen of any kind was noted after the test.

NONROTATING NATURAL FREQUENCY TESTS

Full blade specimens were suspended with root ends both fixed and pinned, and excited near predicted mode points in order to measure beam natural frequencies. The suspended blade is shown in Figure 66, while the shaker attachment is shown in Figure 67. The modal frequencies and shapes were determined for flatwise and edgewise loading with the root end both pinned and fixed. For the pin-ended modes, the blade was hung from knife edges; while for the fixed modes, the blade was bolted to the standard UH-1 blade retention which was in turn rigidly mounted to the Contractor's static test rig. Specimen excitation was by a 50-lb electromagnetic shaker. For the flatwise modes, excitation was at the quarter chord, edgewise excitation was at the leading edge, and flatwise/torsion coupled modes were excited at the trailing edge. Table 41 gives a comparison of the test frequencies obtained from the FREB and the present UH-1 blade. Test results showed that the dynamic characteristics of the FREB are very close to those of the present UH-1H blade.

FATIGUE TESTS OF BLADE COMPONENTS

Component fatigue evaluation consisted of the following tests:

a. Root end fatigue test

b. Free-free beam outboard section tests

c. Tip weight retention ground-air-ground test.

ROOT-END FATIGUE TEST

This testing used the same setup shown in Figure 65 for the root-end static test. Fatigue loads consisted of static CF, flatwise and edgewise moment with simultaneously peaking flatwise and edgewise vibratory moments superimposed on them. Three load spectra were applied: fatigue loads consisting of moments the blade is predicted to see at 107 kt, 6600 lb straight-and-level flight, a high level intended to produce early failure, and an intermediate load level. The testing produced only a drag brace evaluation rather than a blade evaluation because the drag braces used in the testing all failed, leaving the test specimens undeteriorated. Two specimens were tested undamaged, and a third was first tested at the fatigue load level with several damages inflicted (two .75-inch dia. jagged through-holes; see Figure 68) and then tested at the

Figure 66. FREB Suspended for Nonrotating Natural Frequency Test.

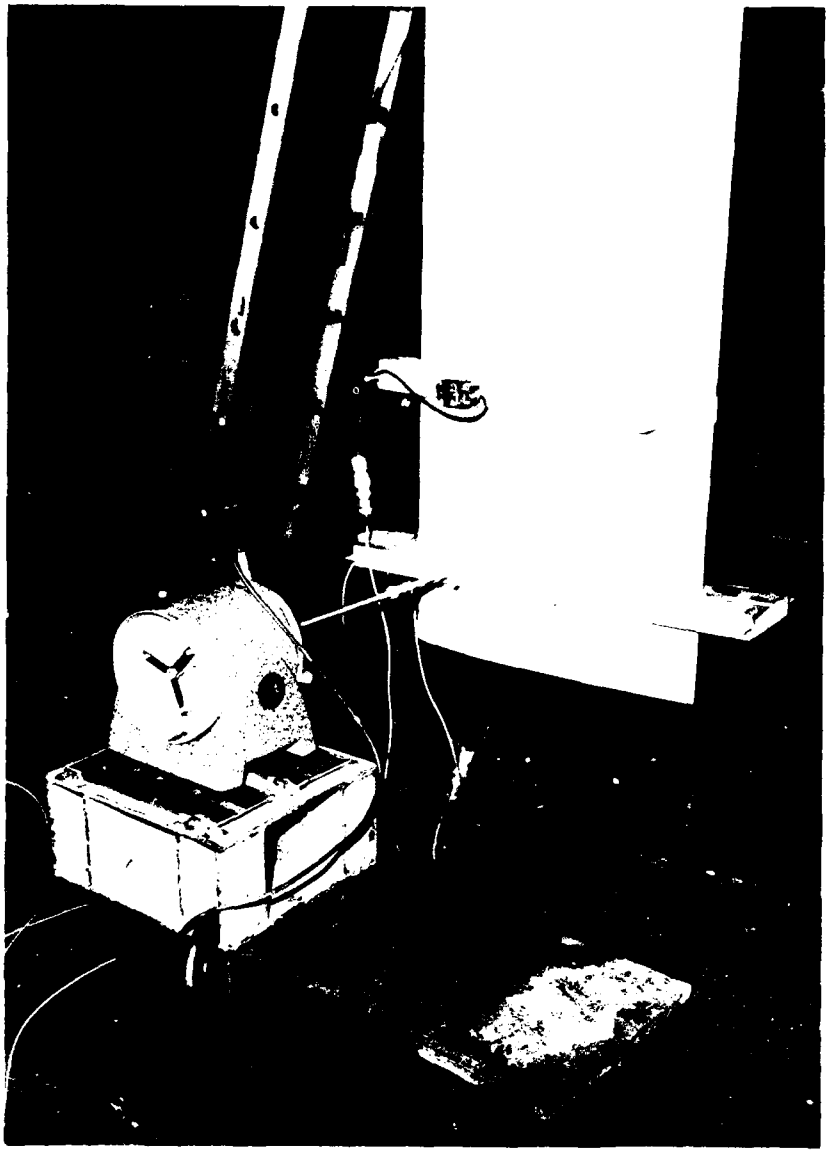

Figure 67. 50-Lb Shaker Attached to FREB for Nonrotating Natural Frequency Test.

TABLE 41. COMPARISON OF BLADE FREQUENCIES FOR THE FREB AND THE PRESENT UH-1H BLADE

MODE	FREQUENCY, Hz	
CANTILEVER	FREB	PRESENT UH-1H BLADE
1st Flatwise	3.7	3.5
2nd Flatwise	8.7	8.2
3rd Flatwise	21.5	20.0
4th Flatwise	24.4	22.8
5th Flatwise	41.0	40.0
1st Flatwise/Torsion	3.6	3.4
2nd Flatwise/Torsion	8.0	6.7
3rd Flatwise/Torsion	9.6	8.0
1st Edgewise	6.5	6.1
2nd Edgewise	8.0	7.7
3rd Edgewise	23.0	22.1
4th Edgewise	25.0	24.3
5th Edgewise	35.0	35.7
PIN-ENDED		
1st Flatwise	5.2	
2nd Flatwise	12.0	
1st Flatwise/Torsion	5.0	
2nd Flatwise/Torsion	12.1	
1st Edgewise	3.6	
2nd Edgewise	10.5	
3rd Edgewise	15.3	
4th Edgewise	21.5	

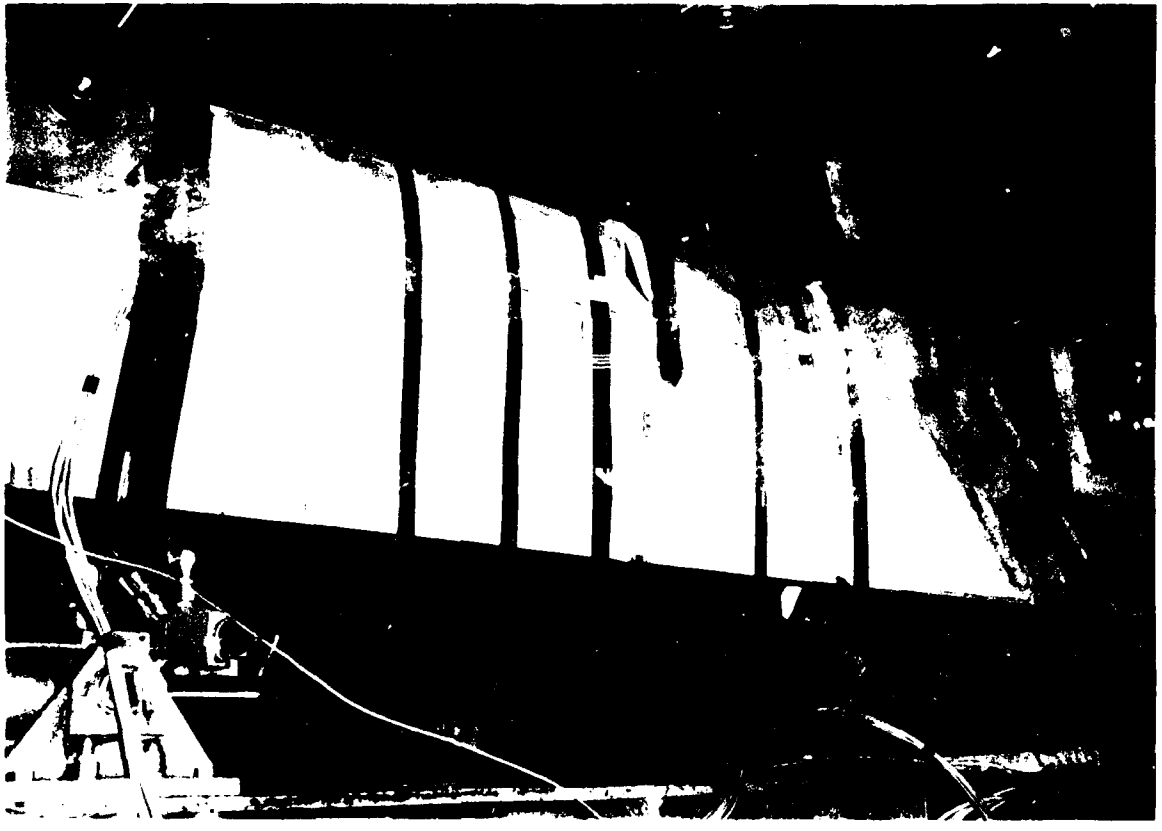

Figure 68. Damage Inflicted on S/N 3 Prior to Fatigue Test.

high load level with the original damages repaired and other damages inflicted and repairs made (see Table 42 and Figures 69 and 70). The drag braces had all seen an unknown spectrum of flight previous to testing, and the drag brace used with specimen 3 had been used for 53 hours of whirl test. The drag brace used with specimen 3, however, had been magnafluxed prior to testing. Typical drag brace failures are shown in Figure 71.

The loads applied during test and the cycles to drag brace failure are given in Table 43. Figure 72 is a projected fatigue curve, based on the data obtained from this testing. In this curve, the runout points are plotted with arrows and the fatigue curve is drawn through these points. This introduces an unknown level of conservatism into the curve with respect to the blade. The curve could be thought of as a drag brace fatigue curve because of the relatively high strength of the blade in comparison to the drag brace.

FREE-FREE BEAM OUTBOARD SECTION TESTS

In order to evaluate the reversed bending fatigue strength of the FREB outboard section, full-length spar-skin-core-spline assemblies were cut into an inboard section 100 inches long and an outboard section 163.5 inches long. The specimens were suspended as shown in Figure 73. Soft springs (bungee cords) supported the blade, and an electromagnetic shaker was used to drive the specimen slightly off a node point. In order to drive the specimens at reasonable frequencies, the edgewise specimens were end-loaded with 30-lb weights while the flatwise specimens were used as received. Table 44 gives a summary of the specimen types, applied loads and cycles to failure.

Specimens 7F and 11E were first tested without damage at a level intended to produce early failure. Specimens 11F and 7E were then tested. Specimen 11F had two ragged through-holes put in the afterbody, and then it withstood an equivalent 10 flight hours of testing at a level approximating that predicted to occur at 107 knots level flight. During this test, the two ragged holes did not deteriorate. Repairs were then made on the two holes, and an equivalent of 100 hours testing failed to produce any deterioration of the repairs. Finally, a large number of damages, including a severe spar dent .030 inch deep were inflicted by hitting the spar with a ball peen hammer. After 182,000 cycles of high-level load, a fatigue crack originated at the spar dent. Figure 74 shows a close-up of the damage to the spar, and Figure 75 shows the resultant fatigue crack. Although a smooth dent .030 inch deep is within acceptable limits (see repair instructions, Appendix B), the hammer-inflicted damage was not a smooth dent and would have had to have been blended out to a depth greater than .030 inch and would, therefore, result in blade scrappage rather than blade

TABLE 42. DAMAGE INFLICTED AND REPAIRS MADE ON ROOT END FATIGUE SPECIMEN #3

ITEM	DAMAGE	REPAIR
A	Damage created by driving a screwdriver completely through the blade in two places. Holes enlarged to approximately .75" by rotating the screwdriver in a conical manner to cause jagged edges.	Repaired with 3" skin patches both sides (after 10 equivalent flight hours of fatigue testing).
B	7" dia. x 1-1/4" deep core removed with router (bottom side only).	Repaired with 7" dia. plug patch.
1	.010" deep scratch in chord direction within 1/4" of hole edge - 1/2" long @ hole $\mathcal{L}$ on top surface.	No repair made.
2	.005" deep scratch, 3/4" long - chordwise in bottom doubler.	No repair made.
3	.010" deep scratch on T.E. spline - chordwise in bottom surface.	No repair made.
4	.004" deep scratch, 1/2" long in honeycomb - chordwise in bottom surface in 2 places.	No repair made.
5	.005" deep scratch, 3/4" long - chordwise in bottom surface.	No repair made.
6	.035" deep nose dent, 5" from doubler edge caused by hitting nose with a 2" dia. steel rod.	No repair made.
7	Max. allowable spline cutout placed at min. allowable distance from doubler edge.	Repaired/Manual
8	.004" deep scratch, 1/2" long - chordwise in bottom surface.	No repair made.

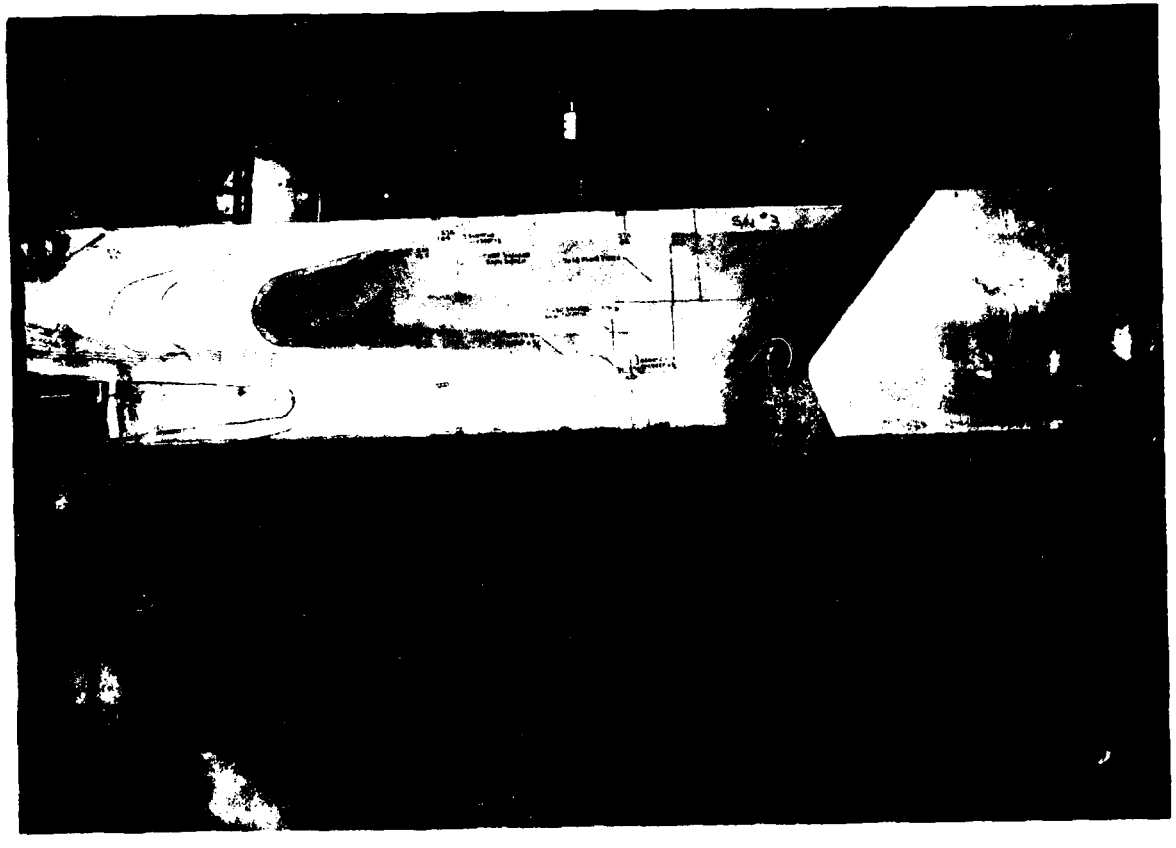

Figure 69. Damage Inflicted on S/N 3 During Test (Bottom Surface).

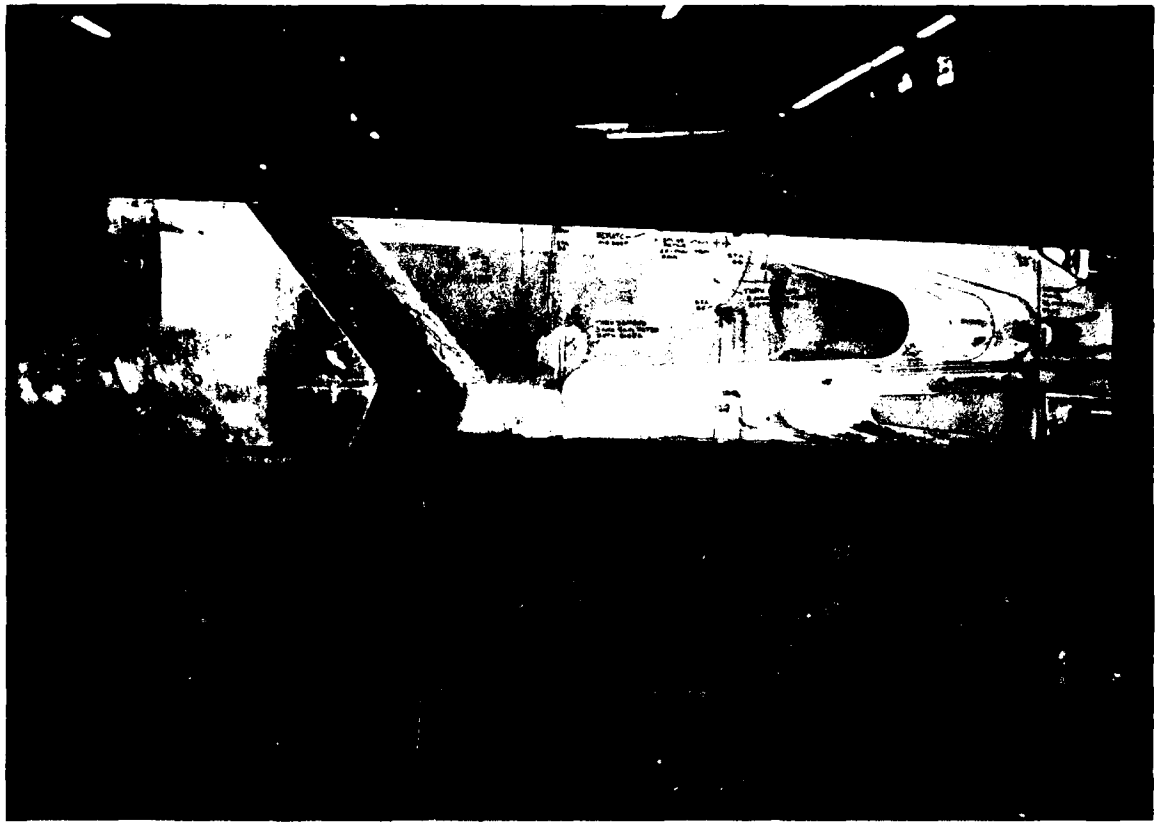

Figure 70. Damage Inflicted on S/N 3 During Test (Top Surface).

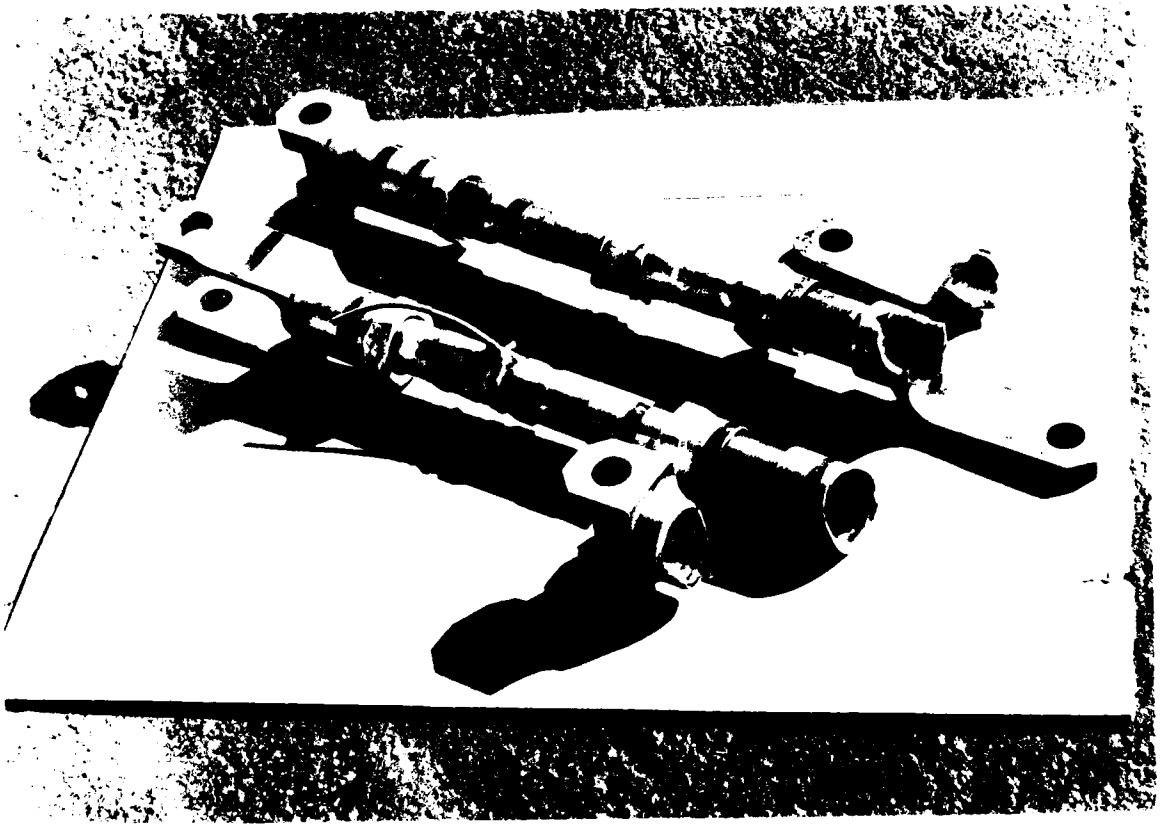

Figure 71. Typical Drag Brace Failures.

TABLE 43. ROOT END FATIGUE TEST SUMMARY

SPECIMEN NUMBER		APPLIED TEST LOADS STATION 34	STATION 64	STATION 82	TEST RESULTS
3 Fatigue (1.07 Kt)	CF, kips	79.42	79.42	79.42	No damage progression after 10 equivalent flight hours (194,000 cycles) at this level with two 3/4" jagged holes completely through the specimen.
	M F/W, in.-kips	16 ± 15.5	5.5 ± 5.5	2 ± 2.5	
	M E/W, in.-kips	27 ± 121	28 ± 97	31 ± 87	
High Level	CF, kips	79.42	79.42	79.42	Testing suspended after drag brace failure at .272 x 10^6 cycles at this level. Above damage was repaired and more damage was inflicted per Table 42. Neither damage nor repairs deteriorated during test.
	M F/W, in.-kips	65 ± 27	30 ± 8	15 ± 3	
	M E/W, in.-kips	19 ± 190	36 ± 145	5.5 ± 134	
4 High Level	CF, kips	79.42	79.42	79.42	No damage inflicted or repaired. Testing suspended at 108 x 10^6 cycles intermixed with 2000 GAG* cycles by drag brace failure.
	F/W, in.-kips	57 ± 25.5	24 ± 9	14 ± 4	
	E/W, in.-kips	17 ± 178	38 ± 148	16 ± 128	
5 Intermediate Level	CF, kips	79.42	79.42	79.42	No damage inflicted or repaired. Testing suspended at 3.02 x 10^6 cycles intermixed with 5000 GAG* cycles by drag brace failure.
	M F/W, in.-kips	49 ± 24.5	24 ± 8.7	13 ± 4	
	M E/W, in.-kips	70 ± 150	83 ± 17.2	32 ± 103.5	

* GAG loading consisted of cycles of CF load from 0 to 79.42 kips.

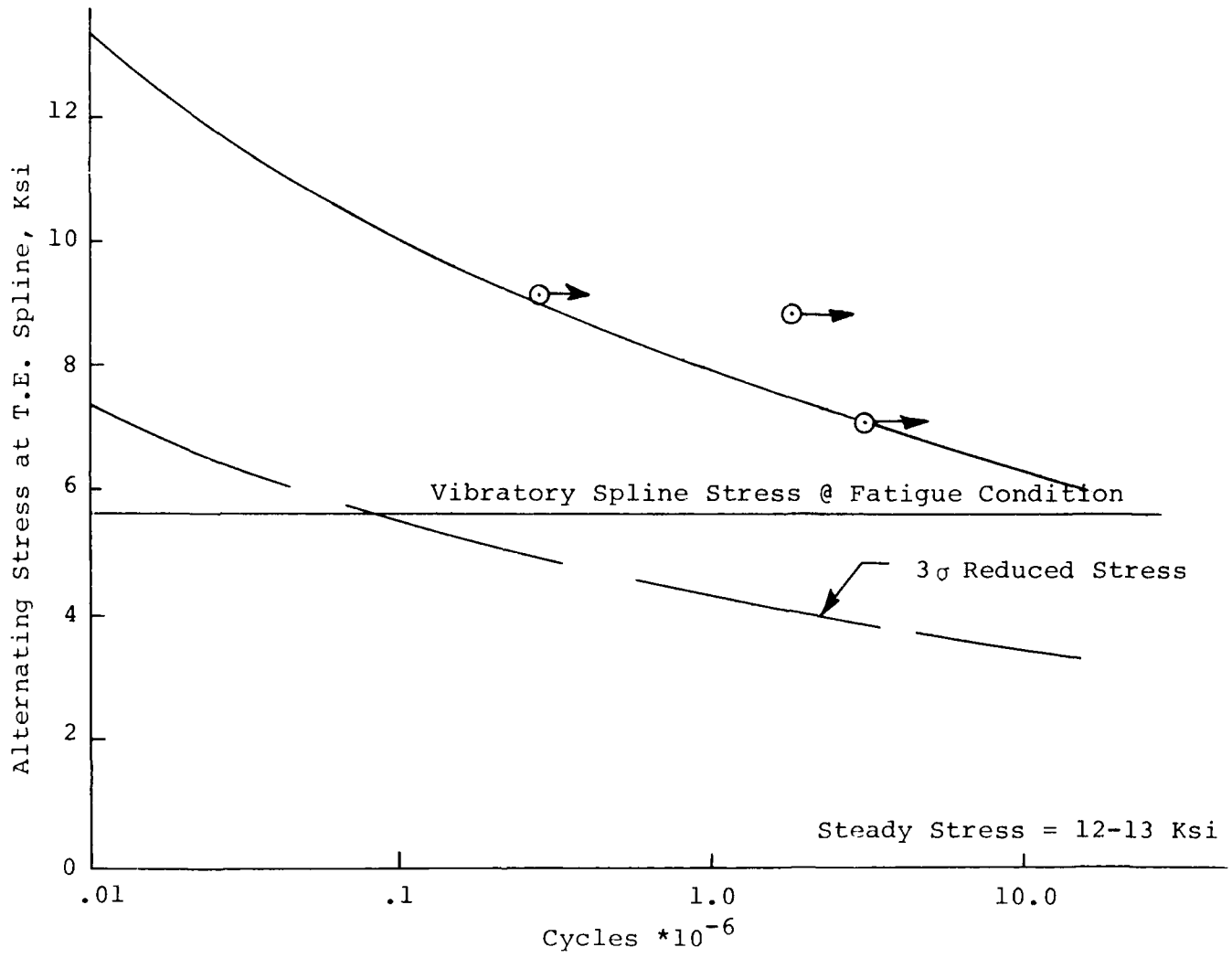

Figure 72. S/N Curve for Root End Fatigue Specimens.

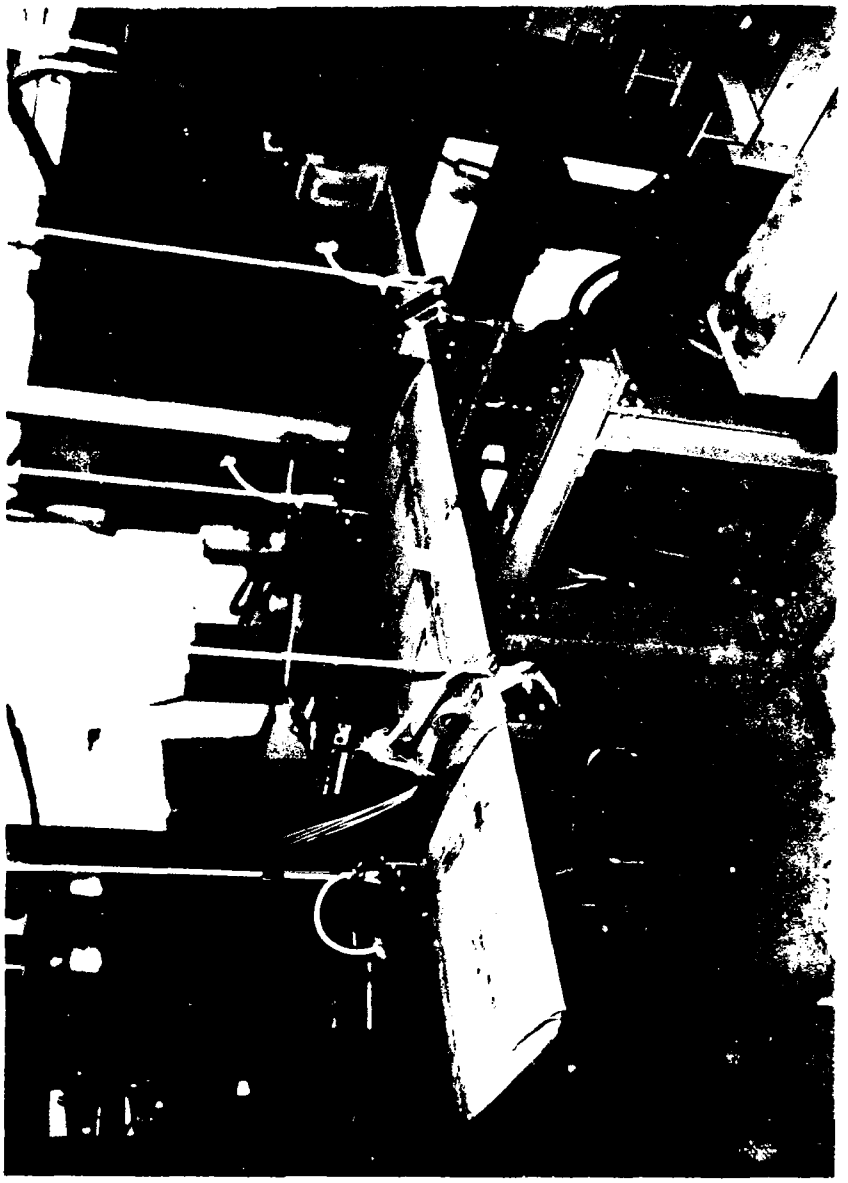

Figure 73. Test Setup for Free-Free Beam Fatigue Tests.

TABLE 44. FREE-FREE BEAM SPECIMEN TEST SUMMARY

SPECIMEN NUMBER	LOAD DIRECTION (AND LEVEL)	DAMAGE	REPAIRS	CYCLES @ FAILURE	COMMENTS
007F	Flatwise (± 55.5 in.-kips)	None	None	351,000	Failure originated @ spar rebate
011E	Edgewise (± 94.7 in.-kips)	None	None	152,200	Failure originated on TE spline
011F	Flatwise (± 6.5 in.-kips)	2 through holes	4 patches	Withstood 194,400 as damaged	No deterioration
				Withstood 1.94×10^6 cycles after repair	No deterioration
	Flatwise (± 55.5 in.-kips)	Patches, scratches and dent		182,160	Failed at inflicted spar dent
007E	Edgewise (± 18 in.-kips)	1 through hole 1 C/W slit	None	Withstood 194,400 as damaged	No deterioration
		Increase area of above damages	None	Withstood another 194,400 as damaged	No deterioration
			One repair	Withstood 1.94×10^6 cycles	No deterioration
	Edgewise (High Level) (± 94.7 in.-kips)		Additional repairs	Failed after 104,400 cycles	Originated @ top of spline

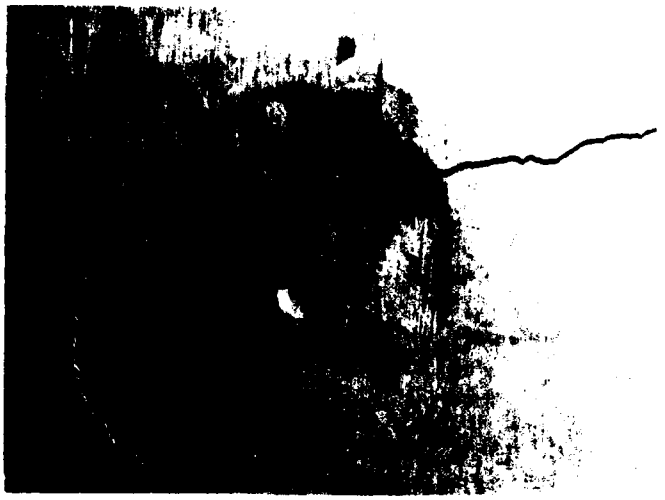

←—T.E. L.E.—→

Figure 74. Hammer Damage to Flatwise Free-Free Beam Specimen 011F.

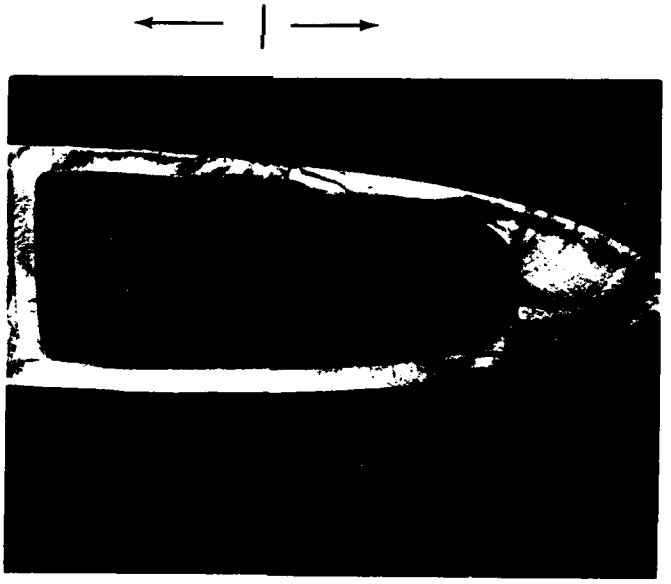

Figure 75. Spar Cross Section Through Fatigue Crack, S/N 011F.

repair. Specimen 7F withstood a failing level of flatwise load for 351,000 cycles before a fatigue crack originated at the spar rebate. A fatigue curve generated from these two data points is shown in Figure 76, along with reference load levels of the peak flatwise moment predicted at station 210 and the fatigue moment predicted at station 210.

The edgewise testing of specimens 11E and 7E was conducted in a similar manner. Specimen 11E was tested at a high load level intended to fail the specimen in a short time. A crack was started on the spline, and failure was noted by a distinct change in driving power required at 152,000 cycles. The spline crack and its effect on the skin are shown in Figure 77. Specimen 7E was first damaged with a through-hole and a chordwise slit. The specimen withstood 10 equivalent flight hours at the fatigue level without deterioration of the holes. One of the holes was then enlarged to 3 inches in diameter, and 1/2 inch deep, and testing continued for an additional 10 hours equivalent, again with no deterioration. After repair, another 10 equivalent flight hours was withstood at the fatigue level, again without specimen deterioration. The load level was then increased to the high-level (early failure) fatigue load, and a failure was finally noted on the spline after an additional 104,000 cycles. These two points were interpreted to give the fatigue curve of Figure 78.

In summary, this free-free beam testing confirmed the damage resistance of the fiberglass afterbody. Although this part of the blade was repeatedly and progressively damaged, all failures in this test sequence originated from either the spar or the spline. The fatigue curves generated from this testing, although based on an extremely small population, indicate that the blade outboard of the doublers should have adequate fatigue life. More extensive testing would be required to substantiate the blade for flight, but the results of this preliminary testing gave highly encouraging results.

TIP WEIGHT RETENTION GROUND-AIR-GROUND TEST

Figure 79 shows the tip weight configuration used in the FREB. This configuration was chosen to allow maximum accessibility of the tip weights for ease of rebalancing after repair. The four bolted attachments which fasten the tip cap to the spar carry all of the centrifugal force of the tip weight assembly, and this tip weight retention test was intended to prove the capability of the bolted attachments under simulated ground-air-ground cycling.

For the test setup, 16 inches of spar was clamped within the fixture. Two holes were bored into the spar leading edge and two into the tip cap attachment fitting, and inserts were put

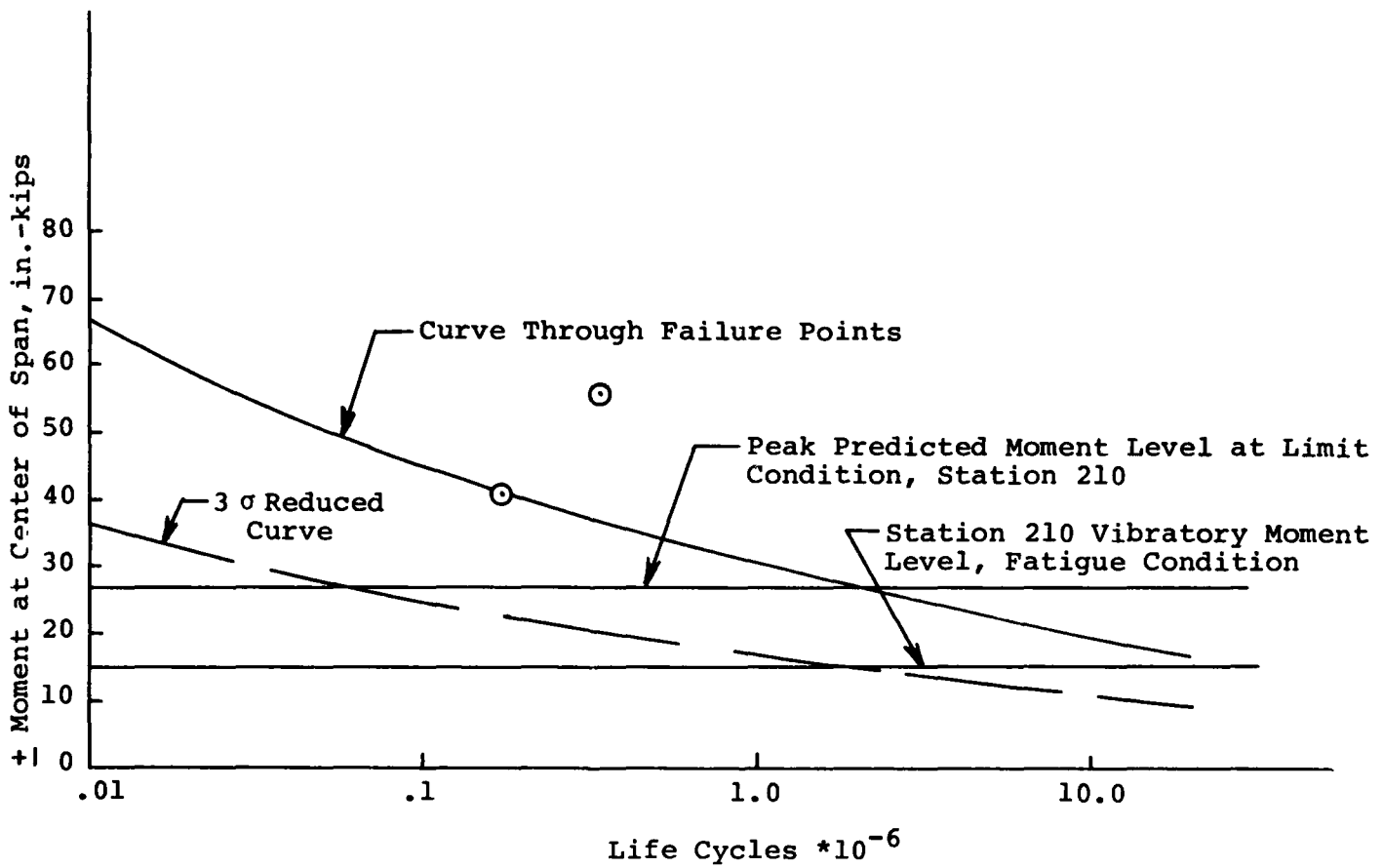

Figure 76. Flatwise Free-Free Beam Fatigue Curve.

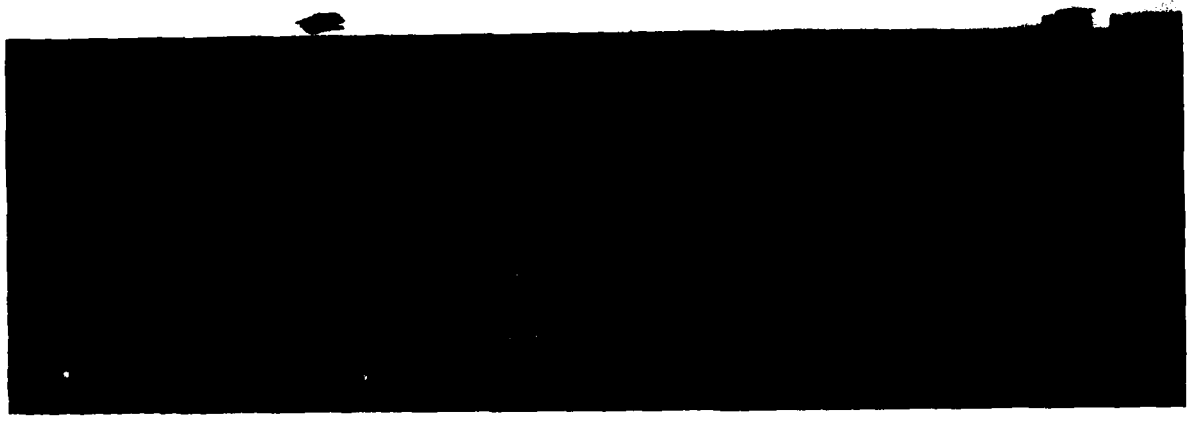

Figure 77. Spline Crack Failure on Specimen 7E.

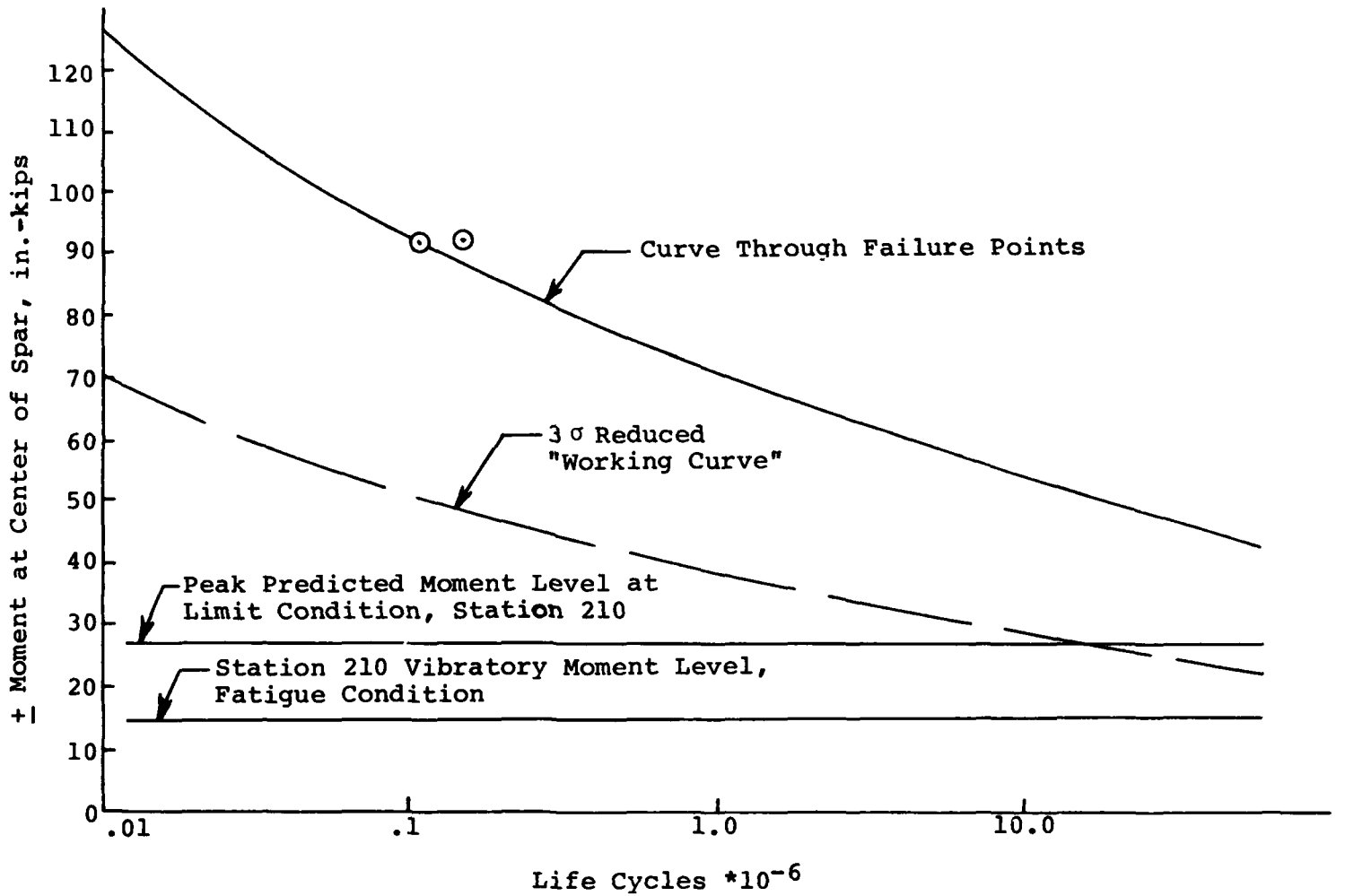

Figure 78. Edgewise Free-Free Beam Fatigue Curve.

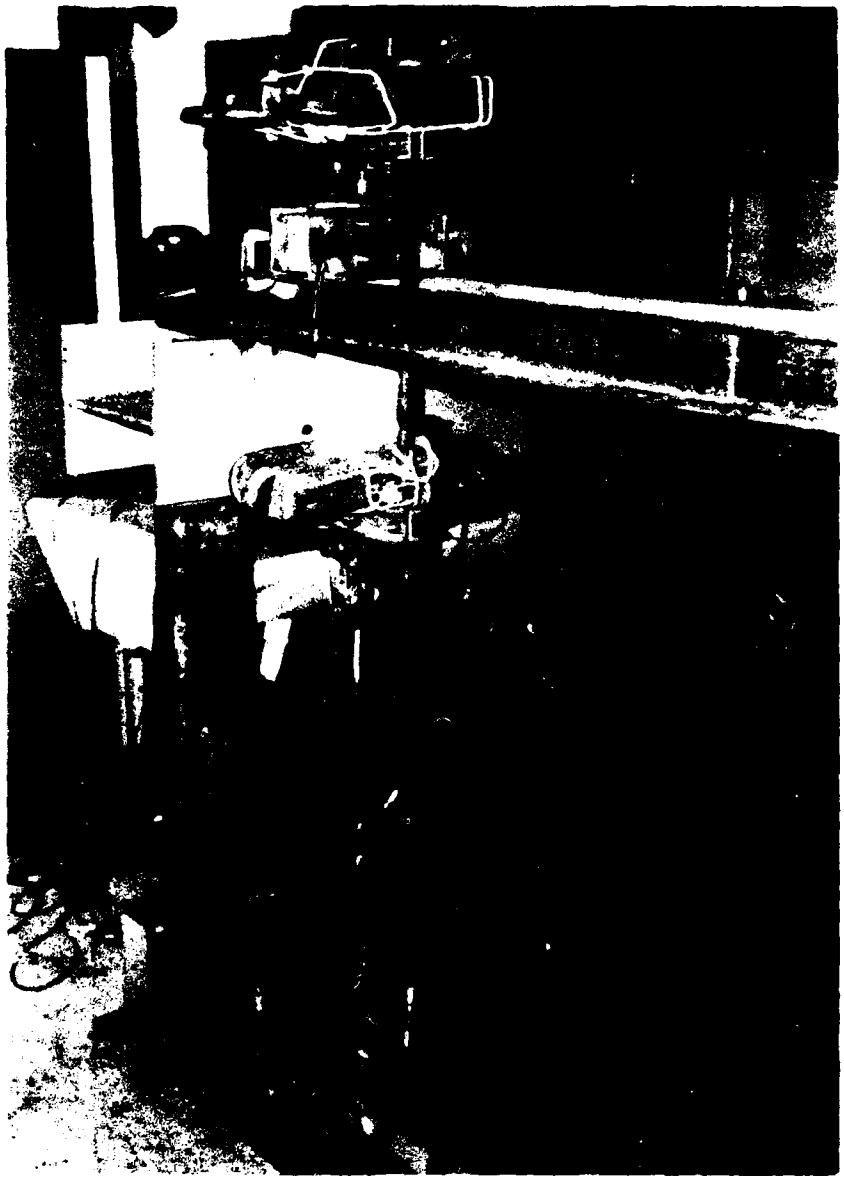

Figure 79. Tip Weight Retention Test Setup.

into these holes to accept the four attaching bolts. During specimen buildup, it was found that the bored holes were sufficiently oversize that they would have been rejected at inspection. This oversize hole produced a loose insert fit. Despite this discrepancy, it was decided to test the specimen without rework.

Loads were applied which went from 10% of the maximum tip weight attachment CF (369 lb) to 110% (4055 lb) at 324 rpm for each cycle. The original intention was to test to failure or 1000 cycles, whichever occurred first. No failure occurred during the first 1000 cycles, so an additional 1000 cycles were run with the same result. The load was changed to 53 lb to 5582 lb, and an additional 400 cycles were run, again with no failure. This testing showed the tip weight retention system to be adequate, with an additional measure of conservatism resulting from the poor fit of the inserts.

WHIRL TOWER TESTS

Whirl tower testing of the FREB was intended to demonstrate the structural integrity, balance, track and aerodynamic performance of the blade and blade repairs under combined CF, flatwise and edgewise loads. A total of 50 hours of testing was conducted on the Contractor's 1300-hp whirl test rig, shown in Figure 62.

The test consisted of approximately a 15-hour whirl test of the blades as manufactured, a 10-hour whirl test of damaged blades, and 25 hours whirl testing of damaged/repaired blades. The first 6 hours of whirl testing was devoted to investigation of blade track, blade stability, overspeed integrity and blade loading by gradually increasing the rotor speed to 315 rpm, followed by thrust buildup in 500-pound increments to 9900 pounds.

Figure 80 shows a flow chart of the whirl test, including where the various damage and repair events occurred in the test sequence. Table 45 goes with Figure 80 and describes the damage and repair events in more detail. The whirl test was designed to demonstrate three aspects of the FREB:

- The integrity of the virgin blade under combined flatwise, edgewise and CF loads
- The integrity of damaged blades under combined flatwise, edgewise and CF loads
- The integrity of the blade repairs under combined flatwise, edgewise and CF loads.

Specimens 8 & 9:

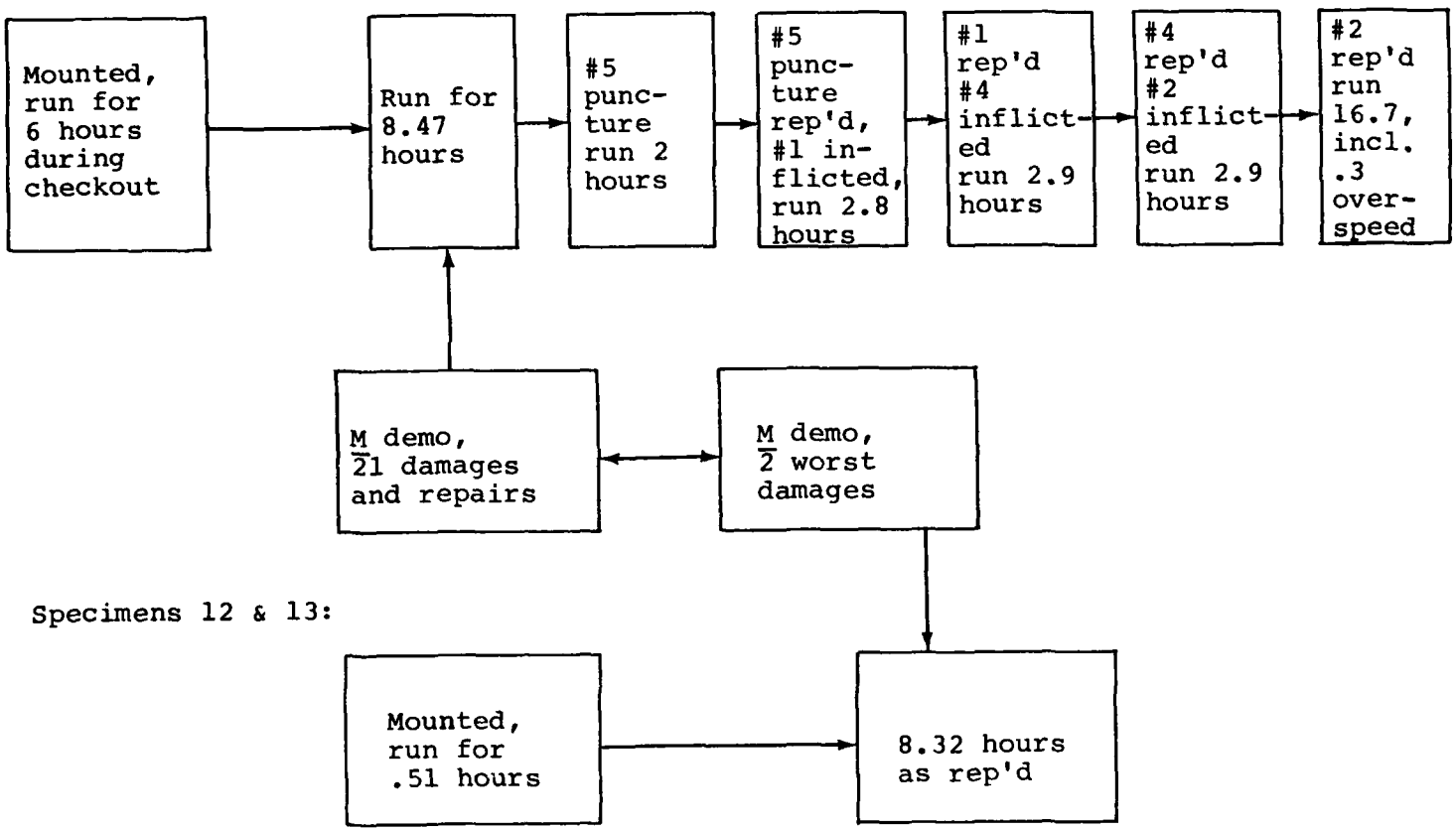

Specimens 12 & 13:

Note: See Table 45 for damage number description.

Figure 80. Whirl Test Flow Chart.

TABLE 45. WHIRL TOWER DAMAGE SUMMARY

EVENT NUMBER IN TEXT	BLADE S/N AND LOCATION	TYPE OF* DAMAGE	RADIUS	CHORD	DIMENSIONAL DESCRIPTION	TYPE REPAIR	WHIRL TEST HOURS	
							REPAIRED STATE	DAMAGED STATE
	8T	*Nick	93.6	1.6	1.225" x 1.78" x .003"	Blend Spar	19.27	0
		*Tear	95.4	10.6	.479" x 5.071" x .558"	Skin Patch Plug		
		*Dent	165.0	12.7	250" x 2.500" x .030"	Skin Patch		
		*Tear	195.2	11.5	.793" x 6.681" x .418"	Plug		
		*Battle Damage	241.2	15.1	.700" x 1.999" x Thru	Double Plug		
		*Puncture	283.5	11.2	.663" x .774" x .238"	Skin Patch		
	8B	*Puncture	102.3	10.3	.782" x .585" x .821"	Skin Patch		
		*Puncture	117.6	13.6	.396" x .709" x 1.093"	Skin Patch		
		*Dent	207.3	13.2	.125" x .875" x .030"	Skin Patch		
		*Nick	228.9	4.6	1.580" x 2.141" x .003"	Blend Spar		
		*Battle Damage	241.2	15.1	700" x 1.999" x Thru	Double Plug		
	9T	*Nick	135.0	21.0	.250" x .015" x Thru	Blend Spline		
		*Puncture	111.9	14.1	.583" x .862" x .341"	Skin Patch		
		*Battle Damage	148.2	10.6	1.149" x 1.215" x Thru	Double Plug		
		*Nick	151.8	3.7	1.164" x 1.832" x .003"	Blend Spar		
		*Puncture	176.4	10.6	.717" x 2.047" x .329"	Plug		
		*Puncture	195.9	18.7	.322" x .773" x .489"	Skin Patch		
		*Tear	253.5	10.2	.125" x .875" x .030"	Skin Patch		
	9B	*Nick	36.2	2.2	.060" x .250" x .015	Blend Doubler		
		*Puncture	99.6	11.5	.341" x .601" x .782"	Skin Patch		
		*Puncture	110.8	9.0	.958" x 1.877" x .334"	Plug		
		*Battle Damage	148.2	10.6	1.149" x 1.215" x Thru	Double Plug		
		*Tear	269.0	13.5	1.250" x 6.500" x .030"	Skin Patch		
2	8T	*Tear	141.6	11.0	.48" x 5.07" x .50"	Plug Patch	.3	2.9
1	8T	*Battle Damage	81.0	9.25	1.00" x .86" x Thru	Double Plug	6.0	2.8
3	8T	*Dent	274.0	0.0	.3" x 0.0" x .06"	Blend	0	2.4
5	9T	*Puncture	281.0	8.0	.66" x .77" x .24"	Plug Patch	8.8	2.0
4	9B	*Battle Damage	81.0	12.5	1.35" x 3.88" x Thru	Double Plug	3.2	2.8

*Through damage is described as a hole in both the top and bottom surfaces.

Blades numbers 8 and 9 had a total of 26 damages and repairs by the completion of their whirl testing. The number and distribution of these repairs were far in excess of the maximum number that would be allowed on a field-deployed set of blades. Even with this excess of repairs, the blades were shown to be structurally sound.

At the conclusion of each test sequence, the thrust was reduced and the rotor blades whirled to the 10% overspeed condition (356 rpm) in flat pitch to further evaluate the integrity of the repairs.

During the entire whirl test sequence, the undamaged blades showed no distress, the damage inflicted to the blades did not progress, and the repairs did not deteriorate. The applied loads included 10% rotor overspeed, as well as full thrust of 9900 lb. Blade balance and track before damage, after damage and after damage repair remained within acceptable limits. Figure 81 compares the thrust versus horsepower requirements of the FREB to that of the present UH-1H blade under similar test conditions.

The successful completion of the whirl tower testing with the two sets of blades indicates that both the blade and the repair technique have accomplished the objective of developing a reliable, structurally sound solution to the problem of frequent blade damage.

LIFE-CYCLE COST ANALYSIS

The cost projections discussed in the life-cycle cost analysis section were made based upon assumed levels of repairability and fatigue life for the various design concepts. Concept 2 was chosen as the most likely to meet the requirements of the program, and it was thus chosen as the final design.

Subsequent evaluation of Concept 2, in both the maintainability demonstration plan and the fatigue testing, has shown that the FREB, in all probability, demonstrates the same levels of fatigue life and repairability predicted for it earlier. Consequently, the curves and comparisons given earlier for Concept 2 are still applicable to the final design.

FATIGUE LIFE SUBSTANTIATION

The calculation of rotor blade fatigue life requires accurate knowledge of the flight loads, the flight spectrum (or frequency of occurrence of the loads) and the fatigue strength (S-N data) of critical blade sections. Since no flight test of the FREB was conducted, flight loads for this configuration are not available; however, its fatigue life may be estimated

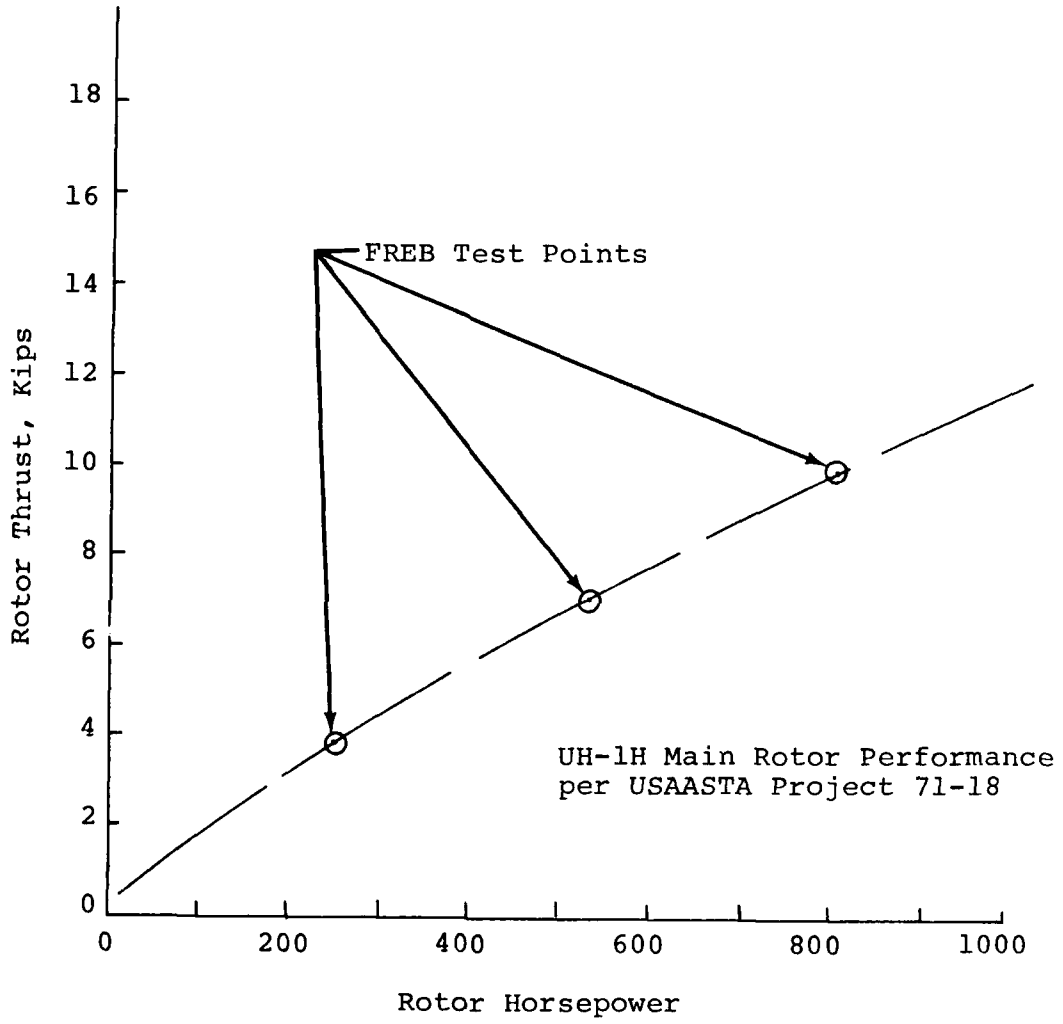

Figure 81. Comparison of Thrust/Horsepower for Standard UH-1H Blade and FREB.

by comparison of fatigue strength, using the assumption that flight loads are the same as on the present blade. This assumption may be considered valid because of the dynamic similarity that was maintained in designing the FREB.

Previous analysis had shown that station 81.0 was another critical location for both blades. The fatigue life for the drag brace (P/N 204-011-140-1) from Reference 3 was predicted to be 3716 hours. During the fatigue testing of the FREB root end, three drag braces failed in fatigue while the FREB specimen sustained no damage. The stress at station 81 on the spline during the root end fatigue testing went from $\pm$ 6 to $\pm$ 9 ksi, well above the vibratory stress predicted for this location during the 107-knot condition. The blade specimens showed no signs of deterioration from testing, and the drag braces failed repeatedly, thus indicating that the FREB root end is stronger than the UH-1 attaching hardware. A life for the root end in excess of 3716 hours is, therefore, predicted.

Some estimate of the fatigue life of the FREB can be made by comparing FREB bench test data to the fatigue life predictions given for the present UH-1D main rotor blade in Reference 3. In this reference, the blade life is based on edgewise vibratory moment at station 192, where the spline is the critical component. Figure 82 shows the 3 reduced S/N curves for the present UH-1 blade at station 192 on the spline and for the FREB at station 210 on the spline. The present UH-1 curve was used to predict a life of 2200 hours. The FREB curve shows a significant increase in life at load, indicating that the critical outboard station on the FREB should have a fatigue life well in excess of the 3000-hour life used for life-cycle cost predictions.

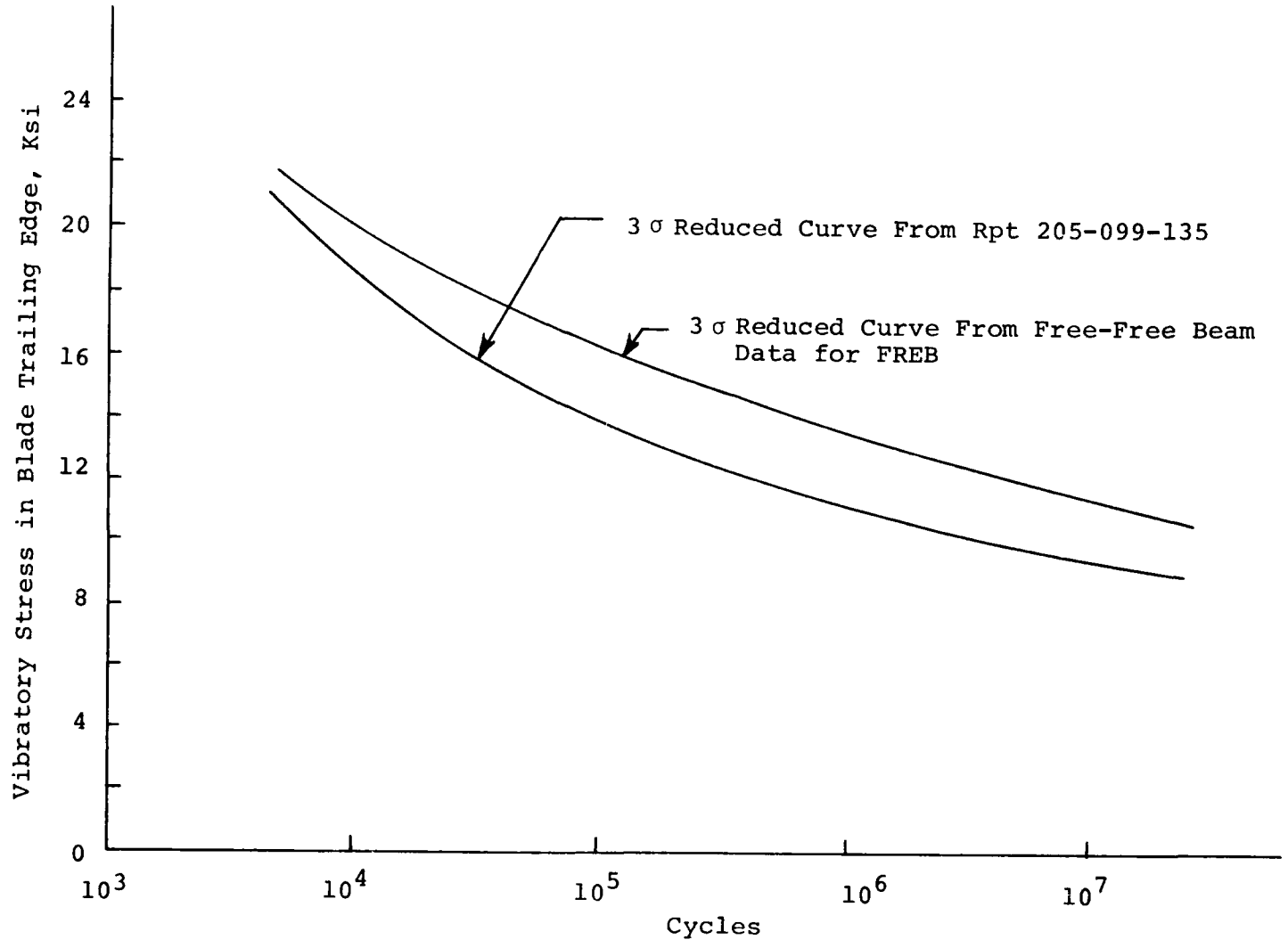

Figure 82. Comparison of S/N Curves for FREB and Present UH-1 Outboard Blade Section.

CONCLUSIONS

The Field Repairable/Expendable Main Rotor Blade Development Program has shown the feasibility of combining requirements for a high degree of maintainability and minimum cost with all of the other prime requirements for a helicopter main rotor blade.

The blade design that was built and tested during this program was shown to be structurally sound in new, damaged and repaired condition. A computer life-cycle cost model was used to compare the total projected life-cycle cost of the FREB to that of the present UH-1 main rotor blade. The long life, low cost and high repairability of the FREB combined to reduce the overall costs of the blades during the life-cycle of the UH-1 helicopter by approximately 40% when compared to the projected life-cycle cost of the present UH-1 helicopter.

RECOMMENDATIONS

1. The program detailed in this report encompassed a substantial amount of the work required to qualify the FREB for fleet use on the UH-1H helicopter. The substantial decrease in helicopter life-cycle costs available from the use of this blade would make additional expenditures to qualify these blades and equip the Army's fleet with them highly cost effective. It is recommended that the above savings projections be verified by introduction of at least a trial quantity of blades.

2. The successful completion of this program demonstrates that repairability and maintainability considerations can be successfully integrated into preliminary component design, resulting in substantially decreased component life-cycle costs. The Army should require this early integration of R&M considerations into all future procurements.

3. The technique of field adhesive bonding of repairs and the kit concept of material packaging should be studied for their possible application to other items in the Army inventory.

REFERENCES

1. Frengley, M. C., DEVELOPMENT PROGRAM FOR FIELD-REPAIRABLE/ EXPENDABLE MAIN ROTOR BLADES; PHASE I - PRELIMINARY DESIGN, Kaman Aerospace Corporation; USAAMRDL Technical Report 73-102, Eustis Directorate, U. S. Army Air Mobility Research and Development Laboratory, Fort Eustis, Virginia, April 1974.

2. Carr, P. V., and Hensley, O. L., UH-1 AND AH-1 HELICOPTER MAIN ROTOR BLADE FAILURE AND SCRAP RATE DATA ANALYSIS, Bell Helicopter Company; USAAVLABS Technical Report 71-9, Eustis Directorate, U. S. Army Air Mobility Research and Development Laboratory, Fort Eustis, Virginia, January 1971, AD 881132L.

3. Report #205-099-313, STRUCTURAL ANALYSIS OF MAIN ROTOR HUB AND BLADE ASSEMBLY FOR 48 FOOT DIAMETER ROTOR, Bell Helicopter Company, Fort Worth, Texas.

4. STRUCTURES MANUAL, Sikorsky Division of United Technologies Corporation.

5. Maloney, P. F., and Akeley, C. R., DESIGN STUDY OF REPAIRABLE MAIN ROTOR BLADES, Kaman Aerospace Corporation; USAAMRDL Technical Report 72-12, Eustis Directorate, U. S. Army Air Mobility Research and Development Laboratory, Fort Eustis, Virginia, July 1972, AD 749283.

6. Frengley, M. C., Maloney, P. F., and Akeley, C. R., DESIGN STUDY OF EXPENDABLE MAIN ROTOR BLADES, Kaman Aerospace Corporation; USAAMRDL Technical Report 72-48, Eustis Directorate, U. S. Army Air Mobility Research and Development Laboratory, Fort Eustis, Virginia, October 1972, AD 758464.

APPENDIX A

DESIGN SPECIFICATION,
HELICOPTER MAIN ROTOR BLADE

1.0 GENERAL

This specification provides design requirements for a field-repairable/expendable main rotor blade for a medium utility helicopter.

1.1 System Compatibility

The rotor blade shall be aerodynamically, dynamically, and structurally compatible with the airframe of the UH-1H helicopter, and with the missions for which that helicopter is used.

1.1.1 The vibration level attributable to the main rotor shall not be increased from that of the UH-1H helicopter as equipped at the date of this specification.

1.1.2 The loads applied to the rotor hub by the field-repairable/expendable blades shall not be so high as to reduce the fatigue life of the hub structure nor the service life of bearings or other components. The static strength of the hub shall not be exceeded.

1.1.3 Clearance from the fuselage to the field-repairable/expendable blade shall not be significantly less than that to the current blade, i.e., the blade installed on the main rotor of the UH-1H helicopter at the date of this specification.

1.1.4 The blade shall extend from the root cutoff at rotor station 24.5 to the tip at rotor station 288.0 (24.5 and 288.0 inches, respectively, from the center of rotation). The tip cap and tracking nib may extend beyond rotor station 288.0 by no more than 1.63 inches, but major structural components shall not.

1.1.5 The chord length shall be 21.0 inches, constant from root to tip.

1.1.6 The maximum thickness of the clean airfoil section shall be 2.52 inches.

1.1.7 The blade shall be twisted 10.9° from the center of rotation to the tip (27.27' per foot).

1.1.8 The root attachments shall be a 2.5-inch bolt at rotor station 28.0 and chord station 3.750 (measured from the leading edge) and a 1.125-inch bolt at rotor station 26.0 and chord station 19.5. The thickness through the main retention shall be 4.5 inches, and 1.9 inches through the drag strut fitting.

1.2 Interchangeability

It shall be possible to remove any one blade of the field-repairable/expendable series and replace it by another of the series and achieve balance, track, and acceptable flying qualities without adjustment of weights. The only acceptable adjustments will be to the pitch link and trim tab.

1.3 Expendability

To meet the requirement that the cost impact of abandoning the blade be minimized, the blade price in quantity production shall not exceed $4000 per unit.

1.4 Reliability

The occurrence of damage due to inherent causes shall be minimized.

1.4.1 If any materials are used which are not known to be corrosion resistant, such materials will be protected against corrosion per MIL-F-7179D, Type 1.

1.4.2 The leading edge shall be protected against erosion by rainfall as defined for Category 2 of AR 70-38. The blade shall be assumed to operate in the 12-hour rainfall defined in 2-8c of AR 70-38 for 10% of its allowable service life. The leading edge shall not be eroded sufficiently to cause significant degradation in aerodynamic performance or structural integrity.

1.4.3 The leading edge shall be protected against abrasion by sand and dust as defined for Category 4 of AR 70-38. The blade shall be assumed to hover in ground effect for 3% of its allowable service life, in sand and dust particles as defined in 2-10f and 2-10g of AR 70-38, except that, for unit ground area, sand particles shall be distributed up to the rotor height, with half the particles below 1/10 rotor height, and dust particles will be distributed to the rotor height.

1.4.4 The number of adhesive bond lines subject to delamination shall be minimized. The basic blade (excluding root and tip reinforcement and hardware) shall be made up of not more than eight components.

1.5 Vulnerability

The severity of damage due to external causes shall be minimized.

1.5.1 Thin sheet components shall be of such thicknesses and materials as to resist damage due to impact equivalent to a 1-pound steel ball dropped from a height of 2 feet.

1.5.2 Thin sheet components shall be of materials such that puncture damage will not immediately propagate into a tear.

1.5.3 Internal support structure shall be of resilient material such that negligible surface damage does not cause internal damage.

1.5.4 Impact with immovable objects, such as a tree strike, having energy insufficient to cause significant damage to structural components shall not cause delamination of adhesive bond joints.

1.5.5 No component shall be of any material that will shatter or disintegrate due to nonexplosive ballistic damage, up to and including penetration by a 23mm API round.

1.6 Survivability

The rotor blade shall be designed so that initially marginal damage shall not become catastrophic before the aircraft can return to base.

1.6.1 Where possible, primary structure shall be designed with alternate load paths, each capable of carrying the centrifugal force and bending moments associated with undamaged blades in maneuvers up to 1.2 g at cruise speed, for a minimum of ten (10) hours.

1.6.2 Materials shall be used throughout whose crack propagation rates are slow enough that initially marginal damage shall not become catastrophic for a minimum of ten (10) hours, under the centrifugal force and bending moments associated with undamaged blades in maneuvers

up to 1.2 g at cruise speed.

1.6.3 On impact with immovable objects, damage shall be confined to deformation, or bending, and no component shall fracture or separate.

1.6.4 Nonexplosive ballistic damage, up to and including penetration by a 23mm API round, shall not be catastrophic; that is, material dislodged or detached from the blade shall be of insufficient mass to cause an unmanageable increase in vibration level in the aircraft.

1.7 Maintainability

All allowable repairs shall be safely and reliably accomplishable at the using unit level. Routine maintenance shall be performed at the using unit level.

1.7.1 Repairs requiring replacement of primary structural material shall not be permissible, and damage to such material shall be cause for scrap. Delamination of adhesive bonds involving primary structure shall be cause for scrap.

1.7.2 The skill level of the maintenance personnel shall be that of a UH-1 helicopter repairman, MOS 67N20.

1.7.3 No more than two men shall be required to accomplish any individual maintenance action, exclusive of blade removal and replacement.

1.7.4 The time goal to accomplish any individual repair shall be no greater than 3.0 hours, including any required adhesive cure time and correction of balance and track.

1.7.5 Not more than 5% of the repairable damage occurrences shall require removal of the blade from the aircraft.

1.7.6 The maximum elapsed corrective maintenance time (at the 95th percentile confidence level) to return the aircraft to operational readiness status shall be 3.0 hours, for the entire population of corrective maintenance tasks.

1.7.7 Blade balance shall be corrected using easily accessible adjustable weights installed at the tip. The amount of weight change shall be simply defined and related to each individual repair.

1.7.8 Dents, nicks, and scratches shall be repaired by blending and/or filling, unless structural or contour degradation is not significant.

1.7.9 Repairs to punctures, tears, and cracks shall be designed to minimize stress concentrations, and shall be permissible only in those areas and materials where stress concentrations will not cause subsequent secondary failures.

1.7.10 Punctures, tears, and cracks shall be cleaned up and repaired using standard, prepackaged repair kits. The repair kits shall contain patch materials (protected against contamination), cleaning materials, and adhesives in measured quantities appropriate to the patch size.

1.7.11 Heat and pressure sources will preferably be self-contained in the repair kits, but use of aircraft on-board auxiliary power will be permissible.

1.7.12 Support equipment needed to effect repairs shall be minimized and shall be suitable for deployment at company level.

1.8 Radar Cross Section

The radar return, at all frequencies appropriate to possible threat radars, shall not exceed that of an all-metal blade of 288.0 inches radius, 21.0 inches chord, and NACA 0012 airfoil section.

1.8.1 The total of the appropriately weighted returns from both leading- and trailing-edge aspects shall not exceed that of the target described above.

1.8.2 The peak return at any aspect shall not exceed the peak return from the target described above.

1.9 Acoustic Signature

The acoustic detectability of the field-repairable/expendable blade shall not exceed that of a blade of 288.0 inches radius, 21.0 inches chord, and NACA 0012 airfoil section, with square tips.

2.0 WEIGHT AND BALANCE

The weight and balance characteristics shall not represent a degradation from the current blade, in terms of rotor system and control system loads, but the field-repairable/expendable blades need not be directly interchangeable with the current blade.

2.1 Total Weight

The total weight, including balance adjustment, of the field-repairable/expendable rotor blade, based on nominal component dimensions and material densities, shall not exceed 203.5 pounds.

2.2 Mass Moment About Center of Rotation

The nominal first moment of mass about the center of rotation shall not exceed 29,000 in.-lb.

2.3 Chordwise Center of Gravity

The nominal center of gravity shall not be farther than 5.78 inches (27.5% chord) from the leading edge.

2.4 Dynamic Mass Axis

The dynamic mass axis, or span-weighted chordwise center of gravity, as obtained by dividing the nominal produce of inertia about the leading edge and center of rotation by the nominal first moment of mass about the center of rotation, shall not be farther than 5.15 inches (24.5% chord) from the leading edge.

2.5 Kinetic Energy

In order to provide sufficient response time in the event of an engine failure, the second moment of mass about the center of rotation shall not be less than 1000 slug-ft^2 for one nominal blade.

3.0 STRUCTURE

The strength and stiffness of the blade structure shall not allow a significant decrease in fatigue life, nor a significant degradation in dynamic characteristics, from those of the current blade.

3.1 Static Strength

The bending strength of the blade shall be capable of supporting the blade as a cantilever under an ultimate acceleration of at least 4.0 g.

3.2 Fatigue Strength

The fatigue life under the maneuver spectrum defined for the UH-1H utility mission shall not be less than 2000 hours.

3.3 Flatwise Stiffness

The flatwise bending stiffness shall be such that the downward deflection at the blade tip, under 1.0 g acceleration, with the root fixed in a horizontal attitude, shall not exceed 8.0 inches.

3.4 Edgewise Stiffness

In order to provide sufficient margin beyond ground self-excited mechanical instability limits, the edgewise bending stiffness at rotor station 81.0 shall not be less than 2.2 billion lb-in^2.

3.5 Torsional Stiffness

In order to ensure that torsional and coupled modes of blade vibration have no greater significance than those of the current blade, the torsional stiffness of the field-repairable/expendable blade shall average, over the span, no less than 29.0 million lb-in^2 and shall not be less than 31.0 million lb-in^2 at rotor station 81.0.

4.0 SPARS

4.1 Spars composed of more than one component shall have structural material apportioned between the components so that residual strength after complete failure of any one component will allow operation for a minimum of ten (10) hours under the loads and moments defined in 1.6.1.

4.2 Thicknesses and types of adhesives between spar components shall be selected so as to delay crack propagation across any bond line for a minimum of ten (10) hours of operation under the loads and moments defined in 1.6.1 and 1.6.2.

4.3 Spars composed of one component shall be made from

material whose crack propagation rate shall allow normal operation for a minimum of ten (10) hours from failure initiation to critical failure, under the loads and moments defined in 1.6.2.

4.4 Both internal and external surfaces of the spars shall be resistant to or protected from corrosion so as to remain serviceable for a minimum of five (5) years.

4.5 Spar repairs shall be limited to blending and/or filling of dents, scratches, and nicks.

5.0 SKINS

5.1 Skin materials shall be corrosion resistant.

5.2 Skin thicknesses and materials shall be selected so that impact as defined in 1.5.1 shall cause negligible or no damage.

5.3 The structural design of the blade shall be such that a complete chordwise skin failure aft of the spar shall not be catastrophic.

5.4 The crack propagation rate of the skin material shall be such as to allow normal operation for a minimum of ten (10) hours from failure initiation to a complete chordwise skin failure, aft of the spar, under loads and moments as defined in 1.6.2.

5.5 Thicknesses and types of adhesives between skins and adjacent primary structure shall be selected so as to delay crack propagation from skin to adjacent structure for a minimum of ten (10) hours of normal operation under loads and moments as defined in 1.6.1 and 1.6.2.

5.6 To minimize stress concentrations in adjacent structure due to a failure in the skin, the modulus of elasticity of the skin material shall not be greater than that of any adjacent primary structural material.

5.7 Nicks and scratches in nonmetallic skins less than one-half the skin thickness shall be considered negligible, but they may be filled to improve appearance.

5.8 Any damage to nonmetallic skins exceeding one-half the skin thickness shall be removed and repaired using a suitable patch kit.

5.9 Skin repairs and patch kits shall be so designed that the fatigue life of a patched skin shall be no less than the allowable service life of the undamaged blade.

5.10 Nicks and scratches in metal skins shall be polished out to a depth not more than one-half the skin thickness, or .015 inch, whichever is least.

5.11 Any damage to metal skins exceeding one-half the skin thickness or .015 inch shall be cause for scrapping the blade.

5.12 Dents less than .030 inch deep and having unbroken surfaces, in either metal or nonmetal skins, shall be considered negligible.

6.0 SKIN INTERNAL SUPPORT STRUCTURE

6.1 Internal structure under and between the skins shall be of corrosion-resistant material.

6.2 Entrapment and migration of moisture internally shall be minimized.

6.2.1 Honeycomb internal structure shall be nonperforated.

6.3 For any given damage occurrence, damage to the internal structure shall be no more severe than damage to the skin.

6.4 If damage to internal structure is expected to accompany skin damage as defined in 5.8, repair material for internal structure must be included in the patch kits.

7.0 TRAILING EDGE

If a separate structural spline is used in the trailing edge, it shall meet the following requirements.

7.1 The spline shall be fabricated from corrosion-resistant material, or protected from corrosion so as to remain serviceable for a minimum of five (5) years.

7.2 The spline shall suffer no significant damage from impact equivalent to that of a 24-ounce ball-peen hammer allowed to swing freely through a 2-foot arc on a 3-foot radius.

7.3 Nicks, scratches, and cracks not extending under the skin shall be repairable by blending. Permissible limits of material removal will be determined from the overall structural characteristics of the blade.

7.4 Surfaces exposed by repair shall be protected from corrosion so as to remain serviceable for a minimum of five (5) years.

7.5 Repairs requiring replacement of spline structural material shall not be permissible.

7.6 Spline material shall be selected so that its crack propagation rate shall allow operation for a minimum of ten (10) hours between failure initiation and complete spline failure, under loads and moments as defined in 1.6.2.

8.0 LEADING-EDGE ABRASION SHEATH

8.1 Nonremovable leading-edge protection material shall be capable of operating in the sand and rain environments described in 1.4.2 and 1.4.3 for at least the allowable service life of the blade without being abraded, eroded, or corroded through to its substrate.

8.2 Any leading-edge protection material which is not capable of meeting the requirement of 8.1 shall be designed to be removable.

8.3 Removable leading-edge protection material shall be capable of operating in the sand and rain environments of 1.4.2 and 1.4.3 for a minimum of 500 hours without being abraded, eroded, or corroded through to its substrate.

8.4 For any removable leading-edge sheath, it shall be possible to remove the protection material and clean off its supporting adhesives without any damage to other blade components.

8.5 Removable leading-edge sheaths shall be replaced using prepackaged kits including replacement parts, cleaning materials, and adhesives.

8.6 Replaced leading-edge sheaths shall be capable of meeting the requirement of 8.3.

9.0 LEADING-EDGE BALLAST

9.1 Impact with an immovable object, such as a tree strike, with insufficient energy to bend or severely deform the blade shall not detach the leading-edge ballast from its surrounding structure.

9.2 Mechanical retention capable of retaining the leading-edge ballast for a minimum of ten (10) hours under normal centrifugal force, in the event of severe blade damage detaching the adhesive bond between the ballast and surrounding structure, shall be provided.

9.3 Removal and replacement of leading-edge ballast shall not be permitted.

10.0 ROOT REINFORCEMENT

10.1 If the root reinforcement is designed to be attached outside the basic blade structure, the reinforcement shall be capable of carrying the centrifugal force and bending moments as defined in 1.6.1 for a minimum of ten (10) hours with the reinforcement completely detached from one or the other surface of the blade.

10.2 Nicks and scratches shall be repaired by blending. Permissible limits of material removal shall be determined from the structural characteristics of the blade root.

10.3 Cracks, dents, and punctures shall be cause for scrapping the blade.

10.4 Repairs requiring replacement of material other than nonstructural filler or paint shall not be permissible, and such damage shall be cause for scrapping the blade.

11.0 TIP

11.1 Tip covers shall be interchangeable independent of blade disposition. Weights of all tip covers shall fall within a range of .02 pound.

11.2 Tip covers susceptible to abrasion, erosion, or corrosion shall remain serviceable for a minimum of 500 hours between replacements in the rain and sand environments described in 1.4.2 and 1.4.3.

11.3 Adjustable tip balance weights shall be easily removed and replaced with standard tools normally available at the using unit level.

11.4 It shall be impossible to reinstall adjustable tip weights in incorrect locations.

12.0 ADHESIVE SYSTEMS

12.1 Adhesives used in the skin and core area shall have a low percentage of volatiles to be compatible with the nonperforated core specified in 6.2.1.

12.2 Adhesives subject to environmental deterioration shall be sealed along all exposed bond line edges.

12.3 Adhesives used to effect repairs by patching shall be capable of supporting the patch for the allowable service life of the blade under the full spectrum of loads and moments appropriate to the patch location.

12.4 Adhesive used to attach a removable leading-edge protection sheath shall be capable of supporting the sheath throughout its replacement life.

12.5 Adhesives used to effect repairs shall have cure times compatible with the elapsed time limitation of 1.7.4.

12.6 Adhesives used to effect repairs shall utilize heat and pressure sources as defined in 1.7.11.

APPENDIX B

REPAIR INSTRUCTIONS

REPAIRABLE/EXPENDABLE MAIN ROTOR BLADE

CHAPTER 1

REPAIR LIMITS

1-1. SPAR (Aluminum)

a. Smooth dents up to 0.060 inch deep in the first 1-inch chord measurement of spar are acceptable as is. Smooth dents up to 0.030 inch deep on the remaining exposed surface of spar are acceptable as is. No dents are allowed in the area of the spar covered by blade skin. Dents exceeding these limits require blade scrappage.

b. Corrosion may be reworked by smooth blending up to 0.060 inch deep in the first 1-inch chord measurement and 0.030 inch deep in remaining exposed spar area. Corrosion extending into bond area of skin and spar is cause for blade scrappage.

c. Erosion is acceptable until blade balance becomes a problem.

d. Nicks and scratches deeper than 0.010 inch should be removed by smooth blending to the maximum depth given in Step a above. Depths greater than 0.060 inch in the first 1-inch chord measurement and 0.030 inch in remaining exposed area of spar will be cause for blade scrappage. Nicks and scratches up to 0.010 inch deep in any exposed area of spar are acceptable as is.

1-2. SKIN AND CORE (Fiberglass and Nomex Honeycomb)

a. Skin cracks up to a diameter of 7.00 inches, tears and delaminated areas up to 1.00 inch diameter with no core damage, and punctures up to 1.00 inch diameter, including those through both skins, may be repaired with a skin patch provided the patch required will overlap the damage by a minimum of 1.00 inch. The edge of required patch shall not be closer than 1/2 inch to spar or spline and be no closer than 1.00 inch of trim tab, end closure and previously installed patch on same side of blade.

b. Punctures, tears and delaminated areas greater than 1.00 inch diameter may be repaired with a plug patch provided the damage is not greater than 7.00 inches in diameter and provided the periphery of damage is no closer than 2-1/2 inches in chord direction and 8.00 inches in span direction of root doublers, tip closure, trim tab and previously installed patch on same side of blade (reference Figure B-1).

c. Nicks and scratches in skin up to 0.004 inch deep are acceptable as is. Nicks and scratches found to be greater than 0.004 inch deep should be repaired if within limits allowed for repair of cracks described in Steps a and b above.

d. Smooth dents up to 0.030 inch deep not having broken skin, core or delamination are acceptable as is. Dents greater than 0.030 inch deep will be treated as a puncture and should be repaired if within limits allowed in Steps a and b above.

e. When more than one puncture, tear or delamination falls within a 7-inch diameter, they shall be treated as one damage. Should damage occur within a previously repaired area that cannot be cleaned out and covered by the next larger patch, then the blade must be scrapped.

1-3. SPLINE (Aluminum)

a. Smooth dents up to 0.030 inch deep are acceptable as is. No damage is allowed in area of spline covered by blade skin. Dents greater than 0.030 inch deep may be reworked by smooth blending to the limits in b below.

b. Corrosion damage must be repaired by smooth blending. Rework of spline to full thickness in a direction perpendicular to the chord line is permitted to within 0.100 inch of blade skin starting 1.00 inch outboard of root doublers (reference Figure B-2). The length of each repair shall not exceed 6.00 inch span dimension inboard of Station 105.5 and 3.00 inch span dimension outboard of Station 105.5. Repairs closer than 5.00 inches apart will not be permitted, and all radii will be a minimum of 1 inch. Damage extending beyond these limits shall require scrapping blade.

c. Nicks and scratches in excess of 0.010 inch depth shall be reworked to limits described in Step b above.

1-4. TRIM TAB (Aluminum)

a. Cracks, punctures, tears and delaminations in the tab from the spline trailing edge forward requires scrapping blade.

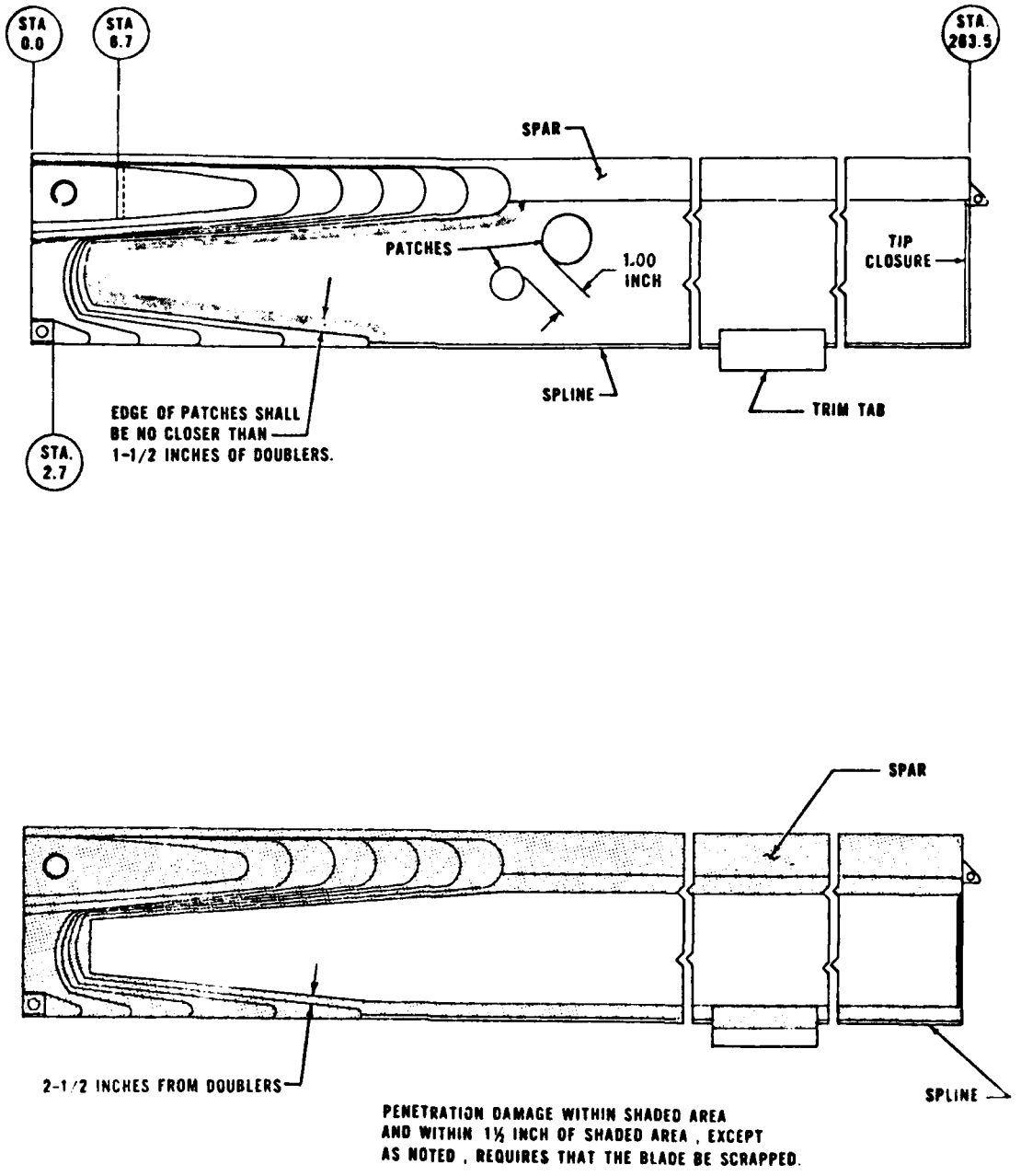

Figure B-1. Repair Limits for Skin and Core Areas.

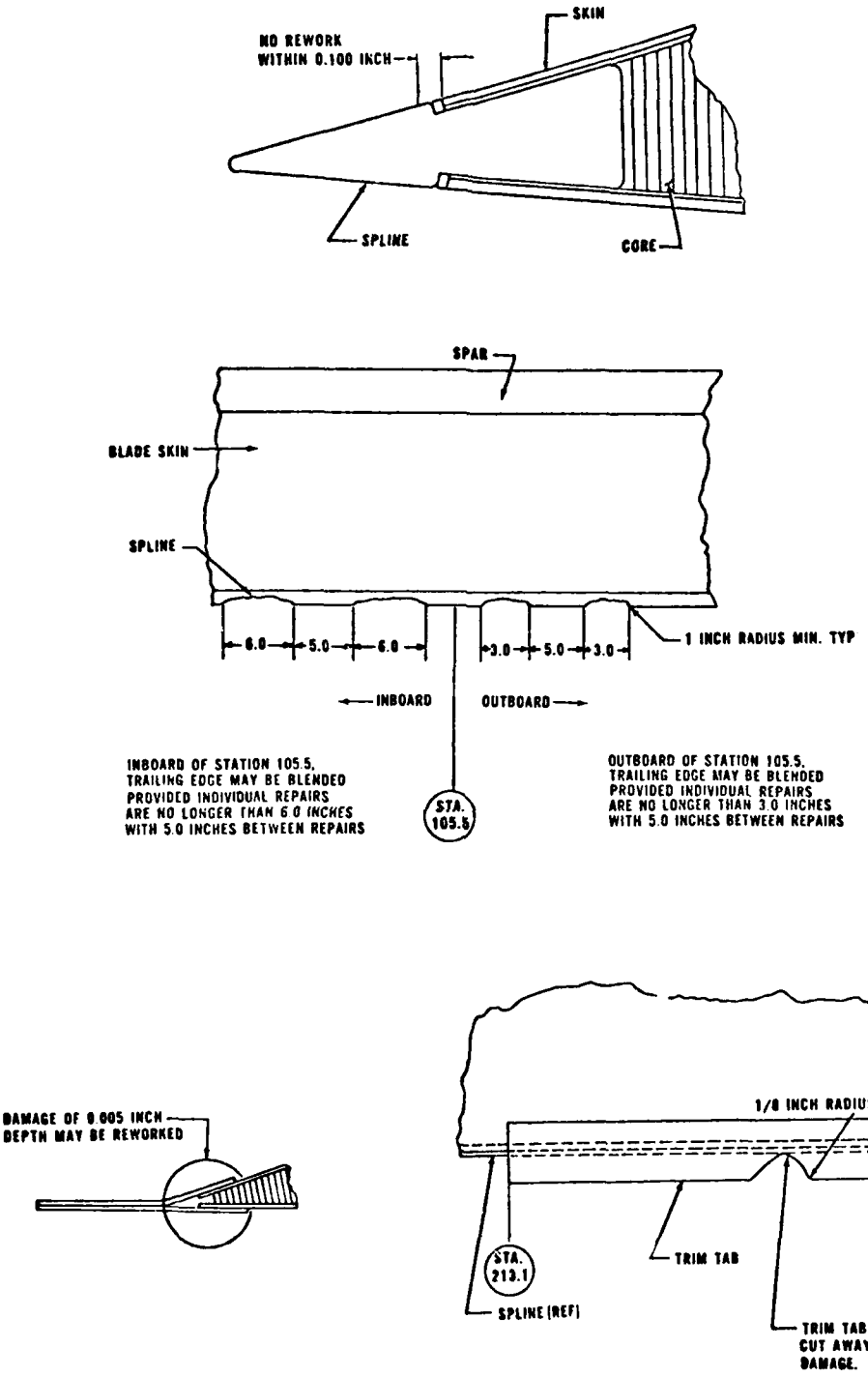

Figure B-2. Blend Limits for Spline and Trim Tab.

b. Bends, dents and distortion of tab aft of spline may be mechanically straightened providing none of the items in Step a above occur.

c. Smooth dents up to 0.030 inch deep in the area of the tab forward of the spline are acceptable providing there is no evidence of bond line delamination.

d. Corrosion, nicks and scratches may be smooth blended to a maximum depth of 0.005 inch. Damage forward of the spline trailing edge greater than this limit requires blade scrappage. Damage located in the tab aft of the spline which is greater than 0.005 inch deep can be reworked to the extent of completely cutting away the damage (reference Figure B-2). This type of repair is limited only to the trim tab's ability to perform its trim function. All edges of cuts shall be blended smooth and all corners shall have a minimum of 1/8 inch radius.

1-5. ROOT DOUBLERS (Aluminum)

a. Corrosion, nicks and scratches greater than 0.005 inch deep, but less than 0.015 inch deep, shall be smooth blended to a maximum of 4 square inches per repair and a maximum of 4 such repairs per each side of blade. Damage exceeding these limits require blade scrappage.

b. Internal voids less than one square inch and at least 1/4 inch from an outside edge are acceptable provided no more than 3 such voids, separated by at least 3 inches, exist per each side of the blade. Edge voids 1/4 inch deep and 1/2 inch long are acceptable providing no more than two voids, separated by six inches per blade side, exist. Voids extending beyond these limits require blade scrappage.

1-6. GRIP AND DRAG PLATES (Aluminum)

a. Corrosion, nicks and scratches 0.010 inch deep are permissible without repair. Damage greater than 0.10 inch deep, within 1/4 inch of the grip and drag bushings, require blade scrappage. Smooth blending of damage from 0.010 inch deep to 0.020 inch deep is permitted on all surfaces outboard of Station 6.7 on the grip plates and Station 2.7 on the drag plates. No more than 2 such repairs are allowed per side of blade. A maximum depth of 0.030 inch in the grip and drag plates, inboard of Stations 6.7 and 2.7, respectively, may be reworked by smooth blending. Such rework may not exceed 1 square inch on the grip plate and 1/4 square inch on the drag plate with one such repair per blade side permitted. Damage to the sides of the grip plates, inboard of Stations 6.7, and

2.7 on the drag plates, may be reworked by smooth blending to a maximum depth of 0.100 inch. Damage exceeding these limits will cause blade scrappage.

1-7. GRIP PAD (Steel)

a. Corrosion, nicks and scratches in excess of 0.010 inch deep must be reworked by smooth blending. No rework is permitted within 1/4 inch of the grip bushing. Damage may be reworked to a maximum depth of 0.030 inch. Blending is not to exceed 1 square inch, with no more than 1 such area permitted. Damage to the sides may be smooth blended to a maximum depth of 0.100 inch, with 2 such repairs allowed separated by a minimum of 1/2 inch.

1-8. GRIP BUSHING (Steel)

a. Corrosion or scratches may be polished from the inside diameter to the extent that the I.D. is not made greater than 2.505 inches. Beyond this limit, the blade must be scrapped.

b. Local polishing in excess of the 2.505-inch dimension is acceptable if only a burr needs to be removed. Example would be a burr created by a scratch from the top of the bushing I.D. to the bottom.

1-9. DRAG BUSHING (Steel)

a. Corrosion or scratches may be polished from the inside diameter to the extent that the I.D. is not made greater than 0.877 inch. Beyond this limit, the blade must be scrapped.

b. Local polishing in excess of the 0.877-inch dimension is acceptable if only a burr needs to be removed. Example would be a burr created by a scratch from the top of the bushing I.D. to the bottom.

1-10. ROOT CLOSURE (Fiberglass)

a. Cracks, punctures and tears require that the blade be scrapped.

b. Dents are acceptable as is provided the surface is not broken and delamination of the closure from adjacent structure has not occurred.

c. Nicks and scratches are acceptable as is provided the damage has not penetrated through the closure skin.

d. Any damage extending into adjacent structure and/or accompanied by delamination of root closure is cause for blade scrappage.

1-11. TIP CAP (Aluminum)

a. Corrosion, nicks and scratches, which do not extend into the area of attaching bolt head mating surfaces, may be repaired by smooth blending, not to exceed 0.060 inch deep. Damage beyond this limit is cause for tip cap replacement.

b. Smooth dents 0.030 inch deep are acceptable as is.

c. Erosion is acceptable as is, provided blade balance is not a problem.

d. Cracks, bends, distortions and punctures are cause for tip cap replacement.

1-12. TIP CLOSURE (Fiberglass)

a. Cracks, punctures and tears require that the blade be scrapped.

b. Dents are acceptable as is provided the surface is not broken and delamination of the closure from adjacent structure has not occurred.

c. Nicks and scratches are acceptable as is provided the damage has not penetrated through the closure skin.

d. Any damage extending to adjacent structure and/or accompanied by delamination to tip closure is cause for blade scrappage.

CHAPTER 2

REPAIR PROCEDURES

2-1. SKIN PATCHES

NOTE

Refer to Paragraph 1-2 to determine if damage is acceptable or repairable or if blade must be scrapped.

NOTE

This procedure applies to the three sizes of available patches (3, 5 and 9 inches in diameter). Refer to Table B-9 for complete list of blade repair kits. Select patch size which will permit 1 inch overlap all around damage after clean-up.

NOTE

Generally, skin patches may be used only when the underlying core is undamaged. The exception to this rule is when core damage is less than one inch in diameter. In such cases, the damage cavity (frayed ends of honeycomb material) is smeared with adhesive prior to application of patch. When core damage exceeds one inch in diameter, plug/patches may be installed per instructions given in Paragraph 2-2.

NOTE

When damage passes through both skins and core damage is less than one inch in diameter, repair is permissible by applying one patch to each skin (reference Figure B-3).

NOTE

Patches may be applied to the top and/or bottom surface(s) of a blade while the blade remains installed on the helicopter.

NOTE

Using a tape rule, measure and record the location of damage on the blade. Before starting

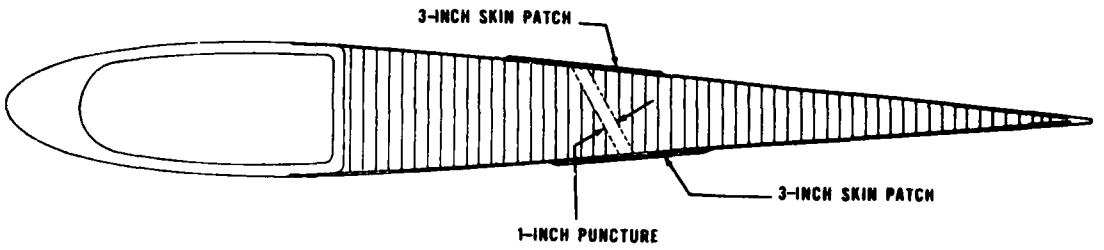

Figure B-3. Typical Double Skin Patch Repair.

repair, check balance weight assembly in spar tip to ensure that a sufficient quantity of weights (washers) is available to make balance adjustment after repair is accomplished. Table B-8 in Paragraph 2-9 specifies the quantities of weights required for various types of repairs. Scrap the blade without attempting repair if available quantity of weights is insufficient.

NOTE

Before starting repair, eliminate teeter movement. Position damaged blade so person making repair has access to damage. Do not cause blade bending greater than normal droop.

TABLE B-1. TOOLS AND EQUIPMENT, SKIN PATCH REPAIR

PART NUMBER	NOMENCLATURE
	Pressure/Heat Pack
	Compressed Air Source
	Electrical Source, 110 Volt, AC
	Electrical Extension Cord, 16-3
	Safety Goggles, Plastic

a. Damage Clean-up and Bond Surface Preparation.

(1) Using a pencil and template (kit item), draw a 5-inch circle for a 3-inch patch; 7-inch circle for 5-inch patch; and 11-inch circle for 9-inch patch around the damaged area, so as to allow at least 1-inch overlap outside of damage.

(2) Dampen cheesecloth (kit item) with methyl-ethyl-ketone (Item 300, Table B-11), and rub off paint from area within the circle.

CAUTION

Care must be taken to prevent thinner from entering core area of blade.

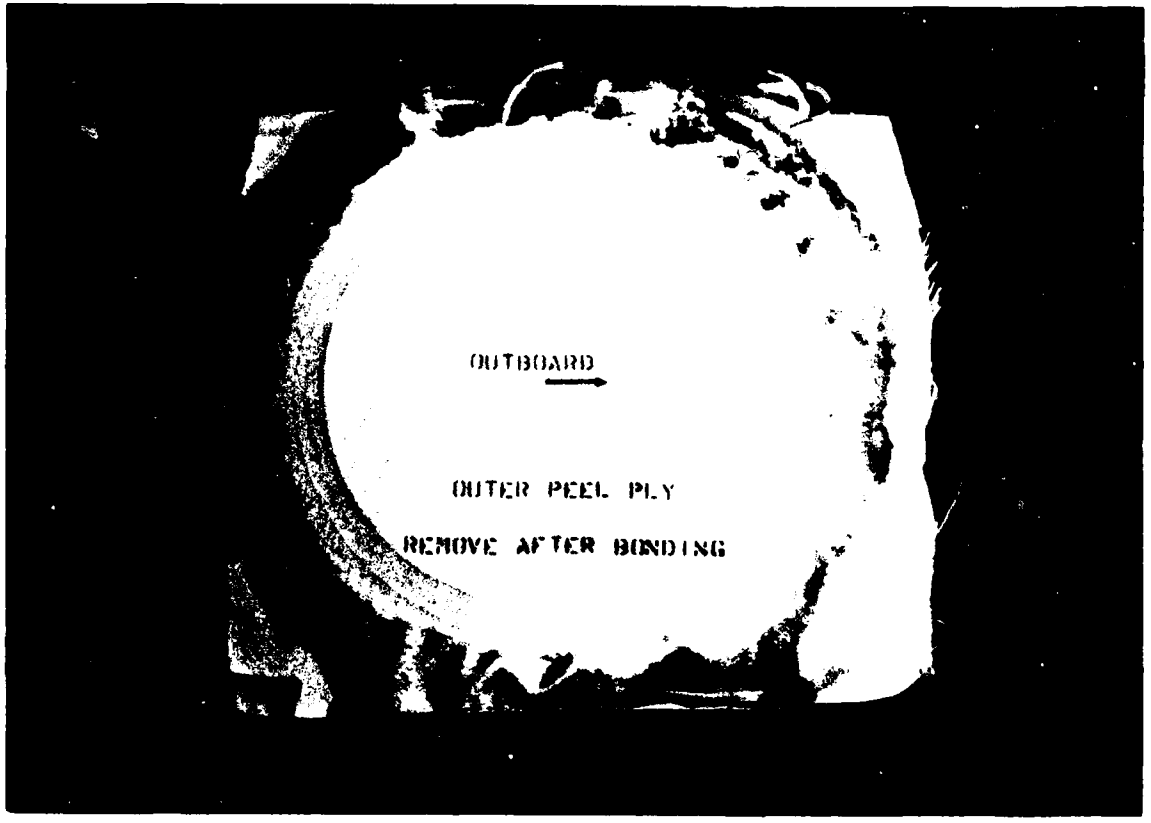

Figure B-4. Patch Outer Marking.

(3) Using 220 grit abrasive paper (kit item) to begin with, and finishing with 120 grit abrasive paper (kit item), sand the yellow primer from the surface of the blade to which the patch is to be bonded.

CAUTION

Excessive sanding will seriously weaken the blade skin. Sand only until the yellow color is removed.

(4) Using a pencil and template (kit item), draw a circle (around the damage area) 1/2 inch larger in diameter than the patch to be applied.

(5) Using 1-inch wide masking tape (kit item), mask the patch area. To accomplish this, cut the tape into short lengths and apply them to the blade just outside the circle drawn in Step (4). The masked circle will be approximately 1/2 inch in diameter larger than the patch to be applied, thus leaving a 1/4-inch margin all around for adhesive squeeze-out. This adhesive will be feathered in a sanding operation after it has cured.

(6) Clean the skin area to be bonded using cheesecloth dampened with methyl-ethyl-ketone (Item 300, Table B-11). Wipe dampened area with clean dry cloth before dampness evaporates.

CAUTION

The areas to be bonded must be clean, dry and free of grease, wax and other foreign matter.

NOTE

Skin patches are prefabricated from several plies of material as shown in Figure B-5. There is a peel ply on the outer surface which will serve to keep squeezed-out adhesive from contacting the pressure/heat pack during the curing process. The peel ply is to be removed after the adhesive has cured. An arrow is stenciled on the peel ply to indicate proper orientation of the patch when being applied to the blade. Patches are packaged in plastic bags in order to keep the bond surfaces contamination-free.

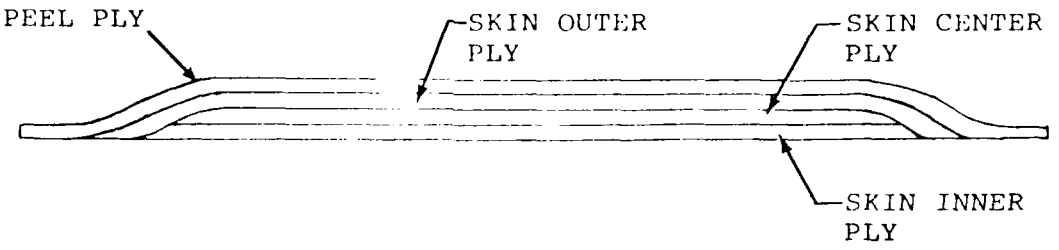

(PLY THICKNESSES DRAWN OVERSIZE FOR CLARITY)

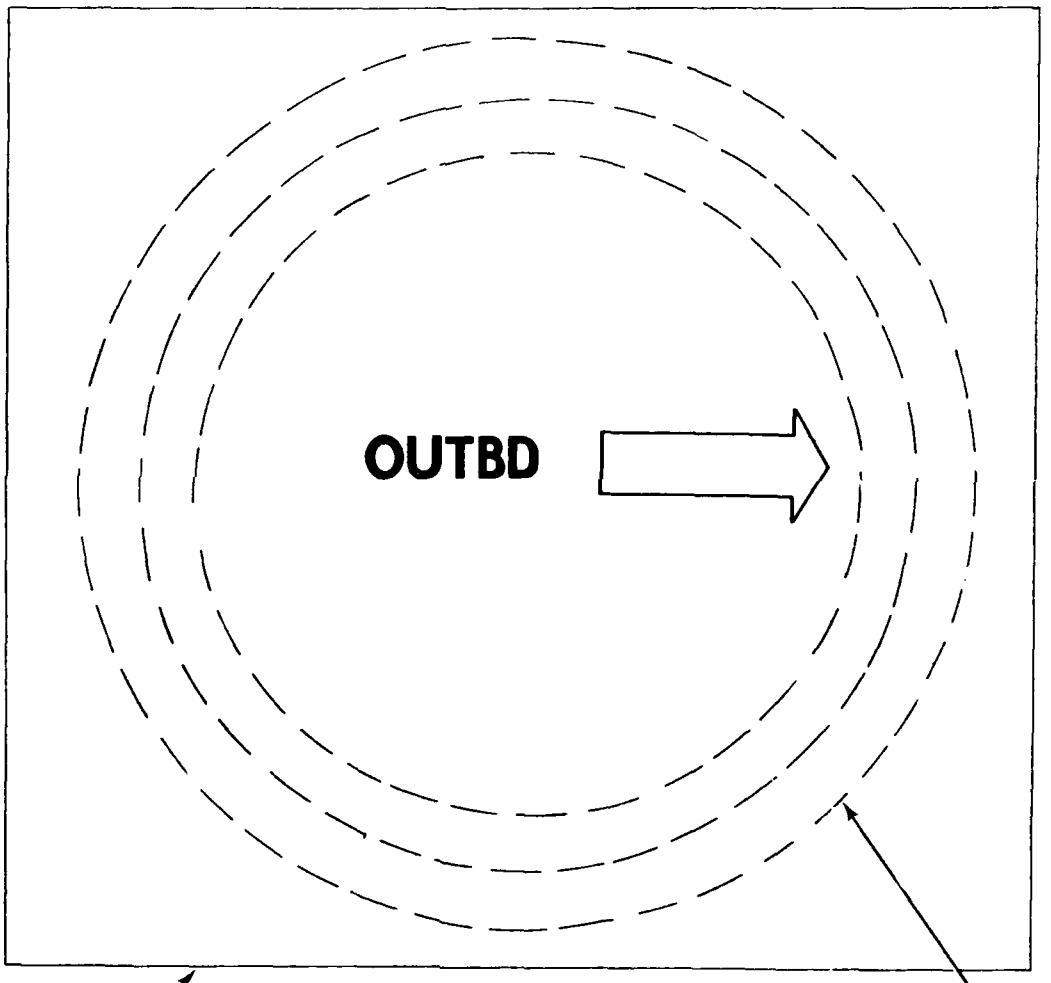

Figure B-5. Typical Skin Patch Construction.

b. Mixing and Application of Adhesive.

NOTE

The quantity of adhesive used in the next step will vary with the size of patch to be applied. A 9-inch diameter patch will require one-third of a 32-gram package of 2-part adhesive. A 5-inch diameter patch, one-eighth of a package, and a 3-inch diameter patch will use one-tenth of a 32-gram package. One tube and one cup are in each package. The cup contains resin and the tube contains curing agent.

CAUTION

Never mix less than a complete 32-gram, 2-part package of adhesive. When less than a full batch is required, mix the full batch and then discard excess after the repair is completed.

(1) Empty the tube (curing agent) into the cup (resin) (Item 200, Table B-11). Stir adhesive with wooden spatula (kit item) until all streaks have disappeared and color is uniform.

CAUTION

These chemicals contain toxic ingredients. Provide adequate ventilation and protect the skin and eyes from contact with uncured resins or curing agent. Wear safety goggles for protection of eyes. Wear plastic gloves (kit item) over cotton gloves (kit item) for protection of hands. If skin is exposed to direct contact with uncured resin or curing agent, wash with warm water and soap. Avoid use of solvents for cleaning the skin.

NOTE

The pot life of adhesive after mixing is only 15 minutes at 72°F. Continue repair procedure without delay.

(2) Using a clean 1-inch-wide paint brush (kit item), new brush only, and/or wooden spatula, apply a light coat of adhesive to blade skin within area previously masked off.

NOTE

If core is damaged and damage is not greater than 1 inch in diameter, smear the damage cavity (frayed ends of honeycomb material) with adhesive prior to applying patch. It is not necessary to rout out the core damage (reference Figure B-3).

CAUTION

Do not pack adhesive into cells of honeycomb core material. To do so will adversely affect blade balance.

(3) Remove the patch from its plastic bag, being careful not to contaminate its inner surface. Using the same brush used to apply adhesive to blade skin, apply a thin coat of adhesive to inner patch surface.

(4) Position patch on blade with stenciled arrow pointing outboard and move slightly back and forth under hand pressure to seat it properly and work out air pockets in the adhesive. Patch must overlap damage area all around by at least 1 inch.

(5) Using clean cheesecloth dampened with methyl-ethyl-ketone, wipe off excess extruded adhesive. It will be necessary to temporarily lift the edges of the patch's peel ply to do so.

(6) Insure patch is properly located. Using masking tape (kit item), tape edges of patch in 4 places to eliminate movement.

c. Curing Adhesive.

(1) Place special pressure/heat pack on blade so that rubber bladder section will come in contact with the repair and the hinges attaching the backer plate are at the blade's trailing edge. Secure pressure/heat pack by swinging the hanging section forward and inserting the toggle lock bolts into slots provided. Tighten the toggle lock bolts until stops are contacted (reference Figures B-6 and B-7).

(2) Actuate hand pump on pressure/heat pack until 4 psi reading is observed on gauge.

NOTE

A pressure relief valve is incorporated to prevent application of pressure above 5 psi.

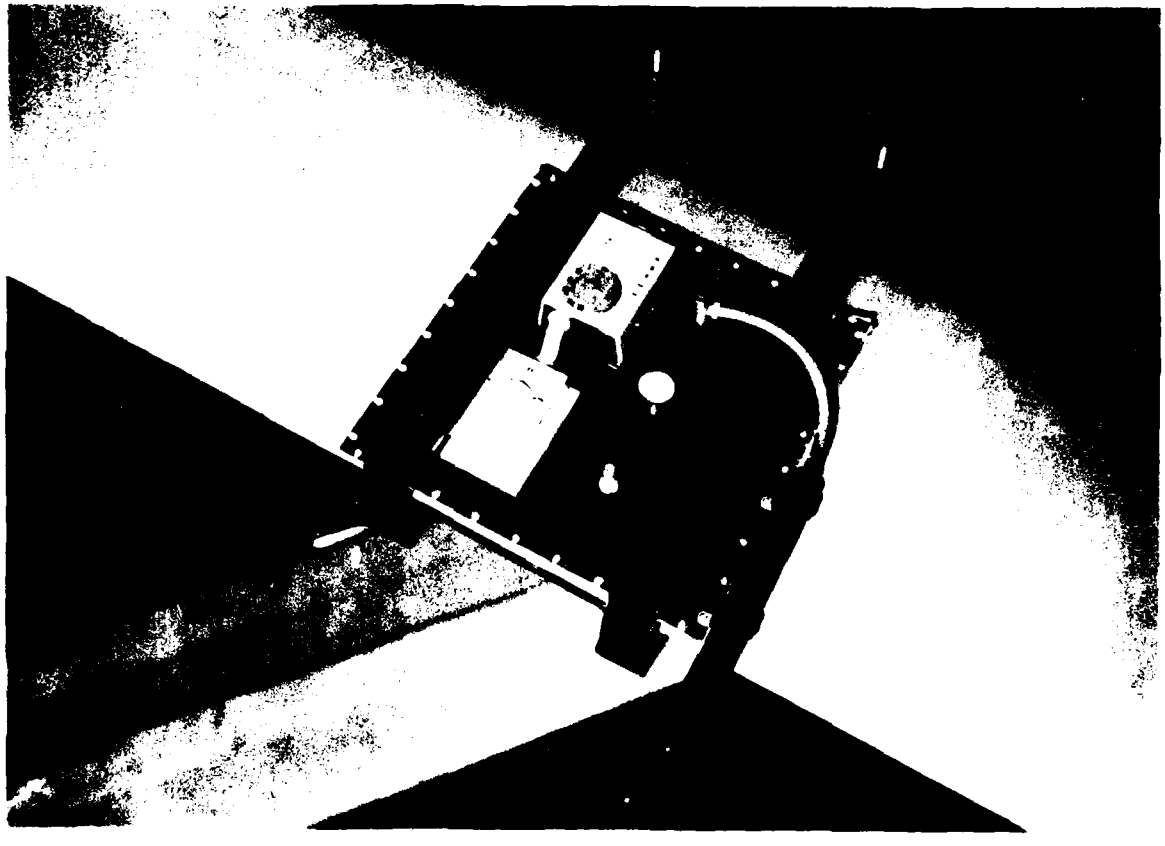

Figure B-6. Pressure/Heat Pack Secured to Blade.

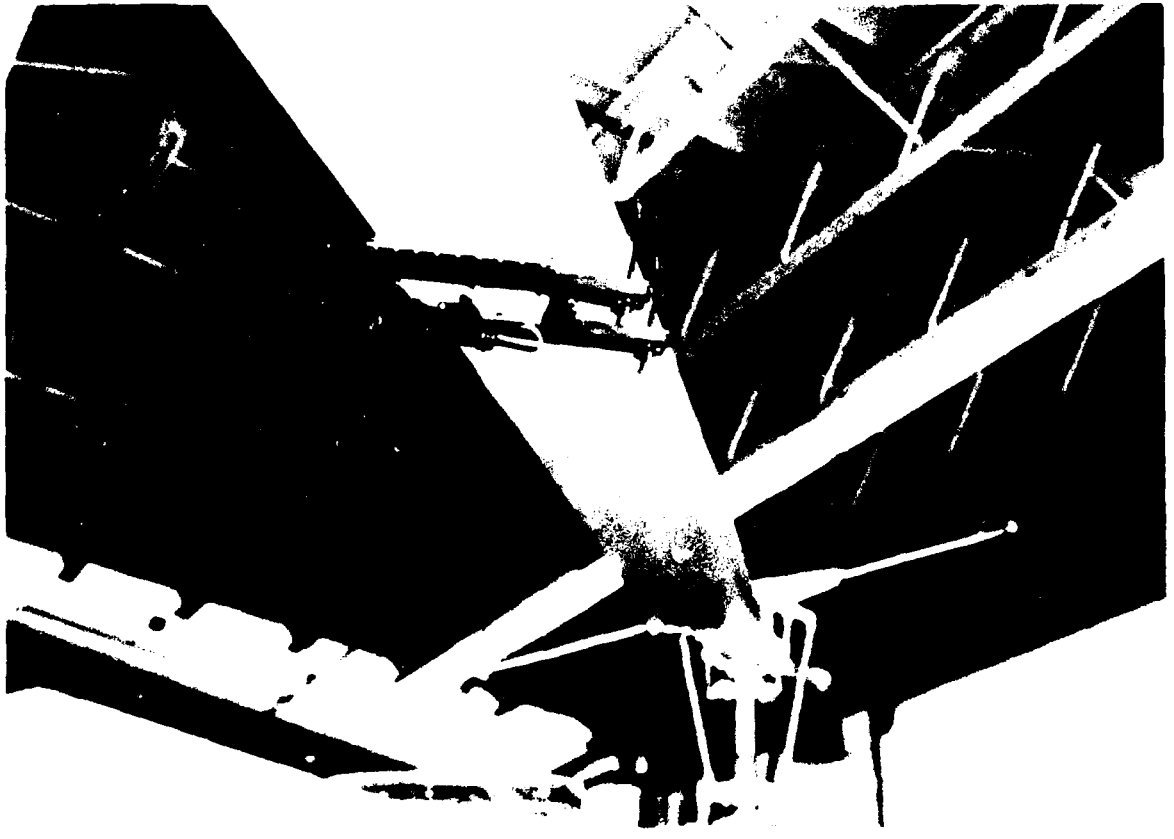

Figure B-7. Pressure/Heat Pack and Blade Perspective.

(3) Connect 110-Volt AC power to pressure/heat pack.

NOTE

A built-in thermostat will automatically maintain the desired curing temperature of 160 F at the skin bond line.

(4) Cure adhesive by maintaining pressure and temperature for 15 minutes.

(5) Disconnect electrical power from pressure/heat pack and relieve air pressure.

NOTE

Relieve air pressure by depressing plunger in valve stem on top of pack assembly.

(6) Remove pressure/heat pack from blade.

(7) Remove peel ply and all masking tape (reference Figure B-8).

d. Refinishing Repair Area.

(1) Using 120 grit abrasive paper, carefully feather the edge of adhesive squeeze-out.

CAUTION

Excessive sanding will result in serious weakening of blade skin.

(2) Paint the repaired area of blade in accordance with instructions given in Paragraph 2-8.

e. Blade Rebalancing.

(1) Refer to Paragraph 2-9 to determine if size and location of skin patch applied above requires adjustment of weights stack-up in blade tip under tip cap. Adjust accordingly.

2-2. PLUG/PATCHES

NOTE

Refer to Paragraph 1-2 to determine if damage is acceptable or repairable, or if blade must be scrapped.

Figure B-8. Removal of Peel Ply.

NOTE

The plug/patch is made from a prefabricated skin patch and Nomex honeycomb plug. The plug comes in two diameters: 3 and 7 inch. Each diameter comes in three depths: 1/4, 1/2 and 1-1/4 inch (reference Figure B-9). There is a peel ply on the outer surface which will serve to keep squeezed-out adhesive from contacting the pressure/heat pack during the curing process. The peel ply is to be removed after the adhesive has cured. An arrow is stenciled on the peel ply to indicate proper orientation of the plug/patch when being installed in the blade. Plugs/patches are packaged in plastic bags in order to keep their bond surfaces contamination-free.

NOTE

This procedure applies to all available sizes of plugs/patches. Refer to Table B-9 for complete list. Measure extent of damage in blade and select plug/patch (diameter and depth of plug) that will replace all of damaged area. After a suitable plug/patch has been selected, refer to Table B-3 to determine the respective number of packages (or fraction of one package) of adhesive that will be required.

NOTE

When damage passes through both skins of blade, two plugs/patches may be applied. The first is applied and allowed to cure before the routing operation of the second is started (reference Figure B-10).

NOTE

This repair may be accomplished to the top and/or bottom surface(s) of a blade while the blade remains installed on the helicopter.

NOTE

Using a tape rule, measure and record the location of damage on the blade. Before starting repair, check balance weight assembly in spar tip to ensure that a sufficient quantity of weights (washers) is available to make balance adjustment after repair is accomplished. Table

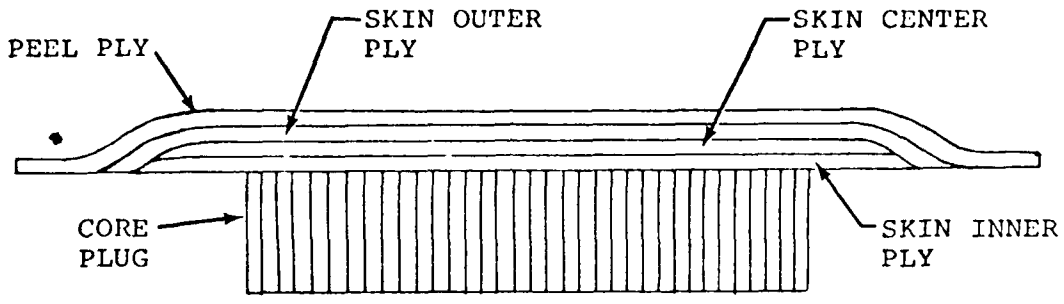

(PLY THICKNESSES DRAWN OVERSIZE FOR CLARITY)

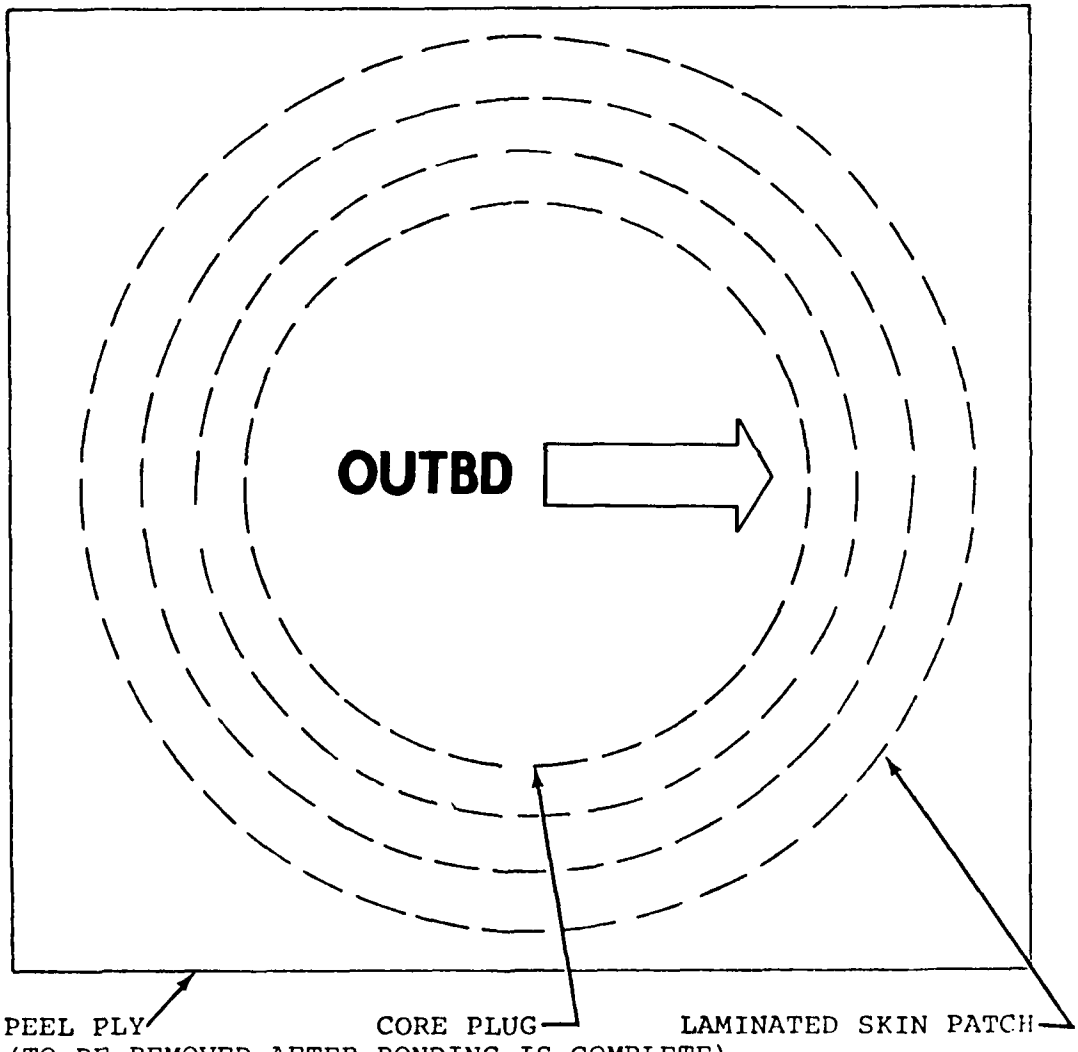

(TO BE REMOVED AFTER BONDING IS COMPLETE)

Figure B-9. Typical Plug Patch Construction.

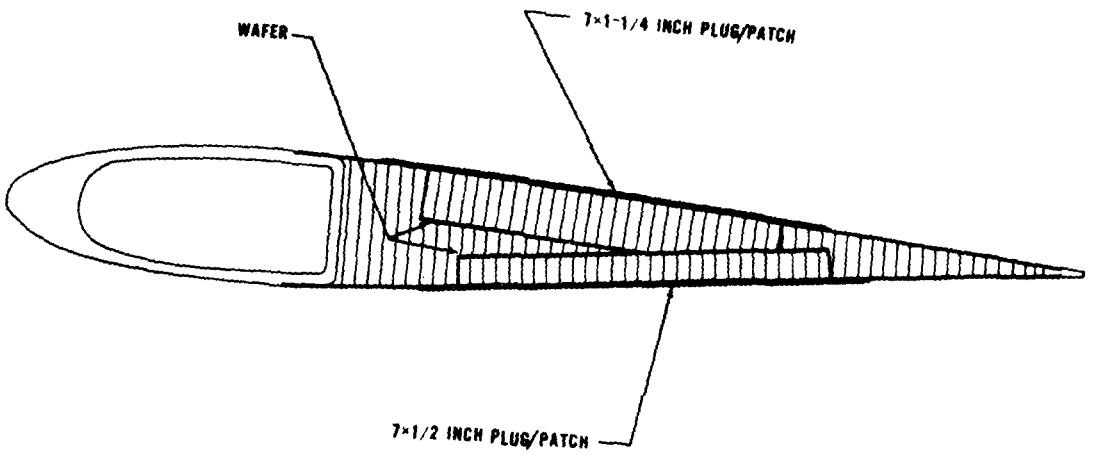

Figure B-10. Typical Double Plug Patch Repair.

B-8 in Paragraph 2-9 specifies the quantities of weights required for various types of repairs. Scrap the blade without attempting repair if available quantity of weights is insufficient.

NOTE

Before starting repair, eliminate teeter movement. Position damaged blade so person making repair has access to damage. Do not cause blade bending greater than normal droop.

TABLE B-2. TOOLS AND EQUIPMENT, PLUG/PATCH REPAIR

PART NUMBER	NOMENCLATURE
	Pressure/Heat Pack
	Router, Electric, Hand Held
	Router Base and Plate
	Router bit, Carbide, 1/4 inch dia., 1-1/2 inches long, Rasp Type
	Compressed Air Source
	Electrical Source, 110 Volt, AC
	Electrical Extension Cord, 16-3

a. Damage Clean-up and Bond Surface Preparation.

(1) Using a pencil and template (kit item), draw 2 concentric circles on the blade around the damage. For a 3-inch plug, 3-inch and 7-inch circles are drawn. For a 7-inch plug, 7-inch and 11-inch circles are drawn.

NOTE

The inner circle drawn in the previous step represents the diameter of a cavity which will be produced in the blade during a later routing operation. The depth of the cavity shall be 1/4, 1/2 or 1-1/4 inches, depending on the depth of the plug selected for use. Because blade core thickness decreases toward the blade

trailing edge, there are limits to how close each different depth cavity can come to the trailing edge without breaking through the opposite skin. These limits are:

Plug Depth	Distance from Trailing Edge
1/4 inch	1 inch
1/2	2
1-1/4	5-1/2

NOTE

The smaller of the two circles drawn in the previous step will be used during routing operation. The smaller circle must be no closer than 1-1/2 inches to the spar or the spline. Also, it must not be closer than 2-1/2 inches in a chordwise direction, nor 8 inches in a spanwise direction to the edge of any root doubler, tip closure, trim tab, or previously installed patch.

(2) Dampen cheesecloth (kit item) with methyl-ethyl-ketone (Item 300, Table B-11) and rub off paint from skin in area between concentric circles.

CAUTION

Care must be taken to prevent thinner from entering core area of blade.

(3) After removing paint, use template and redraw the smaller of the two concentric circles previously drawn in Step a.1. This circle shall be used later during routing operation.

(4) Insert router bit in router collet and set depth of cut to match depth of selected plug plus thickness of wafer. (Both are kit items.)

NOTE

To use plug and wafer as gauge, place plug/patch on flat surface with plug up. Place wafer on plug. Set router base on wafer with router bit along side of plug and adjust router base until router bit comes in contact with inner surface of patch. Lock router base by tightening locking screw (reference Figure B-11).

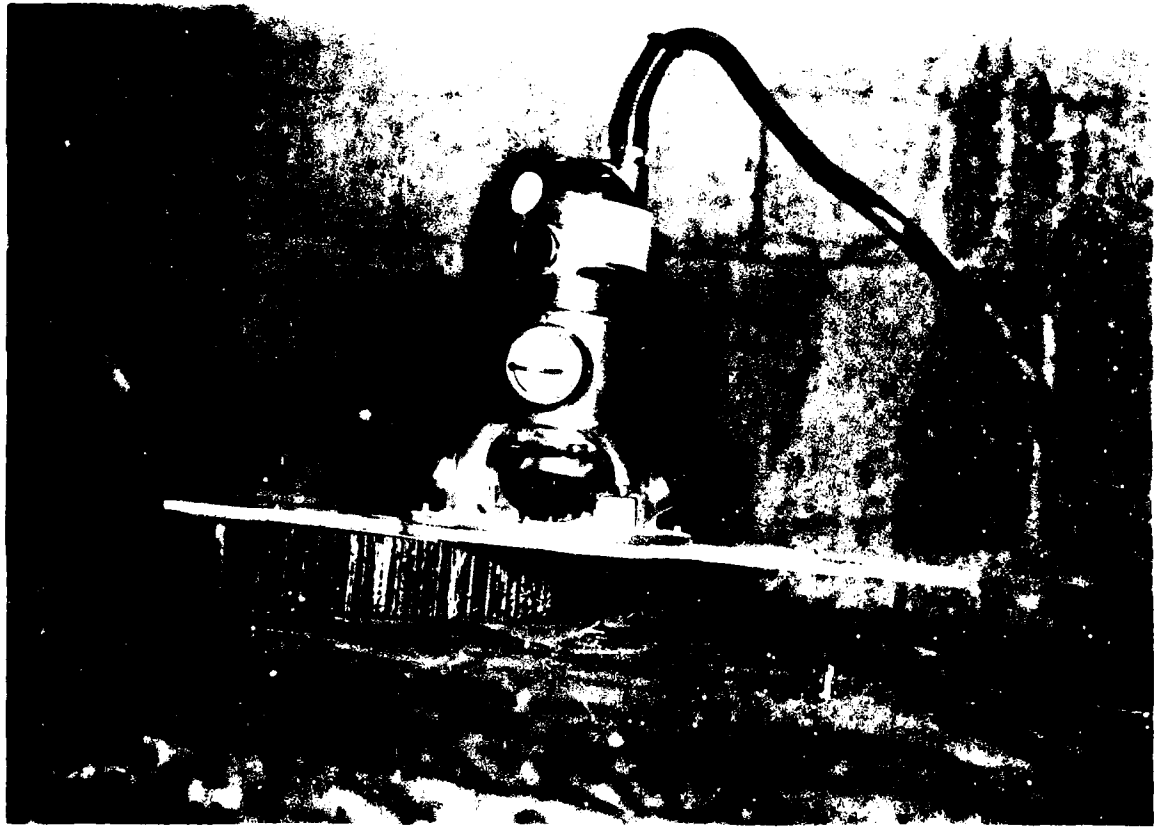

Figure B-11. Using Plug Patch as Gage.

NOTE

When damage is through the blade and a plug patch is to be installed on both sides, proceed with the largest diameter plug first.

WARNING

Fiberglass particles and dust can become eye and skin irritants. Precautions should be taken to protect eyes and skin. As a minimum, the face should be protected during the routing operation with a full coverage shield made of transparent plastic. A hat and shop coat should also be worn.

(5) Start router and grip router handles with both hands. Rest edge of router base on blade (router bit parallel with blade skin and not touching skin). Slowly tilt router forward towards vertical position bringing tip of router bit into contact with blade skin to be removed. Continue this motion until bit is cutting at full depth and router base is resting on blade skin.

NOTE

A special extended length router base is attached to the router to provide stability when bridging larger diameter damage cavities. As the router is moved about during the routing operation, the base extensions must remain parallel with the blade span.

(6) While keeping the router base extensions parallel with the blade span at all times, slowly maneuver the router toward the smaller of the two circles drawn earlier. When the router bit is cutting at the pencil line, carfully move the router in a circular direction, following the drawn line, until a complete circle is cut in the skin (refer to Figure B-12). Remove the router.

(7) Using a flat-bladed screwdriver, lift the edge of the skin inside the cut circle and peel the skin from the core (refer to Figure B-13).

(8) Reinsert the router and with a back and forth motion, rout the core material from within the circle previously cut. The depth of cut should be the same as set in Step (4) (refer to Figure B-14). Remove the router from blade.

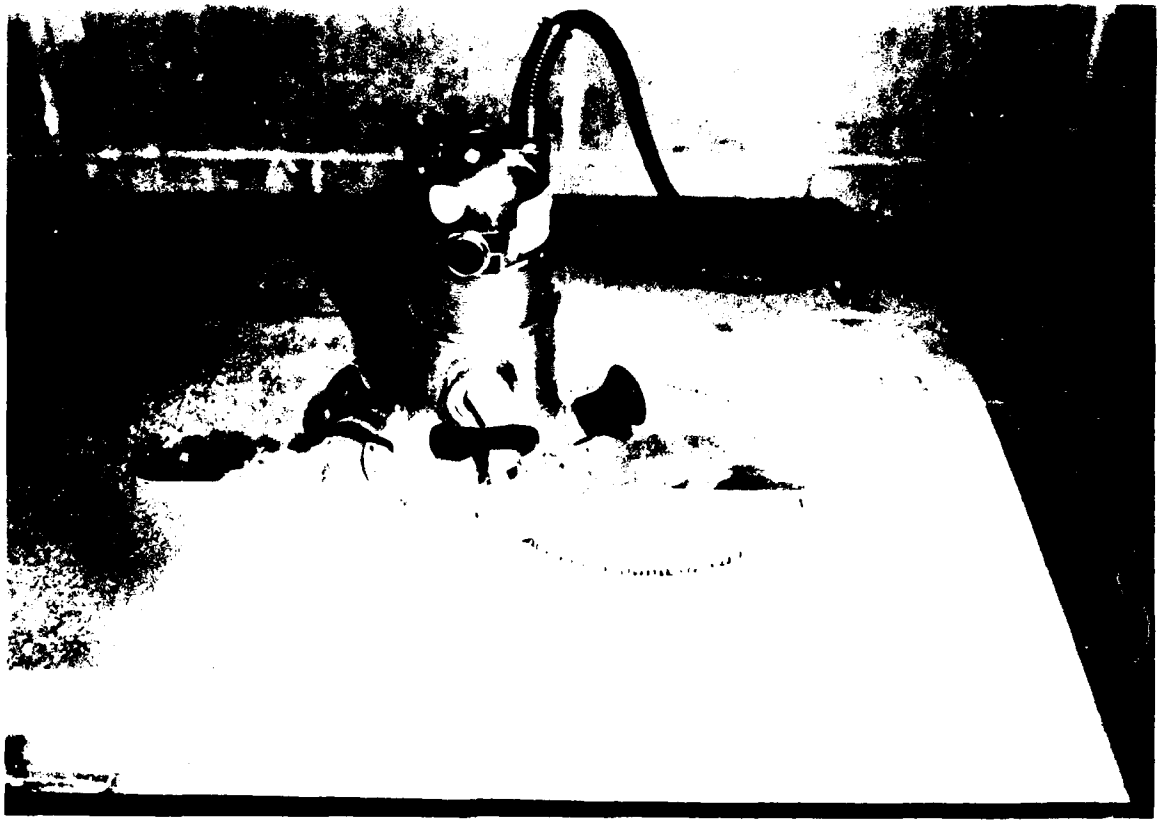

Figure B-12. Routing Skin.

Figure B-13. Peeling of Routed Skin.

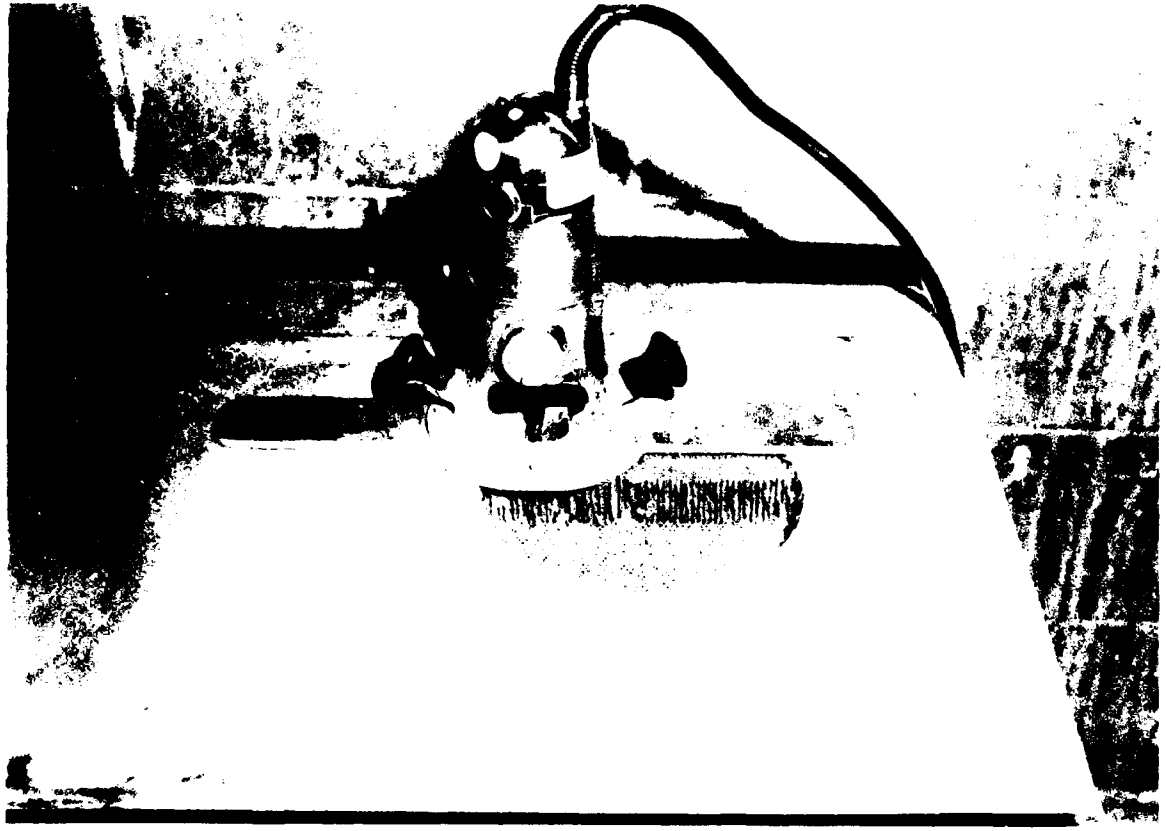

Figure B-14. Routing of Core.

Figure B-15. Installing Plug Patch.

(9) Using 220 grit abrasive paper (kit item) to begin with and finishing with 120 grit abrasive paper (kit item), sand the yellow primer from the surface of the blade skin to which the plug/patch is to be bonded.

CAUTION

Excessive sanding will seriously weaken the blade skin. Sand only until the yellow color is removed.

(10) Remove all debris (cuttings, sanding dust, etc.) from repair area of blade, including core, using compressed air or vacuum cleaner.

(11) Using a pencil and template (kit item), draw a circle 2-1/2 inches in diameter larger than the routed hole produced in Step (8).

NOTE

The template provided for a 3-inch-diameter plug has a 3-inch inside diameter and a 5-1/2-inch outside diameter. The template provided for a 7-inch-diameter plug has a 7-inch inside diameter and a 9-1/2-inch outside diameter.

(12) Using 1-inch wide masking tape (kit item), mask the patch area. To accomplish this, cut the tape into short lengths and apply them to the blade just outside the circle drawn in Step (11). The masked circle will be approximately 1/2 inch in diameter larger than the patch to be applied, thus leaving a 1/4-inch margin all around for adhesive squeeze-out. This adhesive will be feathered in a sanding operation after it has cured.

(13) Clean the skin area to be bonded using cheesecloth (kit item) dampened in methyl-ethyl-ketone (Item 300, Table B-11). Wipe dampened area with clean, dry cheesecloth before dampness evaporates.

CAUTION

The area to be bonded must be clean, dry, and free of grease, oil, wax and other foreign matter.

b. Mixing and Application of Adhesive.

NOTE

The quantity of adhesive used in the next step will vary with the size of plug/patch to be used. The 32-gram adhesive package is made up of two parts, one cup and one tube. The cup contains resin, and the tube contains the proper amount of curing agent. Table B-3 lists the number of packages (or fraction of a package) of mixed adhesive which should be applied to the various sizes of plugs/patches covered in this section.

CAUTION

Never mix less than a complete 32-gram, two part package of adhesive. When less than a full batch is required, mix the full batch and then discard the excess after the repair is completed.

TABLE B-3. PLUG/PATCH ADHESIVE QUANTITY

PLUG DIA.	PLUG DEPTH		
	1/4 In.	1/2 In.	1-1/4 In.
3 Inch	1/3 Pkg.	1/3 Pkg.	2/3 Pkg.
7 Inch	1 Pkg.	1-1/4 Pkg.	2 Pkg.

(1) Empty the tube (curing agent) into the cup (resin), Item 200, Table B-11. Stir adhesive with wooden spatula (kit item) until all streaks have disappeared and color is uniform. Repeat this operation if more than one package is required.

CAUTION

These chemicals contain toxic ingredients. Provide adequate ventilation and protect the skin and eyes from contact with uncured resins or curing agent. Wear safety goggles for protection of eyes. Wear plastic gloves (kit item) over cotton gloves (kit item) for protection of hands. If skin is exposed to direct contact with uncured resins or curing agent, wash with warm water and soap. Avoid use of solvents for cleaning the skin.

NOTE

The pot life of adhesive after mixing is only 15 minutes at 72°F. Continue repair procedure without delay.

(2) Remove the perforated fiberglass wafer from its plastic bag being carful not to contaminate it during handling (reference Figure B-16). Using a clean, 1-inch paint brush (kit item), apply a liberal coat of adhesive to one side of wafer (reference Figure B-17).

CAUTION

Do not pack adhesive into cells of honeycomb core material. To do so will adversely affect blade balance.

(a) Repair on top side of blade will allow wafer to be placed in cavity with adhesive side down (reference Figure B-18).

(b) Repair on underside of blade will require wafer to be placed on plug side of plug/patch (reference Figure B-19).

(3) Apply a liberal coat of adhesive to the remaining exposed side of wafer (reference Figure B-20).

NOTE

The wafer will serve as bond joint between original core and the plug core.

CAUTION

Do not pack adhesive into cells of core material. Blade balance will be adversely affected.

(4) Using wooden spatula or brush, apply a liberal coat of adhesive to walls of cavity in blade core. Apply a thin coat of adhesive to blade skin in area previously masked off.

(5) Remove the plug/patch from its plastic bag, being careful not to contaminate its inner surface. Using a 1-inch paint brush, apply light coat of adhesive to mating surfaces of plug/patch, except plug end, which will contact fiberglass wafer previously installed in core cavity.

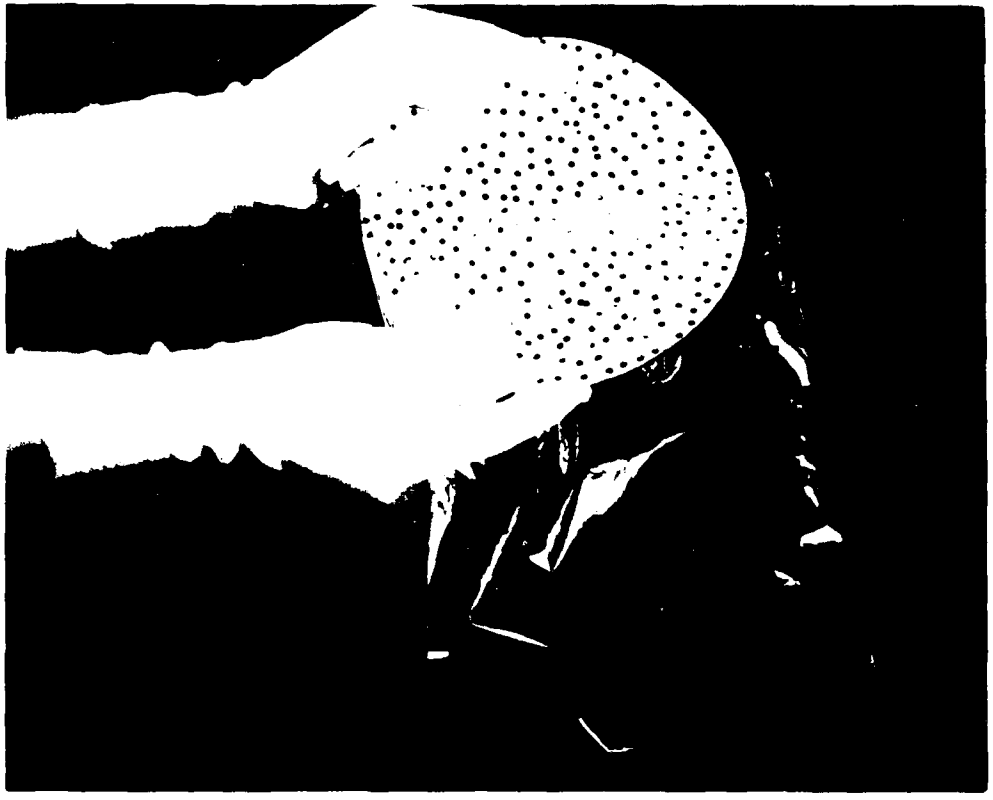

Figure B-16. Perforated Wafer and its Contamination-Free Bag.

Figure B-17. Applying Adhesive to Wafer.

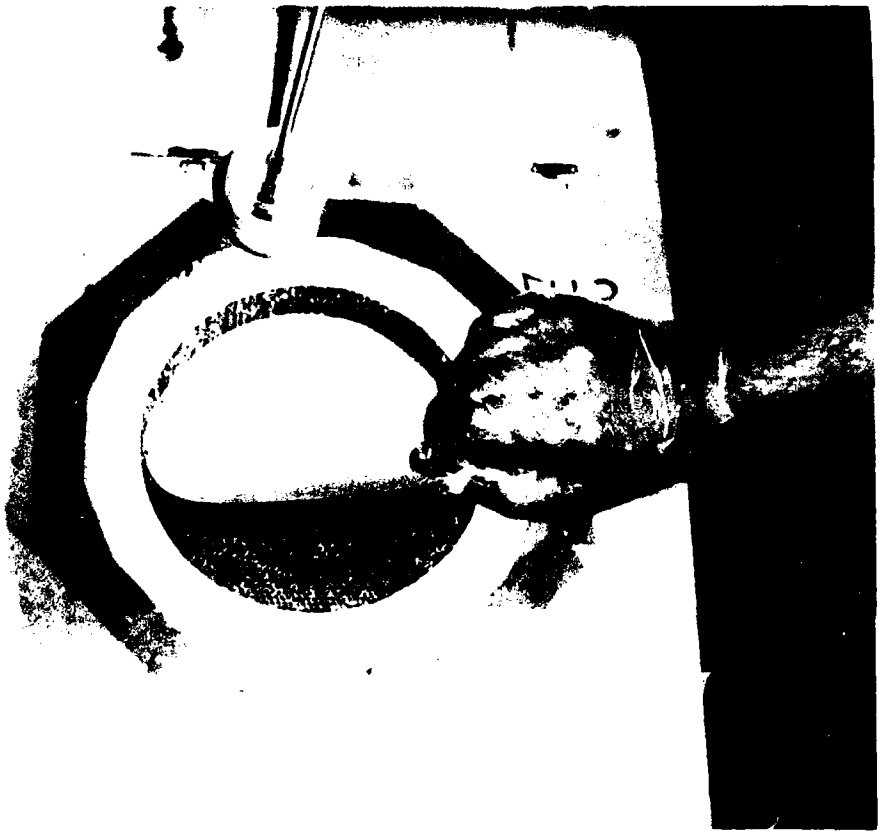

Figure B-18. Placing Wafer in Cavity.

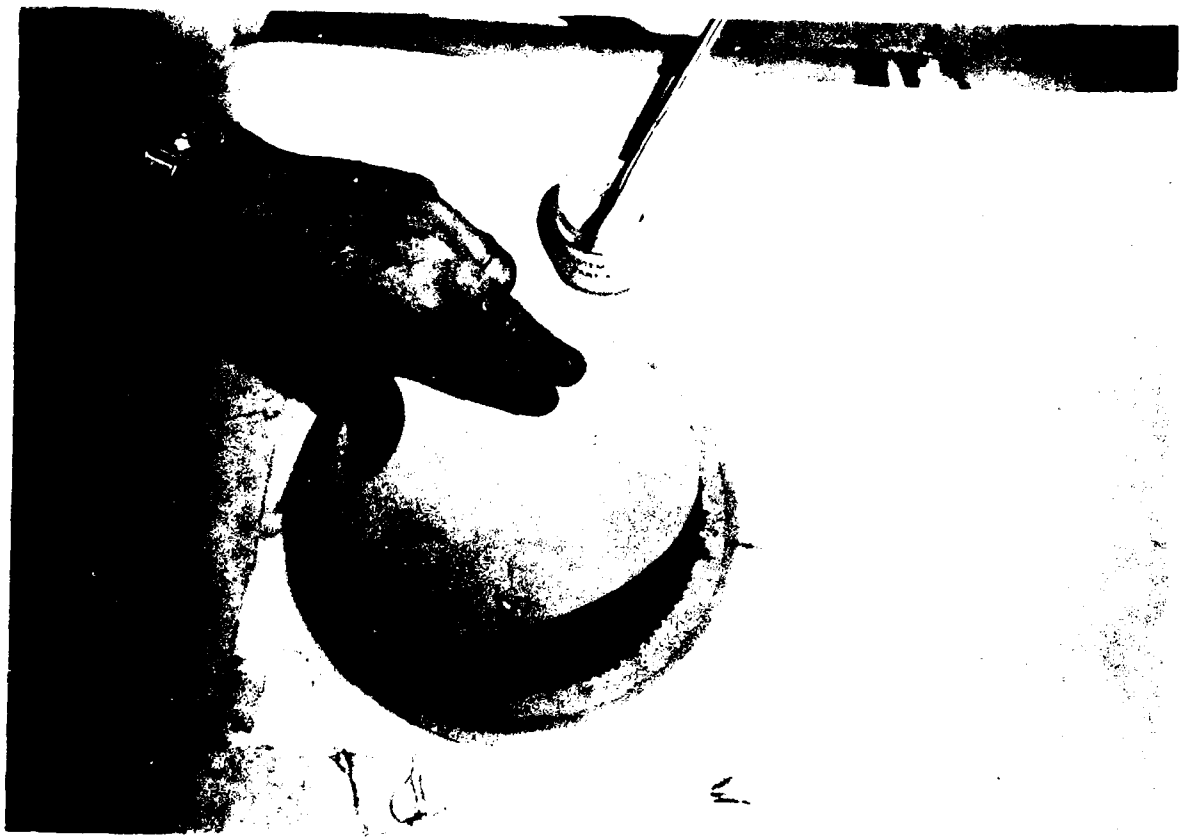

Figure B-19. Placing Wafer on Plug.

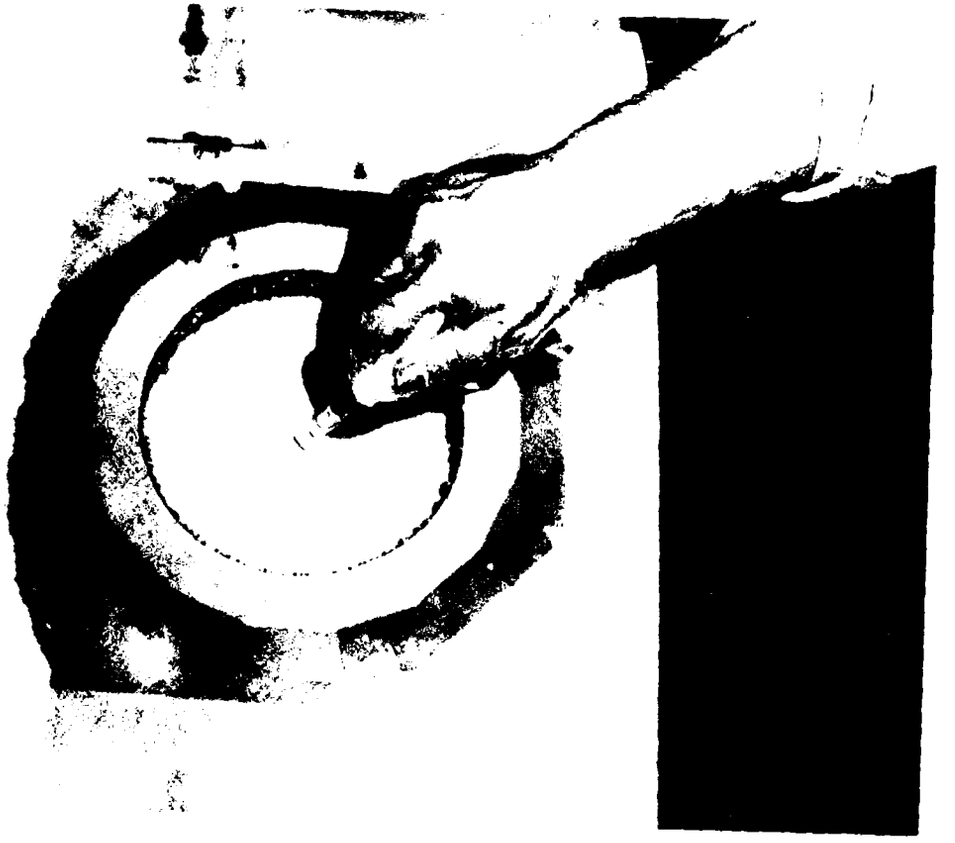

Figure B-20. Applying Adhesive to Remaining Side of Wafer.

CAUTION

Do not pack adhesive into cells of core material. Blade balance will be adversely affected.

(6) Position plug/patch in cavity with stenciled arrow pointing outboard and press firmly into place. Using hand pressure, press out patch area that overlaps blade skin to expel excess adhesive.

(7) Using clean cheesecloth dampened with methyl-ethyl-ketone, wipe off excess extruded adhesive. It will be necessary to temporarily lift the edges of the plug/patch peel ply to do so.

c. Curing Adhesive.

(1) Place special pressure/heat pack on blade so that rubber bladder section will come in contact with the repair and the hinges attaching the backer plate are at the blade's trailing edge. Secure pressure/heat pack by swinging the hanging section forward and inserting the toggle lock bolts into slots provided. Tighten the toggle lock bolts until stops are contacted.

(2) Actuate hand pump on pressure/heat pack until 4 psi reading is observed on gauge.

NOTE

A pressure relief valve is incorporated to prevent application of pressure above 5 psi.

(3) Connect 110-volt AC power to pressure/heat pack.

NOTE

A built-in thermostat will automatically maintain the desired curing temperature of 160°F at the skin bond line.

(4) Cure adhesive by maintaining pressure and temperature for 15 minutes for all but the 7-inch diameter x 1-1/4-inch deep plug/patch. For the 7-inch x 1-1/4-inch plug/patch, maintain pressure and temperature for 30 minutes.

(5) Disconnect electrical power from pressure/heat pack and relieve air pressure.

NOTE

Relieve air pressure by depressing plun
valve stem on top of pack assembly.

(6) Remove pressure/heat pack from bla

(7) Remove peel ply and all masking ta
Figure B-8).

d. Refinishing Repair Area.

(1) Using 120 grit abrasive paper, car
the edge of adhesive squeeze-out.

CAUTION

Excessive abrading will result in serio
ening of blade skin.

(2) Paint the repaired area of blade i
with instructions given in Paragraph 2-8.

e. Blade Rebalancing.

(1) Refer to Paragraph 2-9 to determin
location of plug/patch installed above req ires
weights stack-up in blade tip under tip cap. Ad
ingly.

2-3. TIP CAP REPLACEMENT

NOTE

If tip cap is damaged, refer to Paragra
to determine if damage is acceptable or
able, or if tip cap must be scrapped.

TABLE B-4. TOOLS AND EQUIPMENT, TIP CAP F

PART NUMBER	NOMENCLATUI
	Wrench, 7/32 Inch Hex, Internal Wrenching

a. Removal.

(1) Remove four internal wrenching bolts wh retain tip cap to spar (reference Figure B-21).

NOTE

Do not attempt to loosen the four external wrenching hex head bolts which pass through the tip cap at this time. These bolts retain the balance weights to the interior surface of the tip cap.

(2) Remove tip cap from blade spar.

CAUTION

Do not spill balance weights from weight pins while handling tip cap and weight assembly. An O-ring is installed on each pin and will retain the weights below it under normal handling condi tions. Mark forward pin for later reinstallatio in same position.

(3) Remove weights, pins and retainer (as an as from the tip cap by removing four hex-head bolts.

b. Installation.

(1) Transfer weights assembly to replacement ti Ensure that weight pin previously marked as forward pin i installed in that position. Torque hex-head bolts to 50 70 in-lb.

CAUTION

Do not remove individual weights from weights assembly during process of transferring from one tip cap to another.

(2) Install tip cap in blade spar and secure wi four internal wrenching bolts. Torque bolts to 180 - 200 in-lb.

2.4. MECHANICAL STRAIGHTENING OF TRIM TAB

NOTE

Refer to Paragraph 1-4 to determine if damage to trim tab is acceptable or repairable, or if blade must be scrapped.

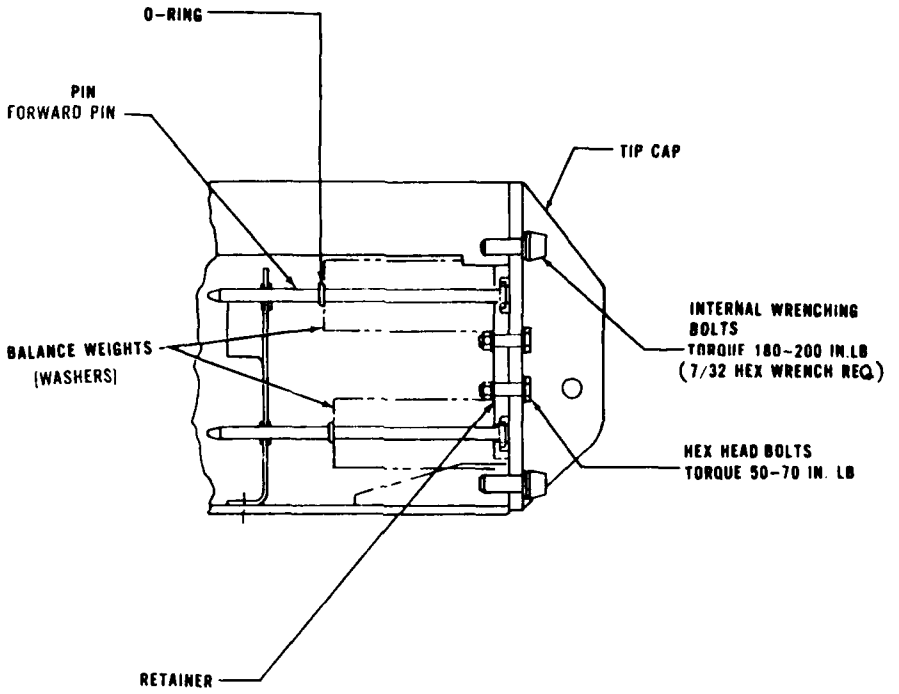

Figure B-21. Tip Cap Replacement.

NOTE

Dents and other distortions may be straightened in accordance with the following instructions, provided cracks or delaminations do not occur in the process. Cracks or delaminations forward of spline will require that the blade be scrapped.

a. Straightening Trim Tab.

CAUTION

Straightening of tab in area forward of spline is not permitted.

(1) Using a broad-faced hammer and suitable backing block, hammer out dents and/or local distortions.

b. Adjusting Bend Angle.

(1) Adjust bend angle of trim tab as required in accordance with TM55-1520-210-20.

c. Refinishing.

(1) Check paint. If cracked, chipped or peeling, refinish affected area in accordance with instructions given in Paragraphs 2-7 and 2-8.

2.5. BLENDING OUT NICKS AND SCRATCHES

NOTE

Refer to Paragraphs 1-1, 1-3, 1-4, 1-5, 1-6 and 1-11 to determine if damage is repairable.

NOTE

Sections of the blade which are fabricated from aluminum alloy and which may be reworked per this procedure are: leading-edge spar, trailing-edge spline, trim tab, root doublers, grip and drag plates, and the tip cap.

TABLE B-5. TOOLS AND EQUIPMENT, BLENDING OUT SCRATCHES	
PART NUMBER	NOMENCLATURE
	Depth Micrometer, 0 - 1 Inch

a. Blending Out Defect.

(1) Using a hand file, abrasive paper, or abrasive wheel, blend out scratch, nick, pitting, etc.

CAUTION

The final polish of smooth blending will be in a spanwise direction. Remove material only to depth necessary for defect elimination. Reworked area shall blend smoothly into surrounding area and have generous blend radii.

CAUTION

Do not use metal (steel or copper alloy) brushes, steel wool or emery cloth on aluminum surfaces, as metal particles may become embedded in the aluminum or entrapped in crevices, thus forming potential corrosion cells.

(2) Remove all filing marks, sanding scratches, etc., by polishing with crocus cloth (Item 501, Table B-11) in a spanwise direction.

b. Inspection.

(1) Using a depth micrometer or other suitable measuring device, check depth of the rework.

NOTE

If extent of rework (depth, length, etc.) exceeds that allowed in repair limits section of these instructions, the blade must be scrapped.

c. Refinishing.

(1) Apply protective alodine finish on reworked aluminum surfaces in accordance with instructions contained in Paragraph 2-7.

(2) Apply touch up primer and paint on reworked surfaces in accordance with instructions contained in Paragraph 2-8.

2-6. POLISHING OUT DEFECTS ON STEEL

TABLE B-6. TOOLS AND EQUIPMENT, POLISHING OUT RUST

PART NUMBER	NOMENCLATURE
	Telescoping Gage Set, 3/4 to 2-1/2 Inch
	O.D. Micrometer, 0 - 1 Inch
	O.D. Micrometer, 2 - 3 Inch
	Depth Micrometer, 0 - 1 Inch

a. Grip and Drag Bushings.

(1) Using 400 grit abrasive paper (Item 502, Table B-11), remove corrosion or pitting from bushing.

(2) Using crocus cloth (Item 501, Table B-11), polish area reworked.

(3) Using telescoping gage and outside diameter micrometer, or other suitable measuring instrument, check effect of rework on inside diameter of bushing. If grip bushing exceeds 2.505 inches or drag bushing exceeds 0.877 inch, the blade must be scrapped and salvaged locally.

NOTE

Local polishing in excess of scrap dimension is acceptable if only a burr needs to be reworked. Example would be a burr created by a scratch from the top of the bushing I.D. to the bottom.

(4) Apply a light film of corrosion-preventive compound (Item 301, Table B-11) to entire I.D. and both ends of bushing.

b. Grip Pad.

(1) Using 180 grit or finer abrasive paper (Item 502, Table B-11), polish out corrosion, pitting, nicks or scratches from grip pad. Final finish to be smooth and in a spanwise direction.

NOTE

Refer to Paragraph 1-7 to determine if damage to grip pad is acceptable or repairable, or if blade must be scrapped.

(2) Apply a light film of corrosion-preventive compound (Item 301, Table B-11) to entire reworked area.

2.7. ALODINE TREATMENT OF ALUMINUM SURFACES

CAUTION

Do not use metal (steel or copper alloy) brushes, steel wool or emery cloth on aluminum surfaces, as metal particles may become embedded in the aluminum or entrapped in crevices, thus forming potential corrosion cells.

(1) Clean the affected area thoroughly with methyl-ethyl-ketone (Item 300, Table B-11) to remove all grease and old paint. Wipe the area with a clean cheesecloth (Item 503, Table B-11).

(2) Wash the cleaned area with a mild soap (Item 304, Table B-11) and clean with fresh water, followed by a clean water rinse. Wipe dry with a clean cheesecloth (Item 503, Table B-11).

(3) Apply alodine solution (Item 302, Table B-11) liberally with a brush or cotton swab.

(4) Allow the alodine solution to remain on the surface for not less than 1 minute, nor more than 5 minutes.

NOTE

Avoid letting the alodine solution dry on the surface. If it has dried, rewet the surface with the alodine.

(5) Rinse the alodized surface with clean fresh water. After rinsing, wipe off excess moisture with a clean,

lintless cloth. Air-blow any moisture from the joints or crevices with clean, dry air and allow to dry completely in open air.

2-8. PAINT TOUCHUP

CAUTION

Because of its effect on rotor balance, repainting the entire blade should not be accomplished. Spot spray the repaired areas only.

a. Preparing the Area to be Painted.

(1) Dampen cheesecloth (Item 503, Table B-11) with lacquer thinner (Item 303, Table B-11) and clean repaired area.

CAUTION

Do not allow lacquer thinner to seep into bonded joints. Thinner will weaken the bond. Cloths wet with thinner should not be left lying on the blade at anytime.

(2) Using 360 grit abrasive paper (Item 502, Table B-11), lightly abrade the surface of fiberglass skins to be painted. Do not abrade metal surfaces to be painted.

CAUTION

Excessive sanding will result in serious weakening of blade skin.

(3) Clean area to be painted using cheesecloth dampened with methyl-ethyl-ketone (Item 300, Table B-11). Wipe area with clean, dry cloth before dampness evaporates.

b. Applying Paint.

NOTE

Epoxy primer (Item 100, Table B-11) is a two-component mix. Component I shall be first poured into an adequate empty container and an equal amount of Component II stirred into Component I. Stir for 10 minutes; then thin by adding 1 part (by volume) of thinner to 2 parts (by volume) of admixed primer. Thinner is a mixture of equal volumes of methyl-isobutyl-ketone

(Item 104, Table B-11) and toluol (Item 105, Table B-11). Stir thoroughly, strain and allow mixture to stand for 1 hour before using.

(1) Spray on a light coat of epoxy primer (Item 100, Table B-11).

(2) Allow primer to air dry for 1 hour.

(3) Spray on a light coat of acrylic lacquer (Item 101, 102 and/or 103, Table B-11), matching the original color of the repaired area.

(4) Allow lacquer to air dry for 1 hour.

2-9. BLADE REBALANCING INSTRUCTIONS

NOTE

These instructions cover rebalancing required subsequent to rework accomplished in Paragraphs 2-1 and 2-2.

TABLE B-7. TOOLS AND EQUIPMENT, BLADE REBALANCE

PART NUMBER	NOMENCLATURE
	Wrench, 7/32 Inch Hex, Internal Wrenching
	Wrench, 0 - 300 in.-lb Torque

a. Remove four internal wrenching bolts which retain tip cap to spar and retain. Remove tip cap from spar.

NOTE

Do not loosen the four external wrenching hex-head bolts.

CAUTION

Do not spill balance weights from weight pins while handling tip cap and weight assembly. An O-ring is installed on each pin and will retain

the weights below it under normal handling conditions.

b. Remove the O-ring retaining balance weights and retain.

c. Remove required quantity of washers from the aft pin and discard and/or move to forward pin as specified in Table B-8.

NOTE

In all cases, weights will be removed from aft pin and discarded and/or moved to forward pin. Never remove weights from forward pin.

NOTE

In those situations when a repair straddles the line separating two zones, consider the entire repair to be in the zone containing the repair center.

d. Place the retaining O-ring on pins.

e. Install tip cap in blade spar and secure with four internal wrenching bolts. Torque bolts to 180 - 200 in.-lb.

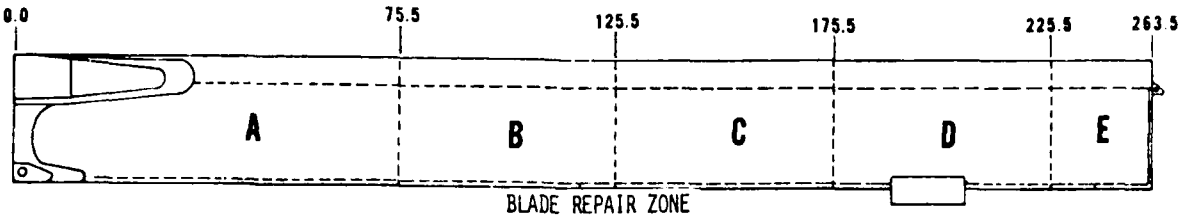

TABLE B-8. BLADE REBALANCE

PARAGRAPH 2-1 REPAIRS						
SKIN/PATCH SIZE	WEIGHT (WASHERS) CHANGE	ZONE A	ZONE B	ZONE C	ZONE D	ZONE E
3 Inch	Discard from aft pin	0	1	1	1	1
	Move forward	4	4	4	4	4
5 Inch	Discard from aft pin	1	2	3	4	4
	Move forward	15	15	15	15	15
9 Inch	Discard from aft pin	5	7	9	12	14
	Move forward	47	47	47	47	47
PARAGRAPH 2-2 REPAIRS						
PLUG/PATCH SIZE	WEIGHT (WASHERS) CHANGE	ZONE A	ZONE B	ZONE C	ZONE D	ZONE E
3 x 1/4 Inch	Discard from aft pin	1	2	3	4	4
	Move forward	15	15	15	15	15
3 x 1/2 Inch	Discard from aft pin	1	2	3	4	4
	Move forward	15	15	15	15	15
3 x 1-1/4 Inch	Discard from aft pin	2	3	5	6	7
	Move forward	23	23	23	23	23
7 x 1/4 Inch	Discard from aft pin	5	7	9	12	14
	Move forward	47	47	47	47	47
7 x 1/2 Inch	Discard from aft pin	5	7	9	12	14
	Move forward	47	47	47	47	47
7 x 1-1/4 Inch	Discard from aft pin	6	9	13	17	21
	Move forward	66	66	66	66	66

TABLE B-9. BLADE REPAIR KITS

KIT NO.	DESCRIPTION	REFERENCE NUMBER
1	3-Inch-Diameter Skin Patch and Related Consumable Materials	K30-202-1
2	5-Inch-Diameter Skin Patch and Related Consumable Materials	K30-202-3
3	9-Inch-Diameter Skin Patch and Related Consumable Materials	K30-202-5
4	3-Inch-Diameter x 1/4-Inch-Deep Plug/5-Inch-Diameter Patch and Related Consumable Materials	K30-202-7
5	3-Inch-Diameter x 1/2-Inch-Deep Plug/5-Inch-Diameter Patch and Related Consumable Materials	K30-202-9
6	3-Inch-Diameter x 1-1/4-Inch-Deep Plug/5-Inch-Diameter Patch and Related Consumable Materials	K30-202-101
7	7-Inch-Diameter x 1/4-Inch-Deep Plug/9-Inch-Diameter Patch and Related Consumable Materials	K30-202-103
8	7-Inch-Diameter x 1/2-Inch-Deep Plug/9-Inch-Diameter Patch and Related Consumable Materials	K30-202-105
9	7-Inch-Diameter x 1-1/4-Inch-Deep Plug/9-Inch-Diameter Patch and Related Consumable Materials	K30-202-107

TABLE B-10. REPAIR KIT CONTENTS

QTY.	UNIT	ITEM	DESCRIPTION	SPEC.	REPAIR KIT DASH NUMBER								
					1	3	5	7	9	101	103	105	107
1	Ea.	Skin Patch	3-Inch-Diameter		X								
1	Ea.	Skin Patch	5-Inch-Diameter			X							
1	Ea.	Skin Patch	9-Inch-Diameter				X						
1	Ea.	Plug/Patch	3-In. x 1/4-In. Plug/ 5-In. Patch					X					
1	Ea.	Plug/Patch	3-In. x 1/2-In. Plug/ 5-In. Patch						X				
1	Ea.	Plug/Patch	3-In. x 1-1/4-In. Plug/ 5-In. Patch							X			
1	Ea.	Plug/Patch	7-In. x 1/4-In. Plug/ 9-In. Patch								X		
1	Ea.	Plug/Patch	7-In. x 1/2-In. Plug/ 9-In. Patch									X	
1	Ea.	Plug/Patch	7-In. x 1-1/4-In. Plug/ 9-In. Patch										X
1	Ea.	Template	1 & 5-In.-Dia. Circles		X								
1	Ea.	Template	1 & 3-1/2-In.-Dia. Circles		X								
1	Ea.	Template	3 & 7-In.-Dia. Circles			X		X	X	X			
1	Ea.	Template	3 & 5-1/2-In.-Dia. Circles			X		X	X	X			
1	Ea.	Template	7 & 11-In.-Dia. Circles				X				X	X	X
1	Ea.	Template	7 & 9-1/2-In.-Dia. Circles				X				X	X	X
1	Pr.	Plastic Gloves	Light Weight, Medium		X	X	X	X	X	X	X	X	X
1	Pr.	Cotton Gloves	Light Weight, Medium		X	X	X	X	X	X	X	X	X
1	Ea.	Paint Brush	1-Inch Wide		X	X	X	X	X	X	X	X	X
50	Ft.	Masking Tape	1-Inch Wide, Small Roll		X	X	X	X	X	X	X	X	X
3	Sq. Yd.	Cheesecloth		CCC-C-440	X	X	X	X	X	X	X	X	X
1	Ea.	Wooden Spatula	Tongue Depressor	LLL-S-007-20	X	X	X	X	X	X	X	X	X
3	Sht.	Abrasive Paper	120 Grit, 9 x 11	P-P-121 & P-P-101	X	X	X	X	X	X	X	X	X
4	Sht.	Abrasive Paper	220 Grit, 9 x 11	P-P-121 & P-P-101	X	X	X	X	X	X	X	X	X
1	Ea.	Wafer	Fiberglass, 3-In.-Dia.					X	X	X			
1	Ea.	Wafer	Fiberglass, 7-In.-Dia.								X	X	X

TABLE B-11. LIST OF CONSUMABLE MATERIALS

ITEM NO.	NOMENCLATURE	COLOR NO.	SPECIFICATION
	PAINTS, PRIMERS, THINNERS AND MARKING COMPOUNDS		
	NOTE: All color numbers to be in accordance with Fed-Std-595.		
100	Primer Coating, Epoxy-Polyamide, Chemical and Solvent Resistant		MIL-P-23377
101	Lacquer, Acrylic, Olive Drab (Camouflage)	34087	MIL-L-81352
102	Lacquer, Acrylic, Insignia White (Gloss)	17875	MIL-L-81352
103	Lacquer, Acrylic, Orange Yellow (Closs)	13538	MIL-L-81352
104	Methyl-Isobutyl-Ketone		TT-M-268
105	Toluol		TT-T-548

TABLE B-11. LIST OF CONSUMABLE MATERI

ITEM NO.	NOMENCLATURE
	ADHESIVES, CEMENTS AND SEALING COM
200	Adhesive, Two-Part Thixotropic Paste, Airline System's Number AS-401-1
	CHEMICALS, COATINGS AND CLEANING CO
300	Methyl-Ehtyl-Ketone
301	Corrosion Preventive Compound, Hot Application, Petrolatum
302	Alodine Solution
303	Thinner, Dope and Lacquer Nitrate
304	Soap, Toilet, White, Floating
305	Tongue Depressor
	ABRASIVES, PAPER, PLASTICS AND MISCE
500	Tape, Masking
501	Cloth, Crocus
502	Abrasive Paper, No. 0000, 000, 180, 220, 240, 320, 360, 400, and 420 Grit, Wet or Dry Type, Commercial Grade
503	Cloth, Cheesecloth Type 2, Class B

11. LIST OF CONSUMABLE MATERIALS (Cont.)

NOMENCLATURE	SPECIFICATION
:SIVES, CEMENTS AND SEALING COMPOUNDS	
/e, Two-Part Thixotropic Paste, : System's Number AS-401-1	
ICALS, COATINGS AND CLEANING COMPOUNDS	
-Ehtyl-Ketone	TT-M-261B
ion Preventive Compound, plication, Petrolatum	MIL-C-11796 Class 3
e Solution	
r, Dope and Lacquer Nitrate	TT-T-266
Toilet, White, Floating	P-S-620
Depressor	LLL-S-007-20
IVES, PAPER, PLASTICS AND MISCELLANEOUS	
Masking	UU-T-106
Crocus	P-C-458
ve Paper, No. 0000, 000, 180, 40, 320, 360, 400, and 420 Wet or Dry Type, Commercial	P-P-121 and P-P-101
Cheesecloth Type 2, Class B	CCC-C-440